Systemic Inflammation, Atherosclerosis and Coronary Thrombosis

Fuijkschot, W.W.

2017

SYSTEMIC INFLAMMATION, ATHEROSCLEROSIS AND CORONARY THROMBOSIS: OF MICE AND MEN

Wessel W. Fuijkschot

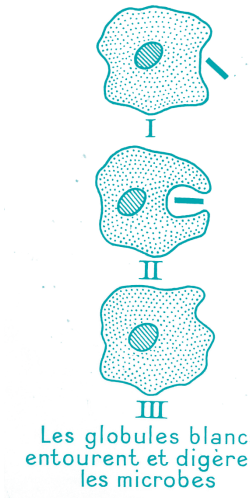

Les globules blancs entourent et digèrent les microbes

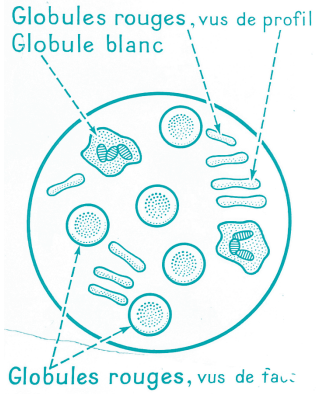

GOUTTE DE SANG
(vue au Microscope)

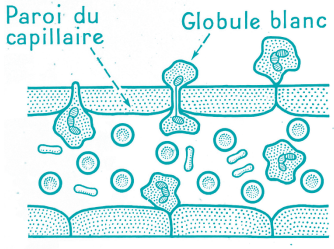

Globule blanc traversant un vaisseau capillaire

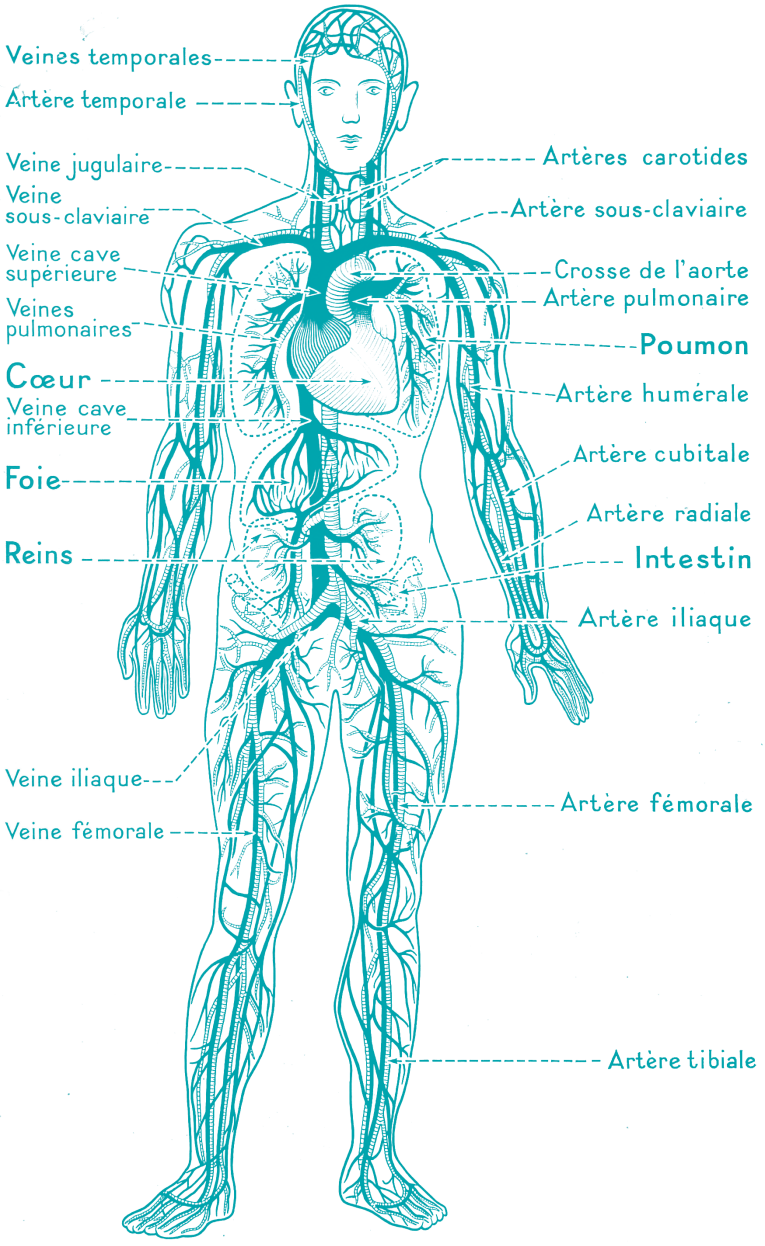

ENSEMBLE DE LA CIRCULATION

Systemic Inflammation, Atherosclerosis and Coronary Thrombosis: Of Mice and Men

Wessel Willem Fuijkschot

VRIJE UNIVERSITEIT

Systemic Inflammation, Atherosclerosis and Coronary Thrombosis: Of Mice and Men

ACADEMISCH PROEFSCHRIFT

ter verkrijging van de graad Doctor aan
de Vrije Universiteit Amsterdam,
op gezag van de rector magnificus
prof.dr. V. Subramaniam,
in het openbaar te verdedigen
ten overstaan van de promotiecommissie
van de Faculteit der Geneeskunde
op dinsdag 12 december 2017 om 13.45 uur
in de aula van de universiteit,
De Boelelaan 1105

door

Wessel Willem Fuijkschot

geboren te Wormerveer

promotoren:	prof.dr. Y.M. Smulders prof.dr. H.W.M. Niessen
copromotor:	dr. P.A.J. Krijnen

Aan mijn grootouders: Minke en Willem Fuijkschot

leescommissie:

prof.dr. M.J.A.P. Daemen
dr. E.C. Eringa
dr. R. Kleemann
prof.dr. E. Lutgens
prof.dr. N.P. Riksen
prof.dr. N. van Royen
prof.dr. A.C. van der Wal

Systemic Inflammation, Atherosclerosis and Coronary Thrombosis: Of Mice and Men

ISBN/EAN: 978-9-46-295780-0
Author: Wessel Fuijkschot
Cover design: Ezekiel Aquino/Ruben Stoel
Lay-out: Kirsty van Nierop/Ron Zijlmans/Rik Westland
Photos: Menno Boermans/Wessel Fuijkschot
Printed by: Proefschriftmaken

Financial support by the Institute for Cardiovascular Research (ICaR-VU), VU University Medical Center, Amsterdam, the Netherlands for the work within this thesis is gratefully acknowledged

The printing of the thesis was additionally kindly supported by:
KINASE, Stichting Medical Business, VU universty medical center department of Internal Medicine, The Dutch Heart Foundation and Marlon Fuijkschot

TABLE OF CONTENTS

1

General introduction and outline of the thesis

GENERAL INTRODUCTION AND OUTLINE OF THE THESIS

Cardiovascular disease

Worldwide, cardiovascular disease is still the number one cause of death, with an annual death toll of 17,5 million lives. Fairly ironic, in most African and Asian countries this rate is augmented each year with enhanced prosperity[1, 2]. Acute myocardial infarction and ischemic stroke account for a large proportion of cardiovascular disease and subsequent morbidity and mortality. A major cause of both events are atherosclerotic plaques vulnerable to rupture or erosion. In the case of myocardial infarction this unstable plaque is typically located in the coronary arteries. The subsequent thrombotic process diminishes myocardial tissue perfusion by reduced coronary artery flow [3]. In the case of ischemic stroke, occlusion is often the result of plaque instability in a carotid artery resulting in a downstream thrombo-embolic process. Our view of the pathogenesis of atherosclerosis has shifted radically in recent decades. Although long presumed as a disease in lipid storage, we now recognize that inflammation is a key contributor to atherosclerosis. Inflammatory cells and mediation in the vascular wall play an important role in disease progression eventually leading to plaque instability and cardiovascular events. As a result, plaque instability is closely related to intra-plaque inflammation[4, 5]. Nonetheless we are still awaiting the results of the first large randomized clinical trials that subject anti-inflammatory interventions to the test[6, 7].

The pathophysiology of plaque rupture on the one hand and occluding thrombus on the other provides the rationale for disease management. Examples of preventive therapies that focus on the vessel wall component are e.g. cholesterol lowering statin treatment and life style advices. In the more acute setting of infarction, percutaneous coronary intervention with stenting or surgical revascularization is often used to restore the patency of the vessel wall and subsequent flow. Anti-thrombotic agents are used preemptively to prevent blood clot formation and subsequent cardiovascular events, which are being augmented by thrombosuction or fibrinolytic approaches in an acute setting. Besides this continuously expanding arsenal, the foundation of treatment of cardiovascular events still predominantly encompasses damage control or tertiary prevention, once an event can occur. Clinicians show great interest in identifying those patients at high risk for an event in order to intervene before myocardial damage has occurred. This is especially promising because it seems that there is a window of opportunity to treat vulnerable or even ruptured plaques before they become clinically overt (i.e. primary prevention vs tertiary prevention) and thus potentially reduce morbidity and mortality. Studies have shown for instance, that sudden coronary occlusion is often preceded by a variable period of plaque instability and/or thrombus formation, underlining the possibility of identifying and treating thrombus initiation and early progression before actual infarc-

tion [8]. In order to properly use this window, it is crucial to understand what factors cause enhanced intra-plaque inflammation leading to vulnerable plaques.

In the search for these factors an important discovery was made that pointed towards systemic over local triggers of plaque destabilization. It was demonstrated that patients with acute myocardial infarction harbor multiple complex coronary plaques, which are associated with adverse clinical outcomes [9]. This finding indicates that plaque instability is not a feature of a single lesion, but it develops in a multifocal pattern, resulting in multiple complex, unstable plaques in anatomically remote locations. Any of these single lesions might progress to total occlusion of a vessel and emerge as the cause of an infarct [9]. This observation supports the concept that plaque instability is not merely a local vascular accident but probably reflects more generalized pathophysiologic triggers with the potential to destabilize atherosclerotic plaques throughout the coronary[9, 10] and carotid vasculature[11].

This concept leads us to the next question: what are possible triggers of widespread/ubiquitous destabilizing of atherosclerotic plaques? Can we understand and thereby predict and prevent increased plaque instability that causes plaque rupture and subsequent thrombosis? Besides very proximate triggers, that cause immediate elevated risk probably via increased myocardial oxygen demand or vasospasm, such as cocaine abuse[12], extreme emotional reactions[13], short term exposure to air pollution[14], sexual activity[15] or physical exercise[16], we are still unaware of the mechanisms that cause these sustained periods[17] of widespread plaque instability.

One possible trigger merits discussion: systemic inflammation. We already described that local inflammatory processes are key in atherosclerotic plaque formation, progression and rupture[18]. Intra-plaque inflammation contributes to many of the characteristics of plaques that are prone to rupture or erode and also plays a role in thrombogenesis[5, 7]. In recent years, it has become more and more obvious that there is a link between systemic inflammation and local plaque enhancement. For instance, several chronic inflammatory states such as systemic lupus erythematosus[19] and rheumatoid arthritis[20] cause plaques to be more vulnerable and therefore could be considered as chronic risk factors for cardiovascular events. In addition, acute infections are suggested to cause an inflammatory activation in the plaque, leading to bursts of pro-inflammatory, proteolytic and prothombotic activity, although definitive evidence is lacking to confirm such a chain of events[21, 22]. In this thesis we study acute systemic inflammation as a factor that may facilitate the initiation of cardiovascular events. Clinical observations predominantly point to an elevated cardiovascular event risk shortly after episodes of acute systemic inflammation. By expanding our understanding of the interaction between acute systemic inflammation and atherosclerotic plaques we may be able to explain the observed increased risk of cardiovascular events as well as provide new leads for preventative therapy.

Acute systemic inflammation and cardiovascular events

Observational epidemiological studies have confirmed what experienced clinicians suspected for many years: cardiovascular events can be triggered by a variety of common non-cardiovascular clinical conditions, particularly those that are associated with systemic inflammation[23-25]. The best documented examples of such conditions include acute (mainly respiratory) infection, and major surgery. Acute systemic infection raises the risk of myocardial infarction by approximately fivefold[23], and risk of stroke by eightfold[26]. The majority of this excess risk is confined to the first days to two weeks after the onset of illness. A post-operational state is another common clinical condition, which increases early cardiovascular risk. A recent nationwide cohort study indicated that the risk of myocardial infarction in patients undergoing total hip or knee replacement is increased by no less than 25-fold, again predominantly during the first days to two weeks[24]

This phenomenon of cardiovascular events occurring in patients hospitalized for non-cardiovascular conditions is clearly important, but the causal mechanisms are unclear, and thus so are targeted preventive strategies. Factors like pain, 'stress', reactive prothrombotic changes, anesthesia and fluid shifts have been invoked, but if any of these are indeed important is unknown.

The acuteness of the increased postoperative cardiovascular risk suggests an effect on atherosclerotic plaque stability and/or erosion[27]. Several studies indeed show that at least half of the cases of myocardial infarction following e.g. non-cardiac surgery originate from rupture of unstable plaques[28-30]. Why plaques could become more prone to rupture in these cases is unclear. We do know that plaque instability is related to factors such as fibrous cap strength, intra-plaque hemorrhage and necrotic core area which, in turn, are all influenced by intra-plaque inflammation[4, 31, 32].

Hence, atherosclerotic inflammation after infection or surgery is a plausible explanation for increased risk. We thus hypothesize that such intra-plaque inflammation may occur as a result of systemic to plaque spreading of inflammatory activity. Not only infection, but also major surgery is associated with a marked systemic inflammatory response (the median C-reactive protein on day 3 after knee arthroplasty, a procedure that is well-documented to increase risk[24], is 189 mg/dl[33]). Conceivably, circulating pro-inflammatory cytokines are responsible for causing inflammatory contamination of atherosclerotic lesions. One study showed that plaque area increased in mice after a single injection of serum amyloid A peptide, a marker and mediator of inflammation [34] Furthermore a landmark paper on the role of acute systemic inflammation in atherosclerosis showed increased plaque area and intra-plaque inflammation in mice, briefly after acute myocardial infarction, another form of acute systemic inflammation[35].

We thus believe that systemic infection and major surgery share a common pathway towards increased early cardiovascular event risk by causing plaque inflammation and plaque growth.

To evaluate this hypothesis, we conduct several mouse and human studies of which we report in this thesis. In these studies, we focus on atherosclerosis, but also evaluate the role of inflammation in atherothrombosis.

General outline of thesis

Besides the larger epicardial blood vessels (the coronary arteries), the smaller intramyocardial vessels are believed to play a role in the etiology of acute myocardial infarction. In Chapter 2 we study the accumulation of N(ε)-(carboxymethyl)lysine (CML) in these intramyocardial vessels in ageing mice. Accumulation of CML is associated with (micro)vascular dysfunction and inflammation. The effect of a diet intervention with the anti-inflammatory fish oil constituent, docosahexaenoic acid, on the accumulation of this advanced glycation end product is also evaluated. Next, the effect of acute systemic inflammation induced by either major orthopedic surgery (Chapter 3) or a single LPS injection to induce sepsis (Chapter 4) on atherosclerosis is studied in mice. In Chapter 5 we compare inflammatory cell content in atherosclerotic coronary arteries of AMI patients that died with or without previous sepsis. In Chapter 6 the density of mast cells in atherosclerotic lesions of the coronary arteries after acute myocardial infarction is studied. Recent developments in 18-fluorodeoxuglucose positron emision tomography (18-FDG-PET) have opened the door to non-invasive imaging of inflammatory changes in large artery atherosclerosis[36, 37]. In Chapter 7 we validate simplified methods for quantitative assessment of ^{18}F-FDG uptake in atherosclerosis assessment of the large arteries. In Chapter 8 PET/CT images of large arteries of human patients before and after major orthopedic surgery are taken. In these images the inflammation in atherosclerotic lesions is quantified in order to evaluate the short-term effects of surgery on intra-plaque inflammation. Most acute myocardial infarctions have their origin in a ruptured plaque with subsequent thrombosis. In 2 chapters the role of inflammation in intra-coronary thrombus formation was studied. In Chapter 9 inflammatory cell and platelet content is quantified and compared with thrombus age and in Chapter 10 we analyze the relation between thrombus age and inflammatory cell content with respect to a phenomenon of the smaller intramyocardial vessels: microvascular injury. A short summary and discussion will be presented in Chapter 11.

REFERENCES

1 Global status report on noncommunicable diseases 2014. Geneva, World Health Organization. 2014

2 Global atlas on cardiovascular disease prevention and control. Geneva, World Health Organization. 2014

3 White HD and Chew DP. Acute myocardial infarction. Lancet 2008;372(9638):570-584

4 Libby P. Inflammation in atherosclerosis. Nature 2002;420(6917):868-874

5 Libby P, Tabas I, Fredman G and Fisher EA. Inflammation and its resolution as determinants of acute coronary syndromes. Circ Res 2014;114(12):1867-1879

6 Back M and Hansson GK. Anti-inflammatory therapies for atherosclerosis. Nat Rev Cardiol 2015;12(4):199-211

7 De CR, D'Ugo E and Libby P. Inflammation and thrombosis - testing the hypothesis with anti-inflammatory drug trials. Thromb Haemost 2016;116(5)

8 Rittersma SZ, van der Wal AC, Koch KT, Piek JJ, Henriques JP, Mulder KJ, Ploegmakers JP, Meesterman M and de Winter RJ. Plaque instability frequently occurs days or weeks before occlusive coronary thrombosis: a pathological thrombectomy study in primary percutaneous coronary intervention. Circulation 2005;111(9):1160-1165

9 Goldstein JA, Demetriou D, Grines CL, Pica M, Shoukfeh M and O'Neill WW. Multiple complex coronary plaques in patients with acute myocardial infarction. N Engl J Med 2000;343(13):915-22

10 Buffon A, Biasucci LM, Liuzzo G, D'Onofrio G, Crea F and Maseri A. Widespread coronary inflammation in unstable angina. N Engl J Med 2002;347(1):5-12

11 Lombardo A, Biasucci LM, Lanza GA, Coli S, Silvestri P, Cianflone D, Liuzzo G, Burzotta F, Crea F and Maseri A. Inflammation as a possible link between coronary and carotid plaque instability. Circulation 2004;109(25):3158-63

12 Mittleman MA, Mintzer D, Maclure M, Tofler GH, Sherwood JB and Muller JE. Triggering of myocardial infarction by cocaine. Circulation 1999;99(21):2737-2741

13 Edmondson D, Newman JD, Whang W and Davidson KW. Emotional triggers in myocardial infarction: do they matter? Eur Heart J 2013;34(4):300-306

14 Pope CA, III, Muhlestein JB, May HT, Renlund DG, Anderson JL and Horne BD. Ischemic heart disease events triggered by short-term exposure to fine particulate air pollution. Circulation 2006;114(23):2443-2448

15 Moller J, Ahlbom A, Hulting J, Diderichsen F, de FU, Reuterwall C and Hallqvist J. Sexual activity as a trigger of myocardial infarction. A case-crossover analysis in the Stockholm Heart Epidemiology Programme (SHEEP). Heart 2001;86(4):387-390

16 Willich SN, Lewis M, Lowel H, Arntz HR, Schubert F and Schroder R. Physical exertion as a trigger of acute myocardial infarction. Triggers and Mechanisms of Myocardial Infarction Study Group. N Engl J Med 1993;329(23):1684-1690

17 Lee SG, Lee CW, Hong MK, Kim JJ, Park SW and Park SJ. Change of multiple complex coronary plaques in patients with acute myocardial infarction: a study with coronary angiography. Am Heart J 2004;147(2):281-6

18 Libby P, Nahrendorf M and Swirski FK. Leukocytes Link Local and Systemic Inflammation in Ischemic Cardiovascular Disease: An Expanded "Cardiovascular Continuum". J Am Coll Cardiol 2016;67(9):1091-1103

19 Stojan G and Petri M. Atherosclerosis in systemic lupus erythematosus. J Cardiovasc Pharmacol 2013;62(3):255-62

20 Salmon JE and Roman MJ. Subclinical atherosclerosis in rheumatoid arthritis and systemic lupus erythematosus. Am J Med 2008;121(10 Suppl 1):S3-8

21 Hansson GK, Libby P and Tabas I. Inflammation and plaque vulnerability. J Intern Med 2015;278(5):483-493.

22 Rosenfeld ME and Campbell LA. Pathogens and atherosclerosis: update on the potential contribution of multiple infectious organisms to the pathogenesis of atherosclerosis. Thromb Haemost 2011;106(5):858-867

23 Smeeth L, Thomas SL, Hall AJ, Hubbard R, Farrington P and Vallance P. Risk of myocardial infarction and stroke after acute infection or vaccination. N Engl J Med 2004;351(25):2611-2618

24 Lalmohamed A, Vestergaard P, Klop C, Grove EL, de BA, Leufkens HG, van Staa TP and de VF. Timing of acute myocardial infarction in patients undergoing total hip or knee replacement: a nationwide cohort study. Arch Intern Med 2012;172(16):1229-1235

25 Corrales-Medina VF, Musher DM, Wells GA, Chirinos JA, Chen L and Fine MJ. Cardiac complications in patients with community-acquired pneumonia: incidence, timing, risk factors, and association with short-term mortality. Circulation 2012;125(6):773-781

26 Elkind MS, Carty CL, O'Meara ES, Lumley T, Lefkowitz D, Kronmal RA and Longstreth WT, Jr. Hospitalization for infection and risk of acute ischemic stroke: the Cardiovascular Health Study. Stroke 2011;42(7):1851-1856

27 Cohen MC and Aretz TH. Histological analysis of coronary artery lesions in fatal postoperative myocardial infarction. Cardiovasc Pathol 1999;8(3):133-139

28 Janssen H, Wagner CS, Demmer P, Callies S, Solter G, Loghmani-khouzani H, Hu N, Schuett H, Tietge UJ, Warnecke G, Larmann J and Theilmeier G. Acute perioperative-stress-induced increase of atherosclerotic plaque volume and vulnerability to rupture in apolipoprotein-E-deficient mice is amenable to statin treatment and IL-6 inhibition. Dis Model Mech 2015;8(9):1071-80

29 Gualandro DM, Campos CA, Calderaro D, Yu PC, Marques AC, Pastana AF, Lemos PA and Caramelli B. Coronary plaque rupture in patients with myocardial infarction after noncardiac surgery: frequent and dangerous. Atherosclerosis 2012;222(1):191-5

30 Hanson I, Kahn J, Dixon S and Goldstein J. Angiographic and clinical characteristics of type 1 versus type 2 perioperative myocardial infarction. Catheter Cardiovasc Interv 2013;82(4):622-8

31 Virmani R, Burke AP, Farb A and Kolodgie FD. Pathology of the vulnerable plaque. J Am Coll Cardiol 2006;47(8 Suppl):C13-8

32 Virmani R, Burke AP, Kolodgie FD and Farb A. Vulnerable plaque: the pathology of unstable coronary lesions. J Interv Cardiol 2002;15(6):439-46

33 Reid D, Toole BJ, Knox S, Talwar D, Harten J, O'Reilly DS, Blackwell S, Kinsella J, McMillan DC and Wallace AM. The relation between acute changes in the systemic inflammatory response and plasma 25-hydroxyvitamin D concentrations after elective knee arthroplasty. Am J Clin Nutr 2011;93(5):1006-1011

34 Thompson JC, Jayne C, Thompson J, Wilson PG, Yoder MH, Webb N and Tannock LR. A brief elevation of serum amyloid A is sufficient to increase atherosclerosis. J Lipid Res 2015;56(2):286-293.

35 Dutta P, Courties G, Wei Y, Leuschner F, Gorbatov R, Robbins CS, Iwamoto Y, Thompson B, Carlson AL, Heidt T, Majmudar MD, Lasitschka F, Etzrodt M, Waterman P, Waring MT, Chicoine AT, van der Laan AM, Niessen HW, Piek JJ, Rubin BB, Butany J, Stone JR, Katus HA, Murphy SA, Morrow DA, Sabatine MS, Vinegoni C, Moskowitz MA, Pittet MJ, Libby P, Lin CP, Swirski FK, Weissleder R and Nahrendorf M. Myocardial infarction accelerates atherosclerosis. Nature 2012;487(7407):325-329

36 Rudd JH, Myers KS, Bansilal S, Machac J, Rafique A, Farkouh M, Fuster V and Fayad ZA. (18)Fluorodeoxyglucose positron emission tomography imaging of atherosclerotic plaque inflammation is highly reproducible: implications for atherosclerosis therapy trials. J Am Coll Cardiol 2007;50(9):892-896

37 Tawakol A, Fayad ZA, Mogg R, Alon A, Klimas MT, Dansky H, Subramanian SS, Abdelbaky A, Rudd JH, Farkouh ME, Nunes IO, Beals CR and Shankar SS. Intensification of statin therapy results in a rapid reduction in atherosclerotic inflammation: results of a multicenter fluorodeoxyglucose-positron emission tomography/computed tomography feasibility study. J Am Coll Cardiol 2013;62(10):909-917

2

Prevention of age-induced N(ε)-(carboxymethyl)lysine accumulation in the microvasculature

Wessel W. Fuijkschot; Hjalmar J. de Graaff; Ekatarina Berishvili; Zurab Kakabadze; Koba Kupreishvili; Elisa Meinster; Maaike Houtman; Amber van Broekhoven; Casper G. Schalkwijk; Alexander B. A. Vonk; Paul A. J. Krijnen; Yvo M. Smulders and Hans W. N. Niessen

Eur J Clin Invest 2016;46:334-41

ABSTRACT

Objective: N(ε)-(carboxymethyl)lysine (CML) is one of the major advanced glycation end products in both diabetics and non-diabetics. CML depositions in the microvasculature, has recently been linked to the etiology of acute myocardial infarction and cognitive impairment in Alzheimer's disease, possibly related to local enhancement of inflammation and oxidative processes. We hypothesised that CML deposition in the microvasculature of the heart and brain is age-induced and that it could be inhibited by a diet intervention with docosahexaenoic acid (DHA), an omega-3 fatty acid known for its anti-inflammatory and anti-oxidative actions.

Material and methods: ApoE -/- mice (n=50) were fed a western diet and were sacrificed after 40, 70 and 90 weeks. Part of these mice (n=20) were fed a western diet enriched with DHA from 40 weeks on. CML in cardiac and cerebral microvessels was quantified using immunohistochemistry.

Results: Cardiac microvascular CML depositions significantly increased with an immunohistochemical score of 11.85 [5.92-14.60] at 40 weeks, to 33.17 [17.60-47.15] at 70 weeks (p=0.005). At the same time points, cerebral microvascular CML increased from 6.45; [4.78-7.30] to 12.99; [9.85-20.122] (p=0.003). DHA decreased CML in the intramyocardial vasculature at both 70 and 90 weeks, significant at 70 weeks (33.17;[17.60-47.15] vs. 14.73;[4.44-28.16] p=0.037). No such effects were found in the brain.

Conclusions: Accumulation of N(ε)-(carboxymethyl)lysine in the cerebral and cardiac microvasculature is age-induced and is prevented by docosahexaenoic acid in the intramyocardial vessels of ApoE -/- mice.

INTRODUCTION

Advanced glycation end products (AGEs) are proteins or lipids that become glycated after exposure to sugars[1]. N(ε)-(carboxymethyl)lysine (CML) is one of the major AGEs and its formation is enhanced in the presence of inflammation and under influence of reactive oxygen species such as superoxide radicals and hydrogen peroxide[2].Vice versa, it is known that CML itself is involved in the generation of oxidative stress and induction of inflammation via interaction and activation of the Receptor AGE (RAGE)[3]. Increased CML serum levels were found to correlate positively with the incidence of cardiovascular events such as acute myocardial infarction[4]. Moreover, CML depositions were locally detected in the major arteries[2] and are believed to contribute to the development of atherosclerosis[5, 6] through both receptor for AGEs (RAGE)-dependent and RAGE-independent pathways[7]. Moreover, intra-plaque levels of CML were associated with increased risk of plaque rupture[8], supporting the concept that CML induces progression of stable to rupture-prone plaques.

Although age-related CML accumulation was found in atherosclerotic vessels[8], it remains unknown whether age-related CML accumulation also occurs in the, non-atherosclerotic, microvasculature of the brain and the heart. This is of great interest, because the intramyocardial blood vessels are more important in the induction of acute events than previously thought[9] and form a potential new therapeutic target. As for the brain, it is known for years that damage to the local microvasculature is related to Alzheimer's disease[10] and coincides with damage to the microvasculature of the kidney and indices of age and hypertension[11]. We have previously shown that CML deposits in the microvasculature of the brain in diabetes mellitus (DM) and in the heart in acute myocardial infarction[9], DM[12] as well as in diastolic heart failure[13]. However, the relation to patients age hasn't been studied and the results from the macrovasculature cannot be directly translated to the microvasculature, since we have found in the human heart that the extent of CML accumulation in the atherosclerotic epicardial coronary arteries does not correlate with that in the downstream intramyocardial microvasculature[9].

To elucidate the role of aging in microvascular CML accumulation, we have now studied CML deposition in the microvasculature in an atherosclerotic mouse model. We have chosen an atherosclerotic model to mimic the situation of elderly humans. Additionally, we have analysed whether putative age-related effects on the microvasculature could be inhibited by the omega-3 (n-3) long chain polyunsaturated fatty acid, docosahexaenoic acid (DHA). As this fish oil constituent has been advocated as a diet intervention against several effects of aging, including cognitive impairment[14, 15] and cardiovascular events[16], in part via its anti-oxidative[17, 18] and anti-inflammatory[19, 20] actions.

MATERIAL AND METHODS

Mice

Apo E -/- mice (6–8 weeks old) were obtained from The Jackson Laboratory (Bar Harbor, Maine, USA). Mice were housed under specific pathogen-free conditions, on a 12-h light–dark cycle and fed a Western Diet for Rodents (5TJN – 1810842, PS Product Supplies, London). The mice were divided into 5 groups (Table 1). Group 1,2 and 3 were fed with a western diet and were respectively sacrificed at 40, 70 and 90 weeks, resulting in extensive atherosclerotic changes of the aorta already at 40 weeks (Fig. 1A). Group 4 and 5 received the western diet enriched with 4% DHA (C22:6, Nu-Chek Prep, Inc, USA) from 40 weeks on and were sacrificed at 70 weeks (group 4) and at 90 weeks (group 5). Survival was recorded during the entire experiment by checking the animals on a daily basis. The survival percentages were calculated per group as the percentage of mice that lived to the time point of planned sacrifice opposed to mice that died preliminary. All procedures were approved by the Animal use and care Committee at the Georgian National Institute for Medical Research.

Table 1 Survival per group

Group (n=10)	Number of mice that reached the endpoint (%)	DHA	Age at sacrifice (weeks)
1	10 (100)	-	40
2	5 (50)	-	70
3	9 (90)	+	70
4	3 (30)	-	90
5	5 (50)	+	90

Number and percentage of mice per group (starting with n=10) that reached the endpoint, based on age of sacrifice and docosahexaenoic acid (DHA) administration (- or +). DHA + mice received DHA from 40 weeks on.

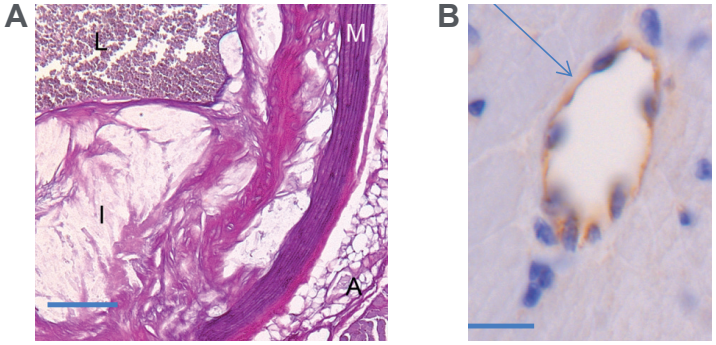

Figure 1 Examples of (immuno)histochemical analyses

Histological (Haematoxylin-eosin) staining of a cross section of the root of an atherosclerotic aorta of an Apo E -/- mouse at the age of 40 weeks. L: lumen of the blood vessel, filled with erythrocytes. I: intima; M: media; **A:** adventitia. Notice the extended calcification and fibrosis showing an advanced lesion (magnification 50 x). Scale bar: 225 µm. **B:** Immunohistochemical staining of CML (arrow) in an intramyocardial blood vessel of an Apo E -/- mouse at the age of 70 weeks (magnification 400 x). Scale bar: 25 µm.

Immunohistochemistry

The heart and brain were embedded in paraffin after overnight fixation (4 % formalin). For immunohistochemical analysis, 4 µm sections were dewaxed, rehydrated and incubated in methanol/H2O2 (0.3%) for 30 minutes to block endogenous peroxidases. Antigen retrieval was performed by heat inactivation in Citrate buffer (pH 6.0) (for the CML staining) and in Tris/EDTA buffer (pH 9.0) (for the SOD2 staining). Previously it was hypothesised that heating could induce CML formation in unfixed rat livers [21], however we have found no evidence that heat induced CML formation in formalin fixed heart and brain tissue occurs (not shown), due to the heating pre-treatment procedure itself. After incubation with normal rabbit serum (1:50; Dako, Glostrup, Denmark) for the CML staining and with normal swine serum (1:20) for the SOD2 staining, both for 10 minutes, sections were incubated for 60 minutes with a biotinylated anti-CML antibody (1:500) or an anti-SOD2 antibody (1:100 dilution). After washing in phosphate-buffered saline (PBS), pH 7.4, sections were incubated for 30 minutes with a rabbit anti-mouse biotin-conjugated antibody (1:500; Dako) for the CML staining or biotin-conjugated swine-anti-rabbit antibody (1:100, Dako) for the SOD2 staining, washed in PBS, incubated with streptavidin-horseradish peroxidase (HRP) (1:200; Dako) for 60 minutes and visualized with 3,3-diamino-benzidine-tetrahydrochloride/H2O2(DAB, 0.1 mg/ml, 0.02% H2O2) for 10 minutes. The slides were subsequently counterstained with haematoxylin, dehydrated and covered. With the staining a PBS and isotype control was included. All these controls yielded negative results (data not shown).

Immunoscoring

Immunoscoring was performed by M.H. E.M. and H.W.N. Agreement was reached between observers. For intensity scoring, each positive vessel in the heart and the brain

was given a score according to the intensity of staining: 1 = weak staining; 2 = moderate staining; or 3 = strong staining[9, 12, 22]. Subsequently, slides were scanned with a PathScan Enabler IV, where after the surface area of the tissue was measured using QuickPHOTO MICRO 3.0 software. To obtain the CML immunohistochemical score, the respective intensity scores (1, 2, and 3) were first multiplied by the amount of blood vessels positive for this score. These three numbers were then added and subsequently divided by the surface area of the tissue, resulting in an immunohistochemical score per mm2. Lastly, the number of SOD2 positive vessels were scored with a microscope and divided by the surface area of the tissue.

Statistics

Values are given as median and interquartile range. Since most of the data were not normally distributed, the Kruskall-Wallis and Mann–Whitney U tests were used to test for differences between groups. The Fisher's exact test was used to compare the survival rates between groups. Results were considered statistically significant if the two-sided p-value was <0.05. Statistical analysis was performed with SPSS (20.0 for Windows, SPSS Inc.) and graphs were made with GraphPad (Prism 6).

RESULTS

CML accumulation in the heart

In 40 week old mice, CML was found to be present in the endothelium of intramyocardial blood vessels (Fig. 1B). These CML depositions were significantly increased in 70 week old mice, namely from an immunohistochemical score of 11.85 [5.92-14.60] at 40 weeks up to 33.17 [17.60-47.15] at 70 weeks (p=0.005) (Fig. 2A). This increase in CML was in line with an increase in the number of CML-positive blood vessels of all three intensity scores, which was significant for intensity scores 2 and 3 (Fig. 3A). The number of blood vessels/mm^2 with intensity score 1 (weak positive) increased from 1.98 [1,27-2.55] to 5.63 [2.33-8.88] (p=0.066), those with intensity score 2 (moderate positive) increased from 2.84;[1.46-3.60] to 5.32;[2.82-8.99] (p=0.050) and those with intensity score 3 (strong positive) from 1.20 [0.65-1.83] to 5.63 [3.20-6.76](p=0.005)
In the 90 week old group (n=3)., the immunohistochemical score and the number of CML-positive blood vessels did not further change significantly. However, compared with 70 week old mice, the numbers of blood vessels with intensity score 1 were lower and those with intensity score 3 were higher, although not significantly.

In 70 and 90 week old mice fed with the DHA-supplemented diet the CML immunohistochemical scores were lower than mice of similar age fed with non-supplemented diet and comparable to the 40 week old mice (Fig. 2A). This difference was significant for the 70 week old mice only , namely 14.73; [4.44-28.16] in the DHA mice versus

33.17; [17.60-47.15] in the non-DHA mice of the same age (p=0.037). This coincided with a decrease in the number of blood vessels with intensity score 1,2 and 3, although this was significant only for intensity score 3, namely 2.10 [0.27-4,59] in the DHA mice versus 5.63; [3.20-6.76] in the non-DHA mice (p=0.039) (Fig. 4A). In 90 week old mice a non-significant decrease in the number of blood vessels positive for scores 1,2 and 3 was found.

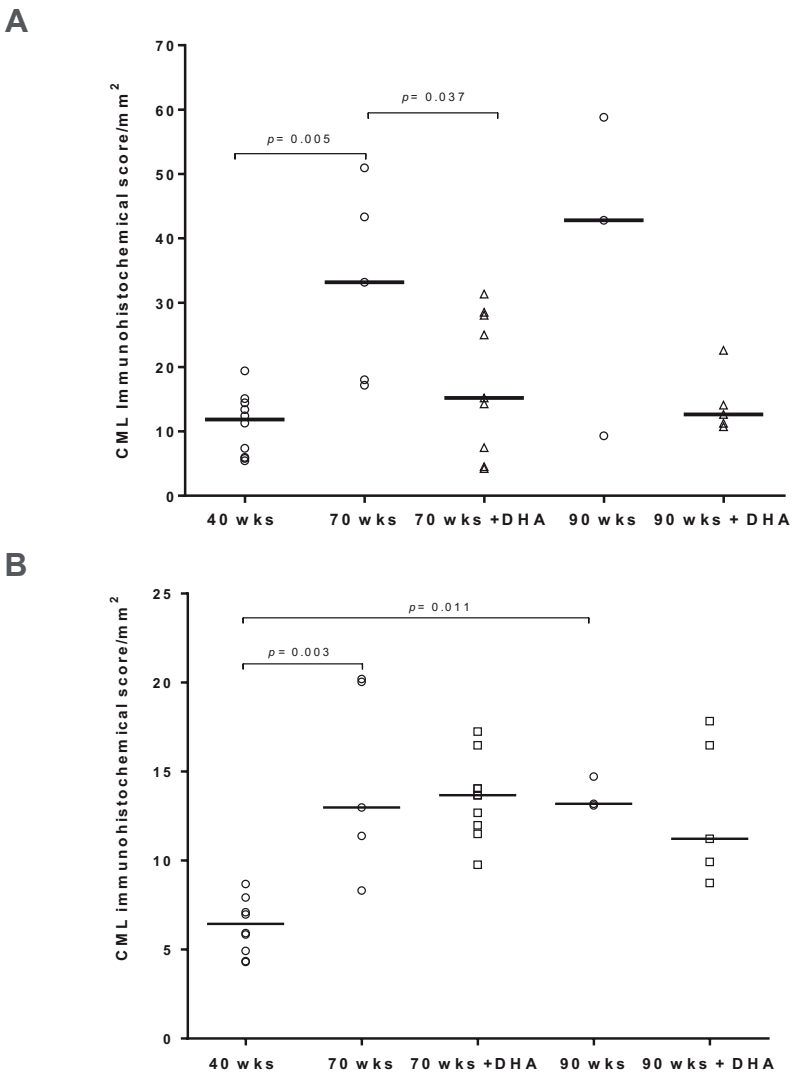

Figure 2 Quantification of N(ε)-(carboxymethyl)lysine (CML) in blood vessel

A: Quantitative analysis of CML in intramyocardial blood vessels **B:** Quantitative analysis of CML in blood vessels of the brain. Bars represent median immunohistochemical scores per mm² (defined in Methods).

CML accumulation in the brain

CML was also found in the non-atherosclerotic blood vessels of the brain in 40 week old mice. Similar to the heart, CML accumulation in the brain was significantly higher in 70 week old mice, namely from an immunohistochemical score of 6.45; [4.78-7.30] at 40 weeks to 12.99; [9.85-20.122] at 70 weeks (p=0.003; Fig. 2B). This corresponded with a significant increase in the number of blood vessels with intensity scores 1, 2 and 3 in these mice (Fig. 3B), namely for intensity score 1 from 0.87;[0.51-1.09 to 2.48;[1.95-2.59] (p=0.002); for intensity score 2 from 1.21;[0.88-1.60] to 1.86;[1.55-2.56] (p=0.027) and for intensity score 3 from 1.01;[0.77-1.17] to 2.42;[1.49-4.17] (p=0.003).

In 90 week old mice, the immunohistochemical score and the number of blood vessels with intensity score 3 were significantly higher than 40 week old mice ($p<0.011$ for both), but not 70 week old mice (Fig. 2B and 3B). ln contrast to the heart, DHA did not have a significant effect on the immunohistochemical scores in both 70 and 90 week old mice. And although the median of intensity scores 2 and 3 was lower in DHA-treated 90 week old mice compared with non-treated 90 week old mice, no significant differences were found in intensity scores between DHA-treated and non-treated mice in 70 and 90 week old mice.

Super Oxide Dismutase

We analyzed the amount of SOD-2 positive vessels in the hearts of the 40 wks, 70 wks DHA - and 70 wks DHA + mice, since the CML scores in these groups differed most. SOD-2 positive blood vessels were scarce and up to a factor 10-100 lower than CML-positive vessels. SOD-2 positive vessels did not significantly differed between the groups, namely 0,22 [0.03-0.32] in the 40 weeks old mice, 0.06 [0.00-0.14] in the 70 weeks old mice without DHA and 0.47 [0.07-0.62] in 70 weeks old mice with DHA (p=0.20).

Survival

Survival rate decreased with age from 100 % (40 weeks) to 50 % (70 weeks) to 30 % (90 weeks) (table 1). Interestingly, 70 and 90 week old mice that were treated with DHA had a higher survival rate than the respective age-related non-treated groups, i.e. 90 % versus 50 % and 50 % versus 30% respectively. We added the survival rates of the DHA + groups, both at 70 and 90 weeks and compare d them with DHA - groups at 70 and 90 and found a survival advantage for the DHA treated group of 70 % vs. 40 % albeit not significant (p=0.111).

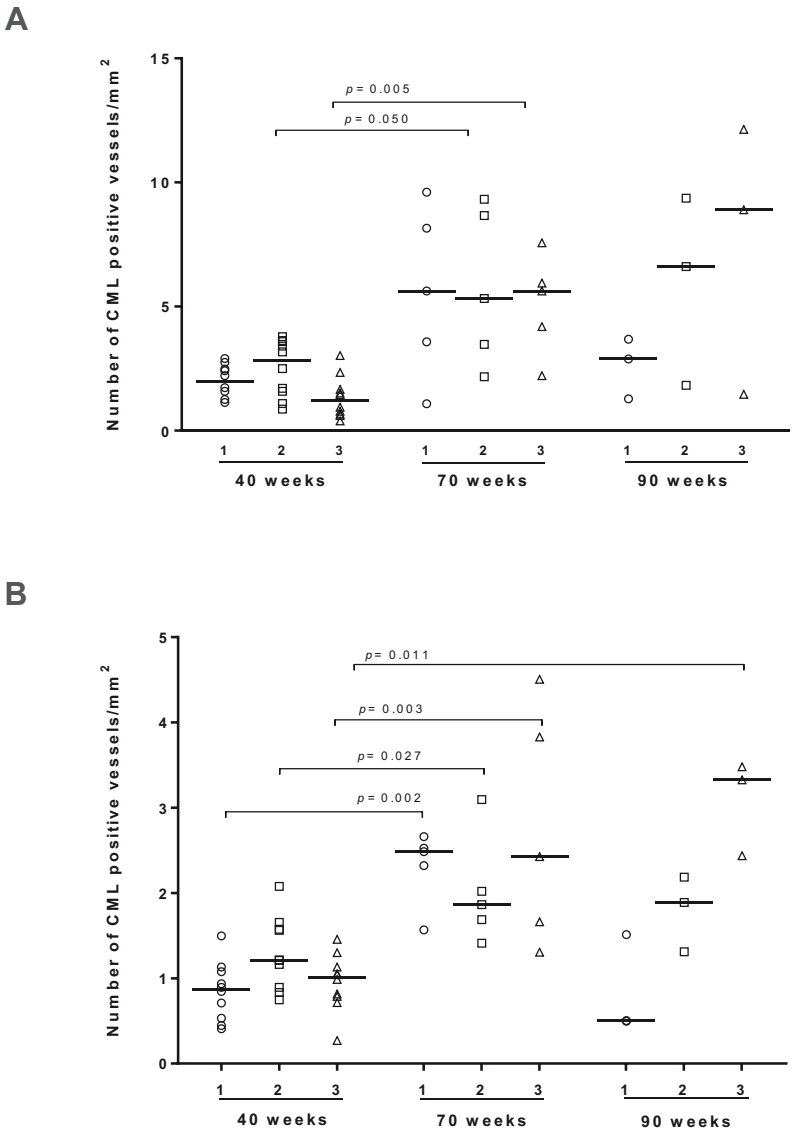

Figure 3 Intensity score of CML in 40,70 and 90 weeks old mice

A: Quantitative analysis of the intensity scores of the CML positive intramyocardial blood vessels and **B:** quantitative analysis of the intensity scores of the CML positive the blood vessels in the brain . The 3 different intensity scores for CML (1 = minor; 2 = moderate; 3 = strong) are defined in detail in Methods. Bars represent median scores.

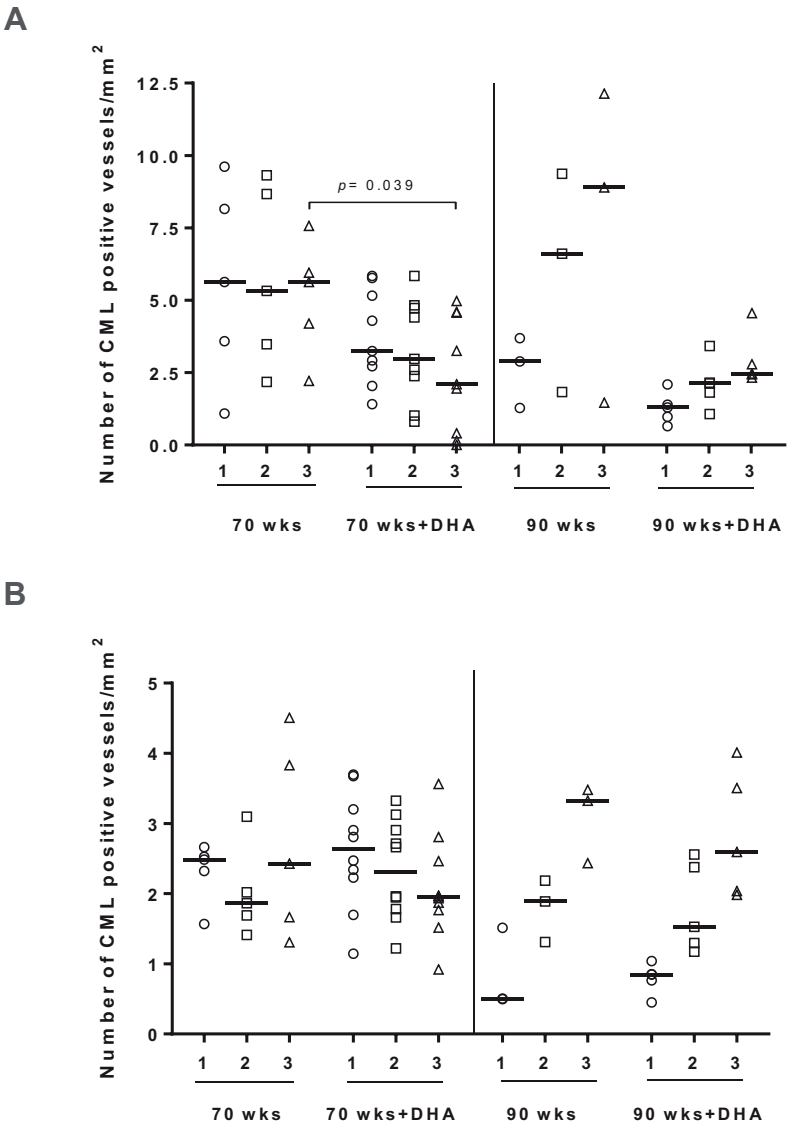

Figure 4 Intensity score of CML in 70 and 90 weeks old mice with and without DHA

A: Quantitative analysis of the intensity levels of the CML positive intramyocardial blood vessels and **B:** quantitative analysis of the intensity scores of the CML positive the blood vessels in the brain . The 3 different intensity scores for CML (1 = minor; 2 = moderate; 3 = strong) are defined in detail in Methods. Bars represent median scores.

DISCUSSION

N(ε)-(carboxymethyl)lysine (CML) is believed to play a role in the development and progression of atherosclerosis[2, 5, 6] and its accumulation in atherosclerotic changed blood vessels increases with age. In the present study we found age-related CML accumulation in non-atherosclerotic microvasculature of the heart and the brain of atherosclerotic mice. Furthermore, we found that the polyunsaturated fatty acid DHA, inhibited this age-related microvascular CML accumulation in the heart, but not in the brain.

Age-related CML accumulation in tissue was previously shown in collagen of the skin[23], in human articular cartilage[24] and in atherosclerotic changed arteries [2]. We now add to this, that CML accumulates age-related in the non-atherosclerotic intramyocardial microvasculature. This is in line with a study that found that CML levels in human cardiac tissue homogenates increase with age, coinciding with diabetes and coronary heart disease[25], without further specifying the location of this CML. This specific location in the heart is important in relation to the notion that CML accumulation in the intramyocardial non-atherosclerotic vasculature may play a role in the etiology of Acute Myocardial Infarction (AMI), based on the finding that CML accumulation within the intramyocardial vasculature was especially found in patients that died from AMI as opposed to control deaths, independent of the disease state of epicardial coronary arteries. This CML accumulation occurred prior to the onset of AMI[9] and therefore is not a reflector of AMI. Moreover, we have shown this CML accumulation also in diabetes[12, 22] and diastolic heart failure[13].

We have previously described CML depositions in non-atherosclerotic changed vessels of the brain in diabetes in humans and rats[22]. It has been suggested that this could influence the microcirculation of the brain, contributing to the development of cognitive impairment, the so-called diabetes-associated cognitive decline[22]. We now have found age-related CML accumulation in the non-atherosclerotic microvasculature of the brain. Interestingly, it was described that CML accumulation in the microvasculature of the brain is related to cognitive impairment[26,28]. Indeed age-related functional effects of CML in cultured hippocampal microvessels and cultured choroidal explants of rats were described[26, 27].

There are several mechanisms by which CML may play a pathophysiological role in the vascular cell function[28, 29], including formation of inflammatory cytokines and growth factors coinciding with pro-thrombogenic alteration of the endothelium, impaired vasodilatation and increased expression of adhesion molecules and chemokines on vascular cells[30]. The deleterious consequences of aging in the vasculature could in part be explained through the now described age-related CML accumulation in the blood vessels.

Another interesting finding of our study was the observation that the omega-3 fatty acid DHA, inhibited CML accumulation in the non-atherosclerotic intramyocardial vessels to control levels. It is believed that DHA lowers blood pressure, has antiplatelet actions and has anti-atherogenic effects f.i. via reduction of triglyceride concentration, via reduction of expression levels of adhesion molecules and on smooth muscle cells proliferation and migration[31-33] . It was also found that DHA has a direct antiarrhythmic effect on the heart[34, 35]. The mechanisms by which DHA prevents CML deposition in the microvasculature of the heart in our study, is unknown, but it is reasonable to assume that the anti-inflammatory role of DHA in combination with its superoxide scavenging role and inhibition of lipid peroxidation activity could prevent CML formation. More specific, it is known that DHA increases SOD activity[36, 37], that in turn reduces reactive oxygen species[38]. We therefore wondered if the effects of DHA on CML in the heart could be explained by an increase in vascular SOD-2. Indeed an age-accompanied decrease with SOD-2 activity was found in the small vessels of the heart, with an increase of SOD-2 in the mice that were fed DHA, albeit not significant. It has to be noticed that the amount of SOD-2 positive vessels is minor compared to the amount of CML positive vessels.

It was previously found that omega-3 fatty acid dietary administration in rats increased activity of superoxide dismutase and decreased lipid peroxidation in tissue homogenates of the cerebral cortex thus as such theoretically could inhibit ROS-driven CML accumulation[39-41], we didn't find any significant effect of DHA in the brain. We can only speculate why DHA did have an effect on CML depositions in the microvasculature of the heart but not of the brain. This could point to a difference in properties of endothelial cells in the heart and the brain, as it is known that dependent on the location in the body, endothelial cells have their own molecular make up that drives basic behavior, as well as their responses on inflammatory stimuli[42, 43]. Clearly the specialized brain endothelium, forming the blood brain barrier, has different properties than the endothelium of the intramyocardial vessels[44]. Obviously this interesting observation needs further research for a more precise explanation. The study has in our opinion one important limitation, namely the low survival in the 90 weeks group (n=3) that made a proper statistical comparison difficult.

In conclusion, we have found that aging induces CML accumulation in the non-atherosclerotic microvasculature of the heart and the brain in ApoE -/- mice and that DHA inhibits CML accumulation in the heart, but not in the brain. Further experiments are necessary to better understand the consequences of the age-dependent increase of CML in non-atherosclerotic microvascular vessels and the underlying pathophysiology and therapeutic possibilities of the effects of DHA on age-related CML accumulation.

ACKNOWLEDGEMENTS

This work was supported by a New Horizons grant of the European Association for the Study of Diabetes (EASD) and an unrestricted grant of Nutricia Advanced Medical Nutricion. The sponsors had no involvement in the analysis of data and the writing of the manuscript.

REFERENCES

1 Goldin A, Beckman JA, Schmidt AM, Creager MA. Advanced glycation end products: sparking the development of diabetic vascular injury. Circulation 2006 August 8;114(6):597-605

2 Schleicher ED, Wagner E, Nerlich AG. Increased accumulation of the glycoxidation product N(epsilon)-(carboxymethyl)lysine in human tissues in diabetes and aging. J Clin Invest 1997 February 1;99(3):457-68

3 Baynes JW, Thorpe SR. Role of oxidative stress in diabetic complications: a new perspective on an old paradigm. Diabetes 1999 January;48(1):1-9

4 Hanssen NM, Beulens JW, van DS et al. Plasma advanced glycation end products are associated with incident cardiovascular events in individuals with type 2 diabetes: a case-cohort study with a median follow-up of 10 years (EPIC-NL). Diabetes 2015 January;64(1):257-65

5 Nerlich AG, Schleicher ED. N(epsilon)-(carboxymethyl)lysine in atherosclerotic vascular lesions as a marker for local oxidative stress. Atherosclerosis 1999 May;144(1):41-7

6 Wang Z, Jiang Y, Liu N et al. Advanced glycation end-product Nepsilon-carboxymethyl-Lysine accelerates progression of atherosclerotic calcification in diabetes. Atherosclerosis 2012 April;221(2):387-96

7 Del TS, Basta G. An update on advanced glycation endproducts and atherosclerosis. Biofactors 2012 July;38(4):266-74

8 Hanssen NM, Wouters K, Huijberts MS et al. Higher levels of advanced glycation endproducts in human carotid atherosclerotic plaques are associated with a rupture-prone phenotype. Eur Heart J 2014 May;35(17):1137-46

9 Baidoshvili A, Krijnen PA, Kupreishvili K et al. N(epsilon)-(carboxymethyl)lysine depositions in intramyocardial blood vessels in human and rat acute myocardial infarction: a predictor or reflection of infarction? Arterioscler Thromb Vasc Biol 2006 November;26(11):2497-503

10 Zipser BD, Johanson CE, Gonzalez L et al. Microvascular injury and blood-brain barrier leakage in Alzheimer's disease. Neurobiol Aging 2007 July;28(7):977-86

11 O'Rourke MF, Safar ME. Relationship between aortic stiffening and microvascular disease in brain and kidney: cause and logic of therapy. Hypertension 2005 July;46(1):200-4

12 Schalkwijk CG, Baidoshvili A, Stehouwer CD, van H, V, Niessen HW. Increased accumulation of the glycoxidation product Nepsilon-(carboxymethyl)lysine in hearts of diabetic patients: generation and characterisation of a monoclonal anti-CML antibody. Biochim Biophys Acta 2004 March 22;1636(2-3):82-9

13 van HL, Hamdani N, Handoko ML et al. Diastolic stiffness of the failing diabetic heart: importance of fibrosis, advanced glycation end products, and myocyte resting tension. Circulation 2008 January 1;117(1):43-51

14 Barberger-Gateau P, Letenneur L, Deschamps V, Peres K, Dartigues JF, Renaud S. Fish, meat, and risk of dementia: cohort study. BMJ 2002 October 26;325(7370):932-3

15 Solfrizzi V, Frisardi V, Capurso C et al. Dietary fatty acids in dementia and predementia syndromes: epidemiological evidence and possible underlying mechanisms. Ageing Res Rev 2010 April;9(2):184-99

16 Mozaffarian D, Wu JH. Omega-3 fatty acids and cardiovascular disease: effects on risk factors, molecular pathways, and clinical events. J Am Coll Cardiol 2011 November 8;58(20):2047-67

17 Kiecolt-Glaser JK, Epel ES, Belury MA et al. Omega-3 fatty acids, oxidative stress, and leukocyte telomere length: A randomized controlled trial. Brain Behav Immun 2013 February;28:16-24

18 Richard D, Kefi K, Barbe U, Bausero P, Visioli F. Polyunsaturated fatty acids as antioxidants. Pharmacol Res 2008 June;57(6):451-5

19 Micallef MA, Garg ML. Anti-inflammatory and cardioprotective effects of n-3 polyunsaturated fatty acids and plant sterols in hyperlipidemic individuals. Atherosclerosis 2009 June;204(2):476-82

20 Madsen T, Schmidt EB, Christensen JH. The effect of n-3 fatty acids on C-reactive protein levels in patients with chronic renal failure. J Ren Nutr 2007 July;17(4):258-63

21 Miki HC, Nagai R, Miyazaki K et al. Conversion of Amadori products of the Maillard reaction to N(epsilon)-(carboxymethyl)lysine by short-term heating: possible detection of artifacts by immunohistochemistry. Lab Invest 2002 June;82(6):795-808

22 van Deutekom AW, Niessen HW, Schalkwijk CG, Heine RJ, Simsek S. Increased Nepsilon-(carboxymethyl)-lysine levels in cerebral blood vessels of diabetic patients and in a (streptozotocin-treated) rat model of diabetes mellitus. Eur J Endocrinol 2008 May;158(5):655-60

23 Dyer DG, Dunn JA, Thorpe SR et al. Accumulation of Maillard reaction products in skin collagen in diabetes and aging. J Clin Invest 1993 June;91(6):2463-9

24 Verzijl N, DeGroot J, Oldehinkel E et al. Age-related accumulation of Maillard reaction products in human articular cartilage collagen. Biochem J 2000 September 1;350 Pt 2:381-7

25 Hu S, He W, Liu Z, Xu H, Ma G. The accumulation of the glycoxidation product N(epsilon)-carboxymethyllysine in cardiac tissues with age, diabetes mellitus and coronary heart disease. Tohoku J Exp Med 2013;230(1):25-32

26 Hagino N, Kobayashi S, Tsutsumi T et al. Vascular change of hippocampal capillary is associated with vascular change of retinal capillary in aging. Brain Res Bull 2004 February 15;62(6):537-47

27 Kobayashi S, Nomura M, Nishioka T et al. Overproduction of N(epsilon)-(carboxymethyl)lysine-induced neovascularization in cultured choroidal explant of aged rat. Biol Pharm Bull 2007 January;30(1):133-8

28 Wautier JL, Zoukourian C, Chappey O et al. Receptor-mediated endothelial cell dysfunction in diabetic vasculopathy. Soluble receptor for advanced glycation end products blocks hyperpermeability in diabetic rats. J Clin Invest 1996 January 1;97(1):238-43

29 Brownlee M. Negative consequences of glycation. Metabolism 2000 February;49(2 Suppl 1):9-13

30 Basta G, Schmidt AM, De CR. Advanced glycation end products and vascular inflammation: implications for accelerated atherosclerosis in diabetes. Cardiovasc Res 2004 September 1;63(4):582-92

31 Shiina T, Terano T, Saito J, Tamura Y, Yoshida S. Eicosapentaenoic acid and docosahexaenoic acid suppress the proliferation of vascular smooth muscle cells. Atherosclerosis 1993 December;104(1-2):95-103

32 Mizutani M, Asano M, Roy S et al. Omega-3 polyunsaturated fatty acids inhibit migration of human vascular smooth muscle cells in vitro. Life Sci 1997;61(19):L269-L274

33 Durrington PN, Bhatnagar D, Mackness MI et al. An omega-3 polyunsaturated fatty acid concentrate administered for one year decreased triglycerides in simvastatin treated patients with coronary heart disease and persisting hypertriglyceridaemia. Heart 2001 May;85(5):544-8

34 Burr ML, Fehily AM, Gilbert JF et al. Effects of changes in fat, fish, and fibre intakes on death and myocardial reinfarction: diet and reinfarction trial (DART). Lancet 1989 September 30;2(8666):757-61

35 McLennan PL, Bridle TM, Abeywardena MY, Charnock JS. Comparative efficacy of n-3 and n-6 polyunsaturated fatty acids in modulating ventricular fibrillation threshold in marmoset monkeys. Am J Clin Nutr 1993 November;58(5):666-9

36 Romieu I, Garcia-Esteban R, Sunyer J et al. The effect of supplementation with omega-3 polyunsaturated fatty acids on markers of oxidative stress in elderly exposed to PM(2.5). Environ Health Perspect 2008 September;116(9):1237-42

37 Lluis L, Taltavull N, Munoz-Cortes M et al. Protective effect of the omega-3 polyunsaturated fatty acids: Eicosapentaenoic acid/Docosahexaenoic acid 1:1 ratio on cardiovascular disease risk markers in rats. Lipids Health Dis 2013;12:140

38 Capo X, Martorell M, Sureda A, Llompart I, Tur JA, Pons A. Diet supplementation with DHA-enriched food in football players during training season enhances the mitochondrial antioxidant capabilities in blood mononuclear cells. Eur J Nutr 2015 February;54(1):35-49

39 Pamplona R, Dalfo E, Ayala V et al. Proteins in human brain cortex are modified by oxidation, glycoxidation, and lipoxidation. Effects of Alzheimer disease and identification of lipoxidation targets. J Biol Chem 2005 June 3;280(22):21522-30

40 Avramovic N, Dragutinovic V, Krstic D et al. The effects of omega 3 fatty acid supplementation on brain tissue oxidative status in aged wistar rats. Hippokratia 2012 July;16(3):241-5

41 Kromhout D, Yasuda S, Geleijnse JM, Shimokawa H. Fish oil and omega-3 fatty acids in cardiovascular disease: do they really work? Eur Heart J 2012 February;33(4):436-43

42 Molema G. Heterogeneity in endothelial responsiveness to cytokines, molecular causes, and pharmacological consequences. Semin Thromb Hemost 2010 April;36(3):246-64

43 Garlanda C, Dejana E. Heterogeneity of endothelial cells. Specific markers. Arterioscler Thromb Vasc Biol 1997 July;17(7):1193-202

44 Ritz K, Denswil NP, Stam OC, van Lieshout JJ, Daemen MJ. Cause and mechanisms of intracranial atherosclerosis. Circulation 2014 October 14;130(16):1407-14

3

Major orthopedic surgery significantly increases plaque area in atherosclerotic ApoE -/- mice

Wessel W. Fuijkschot; Martine C. Morrison; Rianne van der Linden; Paul A.J. Krijnen; Ilse P.A. Zethof; Lars F.H. Theyse; Robert Kleemann; Hans W.M. Niessen and Yvo M. Smulders

Atherosclerosis 2016;255:164-170

ABSTRACT

Objective: Observational studies show a peak incidence of cardiovascular events after major surgery. For example, the risk of myocardial infarction increases 25-fold early after hip replacement. The acuteness of this increased risk suggests abrupt enhancement in plaque vulnerability, which may be related to an acute increase of intra-plaque inflammation, thinning of the fibrous cap and/or necrotic core expansion. We hypothesized that acute systemic inflammation following major orthopedic surgery induces such changes.

Approach and results: Apo E-/- mice were fed a western diet for 10 weeks. Thereafter half the mice underwent mid-shaft femur osteotomy followed by realignment with an intramedullary K-wire, to mimic major orthopedic surgery. Mice were sacrificed 5 or 15 days post-surgery (n=22) or post-saline injection (n=13). Serum amyloid A (SAA) was measured as a marker of systemic inflammation. Paraffin embedded slides of the aortic root were stained to measure total plaque area and to quantify fibrosis, calcification, necrotic core, and inflammatory cells. Surgery mice showed a pronounced elevation of SAA and developed increased plaque and necrotic core area already at 5 days, which reached significance at 15 days ($p=0.019$; $p=0.004$ for plaque and necrotic core, respectively). Macrophage and lymphocyte density significantly decreased in the surgery group compared to the control group at t=15 days ($p=0.037$; $p=0.024$, respectively). The density of neutrophils and mast cells remained unchanged.

Conclusions: Major orthopedic surgery in Apo E-/- mice triggers a systemic inflammatory response. Atherosclerotic plaque area is enlarged after surgery mainly due to an increase of the necrotic core. The role of intra-plaque inflammation in this response to surgical injury remains to be fully elucidated.

INTRODUCTION

Observational epidemiological studies have confirmed what experienced clinicians suspected for many years: cardiovascular events can be triggered by a variety of common non-cardiovascular clinical conditions, particularly those that are associated with systemic inflammation[1-3]. One of the best documented examples of non-infectious systemic inflammation causing an acute increase in cardiovascular risk is major surgery. A recent study indicated that the risk of myocardial infarction in patients undergoing total hip or knee replacement is increased by no less than 25-fold, mainly during the first days to weeks post-surgery[2]. This phenomenon is hardly investigated and the mechanisms which underlie this postoperative risk remain elusive.

The acuteness of the increased postoperative cardiovascular risk suggests an effect on atherosclerotic plaque stability[4]. Several studies indeed show that at least half of the cases of myocardial infarction following non-cardiac surgery originate from rupture of unstable plaques[5-7]. Why plaques could become more prone to rupture briefly after surgery is unclear. Plaque instability is not only related to factors such as fibrous cap strength and intra-plaque hemorrhage, but also to the necrotic core area which, in turn, are all influenced by intra-plaque inflammation[8-11].

Plaque area was shown to increase in mice after a single injection of serum amyloid A peptide, a marker and mediator of inflammation[12]. A recent study addressing the combined effects of major blood loss and surgery reported increased plaque size growth as well as increased plaque vulnerability already after 72 hours[7]. Major orthopedic surgery is known to cause massive systemic inflammation[13]. We therefore hypothesized that acute systemic inflammation caused by major orthopedic surgery could rapidly enhance plaque vulnerability by means of increased intra-plaque inflammation, fibrous cap thinning and/or necrotic core expansion, and we addressed this hypothesis in atherosclerosis-prone Apo E-/- mice.

MATERIALS AND METHODS

Mouse model

Apo E -/- mice (9-10 weeks old) were obtained from Charles River Laboratories (Calco Como,Italy) and were housed in specific pathogen-free rooms, on a 12-h light–dark cycle. All mice were fed a high-fat diet (0.15 % cholesterol) (4022.83, AB diets, Woerden, the Netherlands) for 10 weeks after which the surgery group underwent a mid-shaft femur osteotomy followed by realignment with an intramedullary K-wire, to

mimic major orthopedic surgery. Under general anesthesia (2% isoflurane) and analgesia (0.1 mg/kg buprenorfine), the femur was accessed via a lateral skin incision of the greater trochanter to just proximal of the knee joint. The femur was approached using microsurgical scissors and forceps. With a dental mini-cutter, a mid-shaft osteotomy was performed. After that a stainless steel 0.6 mm K-wire (DePuy Synthes, Amersfoort, The Netherlands) was retrogradely introduced into the medulla of the femur until it exited medial and proximal of the greater trochanter. This was done using an electrical rotary system (Model 3000, Dremel, Breda). The osteomy was reduced and the osteotomy was stabilized by normogradely introducing the K-wire into the medulla of the distal femur until seated in the distal metaphysis. The K-wire was cut flush with the trochanter, where after the wound was closed by interrupted sutures (Monocryl 5-0 FS-2, Eticon) for both the femoral fascia and skin. During the operation bleeding was kept to a minimum by using bipolar radiofrequency micro-forceps (Pfizer, Valleylab Force 30). Blood was sampled after a 4-hour fasting period at several time points surrounding surgery/control (t=-1 day, 1 day, 5 days and 15 days). Mice in both operation (n=22) and control group (n=13) were sacrificed 5 or 15 days post-surgery respectively post-saline injection. All procedures were approved by the Animal use and care Committee at the VU University Medical Centre of Amsterdam.

Analysis of systemic inflammation and serum lipids

Levels of serum amyloid A (SAA), soluble VCAM-1 (CD106) and soluble E-selectin (CD62E) were measured by ELISA (Life Technologies, Bleiswijk, the Netherlands for SAA and R&D Systems, Abingdon, UK, for VCAM-1 and E-selectin). Total serum cholesterol and triglyceride levels were measured in serum by commercially available enzymatic assays (cholesterol CHOD-PAP 11491458 and triglycerides GPO-PAP 11488872, Roche, Woerden, the Netherlands). For determination of the lipid profile, pooled plasma per group was fractionated using an ÅKTA fast protein liquid chromatography system (Pharmacia, Roosendaal, the Netherlands). Fractions were collected and assayed for total cholesterol using an enzymatic assay cholesterol CHOD-PAP 11491458 (Roche) and analysed as reported[14].

(Immuno)histochemistry and morphometry

Dissected hearts including the aortic roots were embedded in paraffin after overnight fixation (4 % formalin) for analysis of atherosclerosis. Serial cross-sections (4 µm) directly distal to the valve area of the aortic root were stained with Alcian Blue (indicative of glycosaminoglycans), Elastica van Gieson, Von Kossa and MAC-3, scanned with a PathScan Enabler IV, after which the mean surface area of plaque and the concordant area of fibrosis (EVG), calcification (Von Kossa) and macrophage area (MAC-3) was analysed blindly from each specimen using QuickPHOTO MICRO 3.0 software or in the case of the MAC-3 staining and the fibrous cap thickness[15] with ImageJ software.

The necrotic core area was calculated by subtracting the area of fibrosis, calcification and macrophages from the total plaque area. For immunohistochemical analysis, serial cross-sections were dewaxed, rehydrated and incubated in methanol/H2O2 (0.3%) for 30 minutes to block endogenous peroxidases. Antigen retrieval was performed using pepsin for 25 minutes at 37 °C (Ly-6G and CD206), boiling in Tris-EDTA buffer, pH 9.0 (Caspase-3) or in citrate buffer, pH 6.0, for 15 minutes at 100 °C using a microwave (MAC-3 and iNOS). Sections were incubated with normal rabbit serum (1:50 dilution, DAKO, X0902) for 10 minutes at room temperature (RT) and subsequently with the primary antibody using rat-anti-mouse-MAC-3 antibody, detecting macrophages (1:30 dilution, BD Pharmingen, clone M3/84, cat. 553322, overnight, RT) or rat-anti-mouse-Ly6G antibody (detecting neutrophilic granulocytes) (1:200 dilution, BD Pharmingen, clone 1Ab, cat. 551459, 1 hour, RT) as appropriate. Thereafter, sections were incubated with biotinylated rabbit-anti-rat (1:300 dilution, DAKO, E0468, 30 minutes)/ Streptavidin-HRP (1:100 dilution, DAKO, P0397, 1 hour). For iNOS staining (to detect type 1 macrophages) the primary antibody polyclonal rabbit-anti-iNOS (1:200 dilution, Abcam, Ab15323, 1 hour, RT) was used and for the Caspase-3 (apoptosis marker) the primary antibody polyclonal Rabbit-anti-Caspase-3 (1:500 dilution, cell signaling technology, cat. 9661-L, 1 hour, RT) was used. Both were followed by incubation with HRP labeled anti-rabbit (100 µl undiluted, DAKO, K4003) for 30 minutes. For the CD206 staining (detecting type 2 macrophages) the primary antibody polyclonal Rabbit-anti-mannose receptor CD206 (1:1000 dilution, Abcam, Ab64693, 1 hour, RT) was used, followed by a swine anti-rabbit HRP secondary antibody (1:100 dilution, DAKO P0217, 30 minutes, RT). For CD45 staining (detecting lymphocytes), antigen retrieval was performed using citrate buffer, pH 6.0, for 15 minutes at 100ºC using a microwave. Sections were incubated in water (97°C) for 30 minutes and subsequently incubated in methanol/H2O2 (0.3%) for 30 minutes. Afterwards, sections were incubated with rat-anti-mouse-CD45 antibody (1:50 dilution, BD Pharmingen, cat. 550539, overnight, 4°C), rinsed in PBS, incubated with rabbit-anti-rat-HRP (1:50 dilution, DAKO, P0450) for 30 minutes. All staining's were visualized with 3,3-diamino-benzidine-tetrahydrochloride/H2O2(DAB, 0.1 mg/ml, 0.02% H2O2) for 10 minutes and counterstained with haematoxylin. Mast cells were stained with Toluidine Blue 1%. MAC-3 area was quantified as percentage MAC-3 positive staining of the total plaque area, using an automated macro in ImageJ software. Numbers of Ly-6G and CD45 positive cells were manually quantified per surface area of the atherosclerotic plaque as cells/µm2. Immunoscoring was performed by R.L and W.W.F. and agreement was reached between both observers.

STATISTICS

Statistical analysis was performed with SPSS (20.0 for Windows, SPSS Inc.). To test for differences in plaque area, necrotic core area and inflammatory cells between groups, an independent sample t-test was used when the data were normally distributed, or a Mann–Whitney U test if not. All data are presented as median and interquartile range. Results were considered statistically significant if the two-sided p-value was <0.05.

RESULTS

Surgery causes acute systemic inflammation

To determine whether major orthopedic surgery was indeed accompanied by an acute systemic inflammatory response we measured serum SAA levels at different time points (t=-1 day, 4 hours, 1 day, 5 days and, in the late-sacrifice group, after 15 days) (Fig. 1A). SAA levels had increased 4 hours after surgery, increased by almost 100-fold after 24 hours, and returned to baseline levels within 5 days. In contrast, SAA values in the control group remained low and stable. Endothelial inflammation markers (VCAM-1 and E-selectin) did not increase in response to trauma (Fig. 1B and 1C).

Surgery transiently decreases body weight and alters lipid profile

Mice in the surgery group had weight loss (6.6%) at 5 days compared to baseline, whereas control mice gained weight (5.8%). Serum cholesterol and triglyceride levels were measured at t=-1 day, 1 day, 5 days and, in the late-sacrifice group, after 15 days. We observed a transient lipid-lowering effect of surgery. This effect was relatively small for cholesterol (Fig. 1D), but more pronounced for triglycerides (Fig. 1E). The lipoprotein profile for cholesterol distribution in VLDL, LDL and HDL-sized particles showed a slight reduction in VLDL which was paralleled by an equally small increase in LDL from t=5 days onward (Fig. 1F-1I).

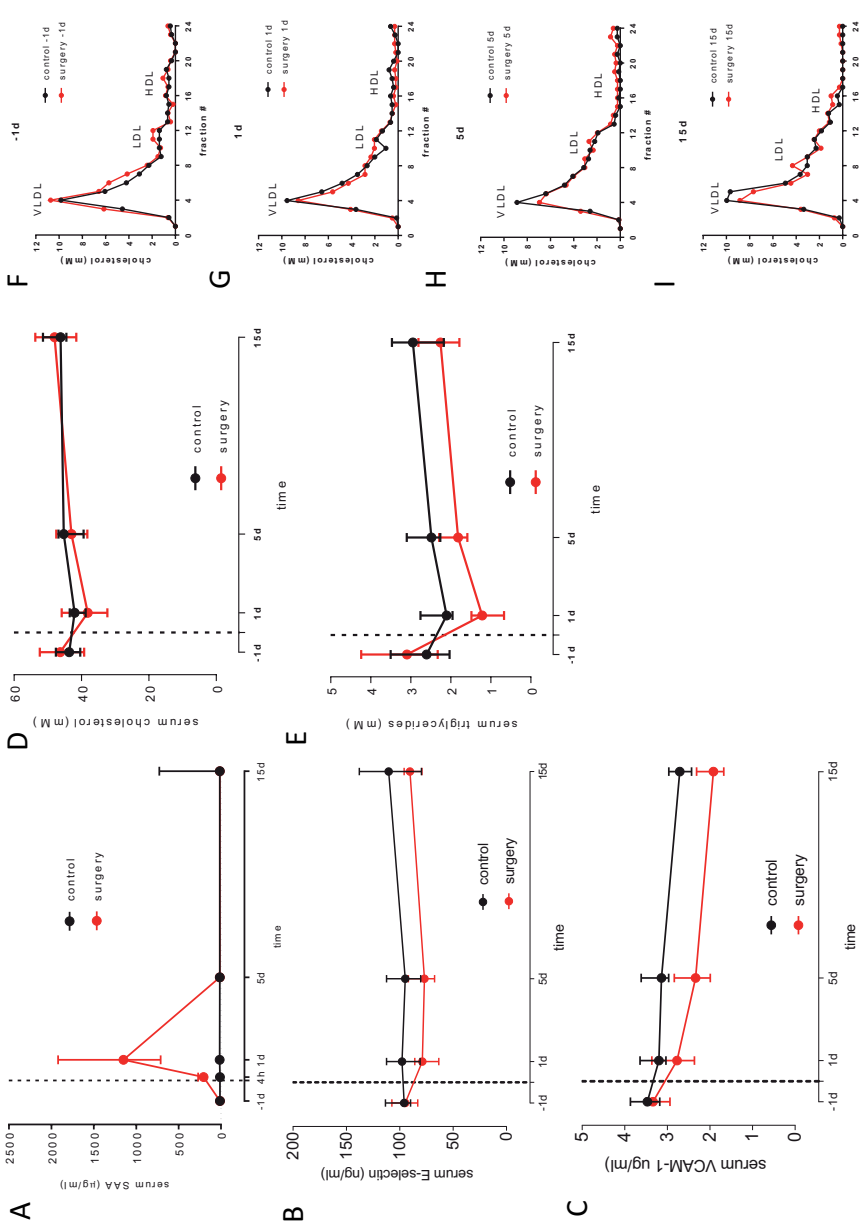

Figure 1 Major orthopedic surgery transiently increases serum SAA levels and decreases serum lipids

The vertical dotted line represents the timing of surgery. Serum levels of **A:** Serum amyloid A (SAA) (µg/ml) **B:** E-selectine (ng/ml) **C:** vascular cell adhesion molecule 1 (VCAM-1) (µg/m) **D:** cholesterol (mM) **E:** triglycerides and **F-H:** lipoprotein profile for cholesterol distribution in Very-low-density lipoprotein (VLDL), High-density lipoprotein (LDL) and Low-density lipoprotein (HDL)-sized particles at baseline and at different time points after surgery (n=22) or control (n=13).

Surgery does not increase the content of inflammatory cells within atherosclerotic lesions

We observed a significant reduction (p=0.037) of the macrophage area relative to the total atherosclerotic plaque area between the surgery and control group at t=15 days (Fig. 2B). Subtyping of typical type 1 macrophages (M1 - iNOS positive area) and type 2 macrophages (M2 - CD206 positive area) relative to total macrophage area (MAC-3 positive area) was performed (Fig. 2D and 2F). At t=5 days, a significantly lower M1 fraction was observed in the surgery group 44% [33-54] versus 55% [47-87] in the control group; p=0.028) which increases significantly to 80% [66-121] (p=0.007) at 15 days. The relative density of M2 macrophages was not affected significantly. No significant differences were found between surgery and control mice in the number of neutrophilic granulocytes (Ly-6g) and mast cells (toluidine blue) (Fig. 2H and 2J). We did however observe a significant reduction in lymphocyte density (Fig. 2L) 15 days post-surgery as compared to the control group (p=0.024).

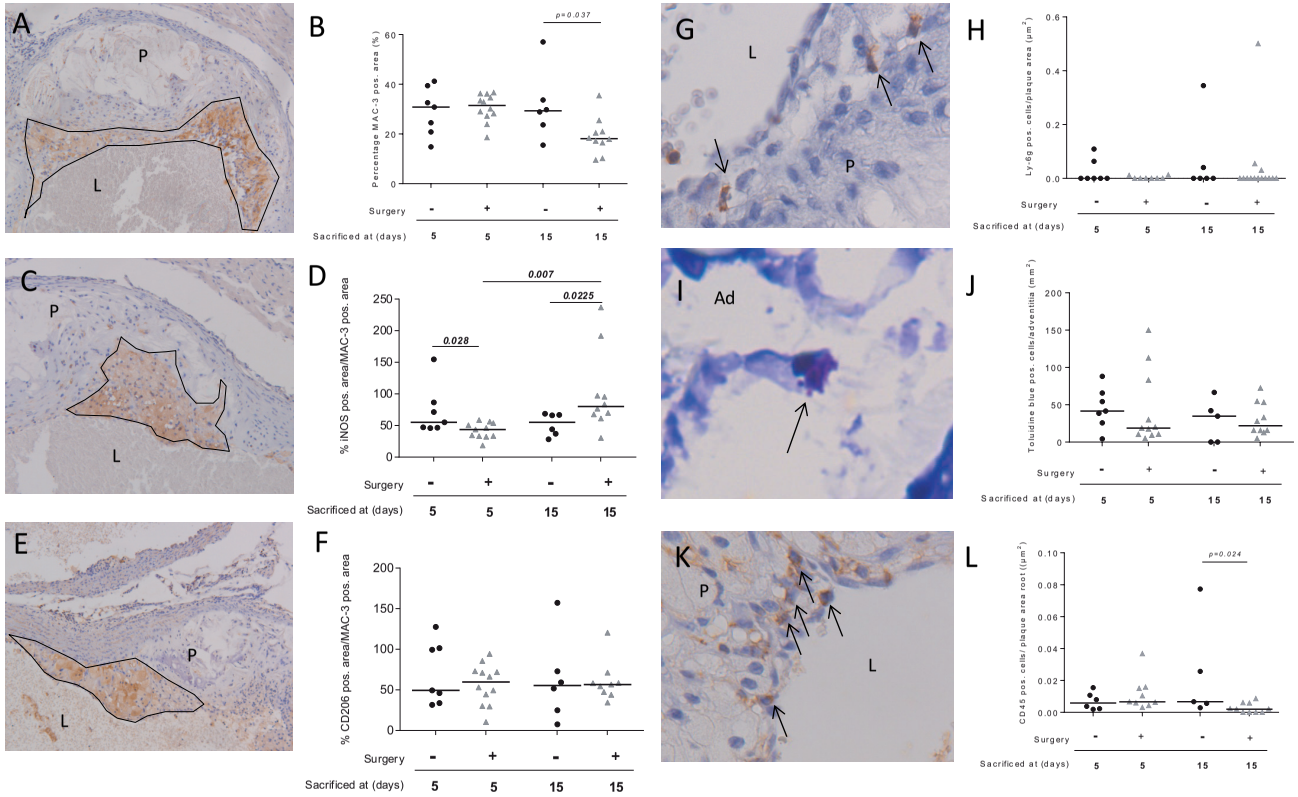

Figure 2 MAC-3 positive area divided by total plaque area (%) at t=15 days post-surgery decreases

A: MAC-3 positive area (encircled) in the plaque **B:** divided by total plaque area (%) **C:** iNOS positive area (encircled) in the plaque **D:** divided by MAC-3 positive area (%). **E:** CD206 positive area (encircled) in the plaque **F:** divided by MAC-3 positive area (%). **G:** Ly-6g positive cells in the plaque **H:** divided by the total plaque area (cells/µm^2). **I:** Toluidine blue stained cells in the adventitia **J:** divided by the area of adventitia (cells/mm^2). **K:** CD45 positive cells in the plaque **L:** divided by the total plaque area (cells/µm^2). Arrows point out positive cells. P=plaque; L=lumen; Ad=adventitia. Magnification of A,C,E 10x; magnification G and K 40x; magnification I 50x. All expressed the aortic root of mice sacrificed at t=5 days post-surgery (n=12) or control (n=7) or t=15 days post-surgery (n=10) or control (n=6).j

Atherosclerotic plaque and necrotic core area increase after surgery

Aortic root sections of all experimental groups showed advanced atherosclerotic lesions infiltrated by macrophages and lymphocytes, with a thin fibrous cap (Fig. 3A-3D). To assess the effect of surgery we measured total plaque area in the root, and evaluated the relative contribution of different plaque components. At t=5 days, a non-significant 5.5% higher plaque area was observed in the surgery group (481 x 103 μm^2 [387-558] versus 456 x 103 μm^2 [394-491] in the control group; p=0.297). This difference became more pronounced and statistically significant at t=15 days; (519 x 103 μm^2 [485-634] in operated mice versus 387 x 103 μm^2 [331-464] in control mice, p=0.019; Fig. 3E). This plaque enlargement was mainly attributable to a 160% increase in the necrotic core area (257 x 103 μm^2 [151-315] in operated mice vs. 99.0 x 103 μm^2 [71.2-155] in control mice, p=0.004; Fig. 3F). The area of the other plaque histological characteristics (fibrosis, macrophages, calcification and apoptosis) did not significantly contribute to the increase in plaque area (Fig. 4). Also, we found no evidence of fibrous cap thinning at t=5 days (28.7 [22.4-42.3] µm in operated mice versus 19.8 [17.5-37.2] µm in control mice, p=0.3), nor at t=15 days (36.7 [29.6-45.2] µm in operated mice versus 24.5 [18.7-42.3] µm in control mice, p=0.6). In addition, we assessed old intra-plaque hemorrhage but only found small non-significant areas of Fe-positivity that had only a very minor contribution to the total area and that did not differ between groups (data not shown). Finally, in the roots of all mice (surgery and control) Alcian Blue positive staining was observed both in the necrotic core area and in the other regions of the plaque, with no differences between the groups.

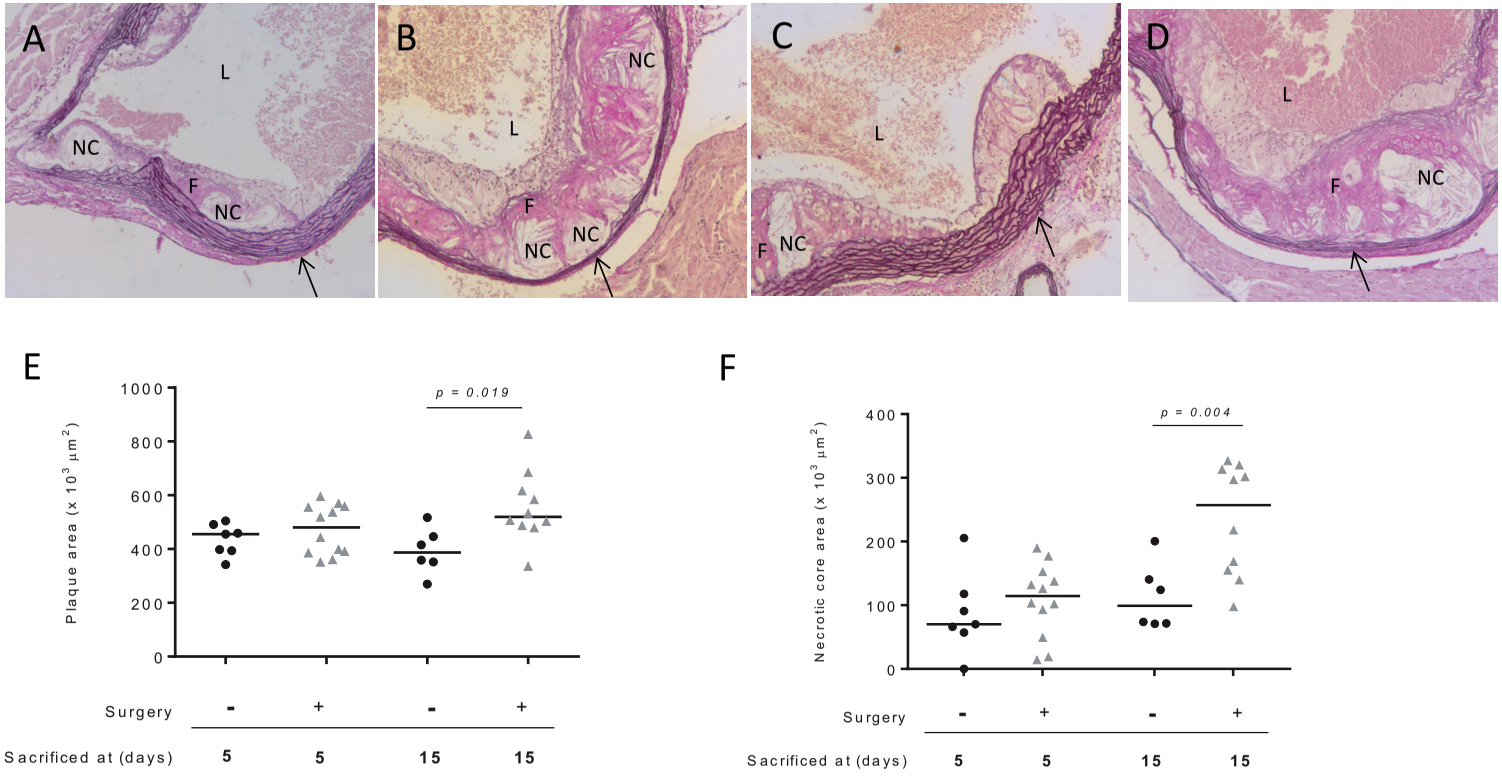

Figure 3 Major orthopedic surgery increases atherosclerotic plaque and necrotic core area

A: Representative images of EVG stained cross-sections of the aortic root after 5 days without surgery, **B:** 5 days with surgery. **C:** 15 days without surgery and **D:** 15 days with surgery. All showing 10x magnified advanced atherosclerotic lesions (encircled) with necrotic cores (NC) and areas of fibrosis (F). The arrows indicate the media, the lumen (L) is largely composed of erythrocytes. **E:** Plaque area (x103 µm^2) and **F:** necrotic core area (x103 µm^2) at the aortic root of mice sacrificed at t=5 days post-surgery (n=12) or control (n=7) or t=15 days post-surgery (n=10) or control (n=6).

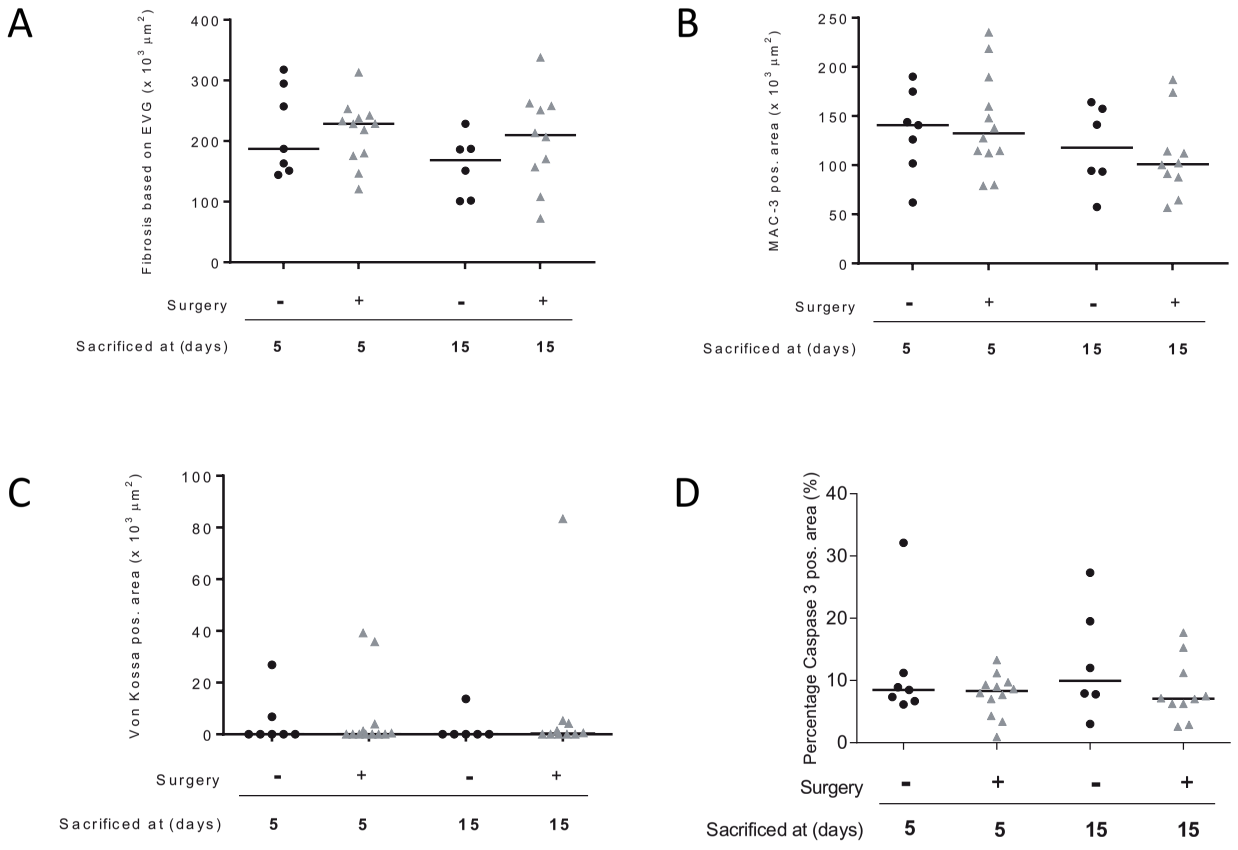

Figure 4 Major orthopedic surgery shows no significant effect on area of fibrosis, macrophages and calcification

Plaque area (x 103 µm^2) of fibrosis based on **A:** an EVG staining, **B:** macrophages based on a MAC-3 staining, **C:** calcification based on a Von Kossa staining and **D:** apoptosis based on a Caspase-3 staining at the aortic root of mice sacrificed at t=5 days post-surgery (n=12) or control (n=7) or t=15 days post-surgery (n=10) or control (n=6) (all p-values > 0.05).

DISCUSSION

Major orthopedic surgery in Apo E-/- mice causes acute systemic inflammation. At 15 days post-surgery we observed a significant increase of plaque area, mainly due to necrotic core enlargement. Plaque necrosis is a characteristic hallmark of atherosclerotic lesions that cause acute atherothrombotic vascular disease[9-11]. Our finding of a post-surgery increase of necrotic core area may reflect increased plaque vulnerability and could, at least partly, explain the increased incidence of cardiovascular events after major orthopedic surgery.

The surgical procedure caused a marked acute systemic inflammatory response as demonstrated by a rapid increase in SAA, a relatively stable inflammation marker that integrates the signals of proatherogenic cytokines (IL1, TNFα, IL6), many of which may have contributed to the effect on the atherosclerotic leasion[16, 17]. Several studies suggest that SAA itself participates in the pathogenesis of atherosclerosis and a recent study shows that it may contribute to plaque vulnerability[18]. For instance, SAA induces TGF-β, increases vascular biglycan content, and increases LDL retention[19]. SAA also stimulates NF-κB activation and induces the expression of pro-atherosclerotic factors, such as ICAM-1, MCP-1, MMP-9 and tissue factor in macrophages[20]. Lastly, SAA displaces apoA-I from the surface of the HDL particle, thus generating free apoA-I, which is cleared faster by the kidney, thus potentially affecting the anti-atherogenic effect of HDL[21]. In addition to the effects on SAA, we observed a slight effect on circulating lipoproteins (i.e. decrease in VLDL and increase in LDL) in the orthopedic surgery group. Although the shift toward more atherogenic particles is relatively small, it may have contributed to the development of atherosclerosis in the orthopedic surgery group.

We did not find indications of fibrous cap thinning after orthopedic surgery, which besides necrotic core expansion is another hallmark of vulnerable, inflammatory plaque[8, 22]. We cannot exclude fibrous cap thinning because it is known to be very heterogeneously distributed, varying between and within lesions[23]. In parallel, we did not find an increased density of inflammatory cells after orthopedic surgery. This may have been caused by the fact that we examined plaques after 5 and 15 days. We cannot exclude inflammatory cell infiltration taking place before these time points and that activated macrophages in particular had already 'dissolved' at 5 days, contributing to the necrotic core. Indeed, death of lesional macrophages promotes the formation of plaque necrosis [9], and could thus be compatible with the decreased plaque macrophage content we observed at later time points. Similarly, activation of lymphocytes may cause loss of CD45-positive epitopes and cells can become undetectable by CD45-staining. It thus

remains possible that surgery-induced intra-plaque inflammation due to infiltration of immune cells contributed to the observed increase in the necrotic core area (and hence total lesion area).

There is a growing understanding that the balance between pro- and anti-inflammatory macrophages in plaque is dynamic[24]. We found an increase in the fraction of M1 pro-inflammatory macrophages at 15 days, supporting a pro-inflammatory postoperative plaque milieu.

We have found no differences between the different groups and time points for Caspase-3, an apoptosis marker, and therefore we cannot conclude that apoptosis is a major driver of the necrotic core expansion after surgery. Of note, however, these test also do not exclude a role for apoptosis. Caspase-3 staining is a temporary phenomenon in apoptosis and after some time, Caspase-3 staining in the necrotic core could be lost. This also emphasizes the need for future studies addressing earlier time points and more in-depth characterization of biomarker profile, and inflammatory cell activity in similar experimental designs.

Several related experimental studies merit discussion. Recently, a study in Apo E-/- mice addressed the combined effects of major blood loss and surgery, and reported increased plaque size after 72 hours, along with signs of plaque vulnerability [7]. However, this effect appeared to be mainly due to excessive blood loss (20% of body weight; which is substantially more than in our model), rather than surgery itself. As in our study, the density of intra-plaque macrophages did not differ, but other inflammatory cell types were not quantified. A few experimental studies addressed the effects of acute systemic inflammation on atherosclerosis. A recent murine model of intra-abdominal sepsis suggested that atherosclerotic plaque area was enhanced by sustained systemic, endothelial and intimal inflammation, and was not explained by infection itself[25]. More specifically, an increase in intra-plaque macrophages was observed 5 months after the induction of sepsis via cecal ligation and puncture. This coincides with a sustained elevated level of IL6, suggesting that this model mimics a chronic inflammatory state, in contrast to our model of transient acute inflammation. No data on macrophage density at earlier time points (nor other inflammatory cell types) were reported. Another study in Apo E-/- mice showed that influenza virus infection caused subendothelial infiltration of a heterogeneous population of cells[26]. These cells were however not quantified per type and plaque area was not assessed. Lastly a study again in Apo E-/- mice demonstrated that the systemic inflammatory response to myocardial infarction aggravates chronic atherosclerosis[22]. Together with the results described herein, these studies support an important role for systemic inflammation in plaque destabilization and might thereby contribute to increased risk of cardiovascular events.

Limitations

Our goal was to evaluate effects of major (orthopedic) surgery on atherosclerotic plaque. Although we found plaques changes congruent with increased event risk, the study wasn't designed to clarify responsible mechanism(s). Our data are compatible with a role for surgery-induced inflammation, but this requires more in-depth studies. In addition, other, non- or indirect inflammatory effects of surgery could be further explored. For instance, hemodynamic disturbances[27], sympathetic nerve system activation[28] or enhanced platelet activity[29] are potential contributors to atherosclerotic lesion development and increased cardiovascular risk. Furthermore it would be interesting to test our findings in advanced mouse models to study actual plaque complications rather than atherosclerotic plaque development alone[30, 31].

CONCLUSION

Major surgery can cause a strong systemic inflammatory response and lead to an increase in plaque and necrotic core area, contributing to plaque vulnerability. These findings may help explain the high incidence of cardiovascular events following major surgery and, in a broader perspective, other clinical conditions of acute systemic inflammation.

REFERENCES

1 Smeeth L, Thomas SL, Hall AJ, Hubbard R, Farrington P, Vallance P. Risk of myocardial infarction and stroke after acute infection or vaccination. N Engl J Med 2004 December 16;351(25):2611-8

2 Lalmohamed A, Vestergaard P, Klop C et al. Timing of acute myocardial infarction in patients undergoing total hip or knee replacement: a nationwide cohort study. Arch Intern Med 2012 September 10;172(16):1229-35

3 Corrales-Medina VF, Musher DM, Wells GA, Chirinos JA, Chen L, Fine MJ. Cardiac complications in patients with community-acquired pneumonia: incidence, timing, risk factors, and association with short-term mortality. Circulation 2012 February 14;125(6):773-81

4 Cohen MC, Aretz TH. Histological analysis of coronary artery lesions in fatal postoperative myocardial infarction. Cardiovasc Pathol 1999 May;8(3):133-9

5 Hanson I, Kahn J, Dixon S, Goldstein J. Angiographic and clinical characteristics of type 1 versus type 2 perioperative myocardial infarction. Catheter Cardiovasc Interv 2013 October 1;82(4):622-8

6 Gualandro DM, Campos CA, Calderaro D et al. Coronary plaque rupture in patients with myocardial infarction after noncardiac surgery: frequent and dangerous. Atherosclerosis 2012 May;222(1):191-5

7 Janssen H, Wagner CS, Demmer P et al. Acute perioperative stress-induced increase of plaque volume and vulnerability in apolipoprotein E-deficient mice is amenable to statin treatment and IL-6-inhibition. Dis Model Mech 2015 June 18

8 Libby P. Inflammation in atherosclerosis. Nature 2002 December 19;420(6917):868-74

9 Virmani R, Burke AP, Kolodgie FD, Farb A. Vulnerable plaque: the pathology of unstable coronary lesions. J Interv Cardiol 2002 December;15(6):439-46

10 Virmani R, Burke AP, Farb A, Kolodgie FD. Pathology of the vulnerable plaque. J Am Coll Cardiol 2006 April 18;47(8 Suppl):C13-C18

11 Santos-Gallego CG, Picatoste B, Badimon JJ. Pathophysiology of acute coronary syndrome. Curr Atheroscler Rep 2014 April;16(4):401

12 Thompson JC, Jayne C, Thompson J et al. A brief elevation of serum amyloid A is sufficient to increase atherosclerosis. J Lipid Res 2015 February;56(2):286-93

13 Reid D, Toole BJ, Knox S et al. The relation between acute changes in the systemic inflammatory response and plasma 25-hydroxyvitamin D concentrations after elective knee arthroplasty. Am J Clin Nutr 2011 May;93(5):1006-11

14 Morrison M, van der Heijden R, Heeringa P et al. Epicatechin attenuates atherosclerosis and exerts anti-inflammatory effects on diet-induced human-CRP and NFkappaB in vivo. Atherosclerosis 2014 March;233(1):149-56

15 Seimon TA, Wang Y, Han S et al. Macrophage deficiency of p38alpha MAPK promotes apoptosis and plaque necrosis in advanced atherosclerotic lesions in mice. J Clin Invest 2009 April;119(4):886-98

16 Kleemann R, Zadelaar S, Kooistra T. Cytokines and atherosclerosis: a comprehensive review of studies in mice. Cardiovasc Res 2008 August 1;79(3):360-76

17 Zhang N, Ahsan MH, Purchio AF, West DB. Serum amyloid A-luciferase transgenic mice: response to sepsis, acute arthritis, and contact hypersensitivity and the effects of proteasome inhibition. J Immunol 2005 June 15;174(12):8125-34

18 King VL, Thompson J, Tannock LR. Serum amyloid A in atherosclerosis. Curr Opin Lipidol 2011 August;22(4):302-7

19 Thompson JC, Jayne C, Thompson J et al. A brief elevation of serum amyloid A is sufficient to increase atherosclerosis. J Lipid Res 2014 November 26

20 Tan SZ, Ooi DS, Shen HM, Heng CK. The atherogenic effects of serum amyloid A are potentially mediated via inflammation and apoptosis. J Atheroscler Thromb 2014;21(8):854-67

21 Santos-Gallego CG, Badimon JJ, Rosenson RS. Beginning to understand high-density lipoproteins. Endocrinol Metab Clin North Am 2014 December;43(4):913-47

22 Dutta P, Courties G, Wei Y et al. Myocardial infarction accelerates atherosclerosis. Nature 2012 July 19;487(7407):325-9

23 van Dijk RA, Virmani R, von der Thusen JH, Schaapherder AF, Lindeman JH. The natural history of aortic atherosclerosis: a systematic histopathological evaluation of the peri-renal region. Atherosclerosis 2010 May;210(1):100-6

24 Moore KJ, Sheedy FJ, Fisher EA. Macrophages in atherosclerosis: a dynamic balance. Nat Rev Immunol 2013 October;13(10):709-21

25 Kaynar AM, Yende S, Zhu L et al. Effects of intra-abdominal sepsis on atherosclerosis in mice. Crit Care 2014;18(5):469

26 Naghavi M, Wyde P, Litovsky S et al. Influenza infection exerts prominent inflammatory and thrombotic effects on the atherosclerotic plaques of apolipoprotein E-deficient mice. Circulation 2003 February 11;107(5):762-8

27 Landesberg G, Beattie WS, Mosseri M, Jaffe AS, Alpert JS. Perioperative myocardial infarction. Circulation 2009 June 9;119(22):2936-44

28 Dutta P, Courties G, Wei Y et al. Myocardial infarction accelerates atherosclerosis. Nature 2012 July 19;487(7407):325-9

29 Santos-Gallego CG, Badimon JJ. The sum of two evils: pneumonia and myocardial infarction: is platelet activation the missing link? J Am Coll Cardiol 2014 November 4;64(18):1926-8

30 Chen YC, Bui AV, Diesch J et al. A novel mouse model of atherosclerotic plaque instability for drug testing and mechanistic/therapeutic discoveries using gene and microRNA expression profiling. Circ Res 2013 July 19;113(3):252-65

31 Van der Donckt C, Van Herck JL, Schrijvers DM et al. Elastin fragmentation in atherosclerotic mice leads to intraplaque neovascularization, plaque rupture, myocardial infarction, stroke, and sudden death. Eur Heart J 2015 May 1;36(17):1049-58

4

LPS-induced systemic inflammation does not alter atherosclerotic plaque area or inflammation in ApoE3*Leiden mice in the early phase up to 15 days

Wessel W. Fuijkschot; Martine C. Morrison; Ilse P.A. Zethof; Paul A.J. Krijnen; Robert Kleemann; Hans W.M. Niessen and Yvo M. Smulders

Accepted for publication in Shock

ABSTRACT

Background and aims: Observational studies show a peak incidence in cardiovascular events during and early after clinical conditions associated with substantial systemic inflammation, such as pneumonia. The acuteness of this increased risk suggests rapid plaque destabilization and associated intra-plaque inflammation. We evaluated whether LPS-evoked acute systemic inflammation would induce such detrimental vascular changes in murine aortas with manifest atherosclerotic lesions.

Methods and results: ApoE3*Leiden mice were fed a high cholesterol diet for 20 weeks to establish atherosclerosis. Thereafter, mice received a single intraperitoneal injection with lipopolysaccharides (LPS) to induce systemic inflammation, or saline for control. Mice were sacrificed 2 or 15 days post-LPS injection (n=17) or post-saline injection (n=13). Serum amyloid A (SAA), a sensitive marker of systemic inflammation, increased 250-fold in LPS-treated mice. Aortic root plaques were assessed for total plaque area, plaque severity and inflammatory cell content. No significant differences in total surface area of atherosclerotic plaque were found between control and LPS groups sacrificed after 2 days (resp. 0.409±0.228 x 105 μm^2 vs. 0.285±0.169 x 105 μm^2) (p=0.31), and 15 days (resp. 0.950±0.938 x 105 μm^2 vs. 0.612±0.413 x 105 μm^2) (p=0.80). Furthermore, plaque type and number of lesions were unaltered and intra-plaque density of macrophages and lymphocytes were comparable in both groups.

Conclusions: Intraperitoneal LPS injection in ApoE3*Leiden mice triggers a profound systemic inflammatory response, but does not increase atherosclerotic plaque area or inflammatory cell density. This model of LPS-induced inflammation in atherosclerosis-prone mice argues against intra-plaque alterations as an explanation for acute inflammation-induced cardiovascular event risk.

INTRODUCTION

Observational epidemiological studies have shown that cardiovascular events can be triggered by a variety of common non-cardiovascular clinical conditions, particularly those that are associated with systemic inflammation[1-4]. The best documented example of such conditions is systemic infection. For instance, lower respiratory tract infection raises the early (2-14 days after onset of symptoms)[1, 2] risk of myocardial infarction by approximately fivefold1, and the risk of stroke by eightfold[1-3]. This phenomenon of cardiovascular events occurring in patients with infection is clearly important, but the causal mechanisms remain unclear. Hemodynamic and hemostatic abnormalities have been implicated, but their exact role is unknown.

Conceivably, acute inflammation may also affect atherosclerotic plaque stability, with subsequent risk of plaque rupture[5-7]. It is, however, unclear whether acute systemic inflammation affects plaque morphology and composition and induces a more unstable phenotype. It is well-established that plaque instability is largely determined by intra-plaque inflammation[8-10]. Several studies support the concept of systemic inflammation inducing detrimental intra-plaque changes. Plaque area increased in Apo E-/- mice 16 weeks after a single injection of serum amyloid A peptide (SAA), a marker and mediator of inflammation[11]. In addition, we recently described that major orthopedic surgery in Apo E-/- mice causes marked systemic inflammation, which was accompanied by increased plaque necrosis area only 15 days after surgery. Furthermore, a recent murine model of intra-abdominal sepsis induced by colon ligature and puncture (CLP) has suggested late (3-5 months after onset) effects on atherosclerotic plaque stability long after the initial infection has ceased[12]. Whether acute systemic inflammation induces pro-inflammatory changes in atherosclerotic plaques in a similar time frame as the acute cardiovascular event risk in humans with infection has, however, not been studied to date. We hypothesized that LPS-evoked acute systemic inflammation would enhance plaque area and intra-plaque inflammation during a pro-inflammatory period of 15 days using ApoE*3Leiden mice with established lesions.

METHODS

Mouse model

Female ApoE*3Leiden transgenic mice (n=30) were obtained from the breeding facility of TNO Metabolic Health Research, Leiden, the Netherlands, and were housed in pathogen-free rooms, on a 12-h light–dark cycle. All mice were fed a high-fat diet (1 % cholesterol) 4021.34, AB diets, (Woerden, the Netherlands) for 20 weeks. Plasma

cholesterol and triglyceride concentrations were used to match mice in the control and LPS group. The control group received an intraperitoneally injection with 100µl phosphate buffered saline (PBS), whereas the test group was injected intraperitoneally with 1µg/100µl LPS (Escherichia coli (E.coli) 055:B5, Sigma-Aldrich, Zwijndrecht, the Netherlands) to induce systemic inflammation. The LPS dose for dyslipidemic high-fat diet treated mice was optimized in previous scouting experiments. To prevent the mice from dehydrating, all received a subcutaneous injection with 250µl NaCl 0.9% on the first day after receiving LPS/PBS injection. Blood was collected after a 4 hours fasting period at several time points around the LPS/PBS injection (t=-1 days, 2 days, 7 days and 15 days) to determine SAA levels. Mice in both LPS and PBS group were sacrificed by the use of a CO2box (100% CO2), either 2 or 15 days after injection. All procedures were approved by the Animal Use and Care Committee at the VU University Medical Centre of Amsterdam.

Analysis of SAA and serum lipids

Levels of serum amyloid A (SAA) were measured by ELISA (Life Technologies, Bleiswijk, the Netherlands). After 16 weeks of diet total serum cholesterol and triglyceride levels were measured in serum by commercially available enzymatic assays (cholesterol CHOD-PAP 11491458 and triglycerides GPO-PAP 11488872, Roche, Woerden, the Netherlands), to match mice in the control and LPS group.

(Immuno)histochemistry and morphometry

Atherosclerosis was analysed by observers blinded to group allocation in 4 serial Elastica von Gieson stained cross-sections (4 µm, at 56 µm intervals) of the valve area of the aortic root. Next, morphometric analysis of lesion number and area was measured using the Pathscan Enabler IV (Meyer Instruments, Houston, TX) with QuickPhoto Micro software (windows version 3.0, Promicra, Prague, Czech Republic). Grading of lesion severity was performed according to the adapted classification of the American Heart Association (AHA)[13] as reported in ApoE*3Leiden mice[14]. This scoring system distinguishes 5 lesion types: Type I (early fatty streak): up to 10 foam cells of a single lesion in the intima (magnification 40 x), no other changes; Type II (regular fatty streak): 10 or more foam cells in a single lesion in the intima (magnification 40 x), no other changes; Type III (mild plaque): foam cells in the intima with presence of a fibrotic cap; Type IV (moderate plaque): progressive lesion, infiltration into media, elastic fibers intact; Type V (severe plaque): structure of media severely disrupted with fragmented elastic fibers, cholesterol crystals, calcium deposits and necrosis may be present.

For immunohistochemical analysis, serial cross-sections were dewaxed, rehydrated and incubated in methanol/H2O2 (0.3%) for 30 minutes to block endogenous peroxidases. For both MAC-3 (macrophages) and CD45 (lymphocytes) staining, antigen retrieval was performed with citrate buffer, pH 6.0, for 15 minutes at 100 °C using a microwave. In

case of MAC-3 staining, sections were incubated with normal rabbit serum (1:50 dilution, DAKO, X0902) for 10 minutes at room temperature (RT) and subsequently with the primary antibody using rat-anti-mouse-MAC-3 antibody, detecting macrophages (1:30 dilution, BD Pharmingen, clone M3/84, cat. 553322, overnight, RT). For CD45 staining (detecting lymphocytes) sections were incubated with rat-anti-mouse-CD45 antibody (1:50 dilution, BD Pharmingen, clone 30-F11, cat. 553076, overnight, 4°C) and rinsed in PBS. Both staining's use rabbit-anti-rat immunoglobin/Horespradish peroxidase (HRP) (1:50 dilution, DAKO, cat. P0450, 30 minutes at RT) as secondary antibody, followed by visualisation with 3,3-diaminobenzidine-tetrahydrochloride/H2O2(DAB, 0.1 mg/ml, 0.02% H2O2) for 10 minutes and counterstaining with haematoxylin. With each staining slides were included incubated without a primary antibody as a negative control and all these controls yielded negative results. MAC-3 area was quantified as percentage MAC-3 positive staining of the total plaque area, using QuickPHOTO MICRO 3.0 software (windows version 3.0, Promicra, Prague, Czech Republic). Numbers of CD45 positive cells were manually quantified per surface area of the atherosclerotic plaque as cells/µm2. Immunoscoring was performed by I.P.A.Z and W.W.F.

Statistics

Statistical analyses were performed using Graphpad Prism software, version 6.0 (La Jolla, CA, USA). To evaluate differences in plaque area, plaque type, lesion number and inflammatory cells between groups, an independent sample t-test was used if the data were normally distributed, or a Mann–Whitney U test if not. Results were considered statistically significant if the two-sided p-value was <0.05.

RESULTS

LPS causes acute inflammation and loss of body weight

LPS-injected mice gave signs of moderate to severe distress[15] starting within 1 hour after injection. They appeared depressed, had squinted eyes, walked hunched and slowly and developed a rough hair coat. These symptoms peaked between day 1 to 3 after injection and gradually resolved within 3 to 5 days after injection. To determine whether the single LPS injection was indeed followed by an acute systemic inflammatory response we measured serum SAA levels at different time points (t= -1 day, 2 days, and, in the late-sacrifice group, after 7 and 15 days) (Fig. 1A). On day 2 after LPS injection, median SAA levels had increased 250-fold, from 13.9 [9.6-16.7] to 3598 [2567-7288] ug/mL, and returned to baseline levels, 9.5 [8.8-11.0] ug/mL on day 7. SAA values in the control group remained low and were stable. In the LPS group median body weight decreased from 26.3 [24.0-27.5] to 22.6 [21.7-24.2] gram at day 3 post-injection, returning largely to baseline levels at day 15 (Fig. 1B) which is in line with acute distress and recovery. In the control group, body weight remained stable as expected.

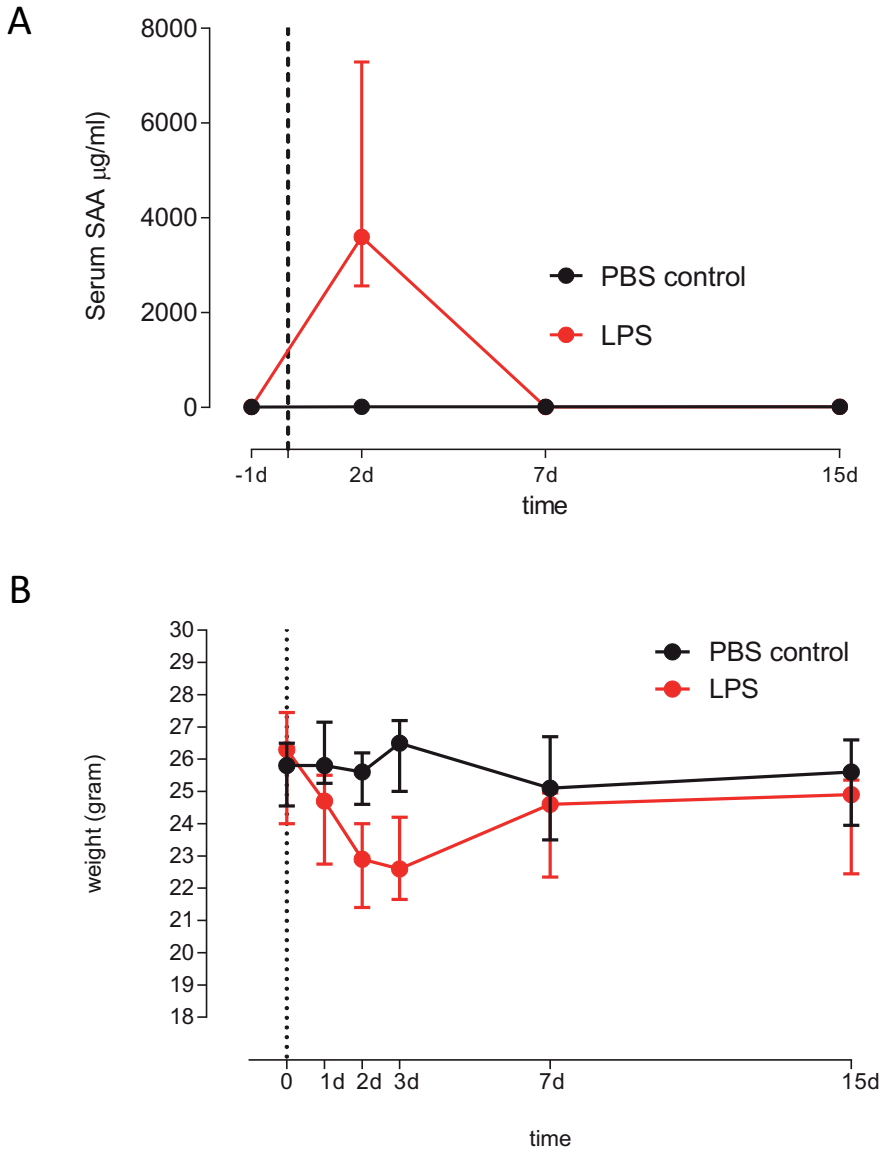

Figure 1 A single LPS injection transiently increases SAA levels and decreases body weight

A: Serum SAA levels in µg/ml and **B:** body weight in grams of control mice (black) and LPS mice (red) at baseline and at different time points after LPS (n=17) or control (n=13) injection. The vertical dotted line represents the timing of LPS or PBS injection. Data presented as median and interquartile range.

LPS-evoked acute systemic inflammation does not alter atherosclerotic plaque area, number, or severity

Atherosclerotic lesion area, severity and number were quantified histologically in the valve area of the aortic root. Aortic root sections of all experimental groups showed atherosclerotic lesions (Fig. 2A) of variable severity (type I to type V).

First, the total atherosclerotic plaque area at the level of the aortic valves in the root was measured (Fig. 2B). No significant differences in total surface area of atherosclerotic plaque were observed between the control and LPS groups sacrificed 2 days (resp. 0.409±0.228 x 105 μm^2 vs. 0.285±0.169 x 105 μm^2) (p=0.31), and 15 days (resp. 0.950±0.938 x 105 μm^2 vs. 0.612 ± 0.413 x 105 μm^2) (p=0.80) after saline/LPS injection While saline treated groups showed no further progression of atherosclerosis between day 2 and 15, treatment with LPS increased the total lesion area with borderline significance (P=0.055). The number of atherosclerotic plaques and percentage of lesion free segments were comparable in both groups (Fig. 2C and 2D).

In a subsequent more refined analysis, lesion severity was scored and lesions were graded on basis of their morphology and cellular composition. The plaque area per lesion type was quantified. No significant difference in plaque area was observed between the experimental groups sacrificed at day 2, with a comparable load of mild plaques (0.839±0.424 x 105 μm^2 vs. 0.764±0.397 x 105 μm^2, respectively; p=0.79), and severe plaques (0.743±0.641 x 105 μm^2 vs. 0.400±0.318 x 105 μm^2, respectively; p=0.23; Fig. 3). Similarly, no differences were found between the control and LPS groups sacrificed at day 15, both with respect to mild plaques (1.007±0.536 x 105 μm^2 vs. 0.992±0.369 x 105 μm^2, respectively; p=0.95), and severe plaques (resp. 1.683±1.349 x 105 μm^2 vs. 1.220±1.103 x 105 μm^2, respectively; p=0.35). Consistent with the global atherosclerosis analysis, the lesion area of mild and severe lesions was greater in mice sacrificed at day 15 as compared to the mice sacrificed at day 2, with most pronounced effects for the severe plaques (respectively p=0.33 in the control mice and p=0.075 in the LPS mice).

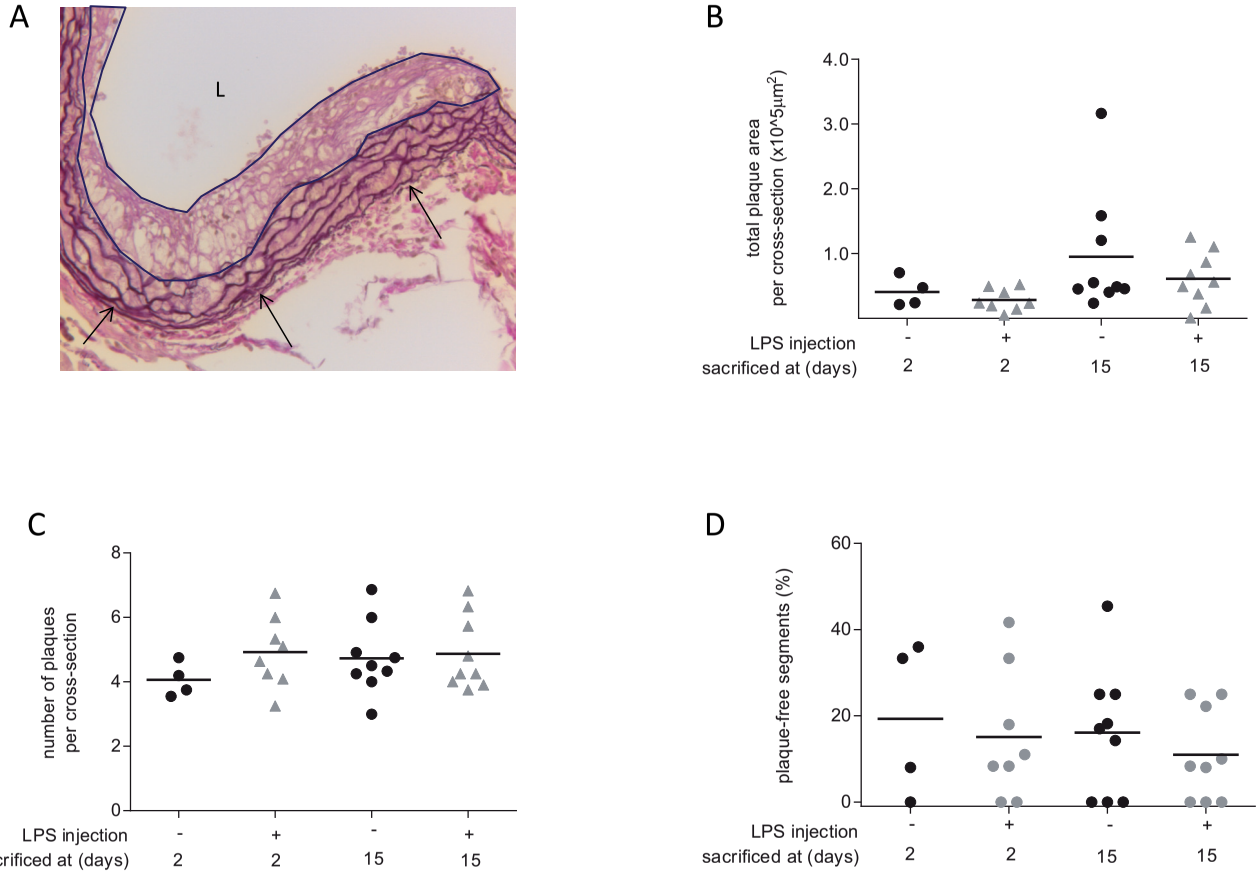

Figure 2 LPS does not increase atherosclerotic plaque area, number and lesion free segments

A: Representative image of EVG stained cross-sections of the aortic root. Showing a 10x magnified aortic root with lumen (L), a severe atherosclerotic lesion (encircled). The arrows indicate the media. **B:** Total plaque area (x105 µm^2). **C:** number of plaques per cross-section and **D:** percentage of lesion free segments at the aortic root of mice sacrificed t=2 days post-LPS (n=8) or control (n=4) or t=15 days post-LPS (n=9) or control (n=9). Data presented as mean and SD.

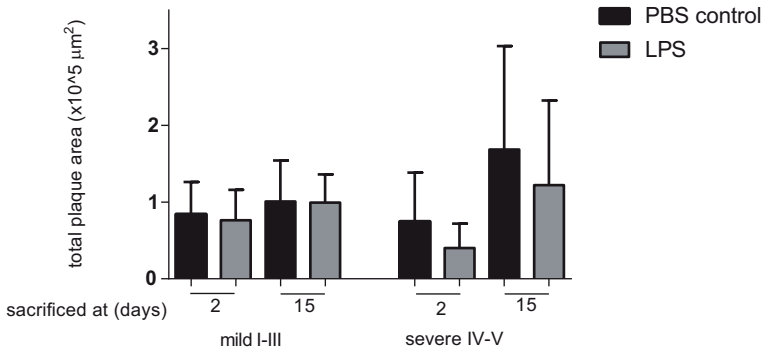

Figure 3 LPS does not increase total atherosclerotic plaque severity

Total surface area (x105 µm^2) of the atherosclerotic plaques per plaque type at the aortic root of mice sacrificed at t=2 days post-LPS (n=8) or control (n=4) or t=15 days post-LPS (n=9) or control (n=9). Data presented as mean and SD.

LPS-induced systemic inflammation does not increase the content of inflammatory cells within atherosclerotic lesions

To evaluate whether LPS injection enhances intra-plaque inflammation, the density of macrophages and lymphocytes in atherosclerotic plaques was determined (Fig. 4). The MAC-3 positive area (indicative of macrophages) divided by total plaque area was comparable in both groups and after 2 days 68.16±7.51% in control vs. 65.37±8.67% in LPS group (p=0.60) and after 15 days 65.16±10.99% vs. 59.97±8.51% (p=0.28). Next, the percentage of macrophage area in the different plaque types was evaluated (Fig. 4B). No significant differences were found between the control and LPS group sacrificed at day 2 or day 15, neither in the mild nor in the severe plaque types. The modest increase of macrophage density in severe plaques in the LPS groups at both time points was not statistically significant (p=0.21 at 2 days and p=0.43 at 15 days).

The number of lymphocytes per surface area of atherosclerotic plaques appeared higher in the control group than in the LPS group sacrificed at day 2 (3.5±2.9 x 10-4 µm^2 vs. 1.1±0.70 x 10-4 µm^2), but this difference was not statistically significant (p=0.37) (Fig. 4C). The lymphocyte density was also comparable in the groups sacrificed after 15 days (2.3±1.0 x 10-4 µm^2 vs. 2.3±1.7 x 10-4 µm^2) (p=0.91). The percentage of lymphocyte-covered area in the different plaque types was evaluated (Fig. 4D) but no significant differences were found between the control and LPS group at both time points, and irrespectively of the severity of the plaques.

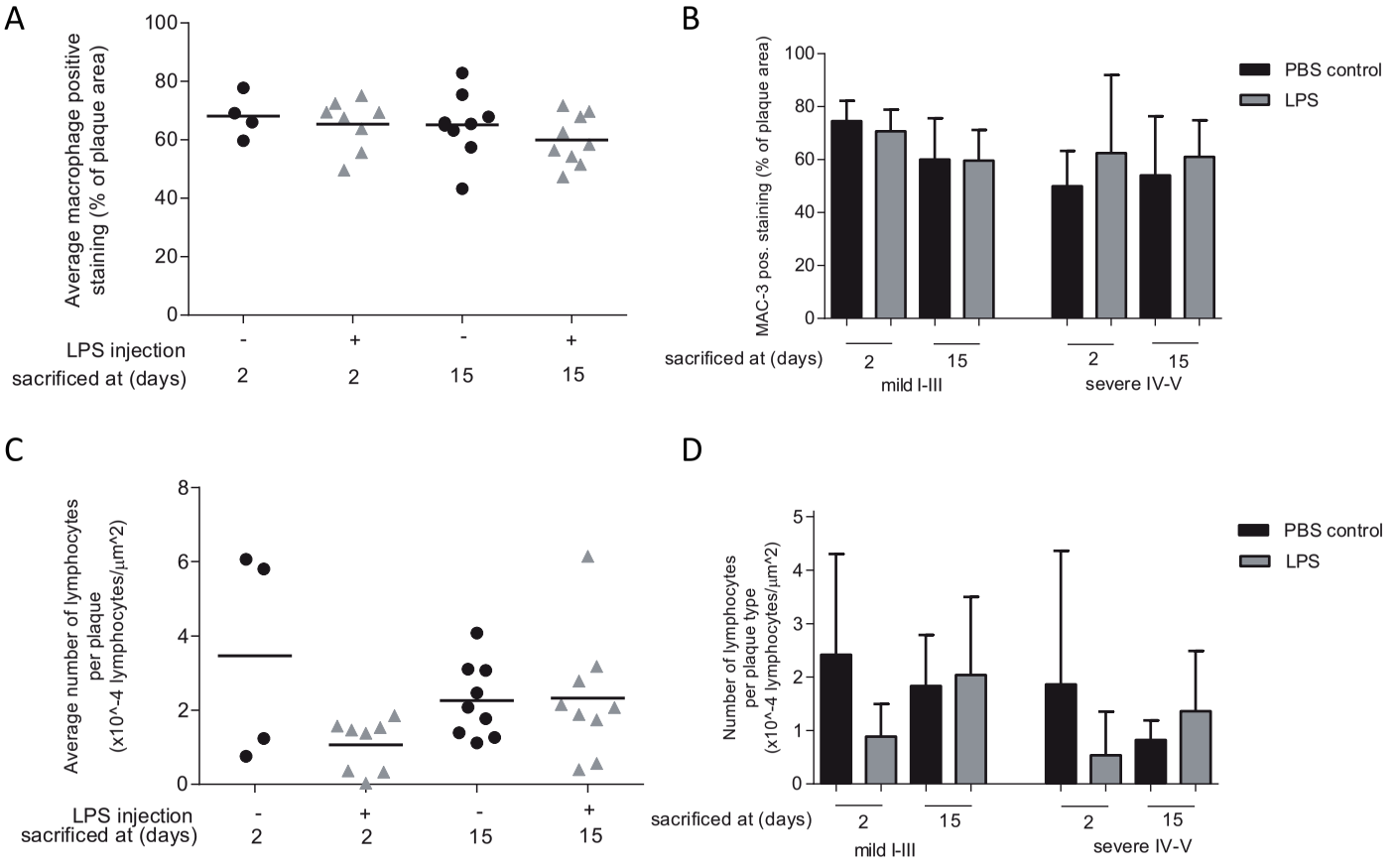

Figure 4 LPS does not increase the content of inflammatory cells within atherosclerotic lesions

A: MAC-3 positive area in the plaque divided by total plaque area (%) **B:** MAC-3 positive area in the plaque divided by total plaque area (%) shown per plaque category (mild and severe). **C:** CD45 positive lymphocytes in the plaque divided by the total plaque area (cells/µm^2). All expressed the aortic root of mice sacrificed at t=2 days post-LPS (n=8) or control (n=4) or t=15 days post-LPS (n=9) or control (n=9). **D:** Data presented as mean and SD.

DISCUSSION

A single LPS injection in ApoE3*Leiden mice triggered a substantial systemic inflammatory response but did not evoke intraplaque changes in size or inflammatory cell density. Thus, this model cannot help explain the high incidence of cardiovascular events following acute systemic inflammation in clinical patients in the early phase of the disease.

The LPS-injection caused a marked acute systemic inflammatory response as demonstrated by mice behavior, weight loss and a rapid increase in SAA, a relatively stable and sensitive inflammation marker that integrates the signals of several pro-atherogenic cytokines, such as IL1, TNFα, and IL6[16, 17]. Several studies suggest that SAA itself participates in the pathogenesis of atherosclerosis[18] and a recent study showed that a single SAA injection in ApoE-deficient mice, a model of spontaneous atherosclerosis, increases atherosclerotic plaque area 16 weeks later[11]. Similar evidence for a long-term effect of acute inflammation on plaque development also comes from a model of intra-abdominal sepsis in ApoE-deficient mice caused by colon ligature and puncture (CLP) in which atherosclerotic plaque area was enhanced at 3 and 5 months and suggested increased intra-plaque macrophage infiltration at 5 months[12]. The aforementioned long-term studies suggest that acute inflammation enhances plaque growth and inflammation after several months, but do not address the question if acute plaque changes occur days after the onset of inflammation, which would help explain the acute event risk in humans with systemic infection. Data is scarce, but some studies have evaluated vessel wall changes shortly after inflammation. The earlier mentioned study using the CLP in ApoE -/- model also described elevated mRNA expression for cytokines and adhesion molecules (TNF-a, CCL2, ICAM-1, VCAM-1) in the aorta's of wild type mice, 1-5 days after CLP, but these observations were not evaluated at a protein level. This finding was however not confirmed in the atherosclerotic mouse model and therefore could be a sign of systemic infection induced pan-aortitis and does thus not prove or disprove enhanced intra-plaque inflammation and atherogenesis. In advance, a study in Apo E-/- mice subjected to an influenza virus infection showed subendothelial infiltration of a heterogeneous population of inflammatory cells within 10 days after infection[19]. These cells were however not quantified per type and plaque area was not assessed. So whether acute systemic inflammation induces pro-inflammatory changes in atherosclerotic plaques in a similar time frame as the acute cardiovascular event risk in humans with infection has, however, not been studied to date. In an attempt to mimic the situation in the clinic, we established an acute systemic inflammatory condition in mice with established lesion by injection of LPS that resulted in markedly elevated levels of SAA. Under these conditions, we found no evidence for acute morphological or structural changes of lesions in the vessel wall which would indicate pro-atherogenic or intra-plaque pro-inflammatory effects, for which we propose three possible, non-mutually exclusive explanations:

Firstly, our hypothesis that acute systemic inflammation evokes similarly acute pro-inflammatory changes in plaques may be incorrect.

Secondly, our LPS-induced systemic inflammatory response could have been inappropriate to disprove the hypothesis. An actual infection model may more closely resemble the pathophysiological process of sepsis than the LPS model[20]. These infection models however are very hard to mimic and to translate to clinically relevant situations. In fact, sepsis is one of the most difficult clinical conditions to model in animals as is also shown by the fact that many promising therapeutic agents that were effective in animal studies failed to demonstrate a similar benefit in human clinical trials[20, 21]. Although LPS causes an acute systemic inflammatory response, it may not mimic real infection sufficiently enough, because it is strictly TLR4 mediated, has a higher and shorter increase in cytokines and has a different hemodynamic response compared to human sepsis[21, 22]. There are some indications that actual infection models, such as the often used CLP model, may better mimic human sepsis[21, 23]. We did however not choose CLP or other models based on alteration of the endogenous protective barrier of the animal [24], because with this technique it remains difficult to control the magnitude of the septic challenge. As a result sepsis is highly variable in severity[21].

Thirdly and finally, inflammatory cell content of plaque could be an inappropriate read-out parameter for acute plaque inflammation. The premise that inflammation is always appropriately reflected by inflammatory cell content may be incorrect, particularly in very acute circumstances. Inflammatory cells may for example decrease in number due to apoptosis after a brief phase of activation. This is known to occur with intra-plaque macrophages, which degrade to necrotic core after activation and LDL uptake[25, 26]. Our recent study in Apo E-/- mice also seems to suggest a similar phenomenon, as major orthopedic surgery caused a strong systemic inflammatory response and lead to an increase in plaque and necrotic core area with concomitant decrease of macrophage and lymphocyte density at day 15 post-surgery[27]. Hence, the activation state rather than cell density may represent the best parameter of acute intra-plaque inflammation. There is, however, limited consensus as to how to quantify pro-inflammatory activity of relevant immune cells, in particular macrophages and lymphocytes.

Strengths and limitations

A strength of this study is that we in contrast to others have focused on the early effects of systemic inflammation on the vessel wall, thus specifically addressing the clinical observation of increased cardiovascular risk shortly after onset of acute inflammation. To our knowledge we are the first that quantify plaque area short (days rather than months) after LPS-induces inflammation. Next, we have chosen, the ApoE3*Leiden model as in these mice plaques grow in a slower, more human-like pace than the ApoE -/- model[28, 29] and because the ApoE protein itself plays a role in controlling the physiological responses

during inflammation such as leukocyte migration[30]. Furthermore ApoE is important for hepatic clearance of LPS and the absence of this apolipoprotein enhances the immune response to LPS[31-33]. Therefore our study may reflect LPS effects more realistically than conditions in which ApoE is fully knocked out. Several limitations of our design merit discussion. We based the number of mice per group on the scarce literature on this topic. Mouse numbers are consequently relatively small and the risk of a type 2 fault is present. Although we could not observe differences that approach significance, including more mice would have made the conclusion stronger. And lastly since atherosclerotic plaque rupture in the ApoE3*Leiden model it is not seen in the aortic root it would have been interesting to analyze the effect is of LPS in experimental models that study actual plaque complications rather than atherosclerotic plaque development alone[34, 35].

SUMMARY

We hypothesized that acute systemic inflammation provoked by lipopolysaccharides rapidly enhances plaque area and intra-plaque inflammation, and we addressed this hypothesis in atherosclerosis-prone ApoE*3Leiden mice. LPS mice showed a pronounced elevation of SAA indicating a marked systemic inflammatory conditions, but no significant differences in plaque area, type and number of lesions were observed 2 and 15 days after LPS injection. In parallel, the plaque density of macrophages and lymphocytes remained unchanged in the early phase. Our study argues against structural/morphological intra-plaque alterations as an explanation for acute inflammation-induced cardiovascular event risk.

FINANCIAL SUPPORT

This study was financed by the Institute for Cardiovascular Research (ICaR-VU; Grant No.ICaR-VU-ID414-2012).

REFERENCES

1 Smeeth L, Thomas SL, Hall AJ, Hubbard R, Farrington P and Vallance P. Risk of myocardial infarction and stroke after acute infection or vaccination. N Engl J Med 2004;351(25):2611-2618

2 Meier CR, Jick SS, Derby LE, Vasilakis C and Jick H. Acute respiratory-tract infections and risk of first-time acute myocardial infarction. Lancet 1998;351(9114):1467-1471

3 Elkind MS, Carty CL, O'Meara ES, Lumley T, Lefkowitz D, Kronmal RA and Longstreth WT, Jr. Hospitalization for infection and risk of acute ischemic stroke: the Cardiovascular Health Study. Stroke 2011;42(7):1851-1856

4 Lalmohamed A, Vestergaard P, Klop C, Grove EL, de BA, Leufkens HG, van Staa TP and de VF. Timing of acute myocardial infarction in patients undergoing total hip or knee replacement: a nationwide cohort study. Arch Intern Med 2012;172(16):1229-1235

5 Cohen MC and Aretz TH. Histological analysis of coronary artery lesions in fatal postoperative myocardial infarction. Cardiovasc Pathol 1999;8(3):133-139

6 Corrales-Medina VF, Madjid M and Musher DM. Role of acute infection in triggering acute coronary syndromes. Lancet Infect Dis 2010;10(2):83-92

7 Madjid M, Vela D, Khalili-Tabrizi H, Casscells SW and Litovsky S. Systemic infections cause exaggerated local inflammation in atherosclerotic coronary arteries: clues to the triggering effect of acute infections on acute coronary syndromes. Tex Heart Inst J 2007;34(1):11-18

8 Virmani R, Burke AP, Farb A and Kolodgie FD. Pathology of the vulnerable plaque. J Am Coll Cardiol 2006;47(8 Suppl):C13-8

9 Libby P. Inflammation in atherosclerosis. Nature 2002;420(6917):868-874

10 Santos-Gallego CG, Picatoste B and Badimon JJ. Pathophysiology of acute coronary syndrome. Curr Atheroscler Rep 2014;16(4):401

11 Thompson JC, Jayne C, Thompson J, Wilson PG, Yoder MH, Webb N and Tannock LR. A brief elevation of serum amyloid A is sufficient to increase atherosclerosis. J Lipid Res 2015;56(2):286-293

12 Kaynar AM, Yende S, Zhu L, Frederick DR, Chambers R, Burton CL, Carter M, Stolz DB, Agostini B, Gregory AD, Nagarajan S, Shapiro SD and Angus DC. Effects of intra-abdominal sepsis on atherosclerosis in mice. Crit Care 2014;18(5):469

13 Stary HC, Chandler AB, Dinsmore RE, Fuster V, Glagov S, Insull W, Jr., Rosenfeld ME, Schwartz CJ, Wagner WD and Wissler RW. A definition of advanced types of atherosclerotic lesions and a histological classification of atherosclerosis. A report from the Committee on Vascular Lesions of the Council on Arteriosclerosis, American Heart Association. Arterioscler Thromb Vasc Biol 1995;15(9):1512-1531

14 Morrison M, van der Heijden R, Heeringa P, Kaijzel E, Verschuren L, Blomhoff R, Kooistra T and Kleemann R. Epicatechin attenuates atherosclerosis and exerts anti-inflammatory effects on diet-induced human-CRP and NFkappaB in vivo. Atherosclerosis 2014;233(1):149-156

15 Burkholder T, Foltz C, Karlsson E, Linton CG and Smith JM. Health Evaluation of Experimental Laboratory Mice. Curr Protoc Mouse Biol 2012;2(145-165

16 Kleemann R, Zadelaar S and Kooistra T. Cytokines and atherosclerosis: a comprehensive review of studies in mice. Cardiovasc Res 2008;79(3):360-376

17 Zhang N, Ahsan MH, Purchio AF and West DB. Serum amyloid A-luciferase transgenic mice: response to sepsis, acute arthritis, and contact hypersensitivity and the effects of proteasome inhibition. J Immunol 2005;174(12):8125-8134

18 King VL, Thompson J and Tannock LR. Serum amyloid A in atherosclerosis. Curr Opin Lipidol 2011;22(4):302-307

19 Naghavi M, Wyde P, Litovsky S, Madjid M, Akhtar A, Naguib S, Siadaty MS, Sanati S and Casscells W. Influenza infection exerts prominent inflammatory and thrombotic effects on the atherosclerotic plaques of apolipoprotein E-deficient mice. Circulation 2003;107(5):762-768

20 Dyson A and Singer M. Animal models of sepsis: why does preclinical efficacy fail to translate to the clinical setting? Crit Care Med 2009;37(1 Suppl):S30-7

21 Dejager L, Pinheiro I, Dejonckheere E and Libert C. Cecal ligation and puncture: the gold standard model for polymicrobial sepsis? Trends Microbiol 2011;19(4):198-208

22 Remick DG, Newcomb DE, Bolgos GL and Call DR. Comparison of the mortality and inflammatory response of two models of sepsis: lipopolysaccharide vs. cecal ligation and puncture. Shock 2000;13(2):110-6

23 Wichterman KA, Baue AE and Chaudry IH. Sepsis and septic shock--a review of laboratory models and a proposal. J Surg Res 1980;29(2):189-201

24 Maier S, Traeger T, Entleutner M, Westerholt A, Kleist B, Huser N, Holzmann B, Stier A, Pfeffer K and Heidecke CD. Cecal ligation and puncture versus colon ascendens stent peritonitis: two distinct animal models for polymicrobial sepsis. Shock 2004;21(6):505-11

25 Virmani R, Burke AP, Kolodgie FD and Farb A. Vulnerable plaque: the pathology of unstable coronary lesions. J Interv Cardiol 2002;15(6):439-46

26 Tabas I. Macrophage death and defective inflammation resolution in atherosclerosis. Nat Rev Immunol 2010;10(1):36-46

27 Fuijkschot WW, Morrison MC, van der Linden R, Krijnen PA, Zethof IP, Theyse LF, Kleemann R, Niessen HW and Smulders YM. Orthopedic surgery increases atherosclerotic lesions and necrotic core area in ApoE-/- mice. Atherosclerosis 2016

28 Gijbels MJ, van der Cammen M, van der Laan LJ, Emeis JJ, Havekes LM, Hofker MH and Kraal G. Progression and regression of atherosclerosis in APOE3-Leiden transgenic mice: an immunohistochemical study. Atherosclerosis 1999;143(1):15-25

29 Zadelaar S, Kleemann R, Verschuren L, de Vries-Van der Weij J, van der Hoorn J, Princen HM and Kooistra T. Mouse models for atherosclerosis and pharmaceutical modifiers. Arterioscler Thromb Vasc Biol 2007;27(8):1706-21

30 Madenspacher JH, Azzam KM, Gong W, Gowdy KM, Vitek MP, Laskowitz DT, Remaley AT, Wang JM and Fessler MB. Apolipoproteins and apolipoprotein mimetic peptides modulate phagocyte trafficking through chemotactic activity. J Biol Chem 2012;287(52):43730-40

31 Rensen PC, Oosten M, Bilt E, Eck M, Kuiper J and Berkel TJ. Human recombinant apolipoprotein E redirects lipopolysaccharide from Kupffer cells to liver parenchymal cells in rats In vivo. J Clin Invest 1997;99(10):2438-2445

32 Laskowitz DT, Lee DM, Schmechel D and Staats HF. Altered immune responses in apolipoprotein E-deficient mice. J Lipid Res 2000;41(4):613-620

33 Kattan OM, Kasravi FB, Elford EL, Schell MT and Harris HW. Apolipoprotein E-mediated immune regulation in sepsis. J Immunol 2008;181(2):1399-1408

34 Chen YC, Bui AV, Diesch J, Manasseh R, Hausding C, Rivera J, Haviv I, Agrotis A, Htun NM, Jowett J, Hagemeyer CE, Hannan RD, Bobik A and Peter K. A novel mouse model of atherosclerotic plaque instability for drug testing and mechanistic/therapeutic discoveries using gene and microRNA expression profiling. Circ Res 2013;113(3):252-265

35 Van der Donckt C, Van Herck JL, Schrijvers DM, Vanhoutte G, Verhoye M, Blockx I, Van Der Linden A, Bauters D, Lijnen HR, Sluimer JC, Roth L, Van Hove CE, Fransen P, Knaapen MW, Hervent AS, De Keulenaer GW, Bult H, Martinet W, Herman AG and De Meyer GR. Elastin fragmentation in atherosclerotic mice leads to intraplaque neovascularization, plaque rupture, myocardial infarction, stroke, and sudden death. Eur Heart J 2015;36(17):1049-1058

5

Systemic inflammation enhances mast cell density in coronary arteries in patients who died of myocardial infarction

Wessel W. Fuijkschot; Linde Woudstra; Rianne van der Linden; Danae Beskers; Ilse P.A. Zethof; Paul A.J. Krijnen; Hans W.M. Niessen and Yvo M. Smulders

Submitted for publication

ABSTRACT

Objective: Cardiovascular events show a peak incidence early after episodes of severe systemic inflammation, such as infection. The acuteness of this increased risk suggests intra-plaque inflammation and subsequent plaque instability. We hypothesized that acute systemic inflammation induces such changes and addressed this hypothesis in an autopsy study of patients with acute myocardial infarction (AMI) and with or without infection at time of death.

Methods: We selected AMI patients with (n=18) and without (n=16) non-cardiac acute inflammation (AI) at time of death. Since infarct duration itself may influence plaque inflammation, we divided the groups by estimated time since AMI (3-6 hours vs. 6 hours-14 days). Stenosis, plaque stability and intra-plaque hemorrhage were assessed in coronary sections. Infiltration of lymphocytes (CD45), macrophages (CD68), mast cells (tryptase) and neutrophilic granulocytes (MPO) in the intima, media and adventitia were assessed.

Results: In 289 coronary artery sections, we found no difference in stenosis, plaque stability characteristics or density of most inflammatory cells between AMI patients with or without AI. Mast cells, however, were more numerous in the intima and media of early AMI patients with AI compared to AMI without AI (1.14 [0.47-3.28] vs. 2.26 [1.43-4.66] p=0.021 in the intima, and 0.00 [0.00-0.76] vs. 0.63 [0.00-3.17] p=0.004 in the media, respectively). Lymphocyte and macrophage density increased with advancing infarct duration, with no clear difference between the AI and non-AI groups.

Conclusions: Acute non-cardiac inflammation may enhance mast cell influx in the intima and media of atherosclerotic coronary arteries and thus contribute to the pathogenesis of acute MI. Our results argue against a role for other inflammatory cells in plaque during acute inflammation. We observed an increase in coronary wall inflammation later in the post-MI period, independent from the presence of systemic infection.

INTRODUCTION

Observational epidemiological studies show that cardiovascular events can be triggered by clinical conditions that are associated with systemic inflammation[1-4]. Respiratory tract infection, for instance, raises the early (2-14 days after onset of symptoms)[1, 2] risk of acute myocardial infarction (AMI) by approximately fivefold1, and the risk of stroke by eightfold[1, 3].

The causal mechanisms behind inflammation-induced cardiovascular event risk remain elusive, but its acuteness suggests an effect on atherosclerotic plaque stability[5-7]. If this indeed occurs and, if so, by which mechanism is unclear. We do however know that intra-plaque inflammation plays an important role in the progression and destabilization of atherosclerotic plaques[8-11]. It is thus worth investigating whether acute systemic inflammation has short-term effects on plaque inflammation.
Several studies previously addressed the issue of acute inflammation and its effect on atherosclerosis, but most focused on intermediate to long-term effects. For example, plaque area was increased in Apo E -/- mice 16 weeks after a single injection of serum amyloid A peptide, a biomarker and inducer of systemic inflammation.[12] Furthermore, a recent murine model of abdominal sepsis showed effects on atherosclerotic plaque stability months after the initial infection had ceased.[13] Whether acute systemic inflammation induces similar pro-inflammatory intra-plaque changes in humans has, however, not been studied to date.

Given the short-term effects of systemic inflammation on cardiovascular event risk, we hypothesized that an acute episode of infection rapidly enhances intra-plaque inflammation. In the coronary arteries, such changes could act in two ways. First, they could contribute to the occurrence of a primary AMI. Secondly, they could enhance the pro-inflammatory plaque changes evoked by recent MI itself, thus bearing relevance for patients who have infection in the early post-MI period[14, 15]. We concluded that both hypotheses could be addressed by analyzing inflammatory cell content in atherosclerotic plaques in coronary arteries of patients who died at different time intervals after AMI, with or without signs of systemic infection.

METHODS

The study included deceased patients referred to the Department of Pathology for clinical autopsy, which was performed within 24 h after death. Relatives of patients provided written consent for the use of autopsy material for scientific research. All patients showed macroscopical evidence of recent AMI, as identified by lactate dehydrogenase

(LDH) decolouration of myocardial tissue. Patients diagnosed with chronic inflammatory disease (e.g. systemic lupus erythematosus or rheumatoid arthritis) , recent surgery (<6 months) and metastatic disease were excluded, since these conditions could influence inflammatory status[4, 16-19]. Patients with clinically and autopsy proven sepsis or severe systemic infection at time of death (acute non-cardiac systemic inflammation; AI) were selected and compared to patients with no signs of infection (no acute non-cardiac systemic inflammation; non-AI). Myocardial tissue specimens were obtained from the center of the infarct area in AMI patients and after formalin-fixation, embedded in paraffin and used for immunohistochemical analyses. AMI patients were categorized into two phases of post-AMI duration based on microscopic criteria: the early post-AMI phase (3-6 hrs old; macroscopic LDH decolouration but no extravasation of neutrophilic granulocytes in the infarct area) and the mid-term to late post-AMI phase (6 hrs to 14 days old; extravasation of neutrophilic granulocytes in the infarct area and/or granulation tissue formation[20-23].

In all patients, the left and right coronary arteries were excised from their root to the point where they enter the myocardium. Sections with the most severe stenosis were identified macroscopically and subsequently processed separately for histological and immunohistochemical analyses. Selected tissue cross-sections were fixed in 4% paraformaldehyde, decalcified in buffered formic acid, and embedded in paraffin.

(Immuno)histochemistry

Paraffin tissue sections (4 µm) of the coronary segments were stained with Elastica von Gieson (EVG) and haematoxylin-eosin (HE) for histological analyses. The degree of stenosis of each individual segment was determined based on EVG stained cross-section as percentage of luminal surface area compared to surface area defined by the internal elastic lamina. All atherosclerotic plaques were evaluated microscopically to verify the presence of a thin fibrous cap. Plaques were classified as unstable if the fibrous cap was thin and/or if multiple inflammatory cells reached up to the luminal endothelial layer of the plaque[24, 25]. If neither of these characteristics were present, plaques were classified as stable. To classify intraplaque hemorrhage (IPH) all coronary segments where stained for erythrocytes with the immunohistochemical GLUT-1 staining and for iron using the histochemical Perls staining. Using a microscope with 250 × magnification, fresh IPH was identified by the presence of >10 extravascular localized intact erythrocytes per plaque, while old IPH was identified by the presence of iron and/or erythrocyte fragments[24, 25]. Ongoing IPH was defined as both fresh and old hemorrhage25. Subsequently, all coronary segments were stained with antibodies detecting GLUT-1 (erythrocytes), CD45 (lymphocytes), CD68 (macrophages), MPO (neutrophils) and tryptase (mast cells). For this, the sections were first deparaffinized, rehydrated and blocked for endogenous peroxidases by incubation in H2O2 (0.3%) diluted in methanol for 30 minutes. Antigen retrieval was performed by heat inactivation in sodium-citrate buffer (10 mM,

pH 6.0) for slides to be stained for CD68, MPO and tryptase or in a Tris/EDTA buffer (pH 9.0) for slides to be stained with GLUT-1. Slides to be stained for CD45 required no antigen retrieval step. The slides were incubated with either or rabbit-anti-human Glut-1 (1:100, Thermo Scientific RB-9052-P), mouse-anti-human CD45 (1:100, Dako M0701), rabbit-anti-human CD68 (1:400, Dako M0814), mouse-anti-human MPO (1:1500, Dako A0398) or mouse-anti-human Tryptase (1:500, Dako M7052) for 1 h at room temperature. The sections were then washed with phosphate-buffered saline and incubated with Real EnVision HRP α-mouse/rabbit (undiluted; Dako) for 30 min at room temperature. The staining was visualized using 3,3′-diaminobenzidine (DAB) (0.1 mg/ml, 0.02% H2O2). The sections were then counterstained with hematoxylin, dehydrated, and covered. With each staining, a phosphate-buffered saline control and an isotype control were included. All these controls yielded negative results (not shown).

Quantification of immune cells and morphometric analysis

In all individual segments of each coronary artery the total surface area of the intima and media and adventitia were determined on the scanned slides using the Panoramic Desk scanner and analyzed with Pannoramic Viewer 1.15.2 software (3DHistech, Budapest, Hungary). The surface area of adventitia was measured from the external elastic lamina until 100 μm into the tunica externa.

Lymphocyte and macrophage infiltration was analyzed with the ImageJ 1.47 software (National Institutes of Health, USA) using a color threshold to determine the surface area of positive anti-CD45 staining respectively anti-CD68 staining and dividing it by the surface areas of the relevant intima, media and adventitia. CD68 positive area was quantified only in the intima, since there were no (large) areas of positive staining present in the media an adventitia. The numbers of extravascular mast cells and neutrophilic granulocytes were counted using a light microscope using a 25x magnification objective (Zeiss, Germany) and then calculated per mm^2 of the surface areas of the intima, media and adventitia.

Statistics

To evaluate differences in plaque area, plaque type, lesion number and inflammatory cells between groups, independent sample t-tests and Mann–Whitney U tests were used as appropriate. Statistical analyses were performed using GraphPad Prism version 7.00 for Windows, (GraphPad Software, La Jolla California USA). Results were considered statistically significant if the two-sided p-value was <0.05.

RESULTS

Baseline characteristics

34 AMI patients with a total of 289 coronary slides were included and categorized into 4 groups based on infarction duration and the presence of acute systemic inflammation (Table 1). Additional clinical details regarding co-morbidity and type of infection in the AI group, are given in supplemental table A.

Table 1 Baseline characteristics

	No AI 3-6 hrs (n=12)	AI 3-6 hrs (n=5)	No AI 6 hrs - 14 days (n=6)	AI 6 hrs - 14 days (n=11)
Demographic characteristics				
Age (years)	67 (56-74)	81 (57-86)	64 (51-72)	72 (69-82)
Male, n (%)	11 (92)	4 (80)	5 (83)	7 (64)
Cardiovascular history				
Hypertension, n (%)	1 (8)	0 (0)	0 (0)	4 (36)
DM, n (%)	1 (8)	2 (40)	2 (33)	2 (18)
Previous infarction, n (%)	3 (25)	0 (0)	1 (17)	3 (27)
Coronary slides used for analysis (n)	120	31	45	93

Variable represent median [interquartile range], percentage of total patients (%). DM2, type 2 diabetes; AF, atrial fibrillation; CABG, coronary artery bypass graft; COPD, chronic obstructive pulmonary disease.

Supplemental table A included patients

Gender	age	Infarct duration	Non-cardiac acute systemic inflammation on autopsy report	Secondary pathologies
M	81	3-6 hrs	Sepsis with pneumonia, arthritis of the knee and fasciitis necroticans upper leg	DM2; aortic prothesis; cholecystectomy; prostate and colon cancer (no metastasis)
M	90	3-6 hrs	Sepsis with betahemolytic Streptococ. group A in blood	AF
F	37	3-6 hrs	Bilateral pneumonia with Staph. Aureus	Systemic sclerosis (dermal tightening, Raynaud, myocardial fibrosis, right heart failure), AF
M	82	3-6 hrs	Pneumonia	Prostate cancer (no metastasis)
M	77	3-6 hrs	Pneumonia	DM2
M	72	6-12 hrs	Sepsis with pneumonia	CABG and mitral valve prothesis (7 yrs < death)
M	69	6-12 hrs	Sepsis with pneumonia, peritonitis	CABG (2 yrs < death); kidney failure with peritoneal dialysis; hypertension
M	64	6-12 hrs	Sepsis	none
M	89	1-3 days	Pneumonia	Previous AMI (27 yrs < death); vascular dementia; hypertension
F	82	1-3 days	Pneumonia	none
F	81	1-3 days	Bilaterial pneumonia	Breast cancer with mastectomy (no metastasis); hypertension; hypercholesterolemia; appendectomy; AF
M	69	5-7 days	Sepsis	Aortic prothesis; DM2; hypercholesterolemia
F	69	5-7 days	Pneumonia + urinary tract infection	Breast cancer with lumpectomy (27 yrs < death); CABG (10 yrs < death); stomach cancer with gastrectomy (8 yrs < death)
M	88	7-14 days	Bilateral pneumonia	Gastrectomy; aortic valve stenosis
F	75	7-14 days	Sepsis with infected grafts femoropopliteal bypass	Fempop (3 months < death); COPD; DM2; hypertension; AMI (5 yrs < death); AF; kidney failure
M	55	7-14 days	Pancreatitis	AMI (3 x) last 1 month before death
F	95	3-6 hrs	no	Trauma capitis
M	60	3-6 hrs	no	none
M	66	3-6 hrs	no	COPD; AF
M	90	3-6 hrs	no	COPD; hypertension; DM2; systemic amyloidosis (no cardial involvement)
M	54	3-6 hrs	no	none
M	74	3-6 hrs	no	Lungcarcinoma with surgery (7 yrs < death; AMI (5 yrs < death);
		3-6 hrs		heart failure (3 yrs < death); Aortic valve stenosis
M	74	3-6 hrs	no	Cholelithiasis
M	64	3-6 hrs	no	AF; previous AMI
M	67	3-6 hrs	no	Dilated cardiomyopathie (ICD); alcoholic fibrosis of heart and liver
M	43	3-6 hrs	no	none
M	71	3-6 hrs	no	Previous AMI with CABG
M	55	3-6 hrs	no	none
M	60	1-3 days	no	none
M	67	1-3 days	no	none
M	72	1-3 days	no	none
M	52	5-14 days	no	DM2; alcohol abuses; prostate cancer with prostectomy (1 yrs < death)
M	47	7-14 days	no	DM2; sarcoidosis (no cardial involvement); old infarctions
F	72	7-14 days	no	Livercirrhosis; aortic valve stenosis with left ventriculair hypertrophy

Infarcted area, stenosis, plaque stability and intra-plaque hemorrhage

In patients with acute MI (3-6 hrs old) and late MI (6 hrs-14 days), no significant differences between the non-AI and AI groups were observed for infarct area, stenosis, plaque instability and intra-plaque hemorrhage (Fig. 1A-1D and suppl. Table B).

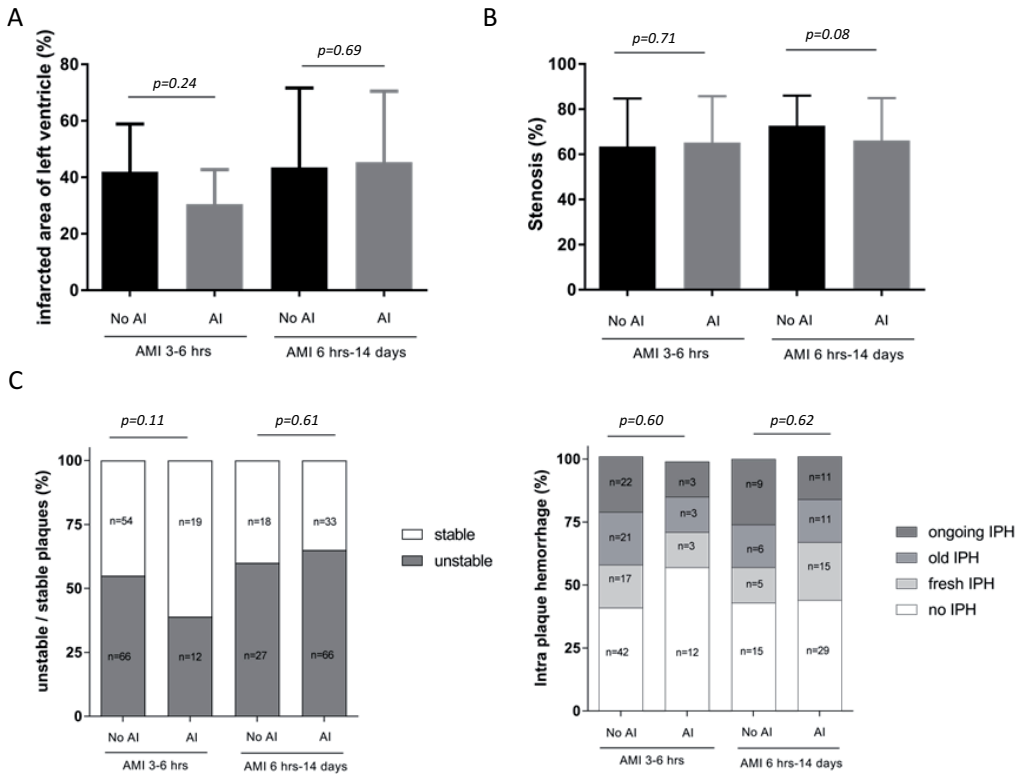

Figure 1 Infarcted area, stenosis and stability per group.

Total surface area (x105 μm^2) of the atherosclerotic plaques per plaque type at the aortic root of mice
A: Infarcted area of the left ventricle divided by total area of left ventricle (%). **B:** Stenosis expressed as percentage of the surface area of the lumen divided by the surface area of the intima ending at the internal elastic lamina. **C:** Number of unstable plaques divided by number of unstable + stable plaques. Percentages are given as well as absolute number of plaques. **D:** Number of plaques without and with (fresh, old or ongoing) hemorrhage. Percentages are given as well as absolute number of plaques. Groups are based on infarct duration (3-6 hrs vs 6hrs-14days) and the presence of non-cardiac acute inflammation (AI) diagnosed at autopsy. AMI; acute myocardial infarction. Bars represent mean and SD.

Supplemental Table B Inflammatory cell densities

	No AI 3-6 hrs	AI 3-6 hrs	No AI 6 hrs - 14 days	AI 6 hrs - 14 days
Lymphocytes (surface area, %)				
Intima	0.26 [0.07-0.70]	0.11 [0.02-0.48]	0.89 [0.37-2.34]	0.31 [0.10-0.98]
Media	0.05 [0.01-0.15]	0.02 [0.00-0.17]	0.20 [0.08-0.59]	0.09 [0.02-0.25]
Acventitia	0.70 [0.27-1.51]	0.53 [0.24-1.49]	3.23 [0.89-5.49]	0.96 [0.33-2.07]
Macrophages (surface area, %)				
Intima	0.40 [0.12-1.56]	0.36 [0.08-1.13]	0.73 [0.34-5.24]	0.83 [0.17-5.04]
Neutrophilic granulocytes (cells/mm^2)				
Intima	1.22 [0.44-2.80]	2.03 [0.37-3.72]	1.57 [0.80-4.58]	1.10 [0.36-2.52]
Media	0.00 [0.00-1.05]	0.00 [0.00-2.49]	0.77 [0.00-3.71]	0.14 [0.00-1.77]
Acventitia	4.02 [0.99-7.67]	3.75 [2.00-9.19]	6.20 [2.66-13.9]	3.96 [1.83-7.65]
Mast cells (cells/mm^2)				
Intima	1.14 [0.47-3.28]	2.26 [1.43-4.66]	1.75 [1.16-3.14]	0.85 [0.21-2.02]
Media	0.00 [0.00-0.76]	0.63 [0.00-3.17]	1.85 [0.00-4.18]	0.41 [0.00-3.33]
Acventitia	14.8 [7.59-43.4]	18.4 [10.5-24.2]	16.1 [9.58-21.6]	11.2 [3.03-27.1]

Data represented as median [interquartile range]

In the non-AI and AI groups combined, late-MI patients (6 hrs-14 days old) were characterized by a higher percentage of unstable plaques (63% versus 52% in the acute MI group; p=0.05, with no differences between the no-AI and AI groups), but no significant differences in any of the other plaque characteristics were found (data not shown).

Lymphocyte infiltration

In patients with acute MI, no significant differences between the non-AI, and the AI group were found (p=0.08; p=0.37; p=0.62, for intima, media and adventitia, respectively; Fig 2A-2C and suppl. Table B). In patients with late MI, lymphocyte densities were significantly higher in the non-AI group (p=0.001; p=0.005; p<0.0001, for intima, media and adventitia, respectively). Overall, lymphocyte densities were significantly higher in late-MI patients in all layers (suppl. Table C and D).

Macrophage infiltration

In both patients with acute MI and late MI, the density of intimal macrophages was similar between the non-AI and AI group (Fig. 2D and suppl. Table B). Overall, macrophage density was higher in the late MI versus the early MI patients (suppl. Table C and D).

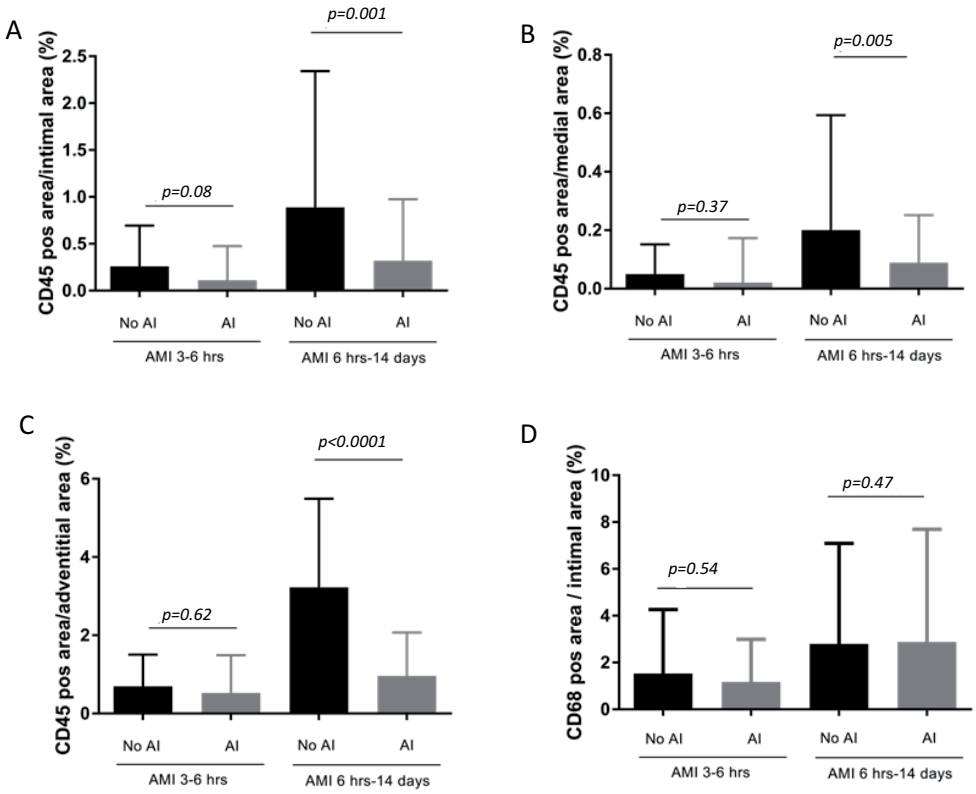

Figure 2 Lymphocyte and macrophage density per group

Percentage of CD45 positive area (indicative of lymphocytes) **A:** in the intima, **B:** media and **C:** adventitia. **D:** Percentage of CD68 positive area (indicative of macrophages) in the intima. Groups are based on infarct duration (3-6 hrs vs 6hrs-14days) and the presence of non-cardiac acute inflammation (AI) diagnosed at autopsy. AMI; acute myocardial infarction. Bars represent median and interquartile range.

Supplemental Table C Inflammatory cell densities early vs. late

	3-6 hrs	6 hrs - 14 days	p-value
Lymphocytes (surface area, %)			
Intima	0.25 [0.06-0.64]	0.55 [0.15-1.48]	0.001
Media	0.05 [0.01-0.15]	0.12 [0.03-0.34]	< 0.001
Acventitia	0.66 [0.26-1.49]	1.35 [0.51-3.13]	< 0.001
Macrophages (surface area, %)			
Intima	0.40 [0.10-1.38]	0.76 [0.18-5.08]	0.002
Neutrophilic granulocytes (cells/mm^2)			
Intima	1.25 [0.44-3.02]	1.30 [0.46-2.90]	0.833
Media	0.00 [0.00-1.23]	0.39 [0.00-2.13]	0.020
Acventitia	4.00 [1.24-7.77]	4.10 [2.16-8.80]	0.125
Mast cells (cells/mm^2)			
Intima	1.51 [0.51-3.84]	1.30 [0.41-2.65]	0.253
Media	0.00 [0.00-0.86]	0.78 [0.00-3.51]	< 0.001
Acventitia	15.6 [7.77-32.4]	13.2 [5.64-25.4]	0.125

Data represented as median [interquartile range]

Supplemental Table D Inflammatory cell densities early vs. late subdivided by non-AI and AI

	No AI, 3-6 hrs	No AI, 6 hrs-14 days	P-value	AI, 3-6 hrs	AI, 6 hrs-14 days	P-value
Lymphocytes (surface area %)						
Intima	0.26 [0.07-0.70]	0.89 [0.37-2.34]	<0.001	0.11 [0.02-0.48]	0.31 [0.10-0.98]	0.016
Media	0.05 [0.01-0.15]	0.20 [0.08-0.59]	<0.001	0.02 [0.00-0.17]	0.09 [0.02-0.25]	0.062
Adventitia	0.70 [0.27-1.51]	3.23 [0.89-5.49]	<0.001	0.53 [0.24-1.49]	0.96 [0.33-2.07]	0.153
Macrophages (surface area %)						
Intima	0.40 [0.12-1.56]	0.73 [0.34-5.24]	0.005	0.36 [0.08-1.13]	0.83 [0.17-5.04]	0.062
Neutrophilic granulocytes (cells / mm^2)						
Intima	1.22 [0.44-2.80]	1.57 [0.80-4.58]	0.043	2.03 [0.37-3.72]	1.10 [0.36-2.52]	0.159
Media	0.00 [0.00-1.05]	0.77 [0.00-3.71]	0.013	0.00 [0.00-2.49]	0.14 [0.00-1.77]	0.993
Adventitia	4.02 [0.99-7.67]	6.20 [2.66-13.9]	0.009	3.75 [2.00-9.19]	3.96 [1.83-7.65]	0.672
Mast cells (cells / mm^2)						
Intima	1.14 [0.47-3.28]	1.75 [1.16-3.14]	0.115	2.26 [1.43-4.66]	0.85 [0.21-2.02]	0.002
Media	0.00 [0.00-0.76]	1.85 [0.00-4.18]	<0.001	0.63 [0.00-3.17]	0.41 [0.00-3.33]	0.982
Adventitia	14.8 [7.59-43.4]	16.1 [9.58-21.6]	0.746	18.4 [10.5-24.2]	11.2 [3.03-27.1]	0.321

Data represented as median [interquartile range]

Neutrophilic granulocyte infiltration

In patients with acute AMI, no significant differences in neutrophil density was found between the non-AI and the AI groups (p=0.32; p=0.22; p=0.35 for intima, media and adventitia, respectively (Fig. 3A-3C and suppl. Table B). Acute systemic inflammation, however, did affect neutrophil densities in late-MI patients, with lower densities in the intima and adventitia in patients with AI (p=0.02 and p=0.04, respectively). Only in the tunica media, late-MI patients showed overall higher neutrophilic granulocyte density compared to acute MI patients (suppl. Table C and D).

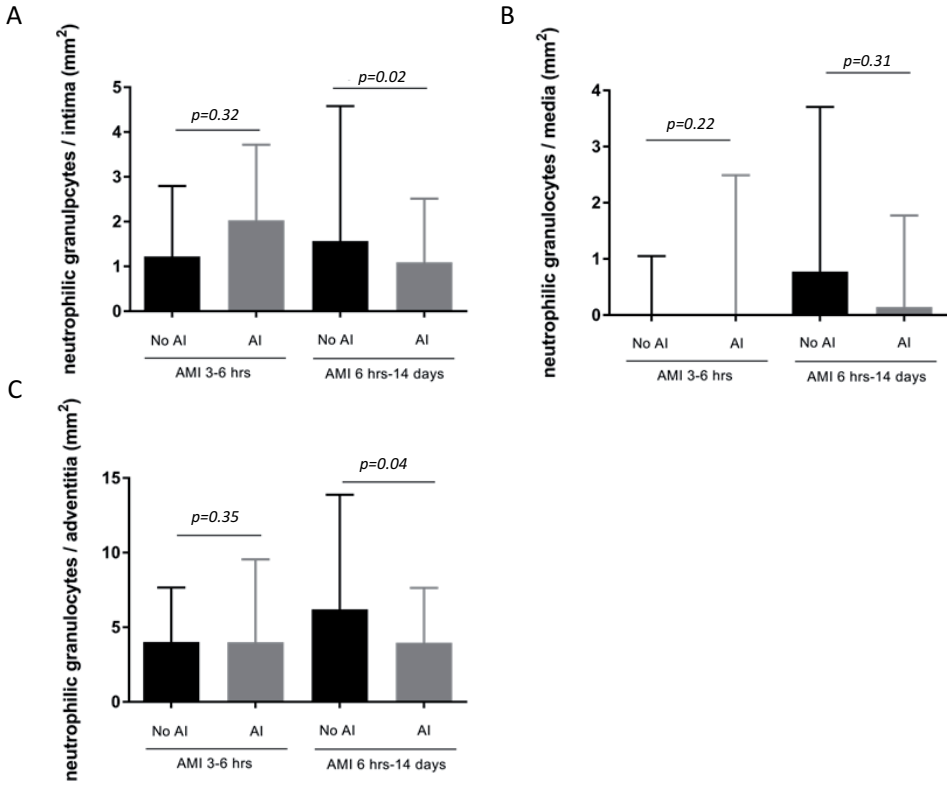

Figure 3 Neutrophil density per group

Percentage of MPO positive area (indicative of neutrophils) **A;** in the intima, **B:** media and **C:** adventitia. Groups are based on infarct duration (3-6 hrs vs 6hrs-14days) and the presence of non-cardiac acute inflammation (AI) diagnosed at autopsy. AMI; acute myocardial infarction. Bars represent median and interquartile range.

Mast cell infiltration

In acute MI patients, mast cells were significantly more dominant in the intima and media in the AI group than in the non-AI group (p=0.02 and p=0.004, respectively), but not in the adventitia (Fig. 4A-4C and suppl. Table B). In late MI patients, systemic inflammation only affected mast cell density in the intima, with significantly lower mast cell counts in the AI versus the non-AI group. In the non-AI and AI groups combined, late-MI patients showed a marked increase in mast cell density in the media compared to early MI patients (suppl. Table C and D).

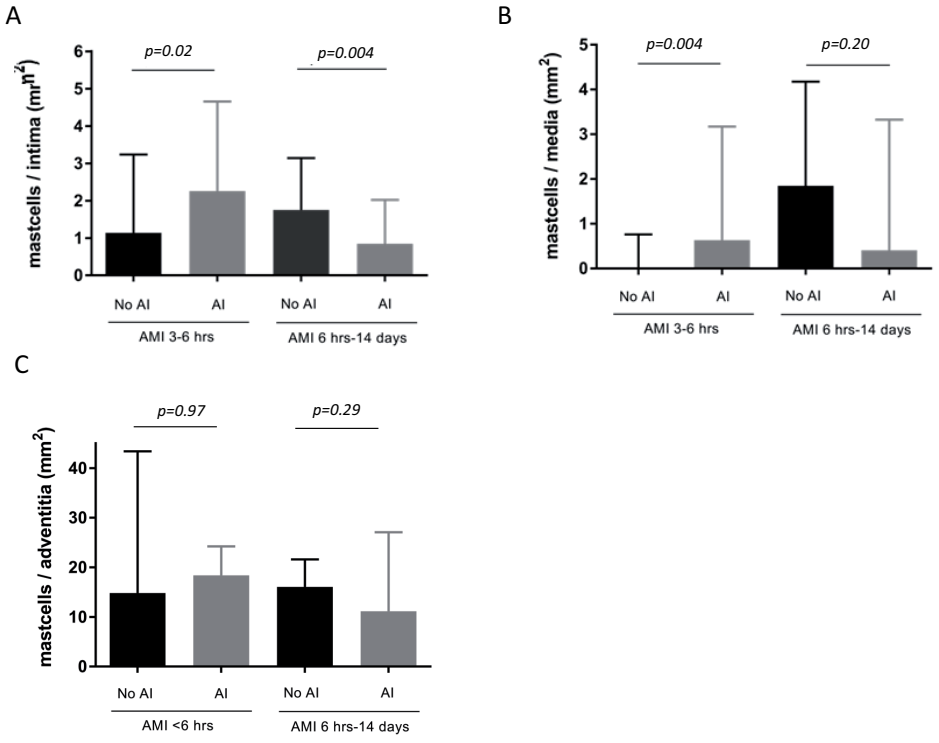

Figure 4 Mast cell density per group

Percentage of tryptase positive cells (indicative of mast cells) **A;** in the intima, **B:** media and **C:** adventitia. Groups are based on infarct duration (3-6 hrs vs 6hrs-14days) and the presence of non-cardiac acute inflammation (AI) diagnosed at autopsy. AMI; acute myocardial infarction. Bars represent median and interquartile range.

DISCUSSION

Given the short-term effects of systemic inflammation on cardiovascular event risk, we hypothesized that an acute episode of infection rapidly enhances coronary wall inflammation and plaque instability. In addition, the presence of infection could contribute to pro-inflammatory changes in the arterial wall evoked by recent MI itself [14].

In acute MI, we found that the presence of acute systemic infection was associated with an increased mast cell density in the intima and media of atherosclerotic coronary arteries. The density of other inflammatory cells, however, was not increased, nor was there a clear effect on histopathological signs of plaque instability. To our knowledge, we are the first to describe an increase of mast cells in coronary arteries as a result of infection. This increase is of potential interest since mast cells in the coronary arterial walls are linked to plaque destabilization[26] and cardiovascular risk[27]. Although mast cells are mostly found and studied in the adventitia, it has recently been suggested that mast cells in the intima and media of atherosclerotic coronary lesions may contribute to the onset of MI through plaque-destabilizing or spasm-inducing properties[26], involving the release of mediators such as histamine, chymase, tryptase, growth factors, and pro-inflammatory cytokines[28, 29]. In several studies in atherosclerotic mouse models, inhibition of mast cells reduced plaque instability[30-34] whereas activation of mast cells had the opposite effect[31, 34, 35]. Moreover, the number of mast cells in human carotid atherosclerotic plaques was shown to be predictive for the occurrence of cardiovascular events, irrespective of their level of activation[27]. In addition, via release of vasoactive mediators, especially histamine, mast cells have been implicated in provoking coronary contraction or even spasms, which can reduce coronary flow, but also destabilize the plaque[36-39]. Thus, our finding of enhanced mast cell density in the media of AMI patients with acute infection may at least partially explain the increased cardiovascular event risk seen shortly after infection [1].
Why only mast cells and not the other inflammatory cells infiltrate the coronary arteries of patients with infection is not clear. This finding does, however, not fully exclude a role for activated lymphocyte and macrophage detection, because their activation may cause loss of epitopes and cells can become less detectable by CD68 and CD45-staining, respectively [18]. Alternatively -and perhaps more likely- is that decreased lymphocyte and macrophage density is a true representation of their role in early AMI occurring during acute infection. This may, for example, be explained by preferential recruitment of these cells in infected tissue elsewhere in the body.

With respect to the mid- to longer-term changes in coronary inflammation after acute MI, our findings corroborate earlier murine and human studies suggesting that MI itself contributes to more widespread plaque inflammation and instability[14, 26]. We did not find

evidence that infection enhanced these post-MI pro-inflammatory changes. An effect of post-AMI infection on plaque stability and subsequent cardiovascular event rate has been proposed[15], but our findings argue against a dominant role for plaque inflammation in this phenomenon.

Important limitations have to be taken into consideration. Firstly, the total number of studied patients is low, particularly in subgroups. This study is the first of its kind, but can, in view of the limited size, only be hypothesis-generating. In addition, the optimum time after MI to study coronary arteries with respect to inflammatory activity is unknown. A maximum period of 6 hours may not fully preclude effects of infarction event itself. For the patients that died between 6 hrs and 14 days after onset of AMI, infection could have been present either pre-AMI, or developed post-AMI at any given time.

In conclusion, we found that the presence of infection enhances mast cell infiltration in the intima and media of coronary arteries, but does not seem to cause recruitment of other inflammatory cells or increase plaque instability. Mast cell involvement may be a partial explanation for the increased cardiovascular event risk seen shortly after infection. We re-established that AMI enhances pro-inflammatory changes of the vessel wall, but did not observe an effect of infection hereon.

REFERENCES

1 Smeeth L, Thomas SL, Hall AJ, Hubbard R, Farrington P and Vallance P. Risk of myocardial infarction and stroke after acute infection or vaccination. N Engl J Med 2004;351:2611-2618

2 Meier CR, Jick SS, Derby LE, Vasilakis C and Jick H. Acute respiratory-tract infections and risk of first-time acute myocardial infarction. Lancet 1998;351:1467-1471

3 Elkind MS, Carty CL, O'Meara ES, Lumley T, Lefkowitz D, Kronmal RA and Longstreth WT, Jr. Hospitalization for infection and risk of acute ischemic stroke: the Cardiovascular Health Study. Stroke 2011;42:1851-1856

4 Lalmohamed A, Vestergaard P, Klop C, Grove EL, de BA, Leufkens HG, van Staa TP and de VF. Timing of acute myocardial infarction in patients undergoing total hip or knee replacement: a nationwide cohort study. Arch Intern Med 2012;172:1229-1235

5 Cohen MC and Aretz TH. Histological analysis of coronary artery lesions in fatal postoperative myocardial infarction. Cardiovasc Pathol 1999;8:133-139

6 Corrales-Medina VF, Madjid M and Musher DM. Role of acute infection in triggering acute coronary syndromes. Lancet Infect Dis 2010;10:83-92

7 Madjid M, Vela D, Khalili-Tabrizi H, Casscells SW and Litovsky S. Systemic infections cause exaggerated local inflammation in atherosclerotic coronary arteries: clues to the triggering effect of acute infections on acute coronary syndromes. Tex Heart Inst J 2007;34:11-18

8 Libby P. Inflammation in atherosclerosis. Nature 2002;420:868-874

9 Maier W, Altwegg LA, Corti R, Gay S, Hersberger M, Maly FE, Sutsch G, Roffi M, Neidhart M, Eberli FR, Tanner FC, Gobbi S, von EA and Luscher TF. Inflammatory markers at the site of ruptured plaque in acute myocardial infarction: locally increased interleukin-6 and serum amyloid A but decreased C-reactive protein. Circulation 2005;111:1355-1361

10 Sadowski M, Zabczyk M and Undas A. Coronary thrombus composition: links with inflammation, platelet and endothelial markers. Atherosclerosis 2014;237:555-561

11 Fuijkschot WW, Groothuizen WE, Appelman Y, Radonic T, van Royen N, van Leeuwen MA, Krijnen PA, van der Wal AC, Smulders YM and Niessen HW. Inflammatory cell content of coronary thrombi is dependent on thrombus age in patients with ST-elevation myocardial infarction. J Cardiol 2017;69:394-400

12 Thompson JC, Jayne C, Thompson J, Wilson PG, Yoder MH, Webb N and Tannock LR. A brief elevation of serum amyloid A is sufficient to increase atherosclerosis. J Lipid Res 2015;56:286-293

13 Kaynar AM, Yende S, Zhu L, Frederick DR, Chambers R, Burton CL, Carter M, Stolz DB, Agostini B, Gregory AD, Nagarajan S, Shapiro SD and Angus DC. Effects of intra-abdominal sepsis on atherosclerosis in mice. Crit Care 2014;18:469

14 Dutta P, Courties G, Wei Y, Leuschner F, Gorbatov R, Robbins CS, Iwamoto Y, Thompson B, Carlson AL, Heidt T, Majmudar MD, Lasitschka F, Etzrodt M, Waterman P, Waring MT, Chicoine AT, van der Laan AM, Niessen HW, Piek JJ, Rubin BB, Butany J, Stone JR, Katus HA, Murphy SA, Morrow DA, Sabatine MS, Vinegoni C, Moskowitz MA, Pittet MJ, Libby P, Lin CP, Swirski FK, Weissleder R and Nahrendorf M. Myocardial infarction accelerates atherosclerosis. Nature 2012;487:325-329

15 Truffa AA, Granger CB, White KR, Newby LK, Mehta RH, Hochman JS, Patel MR, Pieper KS, Al-Khalidi HR, Armstrong PW and Lopes RD. Serious infection after acute myocardial infarction: incidence, clinical features, and outcomes. JACC Cardiovasc Interv 2012;5:769-76

16 Abou-Raya A and Abou-Raya S. Inflammation: a pivotal link between autoimmune diseases and atherosclerosis. Autoimmun Rev 2006;5:331-337

17 Stojan G and Petri M. Atherosclerosis in systemic lupus erythematosus. J Cardiovasc Pharmacol 2013;62:255-62

18 Fuijkschot WW, Morrison MC, van der Linden R, Krijnen PA, Zethof IP, Theyse LF, Kleemann R, Niessen HW and Smulders YM. Orthopedic surgery increases atherosclerotic lesions and necrotic core area in ApoE-/- mice. Atherosclerosis 2016;255:164-170

19 Wu Y and Zhou BP. Inflammation: a driving force speeds cancer metastasis. Cell Cycle 2009;8:3267-73

20 Fishbein MC, Maclean D and Maroko PR. The histopathologic evolution of myocardial infarction. Chest 1978;73:843-849

21 van der Laan AM, Ter Horst EN, Delewi R, Begieneman MP, Krijnen PA, Hirsch A, Lavaei M, Nahrendorf M, Horrevoets AJ, Niessen HW and Piek JJ. Monocyte subset accumulation in the human heart following acute myocardial infarction and the role of the spleen as monocyte reservoir. Eur Heart J 2014;35:376-385

22 White PD, Mallory GK and Salcedo-Salgar J. The Speed of Healing of Myocardial Infarcts. Trans Am Clin Climatol Assoc 1936;52:97-104

23 Krijnen PA, Ciurana C, Cramer T, Hazes T, Meijer CJ, Visser CA, Niessen HW and Hack CE. IgM colocalises with complement and C reactive protein in infarcted human myocardium. J Clin Pathol 2005;58:382-388

24 Kolodgie FD, Virmani R, Burke AP, Farb A, Weber DK, Kutys R, Finn AV and Gold HK. Pathologic assessment of the vulnerable human coronary plaque. Heart 2004;90:1385-91

25 Woudstra L, Biesbroek PS, Emmens RW, Heymans S, Juffermans LJ, van Rossum AC, Niessen HW and Krijnen PA. Lymphocytic myocarditis occurs with myocardial infarction and coincides with increased inflammation, hemorrhage and instability in coronary artery atherosclerotic plaques. Int J Cardiol 2017;232:53-62

26 Kupreishvili K, Fuijkschot WW, Vonk AB, Smulders YM, Stooker W, Van Hinsbergh VW, Niessen HW and Krijnen PA. Mast cells are increased in the media of coronary lesions in patients with myocardial infarction and may favor atherosclerotic plaque instability. J Cardiol 2017;69:548-554

27 Willems S, Vink A, Bot I, Quax PH, de Borst GJ, de Vries JP, van de Weg SM, Moll FL, Kuiper J, Kovanen PT, de Kleijn DP, Hoefer IE and Pasterkamp G. Mast cells in human carotid atherosclerotic plaques are associated with intraplaque microvessel density and the occurrence of future cardiovascular events. Eur Heart J 2013;34:3699-3706

28 Lappalainen J, Lindstedt KA, Oksjoki R and Kovanen PT. OxLDL-IgG immune complexes induce expression and secretion of proatherogenic cytokines by cultured human mast cells. Atherosclerosis 2011;214:357-63

29 Meng Z, Yan C, Deng Q, Dong X, Duan ZM, Gao DF and Niu XL. Oxidized low-density lipoprotein induces inflammatory responses in cultured human mast cells via Toll-like receptor 4. Cell Physiol Biochem 2013;31:842-53

30 Bot I, Bot M, van Heiningen SH, van Santbrink PJ, Lankhuizen IM, Hartman P, Gruener S, Hilpert H, van Berkel TJ, Fingerle J and Biessen EA. Mast cell chymase inhibition reduces atherosclerotic plaque progression and improves plaque stability in ApoE-/- mice. Cardiovasc Res 2011;89:244-52

31 den Dekker WK, Tempel D, Bot I, Biessen EA, Joosten LA, Netea MG, van der Meer JW, Cheng C and Duckers HJ. Mast cells induce vascular smooth muscle cell apoptosis via a toll-like receptor 4 activation pathway. Arterioscler Thromb Vasc Biol 2012;32:1960-9

32 Guo T, Chen WQ, Zhang C, Zhao YX and Zhang Y. Chymase activity is closely related with plaque vulnerability in a hamster model of atherosclerosis. Atherosclerosis 2009;207:59-67

33 Sun J, Sukhova GK, Wolters PJ, Yang M, Kitamoto S, Libby P, MacFarlane LA, Mallen-St Clair J and Shi GP. Mast cells promote atherosclerosis by releasing proinflammatory cytokines. Nat med 2007;13:719-24

34 Bot I, de Jager SC, Bot M, van Heiningen SH, de Groot P, Veldhuizen RW, van Berkel TJ, von der Thusen JH and Biessen EA. The neuropeptide substance P mediates adventitial mast cell activation and induces intraplaque hemorrhage in advanced atherosclerosis. Circ Res 2010;106:89-92

35 Bot I, de Jager SC, Zernecke A, Lindstedt KA, van Berkel TJ, Weber C and Biessen EA. Perivascular mast cells promote atherogenesis and induce plaque destabilization in apolipoprotein E-deficient mice. Circulation 2007;115:2516-25

36 Ozben B and Erdogan O. The role of inflammation and allergy in acute coronary syndromes. Inflamm Allergy Drug Targets 2008;7:136-44.

37 Alevizos M, Karagkouni A, Panagiotidou S, Vasiadi M and Theoharides TC. Stress triggers coronary mast cells leading to cardiac events. Ann Allergy Asthma Immunol 2014;112:309-16

38 Kalsner S and Richards R. Coronary arteries of cardiac patients are hyperreactive and contain stores of amines: a mechanism for coronary spasm. Science 1984;223:1435-7

39 Fassio F and Almerigogna F. Kounis syndrome (allergic acute coronary syndrome): different views in allergologic and cardiologic literature. Intern Emerg Med 2012;7:489-95

6

Mast cells are increased in the media of coronary lesions in patients with myocardial infarction and may favour atherosclerotic plaque

Wessel W. Fuijkschot; Linde Woudstra; Rianne van der Linden; Danae Beskers; Ilse P.A. Zethof; Paul A.J. Krijnen; Hans W.M. Niessen and Yvo M. Smulders

J Cardiol 2017;69:548-554

ABSTRACT

Objective: Mast cells (MCs) may play an important role in plaque destabilization and atherosclerotic coronary complication. Here we have studied the presence of MCs in the intima and media of unstable and stable coronary lesions at different time points after myocardial infarction (MI).

Methods: Coronary arteries were obtained at autopsy from patients with acute MI (up to 5 days old; n=27) and with chronic MI (5 - 14 days old; n=18) as well as sections from controls without cardiac disease (n=10). Herein, tryptase-positive MCs were quantified in the intima and media of both unstable and stable atherosclerotic plaques in infarct-related and non-infarct-related coronary arteries.

Results: In the media of both acute and chronic MI patients, the number of MCs was significantly higher than in controls. This was also found when evaluating unstable and stable plaques separately. In patients with chronic MI the number of MCs in unstable lesions was significantly higher than in stable lesions. This coincided with a significant increase in the relative number of instable plaques in patients with chronic MI compared with control and acute MI. No differences in MC density were found between infarct-related and non-infarct-related coronary arteries in patients with MI.

Conclusions: The presence of MCs in the media of both stable and unstable atherosclerotic coronary lesions after MI suggests that MCs may be involved in the onset of MI and, on the other hand, that MI triggers intra-plaque infiltration of MCs especially in unstable plaques, possibly increasing the risk of re-infarction.

INTRODUCTION

Myocardial infarction (MI) most often is the result of coronary atherosclerotic plaque rupture and resultant thrombus formation. Plaques that are prone to cause MI, so-called unstable or vulnerable plaques, are characterized by a thin fibrous cap and/or an extensive presence of inflammatory cells, including macrophages, lymphocytes and mast cells (MCs). Although best known for their role in allergic reactions, MCs have been shown to be involved in the initiation and progression of atherosclerosis[1, 2]. Notably, MCs may also play an important role in the destabilization of atherosclerotic plaques and coronary atherosclerotic complication. MCs accumulate in the vulnerable shoulder region of human coronary atheromas, at the predilection sites of atheromatous erosion/rupture[3] and at the sites of erosion or rupture in infarct-related coronary arteries[4].

How MCs induce atherosclerotic complications is not completely known. However, evidence supports a role for MCs in the destabilization of atherosclerotic plaques via the local release of vasoactive, neurosensitizing, pro-angiogenic, pro-atherogenic and pro-inflammatory mediators, such as histamine, chymase and tryptase. Release of these mediators can cause vasospasms[5], intraplaque hemorrhage[6], intraplaque neo-vascularization[7, 8] and/or collagen degradation via activation of metalloproteinases resulting in weakening of the fibrous cap[9]. The role of MCs in plaque destabilization was further highlighted in atherosclerotic apolipoprotein E-deficient mice, wherein local activation of MCs resulted in increased intraplaque hemorrhage, macrophage apoptosis and monocyte recruitment[10], whereas inhibition of chymase enhanced plaque collagen content and reduced necrotic core size and intraplaque hemorrhage[11].

It has been suggested that in particular MCs located in the adventitia are associated with coronary atherosclerotic complications. In coronary arteries MCs were found predominantly in the adventitia, i.e. 10 times more as compared to the intima[12]. Furthermore, an increased number of degranulated MCs was found in the adventitia surrounding ruptured plaques in infarct-related coronary arteries in patients with MI[13]. However, knowledge regarding a putative relation between MCs present in the intima and media of vulnerable and stable coronary lesions and MI is scarce. As many of the aforementioned plaque-destabilizing properties of MC take effect in the intima and media of lesions, we hypothesized that MCs located in these layers could be involved in plaque instability. For this, we quantified MCs in these vessel layers of non-ruptured unstable and stable coronary lesions at different time points after MI and compared those with control patients.

MATERIALS AND METHODS

Patient material

A total of 55 patients who were referred to the Department of Pathology of the VU University Medical Center for clinical autopsy between 1999 and 2003, were retrospectively included in this study. In this period approximately 1000 clinical autopsies were conducted at the VU university medical center. In an estimated 10 to 20 % of these cases a recent MI was found. Sections of coronary arteries were obtained at autopsy from patients with acute MI (infarct of up to 5 days old; n=27) and chronic MI (infarct of 5 to 14 days old; n=18) or as a control from patients without cardiac disease (n=10, Table 1 and 2). Control patients were age-matched and sex-matched. All MI patients showed macroscopical evidence for a recent left ventricular MI, as identified by reduced nitro blue tetrazolium (NBT) staining, indicative for a loss of lactate dehydrogenase (LDH) of the injured myocardial tissue, of a mid-ventricular cross section of the heart. The patients were subsequently categorized into two phases of post-AMI healing based on the following microscopic criteria[14, 15]: acute MI patients showed microscopical evidence of jeopardized myocardium (cardiomyocyte condensation, combined with loss of nuclei and cross striations), with or without evidence of extravasation of neutrophilic granulocytes in the infarction area corresponding to an infarct age of between approximately 3 hours to 5 days after MI. chronic MI patients showed microscopical evidence of cell-rich granulation tissue formation and collagen deposition in the infarction area corresponding to an infarct age of approximately 5 to 14 days after MI. The control patients showed normal NBT staining.

Table 1 Characteristics of coronary artery tissue samples

	Control	Acute MI (< 5 days old)	Chronic MI (5-14 days old)
Number of patients	10	27	18
Age (mean, range)	62.6 (37 – 94)	67.4 (24 – 84)	62.8 (31 – 82)
Sex, male / female (n)	6 / 4	18 / 9	13 / 5
Total number of lesions	35	70	46
Number of unstable lesions	16	32	32
Number of stable lesions	19	38	14

Table 2 Patient characteristics

Patient	Sex	Age	Primary cause of death	Secondary pathologies
Control patients without cardiac disease				
1	M	71	Sepsis	Cholecystitis, peritonitis
2	M	73	Pneumonia	Prostate carcinoma
3	M	80	Subdural hemorrhage	Alcohol abuse Liver cirrhosis COPD
4	F	38	Pneumonia	Cervical cancer
5	F	94	Intracranial hemorrhage	Pneumonia
6	M	37	Not found	-
7	M	67	Respiratory insufficiency	Lung cancer
8	F	52	Pulmonary hypertension	CREST syndrome
9	M	55	Sepsis	Pyelonephritis
10	F	59	Pneumonia	Oesophageal cancer
Control patients with myocardial infarction (< 5 days old; aMI)				
1	M	80	AMI	DM Hypertension Hypercholesterolemia
2	M	65	AMI	DM COPD Hypethyroidism
3	F	83	AMI	Burn wounds
4	F	81	AMI	DM Hypertension Thyrotoxicosis
5	F	71	AMI	-
6	M	57	AMI + pulmonary embolism	-
7	F	84	AMI	Pneumonia DM Hypertension
8	M	43	AMI	Systemic scleroderma
9	F	72	AMI	-
10	F	72	AMI + intestinal necrosis	-
11	M	55	AMI + pulmonary embolism	Colon cancer
12	M	72	AMI + pulmonary embolism	Stomach cancer
13	M	70	AMI	-
14	M	60	AMI	-
15	M	58	AMI + sepsis	Enterolcolitis
16	M	79	AMI	-
17	M	51	AMI	-
18	M	79	AMI + intracerebral hemorrhage	Thyroiditis

Patient	Sex	Age	Primary cause of death	Secondary pathologies
19	F	59	AMI + liver and kidney failure	Alcohol abuse Liver cirrhosis
20	M	75	AMI + ruptured aneurysm	Laryngeal cancer DM
21	F	71	AMI	Pneumonia
22	M	75	AMI	-
23	M	65	AMI	Laryngeal cancer
24	M	24	AMI	Alcohol abuse Cocaine abuse Heroin abuse
25	M	82	AMI	Laryngeal cancer Pneumonia
26	F	74	AMI	Hypertension Hypercholesterolemia
27			AMI + aspergillus infection	DM Polymyositis (prednisolone use)
Control patients with myocardial infarction (5-14 days old; cMI)				
1	M	48	AMI	Fever e.c.i.
2	M	62	AMI	-
3	M	56	AMI	-
4	F	76	AMI + a. femoralis hemorrhage	COPD Hypertension Excessive anticoagulants
5	M	78	AMI	-
6	M	67	AMI	Hypercholesterolemia DM
7	M	48	AMI	Hypertension
8	M	74	AMI + cardiac tamponade	-
9	M	71	AMI + sepsis	Pneumonia Hemorrhagic gastritis
10	F	60	AMI + kidney failure	DM Hypertension
11	M	56	AMI	-
12	F	48	AMI + pulmonary embolism	Acute myeloid Leukemia
13	M	65	AMI	-
14	M	82	AMI	-
15	F	61	AMI	-
16	F	78	AMI + cardiac tamponade	-
17	M	31	AMI + pneumonia	-
18	M	69	AMI + sepsis	Ischemic enteritis

M: male. F: female. AMI: acute myocardial infarction. DM: diabetes mellitus. COPD: chronic obstructive pulmonary disease.

All patients were autopsied within 24 hours after death. From all patients, the left and right coronary arteries were excised from their root at the aorta to the point where they enter the myocardium. Sections with the strongest stenosis were identified macroscopically and subsequently processed separately for histological and immunohistochemical analyses. For this, the selected cross tissue sections were fixed in 4% paraformaldehyde and subsequently decalcified in buffered formic acid, where after the sections were embedded in paraffin.

As ruptured culprit lesions or intra-coronary thrombi are rarely found at autopsy in patients with MI, the infarct-related coronary arteries were identified based on the location of the infarcts. The infarct location was determined based on the area of reduced NBT staining, indicative for a loss of LDH, of a mid-ventricular cross section of the heart. The branch of the coronary artery responsible for perfusion of the area of the heart wherein the infarct is situated was then identified as the infarct-related coronary artery.

In the VU University Medical Center patient material can be used for research after completion of the diagnostic process as part of the patient contract and, in case of autopsy, after relatives have given explicit written consent. This is conform the ethical guidelines set up by the World Medical Association (The declaration of Helsinki).

Immunohistochemistry

Coronary artery tissue sections (4 µm thick) were mounted on microscope slides and deparaffinized for 10 min in xylene at room temperature and dehydrated through descending concentrations of ethanol. Endogenous peroxidase activity was blocked by incubation in 0.3% (v/v) H2O2 in methanol for 30 minutes. Tissue sections were subjected to antigen retrieval by boiling in 10 mmol/L sodium citrate buffer, pH 6, for 10 minutes in a microwave oven. The antibodies and normal serum were diluted in PBS containing 1% (w/v) bovine serum albumin (BSA). Tissue sections were pre-incubated for 10 minutes with normal rabbit serum, followed by incubation with mouse-anti-human tryptase mAb (Dako, clone AA1, 1:1000 dilution) for 1 hour. After washing in PBS the slides were incubated with biotin-conjugated rabbit anti-mouse antibody (Dako, 1:500 dilution) for 30 minutes. After washing in PBS the slides were incubated with streptavidin–biotin complex (1:1000 dilution) for 1 hour, followed by incubation with biotinylated tyramine (1:1000 dilutions) for 20 minutes. Staining was visualized with 3, 3'-diaminobenzidine (0.1 mg/mL, 0.02% H2O2). Slides were counterstained with haematoxylin and mounted with Depex.

Quantification of the MCs was performed by three independent investigators (KK, WWF, HWMN). Tryptase-positive MCs were quantified in the intima and media. For each lesion one cross section was scored. Subsequently the surface areas of the scored intima and media were measured with a Leica DM/LM microscope, using QProdit v3.2 (Leica Microsystems, Wetzlar, Germany) as analytical software to present the number of MCs per mm2.

Plaque stability was determined on HE stained slides. For this, after deparaffinization and dehydration, the slides were incubated in haematoxylin for 5 minutes and then rinsed in water. The slides were then incubated in eosin for 2 minutes, rinsed in water with 1% ammonia and the covered. We defined unstable lesions as an atherosclerotic plaque with a thin fibrous cap and/or inflammatory cells infiltrating up to the endothelial layer of the intima[16].

Statistical analysis

Data analysis was performed with GraphPad Prism 4.0 and SPSS version 20 statistics software. Differences in MC number between the different groups in the different layers of the arterial wall as well as between the intima, media or adventitia within the groups were analyzed with an One-way ANOVA and independent samples t-tests when normal distributed, respectively with a Kruskal-Wallis test and subsequent Mann-Whitney U tests, if not. For the comparison between groups of the relative distribution (%) of stable vs. unstable plaques, crosstabs were used resulting in a Fisher's exact test generated p-value. A p value (two sided) of less than 0.05 was considered to be significant.

RESULTS

We quantified MCs per mm^2 in the intima and media of stable and unstable atherosclerotic lesions in coronary arteries at different time-points after onset of MI. Unstable lesions show a thin fibrous cap and inflammatory cells that migrate up to the endothelial layer of the intima Fig. 1A), whereas stable lesions show a profound fibrous cap (Fig. 1B). Tryptase-positive MCs were present scattered throughout the intima and media of coronary atherosclerotic lesions (Fig. 1C).

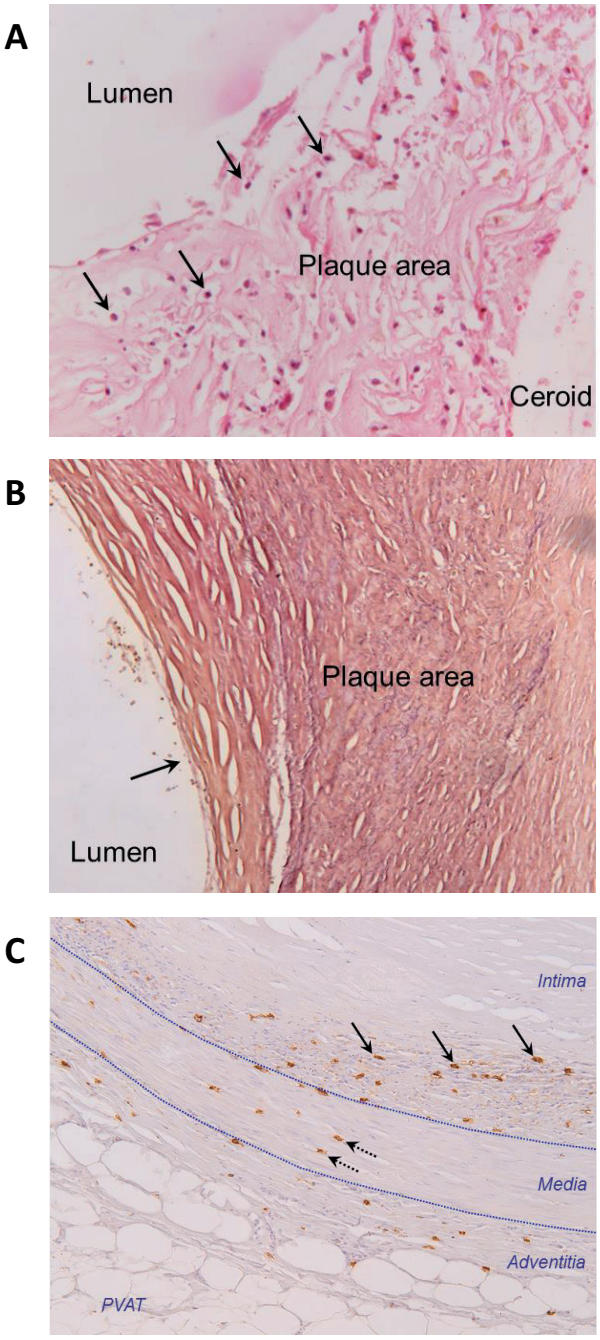

Figure 1

A: Example of an Hematoxylin and Eosin-stained unstable lesion. The atherosclerotic Plaque area shows a thin fibrous cap and inflammatory cells that infiltrate up to the endothelial layer of the intima (arrows). Original magnification 200x. **B:** Example of an Elastica von Gieson-stained stable lesion with a profound fibrous cap (arrow). Original magnification 100x. **C:** Representative image of tryptase-positive mast cells in the intima (solid arrows), media (broken arrows) of a coronary artery. Original magnification 100x.

In all analyzed lesions of MI patients, the density of MCs in the intima was lower than in the media, but not significantly. In contrast, in controls the density of MCs in the intima was significantly higher than in the media (p=0.004). In the intima of all analyzed patients (Fig. 2), there were no significant differences in MC density between control patients, patients with acute MI and patients with chronic MI (controls: 0.9 (0.3-2.7); aMI: 1.2 (0.3-2.8); cMI: 1.5 (0.6-4.6). The density of MCs in the media of both acute and chronic MI patients however, was significantly higher than in controls (controls: 0.0 (0.0-0.9); aMI: 2.4 (0.0-6.5); cMI: 2.3 (0.0-6.8); aMI p=0.001; cMI p=0,009.

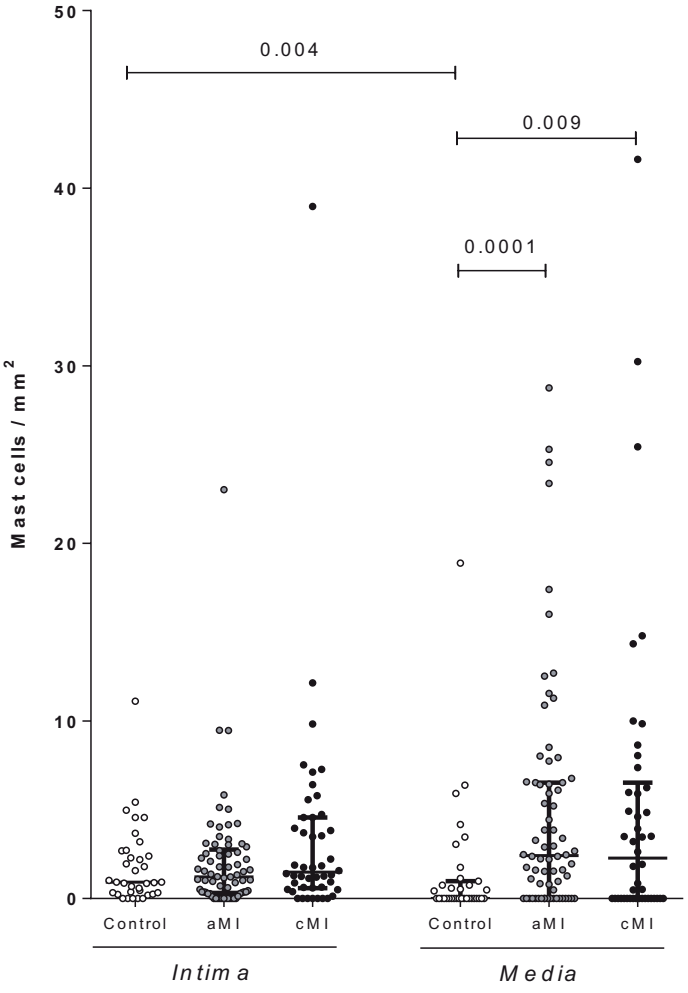

Figure 2

Quantification of tryptase-positive mast cells in the intima and media of coronary lesions in control patients, patients with acute MI (aMI; < 5 days old) and patients with chronic MI (cMI; 5 to 14 days old). Shown are the numbers of mast cells per mm2. Bars represent median and interquartile range.

Next, the density of MCs in the intima and media of unstable and stable lesions was analyzed separately (Fig. 3). In the intima we observed no significant differences in MC density between stable and unstable lesions, not in controls nor in patients with MI (not shown). In contrast, in the media of unstable lesions the MC density was significantly higher in patients with acute and chronic MI than in controls (controls: 0.0 (0.0-0.8); aMI: 2.7 (0.4-6.5); cMI: 3.5 (0.0-8.3); aMI p=0.004; cMI p=0,023). Similarly, stable lesions of acute MI patients had a significantly higher MC density in the media than those of controls (controls: 0.0 (0.0-1.5); aMI: 2.5 (0.4-7.7; p=0.022). However, in chronic MI patients this medial MC density of stable lesions was significantly lower than in patients with acute MI (1.8 (0.0-5.9); p=0.030).

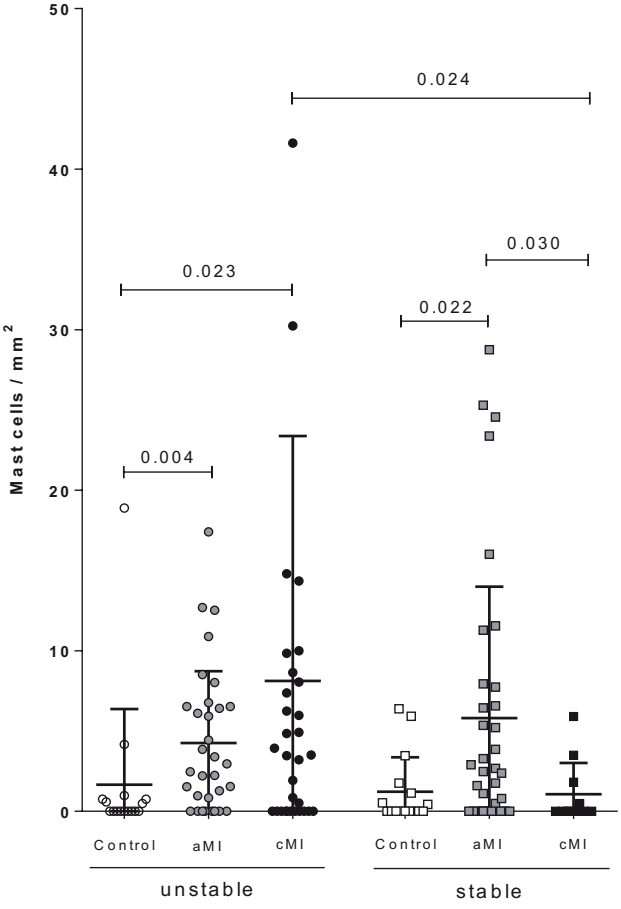

Figure 3

Comparison between the density of tryptase-positive mast cells in the media of unstable and stable coronary lesions in control patients, patients with acute MI (< 5 days old) and chronic MI (5 to 14 days old). Shown are the numbers of mast cells per mm^2 in control patients, patients with acute MI and chronic MI. Bars represent median and interquartile range.

In controls and acute MI patients, no significant differences were observed in the density of MCs in the media between stable and unstable lesions. However, in patients with chronic MI the density of MCs in unstable lesions was significantly higher than in stable lesions (p=0.024).

We subsequently analyzed for differences in the number of infiltrated MCs between the non-infarct and the infarct-related coronary arteries of both acute and chronic MI patients. In both patient groups we did not find significant differences in the number of MCs between infarct- and non-infarct-related coronary arteries. We then compared the number of MCs in unstable lesions, between the coronary arteries of control patients and the non-infarct-related and the infarct related coronary arteries of both aMI and cMI patients. Both in the intima and media, we found no significant differences between the number of MCs between the infarct-related and non-infarct-related arteries both in acute and chronic MI patients. In the intima, these numbers of MCs did not differ significantly compared to control coronary arteries either. However, the numbers of MCs in the media of the infarct-related coronary arteries of acute MI patients (Fig .4A) and the non-infarct-related coronary arteries in chronic MI patients (Fig. 4B) were significantly higher than in the coronary arteries of control patients. Moreover, the number of MCs in the media of non-infarct-related coronary arteries of chronic MI patients was significantly higher than in acute MI patients.

Remarkably, the relative distribution of stable versus unstable plaques differed significantly between acute and chronic MI patients (Fig. 5). Patients with chronic MI had relatively more unstable plaques as opposed to stable plaques than patients with acute MI (p=0.010) and control patients (p=0.040). No significant difference in this distribution was found between patients with acute MI and controls.

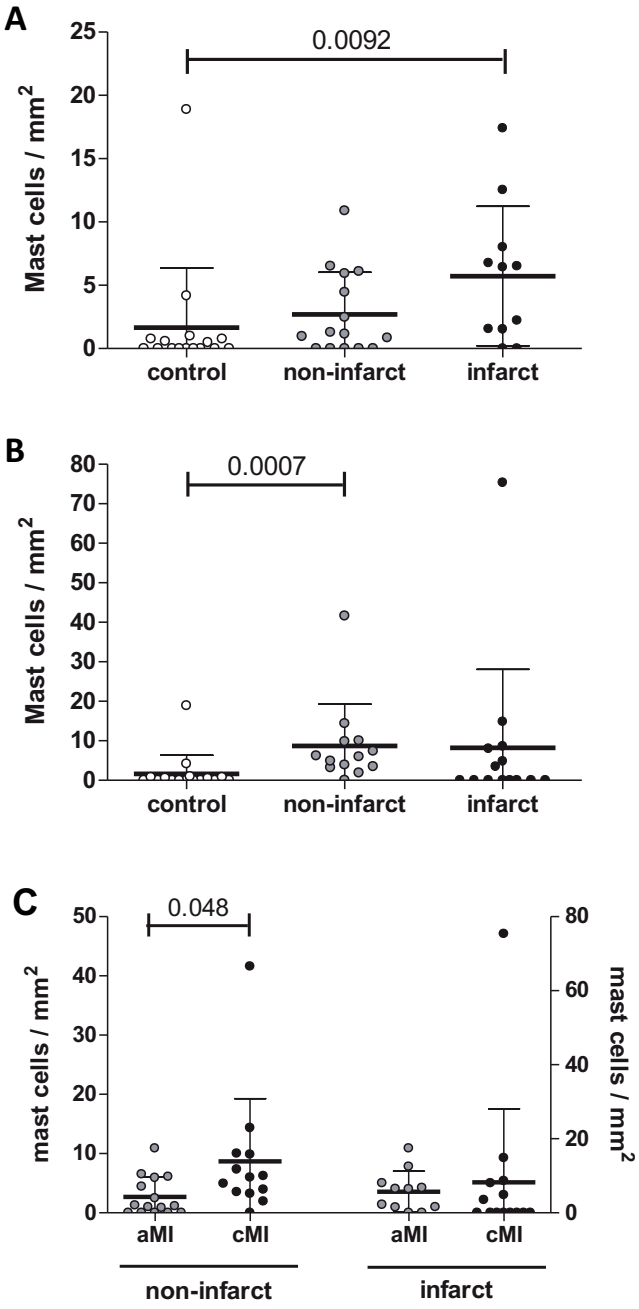

Figure 4

Comparison between the density of tryptase-positive mast cells in the media of unstable lesions, **A:** between the coronary arteries of control patients and the non-infarct-related and the infarct related coronary arteries of acute MI patients (< 5 days old), **B:** the coronary arteries of control patients and the non-infarct-related and the infarct related coronary arteries of chronic MI patients (5 to 14 days old) and **C:** the non-infarct-related and infarct related coronary arteries of acute and chronic MI patients.

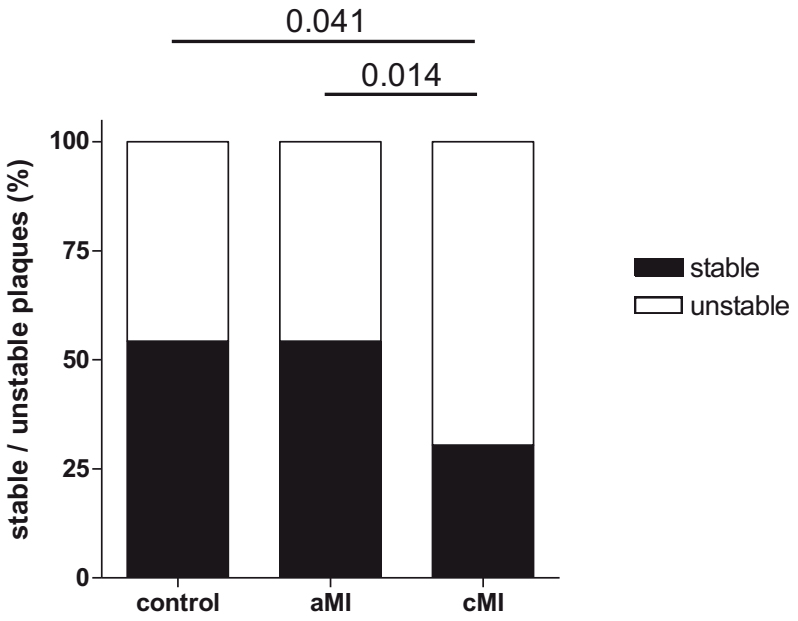

Figure 5

Comparison of the relative distribution (%) of stable and unstable coronary lesions between control patients (control), patients with acute MI (aMI: < 5 days old) and patients with chronic MI (cMI: 5 to 14 days old). P-values are based on crosstabs and the Fisher's exact test.

Finally, we have found no obvious differences in comorbidity occurrence between the groups that could account for the differences in MC density or plaque stability we have observed between the groups (Table 2).

DISCUSSION

Atherosclerotic coronary artery complication most often underlies the induction of MI. Evidence supporting a critical role for MCs in coronary plaque destabilization is accumulating. Perivascular MCs in particular have been associated with coronary atherosclerotic complication[12, 13]. In the present study we found both in the acute and chronic stage after MI a significantly increased presence of MCs compared with controls in the media. Interestingly, in unstable lesions MCs were increased significantly after MI, especially in the chronic stage. In contrast, in the stable lesions a significant decrease was found in the density of MCs in the chronic MI patients. This coincided with a significantly higher percentage of unstable plaques in chronic MI patients compared with controls and acute MI patients.

The increase in MCs in the media in unstable lesions of the infarct related coronary artery we describe here suggests that these cells may contribute to plaque destabilization and thereby to the onset of MI. MCs most likely contribute to plaque destabilization and atherosclerotic coronary complication via the release of atherogenic and vasoactive mediators such as histamine, chymase, tryptase, growth factors and pro-inflammatory cytokines[17, 18]. Indeed, in several studies in atherosclerotic mouse and hamster models inhibition of MCs reduced plaque instability[11, 19-21], whereas activation of MCs increased plaque instability[6, 10, 19], via effects on intraplaque collagen degradation, vascular smooth muscle cell apoptosis, monocyte infiltration and intraplaque hemorrhage. Moreover, the number of MCs in human carotid atherosclerotic plaques was shown to be predictive for the occurrence of cardiovascular events irrespective of their activation[8]. In addition, via release of vasoactive mediators, especially histamine, MCs have been implicated in provoking coronary spasms which can lead to MI directly or indirectly via spasm-induced destabilization followed by complication of unstable coronary lesions[5, 22-24]. Our finding of increased MC infiltration in the media, especially in unstable lesions of acute and chronic MI patients, directly supports such a role. Although a causal relationship between this finding and plaque instability or sensitivity towards spasms remains to be established. These mast cells may migrate into the media from the vaso vasorum. Previous studies have indeed shown high densities of MCs in the adventitia[10, 13].

Given that many of the plaque-destabilizing properties of MCs take effect in the intima and that intraplaque MC numbers in carotid lesions were shown to associate with future cardiovascular events[8], an increased density of MCs in the intima of unstable coronary lesions may have been expected. Remarkably however, we observed no differences in MC density in the intima between stable and unstable lesions or between infarct-related and non-infarct-related coronary arteries in any of the groups, nor between the groups. MC densities were shown before to correlate positively with plaque progression, both in coronary[7] and carotid arteries[7, 25]. However, intimal MC densities between stable and unstable lesions that we describe here, were to the best of our knowledge never analyzed before.

Albeit not significant, we observed that the MC density in the media of specifically unstable coronary lesions increased in time after MI. This increase was significant in non-infarct-related coronary arteries. This suggests that MI itself somehow triggers the infiltration of MCs into coronary lesions. Consequently, through their plaque destabilizing properties these infiltrated MCs may cause further coronary plaque destabilization over time and increase the likelihood of recurrent ischemic events. This hypothesis is strengthened by our finding of a significantly more frequent occurrence of unstable plaques in the coronary arteries in patients with chronic MI as compared to controls and acute MI patients. Indeed, re-infarction is a common event in patients with MI and was shown in a representative trial to occur in 54% of patients within the first year after

MI[26]. Recently, interest is increasing regarding the concept that MI can affect distant vascular remodeling. This concept was first demonstrated in mice wherein MI-induced inflammation augmented neointimal hyperplasia in a remote injured artery[27]. The same research group subsequently showed in humans that luminal narrowing of non-culprit coronary arteries after MI was progressed in comparison with stable angina pectoris, indicative of augmented atherosclerosis[28]. Similarly, in a mouse model, MI caused enhanced inflammation in aortic atherosclerotic plaques[29]. We observed similar proportions of unstable plaques in the coronary arteries of control patients and in acute MI patients. It is known that not all vulnerable plaques lead to plaque rupture[30] and that multiple 'active' plaques often reside in the coronary and other arteries[31]. Moreover, it was shown in patients with unstable angina that inflammation of the coronary arteries was widespread across the coronary vascular bed, regardless of the location of the culprit stenosis[32]. These findings are in line with our findings of increased MC density in media throughout the coronary lesions and challenge the concept of a single vulnerable plaque in coronary syndromes, but perhaps more point to the atherosclerotic burden and specifically the proportional presence of vulnerable lesions as well as the level of plaque inflammation across the coronary vascular bed as factors that increase the likelihood of developing MI.

Finally, as a limitation of the study we would like to point out that the number of studied lesions was relatively small especially from control patients. Further observations in other patients cohorts are warranted to strengthen these results.

In conclusion, in this study we show a presence of MCs in the intima and media of both stable and unstable atherosclerotic coronary lesions after MI, especially significantly increasing in the media of unstable plaques in the patients with chronic MI. These results suggest that MCs present in coronary lesions, may contribute to the onset of MI through their plaque-destabilizing or spasm-inducing properties. MI, in turn, may trigger intra-plaque infiltration of MCs, thereby inducing the transition of stable plaques into unstable plaques resulting in an increased risk of re-infarction.

FUNDING

This study was financed by the Foundation NUTS-OHRA (Grant No. SNO-T-04-16), The European Foundation for the Study of Diabetes (EFSD; Grant No. PT 67543) and The Institute for Cardiovascular Research (ICaR-VU; Grant No.ICaR-VU-ID414-2012).

REFERENCES

1 Bot I, Biessen EA. Mast cells in atherosclerosis. Thromb Haemost 2011 November;106(5):820-6

2 Bot I, Shi GP, Kovanen PT. Mast cells as effectors in atherosclerosis. Arterioscler Thromb Vasc Biol 2015 February;35(2):265-71

3 Kaartinen M, Penttila A, Kovanen PT. Accumulation of activated mast cells in the shoulder region of human coronary atheroma, the predilection site of atheromatous rupture. Circulation 1994 October;90(4):1669-78

4 Kovanen PT, Kaartinen M, Paavonen T. Infiltrates of activated mast cells at the site of coronary atheromatous erosion or rupture in myocardial infarction. Circulation 1995 September 1;92(5):1084-8

5 Ozben B, Erdogan O. The role of inflammation and allergy in acute coronary syndromes. Inflamm Allergy Drug Targets 2008 September;7(3):136-44

6 Bot I, de Jager SC, Bot M et al. The neuropeptide substance P mediates adventitial mast cell activation and induces intraplaque hemorrhage in advanced atherosclerosis. Circ Res 2010 January 8;106(1):89-92

7 Lappalainen H, Laine P, Pentikainen MO, Sajantila A, Kovanen PT. Mast cells in neovascularized human coronary plaques store and secrete basic fibroblast growth factor, a potent angiogenic mediator. Arterioscler Thromb Vasc Biol 2004 October;24(10):1880-5

8 Willems S, Vink A, Bot I et al. Mast cells in human carotid atherosclerotic plaques are associated with intraplaque microvessel density and the occurrence of future cardiovascular events. Eur Heart J 2013 December;34(48):3699-706

9 Johnson JL, Jackson CL, Angelini GD, George SJ. Activation of matrix-degrading metalloproteinases by mast cell proteases in atherosclerotic plaques. Arterioscler Thromb Vasc Biol 1998 November;18(11):1707-15

10 Bot I, de Jager SC, Zernecke A et al. Perivascular mast cells promote atherogenesis and induce plaque destabilization in apolipoprotein E-deficient mice. Circulation 2007 May 15;115(19):2516-25

11 Bot I, Bot M, van Heiningen SH et al. Mast cell chymase inhibition reduces atherosclerotic plaque progression and improves plaque stability in ApoE-/- mice. Cardiovasc Res 2011 January 1;89(1):244-52

12 Stary HC. The sequence of cell and matrix changes in atherosclerotic lesions of coronary arteries in the first forty years of life. Eur Heart J 1990 August;11 Suppl E:3-19

13 Laine P, Kaartinen M, Penttila A, Panula P, Paavonen T, Kovanen PT. Association between myocardial infarction and the mast cells in the adventitia of the infarct-related coronary artery. Circulation 1999 January 26;99(3):361-9

14 Fishbein MC, Maclean D, Maroko PR. The histopathologic evolution of myocardial infarction. Chest 1978 June;73(6):843-9

15 Krijnen PA, Ciurana C, Cramer T et al. IgM colocalises with complement and C reactive protein in infarcted human myocardium. J Clin Pathol 2005 April;58(4):382-8

16 van der Wal AC, Becker AE. Atherosclerotic plaque rupture--pathologic basis of plaque stability and instability. Cardiovasc Res 1999 February;41(2):334-44

17 Lappalainen J, Lindstedt KA, Oksjoki R, Kovanen PT. OxLDL-IgG immune complexes induce expression and secretion of proatherogenic cytokines by cultured human mast cells. Atherosclerosis 2011 February;214(2):357-63

18 Meng Z, Yan C, Deng Q et al. Oxidized low-density lipoprotein induces inflammatory responses in cultured human mast cells via Toll-like receptor 4. Cell Physiol Biochem 2013;31(6):842-53

19 den Dekker WK, Tempel D, Bot I et al. Mast cells induce vascular smooth muscle cell apoptosis via a toll-like receptor 4 activation pathway. Arterioscler Thromb Vasc Biol 2012 August;32(8):1960-9

20 Guo T, Chen WQ, Zhang C, Zhao YX, Zhang Y. Chymase activity is closely related with plaque vulnerability in a hamster model of atherosclerosis. Atherosclerosis 2009 November;207(1):59-67

21 Sun J, Sukhova GK, Wolters PJ et al. Mast cells promote atherosclerosis by releasing proinflammatory cytokines. Nat Med 2007 June;13(6):719-24

22 Alevizos M, Karagkouni A, Panagiotidou S, Vasiadi M, Theoharides TC. Stress triggers coronary mast cells leading to cardiac events. Ann Allergy Asthma Immunol 2014 October 10;112(4):309-16

23 Kalsner S, Richards R. Coronary arteries of cardiac patients are hyperreactive and contain stores of amines: a mechanism for coronary spasm. Science 1984 March 30;223(4643):1435-7

24 Fassio F, Almerigogna F. Kounis syndrome (allergic acute coronary syndrome): different views in allergologic and cardiologic literature. Intern Emerg Med 2012 December;7(6):489-95

25 Jeziorska M, McCollum C, Woolley DE. Mast cell distribution, activation, and phenotype in atherosclerotic lesions of human carotid arteries. J Pathol 1997 May;182(1):115-22

26 Goldstein JA, Demetriou D, Grines CL, Pica M, Shoukfeh M, O'Neill WW. Multiple complex coronary plaques in patients with acute myocardial infarction. N Engl J Med 2000 September 28;343(13):915-22

27 Takaoka M, Uemura S, Kawata H et al. Inflammatory response to acute myocardial infarction augments neointimal hyperplasia after vascular injury in a remote artery. Arterioscler Thromb Vasc Biol 2006 September;26(9):2083-9

28 Okayama S, Uemura S, Nishida T et al. Progression of non-culprit coronary artery atherosclerosis after acute myocardial infarction in comparison with stable angina pectoris. J Atheroscler Thromb 2008 October;15(5):228-34

29 Dutta P, Courties G, Wei Y et al. Myocardial infarction accelerates atherosclerosis. Nature 2012 July 19;487(7407):325-9

30 Libby P, Pasterkamp G. Requiem for the 'vulnerable plaque'. Eur Heart J 2015 November 14;36(43):2984-7

31 Stone GW, Maehara A, Lansky AJ et al. A prospective natural-history study of coronary atherosclerosis. N Engl J Med 2011 January 20;364(3):226-35

32 Buffon A, Biasucci LM, Liuzzo G, D'Onofrio G, Crea F, Maseri A. Widespread coronary inflammation in unstable angina. N Engl J Med 2002 July 4;347(1):5-12

7

Validation of simplified ^{18}F-FDG uptake metrics for quantitative assessment of inflammation in atherosclerotic plaques after major surgery

[*] Wessel W. Fuijkschot; [*] Gem M. Kramer; Maqsood. Yaqub; Paul A.J. Krijnen; Ronald Boellaard; Hans W.M. Niessen; Rachid Saouti; Yvo M. Smulders and Adriaan A. Lammertsma

[*] Both authors contributed equally

Submitted for publication

ABSTRACT

Background: The risk of atherosclerotic events, such as myocardial infarction and stroke, is determined by the stability of atherosclerotic plaques in large arteries which, in turn, correlates with inflammatory activity in these plaques. [^{18}F]-2-fluoro-2-deoxy-D-glucose (^{18}F-FDG) imaging using positron emission tomography (PET) provides a non-invasive assessment of inflammation and, as such, could be a valuable imaging biomarker in atherosclerosis. Systemic inflammation may affect pharmacokinetics of ^{18}F-FDG uptake in atherosclerotic plaques causing inaccurate quantitative assessment using simplified methods. The aim of the present study was therefore to validate the use of simplified quantitative ^{18}F-FDG uptake parameters for evaluation of inflammation in atherosclerotic plaques before and after major surgery, which can be viewed as a model for systemic inflammation caused by localised tissue damage/inflammation.

Methods: Five patients scheduled for a total knee or hip replacement were included in this prospective observational study. Patients underwent ^{18}F-FDG PET/CT scanning on 2 separate occasions: one day prior to surgery and 2 days after surgery. Dynamic scans were acquired and three venous blood samples were collected during the scan to measure plasma and whole blood radioactivity concentrations. Simplified measures (standardized uptake value [SUV] and tissue-to-blood ratio [TBR]) were correlated with fully quantitative measures derived from kinetic modeling using the ascending aorta as image derived input function.

Results: Overall, arterial TBR calibrated using venous blood samples showed the strongest correlation with non-linear regression (NLR) based K_i for carotid artery, ascending aorta and most diseased segment ($R^2 > 0.7$). Performance of TBR was not affected by major surgery. Only SUV normalized to the area under the curve of the arterial input function (SUV_{AUC}) also correlated well with K_i. All other simplified methods (Patlak, uncalibrated TBR and SUV_{bw}) showed no correlation with NLR based K_i ($R^2 < 0.6$) and were highly dependent on VOI definition method.

Conclusions: TBR calibrated using venous blood samples could be used as surrogate simplified measures to assess changes in ^{18}F-FDG uptake in atherosclerotic plaques of patients recovering from major orthopaedic surgery and, more general, patients with systemic inflammation.

INTRODUCTION

The risk of atherosclerotic events, such as myocardial infarction and stroke, is determined by the stability of atherosclerotic plaques in large arteries which, in turn, correlates with inflammatory activity in these plaques[1, 2]. ^{18}F-2-fluoro-2-deoxy-D-glucose (^{18}F-FDG) positron emission tomography (PET) allows for non-invasive imaging of inflammatory changes in large artery atherosclerosis (particularly carotid, aortic and ileofemoral regions)[3, 4]. In general, tissue-to-blood ratio (TBR) is used as an indicator of arterial wall inflammation[5]. Using this ratio, it has indeed been possible to identify patients at risk for vascular events[6-8]. In addition, this ratio showed high inter- and intra-observer agreement and low variability over 2 weeks[9, 10].

An area of particular interest in cardiovascular research is the sharply increased cardiovascular event risk during and shortly after acute systemic inflammation, caused by for example infection or tissue damage due to trauma or surgery. It has been proposed that acute systemic inflammation enhances plaque inflammation[2, 11]. ^{18}F-FDG PET of the arterial wall appears particularly suited to test this hypothesis in man. However, there is an important caveat in the use of simplified uptake measures, as systemic inflammation may modify ^{18}F-FDG kinetics due to competing uptake in inflamed tissues, potentially leading to changes in plasma clearance of ^{18}F-FDG[12 13]. These changes in plasma kinetics are accounted for when analysing data using full kinetic modeling. This, however, requires dynamic scanning over a single bed position. For clinical studies survey of a larger part of the body may be of interest, but whole body scans can only be analysed using simplified ^{18}F-FDG uptake measures. To assess the potential impact of systemic inflammation on the use of simplified ^{18}F-FDG uptake measures, validation against full kinetic modeling is necessary[14]. The aim of this study was therefore to assess the validity of simplified quantitative ^{18}F-FDG parameters, such as TBR and SUV, for quantification of inflammation in atherosclerotic plaques before and after major surgery, which can be viewed as a model for systemic inflammation caused by localised tissue damage/inflammation.

METHODS

Patients

Patients (n=5) scheduled for total knee or total hip replacement, aged > 65 years, were included from the outpatient clinic of the orthopaedic department of the VU University Medical Center (VUmc). Exclusion criteria were: delirium or other cognitive impairment (acute or chronic) that impaired patient judgement, self-reported or objective discomfort

in supine position, recent myocardial infarction (< 6 months), current infections, current use of corticosteroid or non-steroidal anti-inflammatory drugs, chronic inflammatory and/or auto-immune diseases, and renal insufficiency (eGFR <30 mL/min/1.73m^2). Patients underwent ^{18}F-FDG PET/CT scans on 2 separate occasions: one day prior to surgery and 2 days after surgery. Concomitant blood samples were gathered to evaluate inflammatory parameters. Written informed consent was obtained and all study procedures were conform the Helsinki declaration and approved by the VUmc Medical Ethics Review Committee.

PET Imaging

PET/CT scans were obtained using either an Ingenuity TF-128 or a Gemini TF-64 PET/CT scanner (Philips Healthcare, Eindhoven, The Netherlands), both with an axial field of view of 18.4 cm. In all individual patients both pre- and post-surgery scans were obtained using the same scanner. All patients were asked to fast for at least 6 hours prior to the PET scan. Patients were scanned arms down and the field of view was positioned over the thorax such that both ascending aorta and carotid arteries where included. First a low-dose CT during tidal breathing was performed for attenuation correction, immediately followed by a 60 minutes dynamic ^{18}F-FDG PET scan. At the start of the latter scan a 170 MBq bolus of ^{18}F-FDG (5 mL) was injected at a rate of 0.8 mL/s, which was followed by a flush with 35 mL NaCl 0.9% at 2.0 mL/s. The dynamic ^{18}F-FDG data were reconstructed into 19 time frames (1x15, 3x5, 3x10, 4x60, 2x150, 2x300, 4x600 s) using a 3-dimensional row-action maximum-likelihood reconstruction algorithm[15]. All scans were corrected for dead time, decay, scatter and randoms. During the ^{18}F-FDG scan 3 venous blood samples were drawn at 35, 45 and 55 minutes post injection to measure plasma and whole blood radioactivity concentrations[12]. The entire scanning procedure was repeated 2 days after surgery.

PET Data Analysis

Volumes of interest (VOIs) were generated for ascending aorta, carotids and visibly most diseased segment (MDS) both on low-dose CT and PET images of the baseline and post-surgery ^{18}F-FDG scans. For PET based VOI definition, an early frame (25-30s post injection) was used in which the arterial structures were clearly visible. Two different methods for delineating the arterial wall of the ascending aorta were assessed: 1) whole aorta, including the lumen, and 2) only the outer 1-2 voxels of the aorta (Fig. 1). For both carotids and MDS only the whole artery was used, as the spatial resolution of PET/CT does not allow for separate delineation of the arterial wall. Time activity curves (TAC) were generated both for each of the slices in a region (i.e. aorta, carotid or MDS) separately and for all slices of a region combined by projecting the VOIs onto the frames of the dynamic PET scan. Image derived input functions (IDIFs) were obtained by placing 8x8 mm VOIs (2x2 voxels) on the centre of the ascending aorta in 5 consecutive slices.

Again, corresponding TACs were obtained by projecting these VOI onto the dynamic PET scan. IDIFs were scaled using whole blood activity concentrations and calibrated using the plasma-to-blood radioactivity concentration ratios obtained from the venous blood samples (median ratio: 0.92; range: 0.82-1.00).

Non-linear regression (NLR) analyses of the TACs were analysed using non-linear regression (NLR) and the conventional irreversible 2-tissue compartmental plasma input model with an additional parameter for blood volume. For all VOIs the net rates of influx (Ki) were calculated from the individual rate constants: $K_i = K_1 \cdot k_3 / (k_2 + k_3)$. In addition, several simplified measurements were derived from the data: SUV corrected for bodyweight (SUV_{bw}), uncalibrated arterial and venous (TBR, arterial TBR calibrated using venous blood samples, SUV normalized to the area under the curve of the calibrated arterial input function (SUV_{AUC}) and Patlak based K_i[16] (Table 1). Arterial and venous tissue-to-blood ratios (TBR) were calculated by normalizing the SUV of the region of interest to the SUV of the arterial VOI and the superior vena cava (8x8 mm VOIs in 5 consecutive), respectively. All SUV and TBR parameters were calculated for two time intervals, i.e. 40-60 and 50-60 min post injection and Patlak was evaluated for 25-60 and 30-60 min post-injection.

Figure 1

The two delineation methods for assessing the arterial wall of the ascending aorta. Here only one slice is shown, but for analysis VOIs of four consecutive slices were used for both methods.

Table 1 Simplified parameters

Simplified models	
SUV_{bw}	Activity concentration in the VOI normalized by injected dose and body-weight
Arterial uncalibrated TBR	SUV_{bw} normalized to the same interval of the uncalibrated IDIF of the ascending aorta
Venous uncalibrated TBR	SUV_{bw} normalized to the same interval of the uncalibrated IDIF of the superior vena cava
Calibrated TBR	SUV_{bw} normalized to the same interval of the IDIF of the ascending aorta calibrated using whole blood and plasma-to-blood radioactivity concentrations
SUV_{auc}	SUV_{bw} normalized to the area under the calibrated IDIF
K_i	Influx rate constant for an irreversible model (min^{-1})

TBR: tissue-to-blood ratio, IDIF: image derived input function, SUV: standardized uptake value.

Statistical Analysis

Normality of the data was assessed visually using quantile-quantile plots and histograms. The Wilcoxon signed-rank test was used to assess differences in patient and scan characteristics between both scan time points. Differences in uptake metrics between ascending aorta and carotid arteries were evaluated. For all VOIs, simplified uptake metrics were compared with corresponding K_i results obtained from linear regression analysis. In addition, skewness in the comparison of these metrics was assessed using Bland-Altman plots. These analyses were performed for pre and post-surgery scans separately to identify any changes in ^{18}F-FDG kinetics over time. All statistical analyses were performed using SPSS 20 (IBM Corp., Armonk, NY, US).

RESULTS

Five consecutive patients were included (demographics are presented in Table 2). One patient missed the post-surgery scan because he was transferred to another hospital for logistical reasons. Baseline scans were obtained at the morning of surgery, except for one, which was performed one day prior to surgery. All follow-up scans were obtained 2 days post-surgery.

Table 2 Patient's baseline characteristics

Characteristics	
Patients (n)	5
Age (years, range)	74 (70-77)
Male, n (%)	2 (40)
Length (cm)	160 (157-179)
Weight (kg)	68 (59-83)
Injected activity scan 1 (MBq)	161.8 (149-181)
Injected activity scan 2 (MBq)	163.7 (150-172)
Current smoking, n (%)	1 (20)
Hypercholesterolemia	1 (20)
Hypertension, n (%)	3 (60)
Diabetes Mellitus, n (%)	1 (20)
History of CVE, n (%)	2 (40)
Prior CVA, n (%)	2 (40)
Prior MI, n (%)	1 (20)
Laboratory data	
Platelets 10^E9/L	198 [181-220]
Leucocytes 10^E9/L	52 [51-70]
Lymphocytes 10^E9/L	171 [90-213]
Neutrophilic granulocytes 10^E9/L	2.8 [2.8-4.2]
CRP mg/L	15 [4-31]
ESR mm/hour	4 [3-17]
Total cholesterol mmol/L	4.2 [3.0-5.2]
HDL cholesterol mmol/L	1.2 [0.97-1.6]
LDL cholesterol mmol/L	2.2 [1.7-3.0]
Triglycerides mmol/L	1.0 [0.8-1.6]

Variable represent median [interquartile range] or percentage of total patients (%). CVE, cardiovascular event; CVA, cerebral vascular event; MI, myocardial infarction; CRP, C-reactive protein; ESR erythrocyte sediment rate; HDL, high-density lipoprotein; LDL, low-density lipoprotein.

Non Linear Regression

Typical TACs of arterial wall, carotid artery and MDS with associated NLR fits are shown in Fig. 2. As expected a high blood volume fraction was seen ($V_b \sim 0.41 \pm 0.20$). The large blood pool within or near the VOI may compromise the precision of the fitted rate constants. 46 of the 390 VOIs had to be excluded because of a high degree of uncertainty in estimating the individual kinetic parameters K_1, k_2, k_3 and V_b (SD >2 times the parameter). Results of both full kinetic modeling and simplified methods can be found in Table 3.

Simplified Methods

Arterial TBR calibrated using venous blood samples showed the strongest correlation with NLR based K_i for all tissues and strong correlations for both pre- and post-surgery were found for PET-based VOIs of the carotid arteries (R^2: 0.78 – 0.79), ascending aorta (R^2: 0.73 – 0.90) and MDS (R^2: 0.92 – 0.95) (Fig. 3-5 and supplementary data). Bland-Altman plots showed that data were not skewed (not shown). A difference in accuracy between pre- and post-surgery scans was seen only for the ascending aorta, primarily affecting the CT based VOIs (R^2: 0.57 vs. 0.90) (Table 4). This discrepancy was not seen for MDS, although (in the denominator) the ascending aorta was also used for all these VOIs. VOI delineation methods (wall only vs. whole artery) have a limited effect on calibrated TBR performance as seen in Table 4. In contrast to expectations the effects of analyzing per slice or stack of slices were limited. Two outliers in the correlation between NLR based K_i and arterial calibrated TBR (>2 SD) were excluded from the reported R^2 (Fig. 3 and 5). If these regions were included, accuracy of calibrated TBR slightly decreased for the carotid arteries (R^2 >0.67 vs. R^2 >0.74) and MDS (R^2 >0.80 vs. R^2 >0.88) (supplemental Table 1). An overview of the results of all possible combinations of the delineation and analyses methods mentioned above for each of the anatomical regions can be found in supplemental Table 2-4.

When SUV_{AUC}, instead of calibrated TBR, was used for quantification of ^{18}F-FDG uptake, similar correlations with K_i were found, and R^2 remained ≥ 0.7 for most VOI delineation methods. The effect of delineation method (wall only vs. whole artery) on performance of SUV_{AUC} was larger than for calibrated TBR. Patlak based K_i showed a weak correlation with the NLR based K_i for all time intervals (R^2 < 0.6). Moreover, high variability between pre- and post-surgery results was seen, as well as within different tissues and VOI methods.

Using only static images without venous blood sample data decreases correspondence with NLR Ki. Correlation of SUV_{bw} with NLR K_i was poor independent of VOI definition method or time interval after injection used (R^2 < 0.5). This was also true for both baseline and post-surgery measures separately. Normalizing SUV of the region of interest to either arterial or venous blood SUV to obtain uncalibrated TBR improved correlation for certain cases (Table 3). Yet, large variability in performance between different regions was seen (R^2: <0.3 – 0.9) with, in general, improvements limited to carotid arteries. Moreover, large but inconsistent differences were seen between pre- and post-surgery scans. TBR values were similar when normalized to either arterial or venous blood activity.

Table 3 ^{18}F-FDG uptake parameters for several tissues before and after surgery (Median; IQR)

	Carotid artery		Ascending aorta		MDS	
Parameters	**Baseline**	**Post-surgery**	**Baseline**	**Post-surgery**	**Baseline**	**Post-surgery**
Irreversible 2-tissue pharmacokinetic model						
K_1	0.37 (0.18-0.52)	0.31 (0.21-0.43)	0.22 (0.13-0.30)	0.23 (0.17-0.27)	0.16 (0.11-0.27)	0.29 (0.09-0.34)
k_2	1.36 (0.70-1.70)	1.39 (0.83-1.52)	1.41 (0.52-1.62)	1.63 (1.55-1.69)	0.61 (0.34-1.55)	1.47 (0.27-1.59)
k_3	0.025 (0.025-0.029)	0.027 (0.025-0.033)	0.030 (0.025-0.045)	0.035 (0.025-0.069)	0.027 (0.025-0.033)	0.025 (0.025-0.031)
V_b	0.22 (0.19-0.27)	0.15 (0.12-0.21)	0.61 (0.41-0.68)	0.51 (0.36-0.65)	0.49 (0.31-0.56)	0.32 (0.25-0.45)
K_i	0.0086 (0.0069-0.0091)	0.0072 (0.0064-0.0092)	0.0067 (0.0057-0.0083)	0.0060 (0.0042-0.0081)	0.0074 (0.0055-0.0083)	0.0059 (0.0054-0.0091)
Simplified models						
Patlak (25-60 min)	0.0031 (0.0016-0.0043)	0.0034 (0.0024-0.0053)	0.0025 (0.0018-0.0030)	0.0024 (0.0017-0.0027)	0.0023 (0.0016-0.0033)	0.0018 (0.0011-0.0027)
Patlak (30-60 min)	0.0031 (0.0018-0.0046)	0.0035 (0.0015-0.0069)	0.0024 (0.0018-0.0037)	0.0016 (0.0011-0.0020)	0.0025 (0.0014-0.0032)	0.0014 (0.0010-0.0026)
Calibrated TBR (40-60 min)	0.95 (0.84-1.04)	0.79 (0.76-0.97)	0.89 (0.80-0.99)	0.81 (0.66-0.92)	0.89 (0.76-1.00)	0.73 (0.69-0.99)
Calibrated TBR (50-60 min)	0.96 (0.84-1.04)	0.77 (0.73-1.07)	0.92 (0.81-0.99)	0.79 (0.69-0.92)	0.91 (0.74-0.97)	0.74 (0.70-1.04)
SUV_{AUC} (40-60 min)	0.012 (0.010-0.013)	0.0098 (0.0090-0.012)	0.011 (0.010-0.012)	0.0094 (0.0086-0.011)	0.011 (0.0098-0.012)	0.0091 (0.0087-0.011)
SUV_{AUC} (50-60 min)	0.011 (0.0094-0.012)	0.0086 (0.0083-0.012)	0.010 (0.0093-0.011)	0.0088 (0.0079-0.010)	0.010 (0.0090-0.011)	0.0085 (0.0080-0.010)
Venous uncalibrated TBR (40-60 min)	0.98 (0.80-1.03)	0.81 (0.74-1.08)	0.88 (0.78-0.93)	0.86 (0.77-0.91)	0.92 (0.86-0.96)	0.89 (0.81-0.94)
Venous uncalibrated TBR (50-60 min)	0.96 (0.81-1.09)	0.85 (0.71-1.09)	0.89 (0.80-0.95)	0.88 (0.81-0.92)	0.91 (0.85-0.9)	0.88 (0.828-0.94)
Arterial uncalibrated TBR (40-60 min)	0.88 (0.76-0.92)	0.74 (0.70-0.98)	0.80 (0.72-0.85)	0.79 (0.71-0.83)	0.81 (0.72-0.85)	0.82 (0.73-0.86)
Arterial uncalibrated TBR (50-60 min)	0.89 (0.77-0.92)	0.75 (0.67-1.06)	0.81 (0.74-0.86)	0.81 (0.71-0.84)	0.80 (0.71-0.85)	0.84 (0.73-0.88)
SUV_{bw} (40-60 min)	1.82 (1.39-2.09)	1.84 (1.67-2.09)	1.60 (1.31-1.86)	1.71 (1.55-2.39)	1.48 (1.15-1.71)	1.58 (1.47-1.72)
SUV_{bw} (50-60 min)	1.80 (1.35-2.05)	1.83 (1.68-2.00)	1.57 (1.32-1.84)	1.68 (1.53-2.38)	1.43 (1.11-1.66)	1.54 (1.42-1.67)

TBR: Tissue-to-blood ratio, SUV_{AUC}: SUV normalized to the area under the curve of the calibrated arterial input function, SUV_{bw}: Standardized uptake value corrected for bodyweight

Table 4 Correlation of various simplified methods with K_i derived from non-linear regression.

	Carotid artery			
	Baseline		Post-surgery	
Simplified models	**R^2**	**Slope**	**R^2**	**Slope**
PET or CT based VOI				
Calibrated TBR (PET)	0.78	92.9 (71.7-114.1)	0.79	123.4 (90.6-156.2)
Calibrated TBR (CT)	0.82	91.0 (72.6-109.3)	0.88	113.3 (91.8-134.9)
SUV_{AUC} (PET)	0.81	1.09 (0.8-1.31)	0.73	1.00 (0.70-1.32)
SUV_{AUC} (CT)	0.86	1.09 (0.90-1.27)	0.86	0.96 (0.76-1.15)
Arterial uncalibrated TBR (PET)	0.52	51.7 (30.4-73.0)	0.45	74.0 (32.3-115.7)
Arterial uncalibrated TBR (CT)	0.89	78.0 (66.3-89.8)	0.71	87.9 (58.8-116.9)
Venous uncalibrated TBR (PET)	0.35	84.4 (34.6-134.3)	0.32	61.0 (15.5-106.5)
Venous uncalibrated TBR (CT)	0.64	86.0 (58.2-113.9)	0.54	76.2 (39.9-112.4)
Wall only or whole artery				
Calibrated TBR (Wall)*	-	-	-	-
Calibrated TBR (Whole)	0.81	91.3 (78.5-104.2)	0.83	114.0 (96.3-131.7)
SUV_{AUC} (Wall)*	-	-	-	-
SUV_{AUC} (Whole)	0.85	1.09 (0.95-1.22)	0.80	0.95 (0.79 -1.11)
Arterial uncalibrated TBR (Wall)*	-	-	-	-
Arterial uncalibrated TBR (Whole)	0.80	71.8 (61.5-82.1)	0.60	81.4 (59.1-103.7)
Venous uncalibrated TBR (Wall)*	-	-	-	-
Venous uncalibrated TBR (Whole)	0.54	85.7 (62.6-108.7)	0.46	70.0 (44.1-95.9)
Multiple slices or per slice				
Calibrated TBR (Multiple slices)	0.72	84.9 (41.6-128.2)	0.74	121.9 (49.3-194.5)
Calibrated TBR (Per slice)	0.83	92.1 (78.2-106.1)	0.85	112.2 (94.2-130.2)
SUV_{AUC} (Multiple slices)	0.84	1.08 (6.70-1.47)	0.68	0.96 (0.30-1.62)
SUV_{AUC} (Per slice)	0.85	1.09 (0.94-1.23)	0.83	0.95 (0.79-1.12)
Arterial uncalibrated TBR (Multiple slices)	0.79	63.04 (36.7-89.4)	0.44	72.7 (-8.98-154.4)
Arterial uncalibrated TBR (Per slice)	0.81	72.9 (61.2-84.5)	0.64	83.3 (59.2-107.2)
Venous uncalibrated TBR (Multiple slices)	0.43	86.9 (5.72-168.0)	0.31	57.3 (-28.2-142.8)
Venous uncalibrated TBR (Per slice)	0.56	85.4 (60.4-110.4)	0.49	72.1 (44.0-101.4)

* For the Carotid artery only the whole artery was assessed, TBR: Tissue-to-blood ratio, $SUV_{AUC:}$ SUV normalized to the area under the curve of the calibrated arterial input function

Ascending aorta				MDS			
Baseline		Post-surgery		Baseline		Post-surgery	
R^2	Slope	R^2	Slope	R^2	Slope	R^2	Slope
0.73	43.8 (35.0-52.6)	0.90	68.7 (59.9-77.6)	0.92	81.8 (72.5-91.0)	0.95	87.4 (77.8-97.0)
0.57	47.0 (34.6-59.5)	0.90	64.2 (54.9-73.4)	0.87	67.9 (58.2-77.5)	0.90	86.4 (73.1-99.7)
0.60	0.37 (0.27-0.46)	0.86	0.68 (0.58-0.79)	0.88	0.87 (0.75-0.98)	0.90	0.64 (0.54 -0.73)
0.56	0.42 (0.30-0.53)	0.82	0.66 (0.52 -0.80)	0.83	0.70 (0.59-0.817)	0.82	0.62 (0.49-0.75)
0.33	19.6 (10.3-28.8)	0.54	27.1 (17.4-36.8)	0.71	45.4 (34.7-56.2)	0.49	30.0 (16.18 -43.8)
0.30	27.1 (14.2-39.9)	0.45	24.6 (12.6-36.5)	0.64	32.2 (23.5-40.9)	0.27	27.7 (7.18 -48.3)
0.47	25.1 (16.3 33.9)	0.37	19.3 (9.5-29.0)	0.29	36.6 (15.3 -57.8)	0.04	6.27 (-7.54-20.1)
0.29	27.8 (14.3-41.41)	0.25	16.8 (3.84-29.7)	0.22	24.9 (7.8-41.9)	0.01	3.23 (-18.5-25.0)
0.68	50.7 (40.0-61.4)	0.95	75. 8 (68.8-82.8)	0.83	77.1 (63.1-91.0)	0.88	81.7 (67.2-96.1)
0.69	29.6 (23.1 -36.1)	0.88	54.5 (45.6-63.3)	0.91	73.1 (65.1-81.1)	0.96	94.8 (86.9-102.7)
0.72	0.43 (0.35-0.52)	0.90	0.74 (0.64-0.84)	0.83	0.73 (0.60-0.86)	0.86	0.59 (0.47 -0.70)
0.64	0.20 (0.15-0.25)	0.81	0.58 (0.45-0.70)	0.86	0.79 (0.68-0.89)	0.88	0.70 (0.59-0.81)
0.51	26.2 (18.1-34.2)	0.80	36.2 (29.1 -43.3)	0.50	36.1 (22.0-50.2)	0.55	21.9 (12.1-31.8)
0.05	5.85 (-2.84 -14.5)	0.32	11.7 (4.22-19.2)	0.72	39.5 (31.4-47.6)	0.33	37.8 (15.1-60.5)
0.46	29.6 (19.7-39.6)	0.78	25.1 (19.7-30.5)	0.19	-5.85 (-22.6 -10.9)	0.00	0.65 (-11.0-12.3)
0.11	10.0 (1.71-18.3)	0.15	8.10 (-0.46-16.7)	0.39	41.0 (24.3-57.6)	0.04	11.5 (-11.9-35.0)
0.54	42.7 (21.7-63.7)	0.94	67.7 (55.3-80.1)	0.89	24.7 (57.4-86.9)	0.93	92.5 (71.5-113.6)
0.69	45.5 (37.9-53.1)	0.90	66.6 (59.4-73.7)	0.89	74.5 (66.8-82.1)	0.92	85.6 (76.7-94.6)
0.47	0.36 (0.16-0.57)	0.88	0.75 (0.54-0.96)	0.85	0.75 (0.56-0.93)	0.88	0.65 (0.45 -0.85)
0.61	0.39 (0.31 -0.47)	0.84	0.66 (0.67-0.75)	0.86	0.79 (0.70-0.88)	0.85	0.62 (0.53-0.71)
0.24	20.8 (1.01-40.6)	0.36	21.3 (0.02-42.5)	0.64	37.9 (21.7-54.0)	0.35	27.8 (-3.41-58.9)
0.32	22.6 (14.3-30.8)	0.52	26.8 (18.7-34.9)	0.69	39.4 (31.8-47.1)	0.36	29.3 (15.7-42.9)
0.24	23.9 (1.02-46.8)	0.11	14.5 (-7.44-36.5)	0.20	24.7 (-3.98-53.3)	0.00	0.68 (-29.2-30.6)
0.39	26.5 (18.3-34.7)	0.33	18.9 (10.5-27.4)	0.30	33.9 (19.0-48.9)	0.02	6.00 (-8.51-20.4)

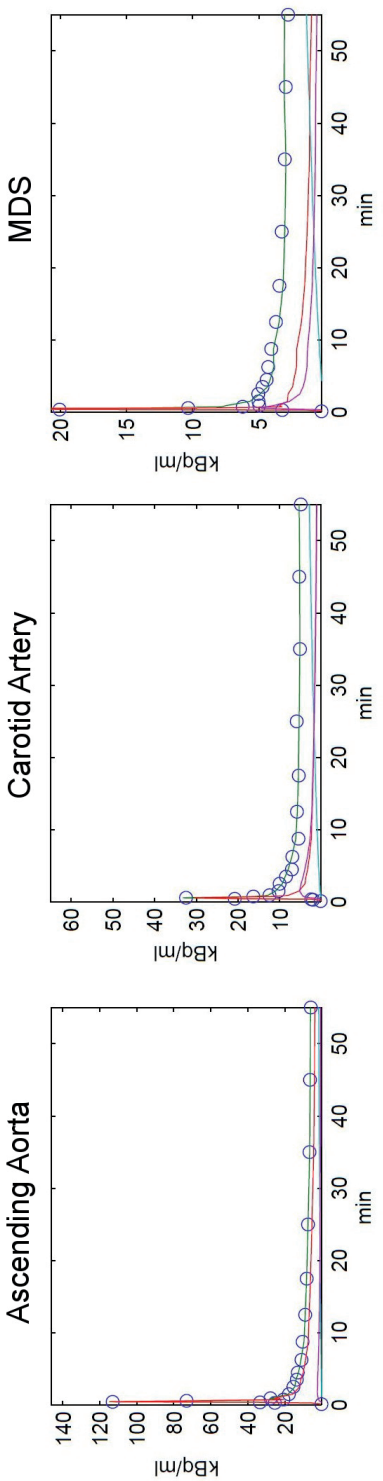

Figure 2

Typical TACs of an ascending aorta, carotid artery and MDS. The green line represents NLR using the standard irreversible 2-tissue plasma input model with blood volume parameter. As shown a large blood volume (V_b) fraction is present, especially in the ascending aorta. (o Data points; Fit of the data points [Green]; V_b fraction [17]; Irreversible compartment [Blue]; Reversible compartment [Purple])

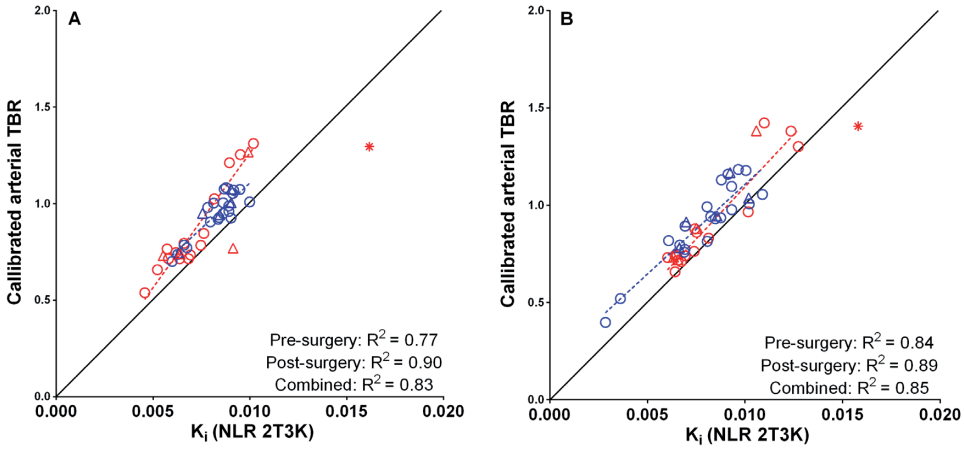

Figure 3

Arterial TBR (tissue-to-blood ratio) calibrated using venous blood samples plotted against K_i obtained from the carotid artery using an irreversible two-tissue compartment model **A:** for PET and **B:** CT based VOIs. Linear regression analysis shown are for the single slice data points. Moreover, the outlier (>3 SD) is excluded from the linear regression analysis. (Blue: baseline; Red: post-surgery; Δ: multiple slices; O: single slice; * Outlier (single slice)).

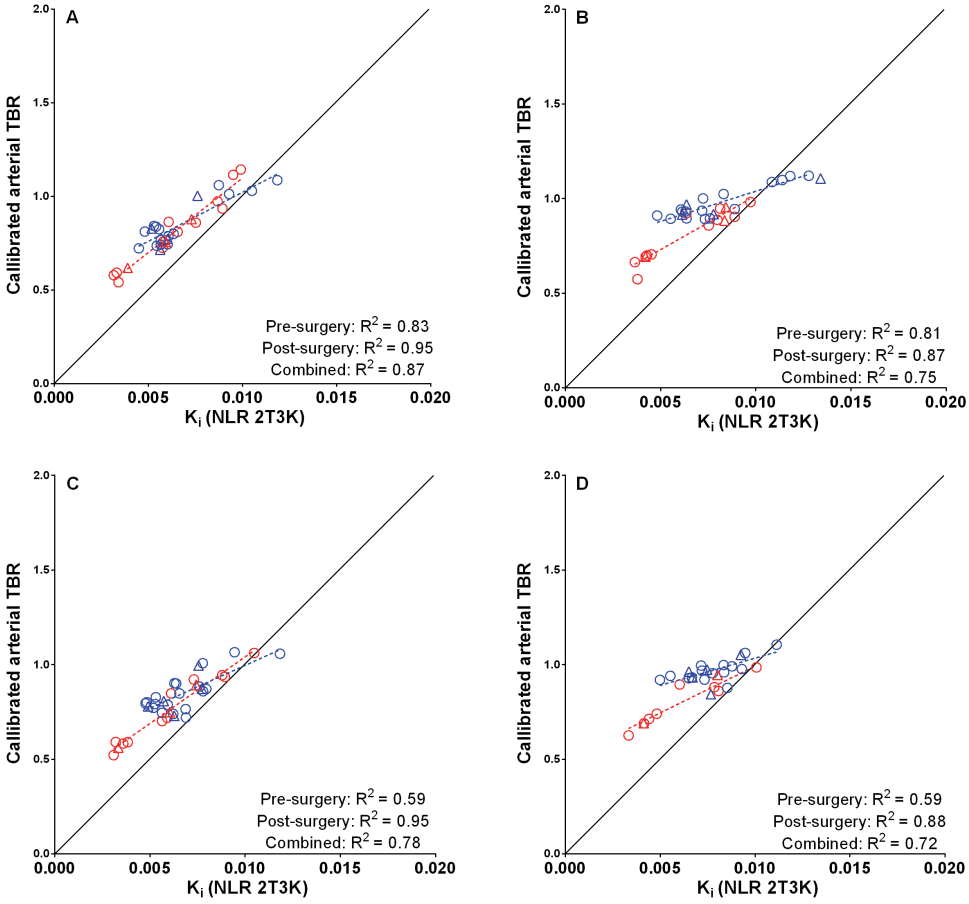

Figure 4

Arterial TBR (tissue-to-blood ratio) calibrated using venous blood samples plotted against K_i obtained from the ascending aorta using an irreversible two-tissue compartment model for PET based VOIs including **A:** wall only, **B:** the whole artery and for CT based VOIs including **C:** wall only and **D:** the whole artery. Linear regression analysis shown are for the single slice data points. (Blue: baseline; Red: post-surgery; Δ: multiple slices; O: single slice).

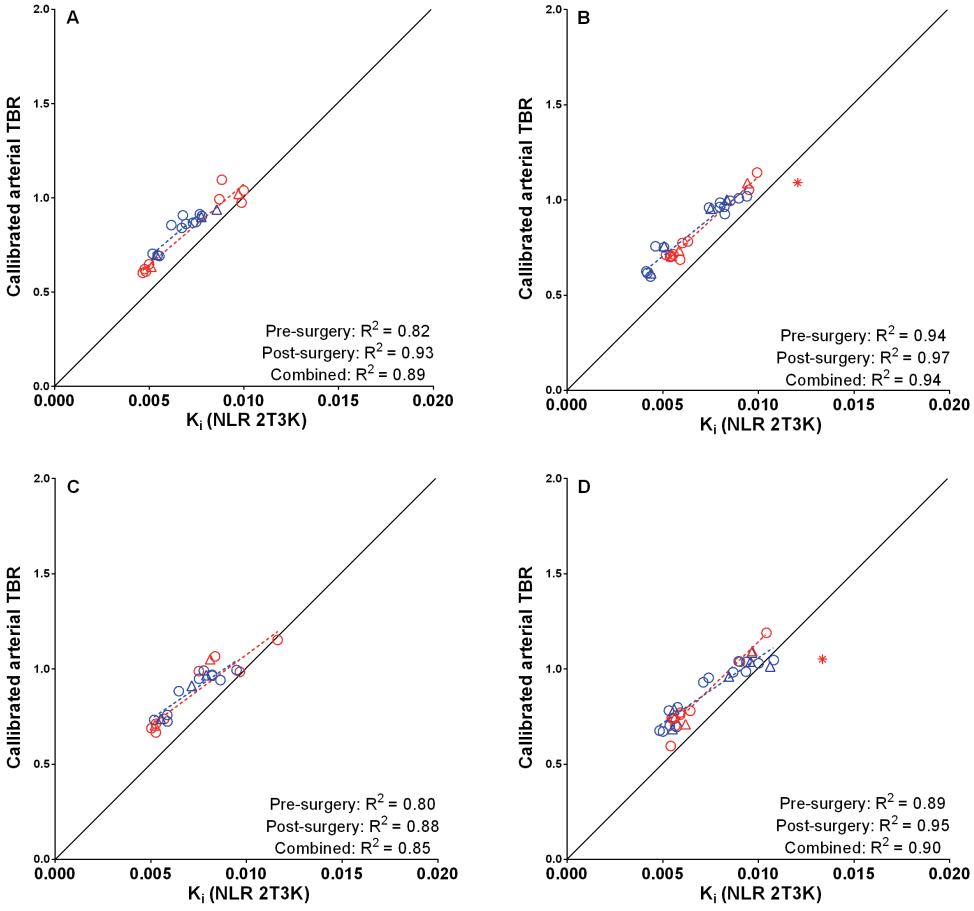

Figure 5

Arterial TBR (tissue-to-blood ratio) calibrated using venous blood samples plotted against K_i obtained from the most diseased segment (MDS) using an irreversible two-tissue compartment model for PET based VOIs including **A:** wall only, **B:** the whole artery and for CT based VOIs including **C:** wall only and **D:** the whole artery. Linear regression analysis shown are for the single slice data points. Moreover, the outlier (>3 SD) is excluded from the linear regression analysis. (Blue: baseline; Red: post-surgery; Δ: multiple slices; O: single slice; * Outlier (single slice)).

DISCUSSION

This study investigated whether simplified ^{18}F-FDG measures can be used as surrogate markers for quantitative analysis of inflammation in atherosclerotic lesions before and after acute systemic inflammation in patients undergoing major orthopaedic surgery. Normalizing SUV to image derived arterial blood pool activity concentrations calibrated using venous blood samples, allowed for accurate quantification showing consistent results before and after surgery independent of VOI definition. Therefore, this simplified measure seems to be the method of choice for evaluating changes in ^{18}F-FDG uptake in the vessel wall due to major orthopaedic surgery across the whole body. With exception of SUV_{AUC} all other simplified methods showed either poor correlation with corresponding NLR results or high variability in performance of different VOI definition methods for different tissue types without a clear preference. Furthermore, results were similar for pre- and post-surgery scans separately, suggesting no significant effects of surgery on the accuracy of simplified ^{18}F-FDG uptake metrics.

Accurate quantification of ^{18}F-FDG uptake in the arterial wall using SUV_{bw} was not feasible due to high blood background activity. Therefore, SUV corrected for background activity derived from the vena cava superior is often used as semi-quantitative measure to evaluate arterial wall inflammation [10]. In the present study, however, large variation was seen in the correlation of uncalibrated TBR with NLR. Correcting TBR using whole blood and plasma-to-blood radioactivity concentrations measured in venous blood samples enhanced correlation for all tissues and VOI types. As plasma-to-blood radioactivity concentrations are stable over time, calibration using a single sample should be sufficient. Nevertheless, more blood samples are advised to avoid inaccurate quantification due to sampling errors. Blood samples can be drawn from the injection site after adequate flushing thereby limiting patient burden, whilst significantly increasing quantitative accuracy[17].

TBR corrected for blood activity concentrations were evaluated using both vena cava superior and ascending aorta. Although no clear differences were seen in performance, the ascending aorta could have some potential advantages over the vena cava. One of these potential advantages is the generally larger diameter of the ascending aorta[18, 19], which may decrease the effects of motion and partial volume effects on accurate quantification and ease VOI definition. In addition, from a pharmacokinetic point of view arterial blood would be preferred, as this resembles tracer delivery to the target region[20]. Even if the blood pool is only used to correct for background as is done in other articles, spill-in from the arterial blood pool into the VOI will probably be more abundant and therefore reflect true spill-in more accurately than in the vena cava.

Accurate quantification of ^{18}F-FDG uptake is also possible although SUV_{AUC}, although this was inferior to calibrated TBR. In addition, quantification using SUV_{AUC} requires an additional (dynamic) scan over the heart and therefore increases patient burden and costs. The same applies to the measurement of Patlak based Ki, which requires a dynamic scan protocol and, therefore, is not applicable for whole body studies. Quantitative performance of Patlak in the present study was poor, probably due to the high V_b fractions. In contrast to full kinetic modeling, for Patlak all activity within the VOI is allocated to the Ki, including those belonging to V_b. Variability of V_b within and between patients increases variation and hampering the performance of Patlak.

The low spatial resolution is one of the challenges when assessing the arterial wall using PET. Delineation of the wall without including (spill-over from) adjacent structures is impossible, especially for smaller arteries. In addition, manual delineation of the arterial wall is more cumbersome than using the entire artery, and a VOI containing only arterial wall may also be more susceptibility to motion artefacts. On the other hand, inclusion of non-arterial wall tissues leads to a higher ^{18}F-FDG background signal, potentially leading to a loss in sensitivity for detecting a specific signal. An advantage of calibrated TBR compared with the other simplified methods was its strong correlation with full kinetic modeling, independent of VOI definition. Both delineation methods are technically feasible and further studies are needed to identify the optimal delineation method under different conditions.

Results of the present study may be relevant for other conditions with systemic inflammation caused by localised tissue damage/inflammation. Nevertheless, for other interventions, these simplified methods need to be assessed again, as different interventions may alter pharmacokinetics in different ways and thus affect the correlation between simplified measures and NLR[21].

CONCLUSION

In patients suffering from systemic inflammation, accurate quantification of the arterial wall is feasible using image derived arterial TBR calibrated using venous blood samples. Performance of this calibrated TBR method is insensitive to VOI definition. Other simplified methods, such as uncalibrated TBR and SUV, do not provide accurate uptake measures.

ACKNOWLEDGEMENTS

We thank the patients and their families for participating in this study. In addition, we acknowledge the staff of the Department of Radiology & Nuclear Medicine of the VU University Medical Center, Amsterdam, The Netherlands, for their help with performing the scans.

FUNDING

This study was financed by the Institute for Cardiovascular Research (ICaR-VU; Grant No.ICaR-VU-ID414-2012).

REFERENCES

1 Libby P. Inflammation in atherosclerosis. Nature 2002;420(6917):868-874

2 Dutta P, Courties G, Wei Y, Leuschner F, Gorbatov R, Robbins CS, Iwamoto Y, Thompson B, Carlson AL, Heidt T, Majmudar MD, Lasitschka F, Etzrodt M, Waterman P, Waring MT, Chicoine AT, van der Laan AM, Niessen HW, Piek JJ, Rubin BB, Butany J, Stone JR, Katus HA, Murphy SA, Morrow DA, Sabatine MS, Vinegoni C, Moskowitz MA, Pittet MJ, Libby P, Lin CP, Swirski FK, Weissleder R and Nahrendorf M. Myocardial infarction accelerates atherosclerosis. Nature 2012;487(7407):325-9

3 Rosenbaum D, Millon A and Fayad ZA. Molecular imaging in atherosclerosis: FDG PET. Curr Atheroscler Rep 2012;14(5):429-437

4 Tawakol A, Migrino RQ, Bashian GG, Bedri S, Vermylen D, Cury RC, Yates D, LaMuraglia GM, Furie K, Houser S, Gewirtz H, Muller JE, Brady TJ and Fischman AJ. In vivo ^{18}F-fluorodeoxyglucose positron emission tomography imaging provides a noninvasive measure of carotid plaque inflammation in patients. J Am Coll Cardiol 2006;48(9):1818-24

5 Rudd JH, Myers KS, Bansilal S, Machac J, Pinto CA, Tong C, Rafique A, Hargeaves R, Farkouh M, Fuster V and Fayad ZA. Atherosclerosis inflammation imaging with ^{18}F-FDG PET: carotid, iliac, and femoral uptake reproducibility, quantification methods, and recommendations. J Nucl Med 2008;49(6):871-878

6 Rominger A, Saam T, Wolpers S, Cyran CC, Schmidt M, Foerster S, Nikolaou K, Reiser MF, Bartenstein P and Hacker M. ^{18}F-FDG PET/CT identifies patients at risk for future vascular events in an otherwise asymptomatic cohort with neoplastic disease. J Nucl Med 2009;50(10):1611-1620

7 Lee SJ, On YK, Lee EJ, Choi JY, Kim BT and Lee KH. Reversal of vascular ^{18}F-FDG uptake with plasma high-density lipoprotein elevation by atherogenic risk reduction. J Nucl Med 2008;49(8):1277-1282

8 Yun M, Jang S, Cucchiara A, Newberg AB and Alavi A. ^{18}F FDG uptake in the large arteries: a correlation study with the atherogenic risk factors. Semin Nucl Med 2002;32(1):70-76

9 Rudd JH, Myers KS, Bansilal S, Machac J, Rafique A, Farkouh M, Fuster V and Fayad ZA. (18)Fluorodeoxyglucose positron emission tomography imaging of atherosclerotic plaque inflammation is highly reproducible: implications for atherosclerosis therapy trials. J Am Coll Cardiol 2007;50(9):892-896

10 Mehta NN, Torigian DA, Gelfand JM, Saboury B and Alavi A. Quantification of atherosclerotic plaque activity and vascular inflammation using [18-F] fluorodeoxyglucose positron emission tomography/computed tomography (FDG-PET/CT). J Vis Exp 2012;63):e3777

11 Fuijkschot WW, Morrison MC, van der Linden R, Krijnen PA, Zethof IP, Theyse LF, Kleemann R, Niessen HW and Smulders YM. Orthopedic surgery increases atherosclerotic lesions and necrotic core area in ApoE-/- mice. Atherosclerosis 2016;255(164-170

12 Frings V, Yaqub M, Hoyng LL, Golla SS, Windhorst AD, Schuit RC, Lammertsma AA, Hoekstra OS, Smit EF and Boellaard R. Assessment of simplified methods to measure [18]F-FLT uptake changes in EGFR-mutated non-small cell lung cancer patients undergoing EGFR tyrosine kinase inhibitor treatment. J Nucl Med 2014;55(9):1417-1423

13 Calder PC, Dimitriadis G and Newsholme P. Glucose metabolism in lymphoid and inflammatory cells and tissues. Current opinion in clinical nutrition and metabolic care 2007;10(4):531-40

14 Lammertsma AA, Hoekstra CJ, Giaccone G and Hoekstra OS. How should we analyse FDG PET studies for monitoring tumour response? Eur J Nucl Med Mol Imaging 2006;33 Suppl 1(16-21

15 Boellaard R, O'Doherty MJ, Weber WA, Mottaghy FM, Lonsdale MN, Stroobants SG, Oyen WJ, Kotzerke J, Hoekstra OS, Pruim J, Marsden PK, Tatsch K, Hoekstra CJ, Visser EP, Arends B, Verzijlbergen FJ, Zijlstra JM, Comans EF, Lammertsma AA, Paans AM, Willemsen AT, Beyer T, Bockisch A, Schaefer-Prokop C, Delbeke D, Baum RP, Chiti A and Krause BJ. FDG PET and PET/CT: EANM procedure guidelines for tumour PET imaging: version 1.0. Eur J Nucl Med Mol Imaging 2010;37(1):181-200

16 Verwer EE, Oprea-Lager DE, van den Eertwegh AJ, van Moorselaar RJ, Windhorst AD, Schwarte LA, Hendrikse NH, Schuit RC, Hoekstra OS, Lammertsma AA and Boellaard R. Quantification of [18]F-fluorocholine kinetics in patients with prostate cancer. J Nucl Med 2015;56(3):365-71

17 Hoekstra CJ, Hoekstra OS and Lammertsma AA. On the use of the injection catheter for venous blood sampling in quantitative FDG PET studies. European journal of nuclear medicine 2000;27(10):1579

18 Prince MR, Novelline RA, Athanasoulis CA and Simon M. The diameter of the inferior vena cava and its implications for the use of vena caval filters. Radiology 1983;149(3):687-9

19 Mao SS, Ahmadi N, Shah B, Beckmann D, Chen A, Ngo L, Flores FR, Gao YL and Budoff MJ. Normal thoracic aorta diameter on cardiac computed tomography in healthy asymptomatic adults: impact of age and gender. Acad Radiol 2008;15(7):827-34

20 Watabe H, Ikoma Y, Kimura Y, Naganawa M and Shidahara M. PET kinetic analysis--compartmental model. Ann Nucl Med 2006;20(9):583-8

21 Cheebsumon P, Velasquez LM, Hoekstra CJ, Hayes W, Kloet RW, Hoetjes NJ, Smit EF, Hoekstra OS, Lammertsma AA and Boellaard R. Measuring response to therapy using FDG PET: semi-quantitative and full kinetic analysis. Eur J Nucl Med Mol Imaging 2011;38(5):832-42

8

Analysis of the effect of major orthopaedic surgery on atherosclerotic plaque inflammation in large arteries using ^{18}F-FDG PET/CT. Study outline and preliminary results

[*]Wessel W. Fuijkschot; [*]Gem M. Kramer; Maqsood. Yaqub; Paul A.J. Krijnen; Hans W.M. Niessen; Adriaan A. Lammertsma and Yvo M. Smulders

[*] Both authors contributed equally

In progress

ABSTRACT

Background: The risk of cardiovascular events is sharply elevated in the first days after major surgery. The cause of this increased risk is unknown, but its acuteness suggests increased plaque inflammation and subsequent plaque instability. [^{18}F]-2-fluoro-2-deoxy-D-glucose (FDG) imaging using positron-emission tomography (PET)/computed tomography (CT) provides a noninvasive assessment of large-artery plaque inflammation. This study assesses whether major orthopedic surgery causes increased inflammation in atherosclerotic lesions.

Methods: In this prospective observational multi-center study, patients scheduled for total knee or total hip replacement undergo ^{18}F-FDG-PET/CT scanning on 2 separate occasions: one day prior to surgery and 2 days after surgery. Venous blood samples are collected twice during the scanning procedure to measure plasma and whole-blood radioactivity concentrations in order to calibrate tissue-to-blood ratio [TBR]) for the aorta, carotid artery and the most diseased segment of these arteries. The first 4 patients of a larger scheduled group (n=20) are included in this preliminary report.

Results: K_i (influx rate constant of ^{18}F-FDG-uptake) after surgery for all arterial regions combined is lower, but not significantly, compared to pre-surgery (Median: 0.0075 vs. 0.0064; P = 0.053). The correlation between absolute as well as relative change in K_i and calibrated TBR after surgery is strong (R^2 >0.7). A significant decrease in TBR after surgery is observed for the ascending aorta as well as all regions combined ($P \leq 0.007$), but the change in uptake after surgery is not statistically significant for the carotid artery and the most-diseased segment separately.

Conclusions: These preliminary findings do not suggest an increase of FDG-activity in the large vessels after surgery. On the contrary, this interim-analysis suggests a decrease of inflammation in the aorta as a result of major orthopaedic surgery, which most likely not related to putative competitive uptake by surgery-induced tissue damage.

INTRODUCTION

The risk of cardiovascular events, mainly acute coronary syndrome and ischemic stroke, is sharply elevated in the first days after major surgery. A recent cohort study suggested that the risk of myocardial infarction in patients undergoing total hip or knee replacement is increased by no less than 25-fold, predominantly during the first weeks[1]. The acuteness of the increased risk suggests plaque instability, which is closely correlated with the degree of intra-plaque inflammation[2]. Major surgery is also associated with a marked systemic inflammatory response (the median C-reactive protein on day 3 after knee arthroplasty, is 189 mg/dl[3]). It thus has been hypothesized that intra-plaque inflammation may occur as a result of systemic inflammation. Indeed, we recently found that plaques become larger and show an increased necrotic core days after major orthopedic surgery in an atherosclerotic mice model[4]. The exact role of intra-plaque inflammation however remains elusive. There are, to date, no human studies to assess the role of intra-plaque inflammation following major surgery.

Recent developments in ^{18}F-fluorodeoxuglucose positron emission tomography (^{18}F-FDG-PET) allow for non-invasive imaging of inflammatory changes in large artery atherosclerosis (particularly carotid, aortic and ileofemoral regions)[5]. Carotid ^{18}F-FDG uptake was shown to be strongly correlated with macrophage density using CD68 immunohistochemistry[6]. Target-to-background ratio (TBR) of ^{18}F-FDG activity is an indicator of arterial wall/plaque inflammation[7], and identifies patients at risk for future vascular events[8-10, 11]. It is based on the standardized uptake value (SUV) ratio of a defined region of interest (ROI) over the background activity, usually derived from the superior vena cava[11, 12]. We recently showed that calibrated TBR using ^{18}F-FDG activity measured in venous blood samples can be used as surrogate simplified measures to assess changes in ^{18}F-FDG uptake in atherosclerotic plaques of patients recovering from major orthopaedic surgery (under review). This allows us to assess the role of generalized plaque inflammation as measured with large-artery ^{18}F-FDG PET/CT as a contributor to cardiovascular event risk in patients recovering from major surgery.

METHODS

Besides being scheduled for total knee replacement or total hip replacement, patients had to be above 65 years since these patients are likely to have ^{18}F-FDG positive atherosclerotic lesions[10, 13, 14]. Exclusion criteria are delirium or other cognitive impairment (acute or chronic) that impairs patient judgement, self-reported or objective discomfort in the supine position, recent myocardial infarction (< 6 months), current infection,

current corticosteroid use, chronic inflammatory diseases and/or auto-immune diseases, renal insufficiency (eGFR <30 mL/min/1.73m^2).

PET/CT scans are obtained using either an Ingenuity TF-128 or a Gemini TF-64 PET/CT scanner (Philips Healthcare, Eindhoven, The Netherlands). In all individual patients the pre- and post-surgery scan are obtained with the same scanner. All patients are asked to fast at least 6 hours prior to the PET scan. Patients are scanned arms down and the field of view was positioned over the thorax such that both ascending aorta and carotid arteries are included. First a low-dose CT during tidal breathing is performed for attenuation correction, directly followed by a 60 minutes dynamic ^{18}F-FDG PET scan (170 ± 17 MBq). ^{18}F-FDG (5 mL) is injected at a rate of 0.8 mL/s, and flushed with 35 mL NaCl 0.9% at 2.0 mL/s. The dynamic ^{18}F-FDG data are reconstructed into 19 time frames (1x15, 3x5, 3x10, 4x60, 2x150, 2x300, 4x600 s) using a 3-dimensional row-action maximum-likelihood reconstruction algorithm (3D-ramla) (voxel size 4x4x4 mm)[15]. All scans are corrected for usual corrections such as dead time, decay, scatter and randoms. During the ^{18}F-FDG scan 3 venous blood samples are drawn at 35, 45 and 55 minutes post injection to measure plasma and whole blood radioactivity concentrations[16]. Weight, height, total injected activity, time of injection, residual activity and exact scan start time of both time points are recorded for each session.

PET Data Analysis

Volumes of interest (VOIs) are drawn on PET images of the baseline and post-surgery ^{18}F-FDG scan. VOIs are generated for the ascending aorta and the carotids in order to quantify diffuse uptake in these vessels. Additionally, a VOI is generated in the visibly most diseased segment (MDS) in either the aorta or in one of the carotid arteries. We assess two different delineation methods for the ascending aorta and MDS: 1. Including the whole artery (including the lumen); 2. Including only the outer 1-2 voxels of the aorta. For the carotids, the whole artery is used as the spatial resolution of the PET/CT scan does not allow for separate delineation of the arterial wall. For these VOIs, time activity curves (TACs) are generated for each of the slices individually in a region (i.e. aorta, carotid or MDS) as well as for all slices of a region combined by projecting them onto the frames of the dynamic PET scan.

Image derived input functions (IDIFs) are obtained by placing a 8x8mm VOI (2x2 voxels) on the centre of the ascending aorta in 5 consecutive slices. Corresponding TACs are obtained by projecting the VOI onto the dynamic PET scan. IDIFs are scaled using whole blood activity concentrations and calibrated using the plasma-to-blood radioactivity concentration ratios obtained from the venous blood samples (median ratio: 0.92; range: 0.82-1.00).

Non-linear regression (NLR) analysis of the TACs is performed using the conventional irreversible 2-tissue compartmental plasma input model (2T3K) with an additional cor-

rection parameter for blood volume (V_b) (Fig. 1). For all VOIs the net rates of influx rates (Ki) are calculated from the individual rate constants: $K_i = K_1 \cdot k_3 / (k_2 + k_3)$. In addition, TBR is calculated by normalizing the SUV to the bloodpool activity in the aorta. The latter is obtained by placing a 8x8mm VOI in 5 consecutive planes of the ascending aorta and calibrated using venous blood samples. TBR is calculated for the time interval of 50-60 min post injection.

Statistical Analysis

Normality of the data is assessed visually using quantile-quantile plots and histogram analyses. The Wilcoxon signed-rank test is used to assess differences in patient- and scan characteristics between both scan time points. A Wilcoxon signed rank test is used to test for significant differences in mean uptake between the pre- and post-surgery scan. P values of less than 0.05 are considered significant. In addition, linear regression analysis is used to evaluate the correlation in between change in full kinetic outcome measures and TBR. All statistical analyses were performed using IBM SPSS Statistics for Windows, Version 21.0. (IBM Corp, Armonk, NY, USA).

RESULTS

Patients characteristics

Four consecutive patients were included in this preliminary report. Demographic characteristics are presented in Table 1. Baseline scans were obtained on the morning of surgery or, in 1 patient, one day prior to surgery. All follow-up scans were obtained 2 days post-surgery.

Table 1 Patient's baseline characteristics

Characteristics	
Patients (n)	4
Age (years, range)	75 (70-78)
Male, n (%)	1 (25)
BMI (kg/m^2)	25.4 (24.1-26.3)
Current smoking, n (%)	1 (25)
Diabetes Mellitus, n (%)	1 (25)
History of CVD, n (%)	2 (50)
Stroke, n (%)	2 (50)
Prior MI, n (%)	1 (25)

Variable represent median [interquartile range] or percentage of total patients (%). BMI, body mass index; CVD, cardiovascular disease; MI, myocardial infarction

Parameters of inflammation and serum lipids

To determine whether major orthopedic surgery is indeed accompanied by an acute systemic inflammatory response, we measured several parameters of inflammation at baseline and 2 days after surgery. CRP, leucocytes, neutrophilic granulocytes and ESR were all increased (Table 2). Serum lipids remained unchanged, besides a moderate decrease in LDL cholesterol.

Table 2 Laboratory data

Laboratory data	Pre-surgery	Post-surgery
Leucocytes 10^E9/L	6.0 [5.2-7.1]	9.0 [3.0-9.6]
Neutrophilic granulocytes 10^E9/L	4.0 [2.8-4.3]	7.2 [6.8-7.9]
CRP mg/L	22 [7-33]	116 [40-262]
ESR mm/hour	4 [2-17]	51 [23-93]
Total cholesterol mmol/L	3.8 [2.8-4.4]	2.9 [2.2-3.9]
HDL cholesterol mmol/L	1.1 [0.94-1.6]	1.2 [0.87-1.4]
LDL cholesterol mmol/L	2.1 [1.5-2.5]	1.3 [0.85-2.1]
Triglycerides mmol/L	0.9 [0.8-1.3]	1.0 [0.65-1.2]

Variable represent median [interquartile range]. CRP, C-reactive protein; ESR erythrocyte sediment rate; HDL, high density lipoprotein; LDL, low density lipoprotein.

^{18}F-FDG Quantitative Uptake Metrics

In every patients at least one area of increased ^{18}F-FDG could be distinguished (MDS). No new focal arterial uptake was seen post-surgery. K_i after surgery for all regions combined was borderline significantly lower than pre-surgery (median: 0.0075 vs. 0.0064; $P = 0.053$) (Fig. 2 and Table 3). Separate assessment per arterial region suggested that this decrease was mainly caused by a lower post-operative K_i of the ascending aorta ($P = 0.052$ vs. $P > 0.26$ for carotid artery and MDS).

The correlation between absolute as well as relative change in K_i and calibrated TBR after surgery was strong ($R^2 > 0.7$) (Fig. 3). The decrease in calibrated TBR after surgery was significantly different for the ascending aorta as well as all regions combined ($P \leq 0.007$). Change in uptake after surgery was not statistically significant for the carotid artery and the MDS.

With exception of K_1 all other pharmacokinetic parameters showed a significant change when all regions were combined ($P < 0.04$). When assessed separately, differences were only seen in one of the regions for each of these parameters respectively (Table 3). Change in K_1 after surgery did not correlate with change in K_i or TBR (Fig. 4).

Table 3 ^{18}F-FDG uptake parameters for several tissues before and after surgery (Median; IQR)

	Carotid artery		Ascending aorta		MDS	
Parameters	Baseline	Post-surgery	Baseline	Post-surgery	Baseline	Post-surgery
Irreversible 2-tissue pharmacokinetic model						
K_1	0.37 (0.18-0.52)	0.31 (0.21-0.43)	0.22 (0.13-0.30)	0.23 (0.17-0.27)	0.16 (0.11-0.27)	0.29 (0.09-0.34)*
k_2	1.36 (0.70-1.70)	1.39 (0.83-1.52)	1.41 (0.52-1.62)	1.63 (1.55-1.69)*	0.61 (0.34-1.55)	1.47 (0.27-1.59)
k_3	0.025 (0.025-0.029)	0.027 (0.025-0.033)	0.030 (0.025-0.045)	0.035 (0.025-0.069)*	0.027 (0.025-0.033)	0.025 (0.025-0.031)
V_b	0.22 (0.19-0.27)	0.15 (0.12-0.21)*	0.61 (0.41-0.68)	0.51 (0.36-0.65)	0.49 (0.31-0.56)	0.32 (0.25-0.45)
K_i	0.0086 (0.0069-0.0091)	0.0072 (0.0064-0.0092)	0.0067 (0.0057-0.0083)	0.0060 (0.0042-0.0081)	0.0074 (0.0055-0.0083)	0.0059 (0.0054-0.0091)
Simplified models						
Calibrated TBR (50-60 min)	0.96 (0.84-1.04)	0.77 (0.73-1.07)	0.92 (0.81-0.99)	0.79 (0.69-0.92)*	0.91 (0.74-0.97)	0.74 (0.70-1.04)

TBR: Tissue-to-blood ratio
*: Significant differences in uptake parameters before and after surgery ($P < 0.05$; Wilcoxon signed rank test). All K's are expressed in min-1

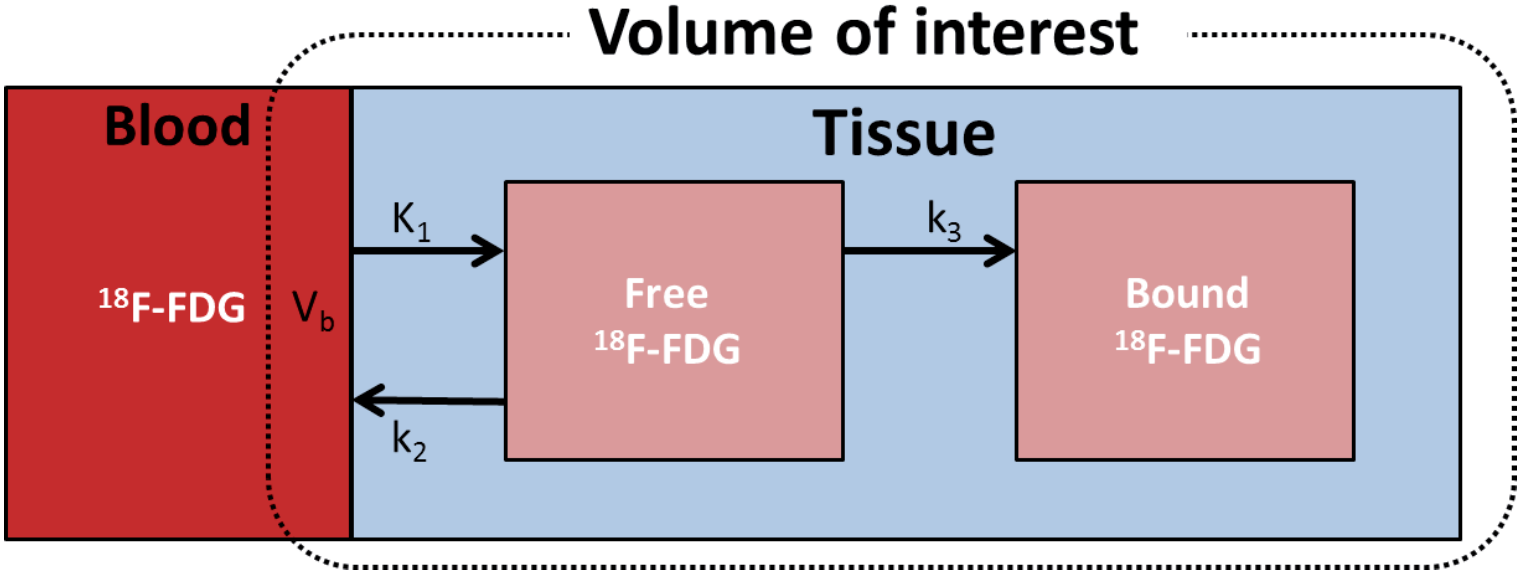

Figure 1

Two-tissue three compartment model with blood volume fraction (2T3K). (K_1 is the rate constant from blood to tissue, k_2 is the rate constant from tissue to blood, k_3 is the rate constant from free 18F-FDG in the tissue to bound 18F-FDG and V_b the blood volume fraction. K_i can be as $K_1 \cdot k_3 / (k_2 + k_3)$ an is the influx rate constant of 18F-FDG. (All K's are expressed in min-1)

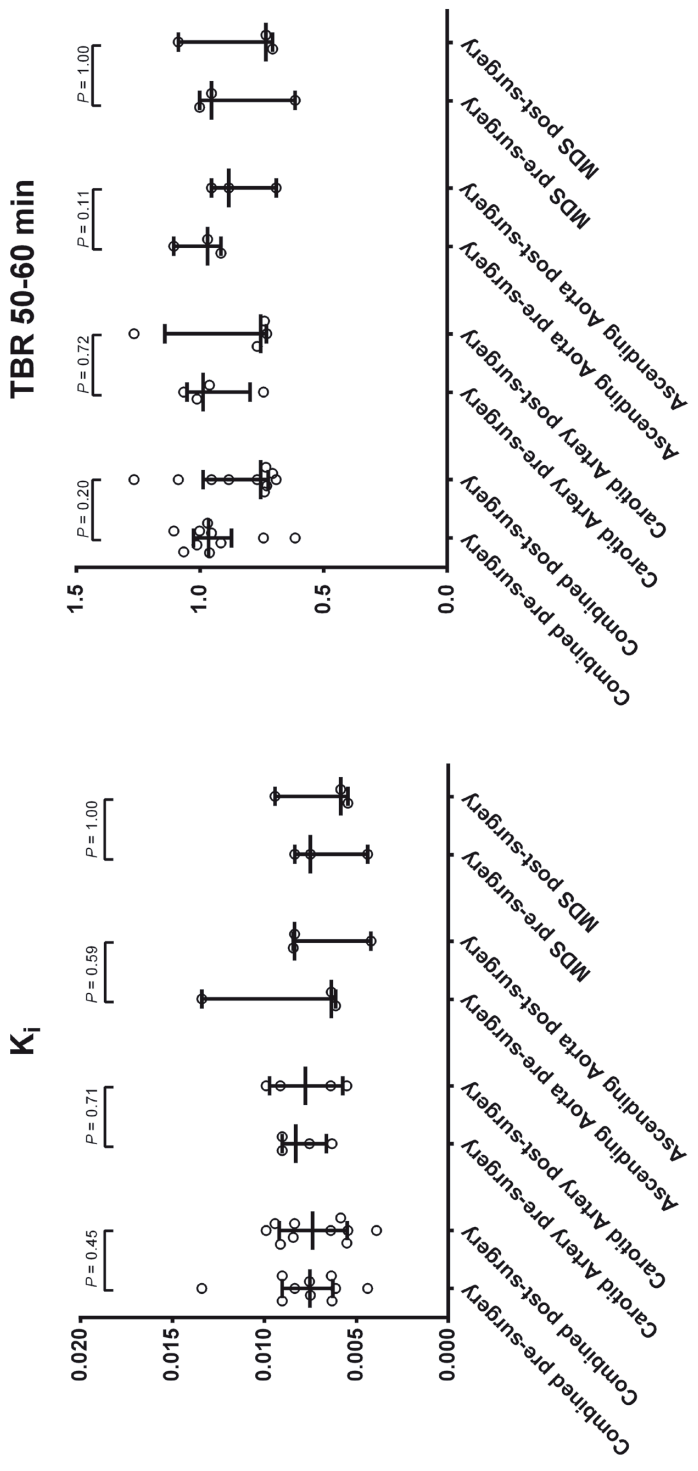

Figure 2

Ki (in min-1) and TBR values of all regions combined as well as separately before and after surgery. Wilcoxon signed rank test was used to calculate statistical significance of the differences between both time points.

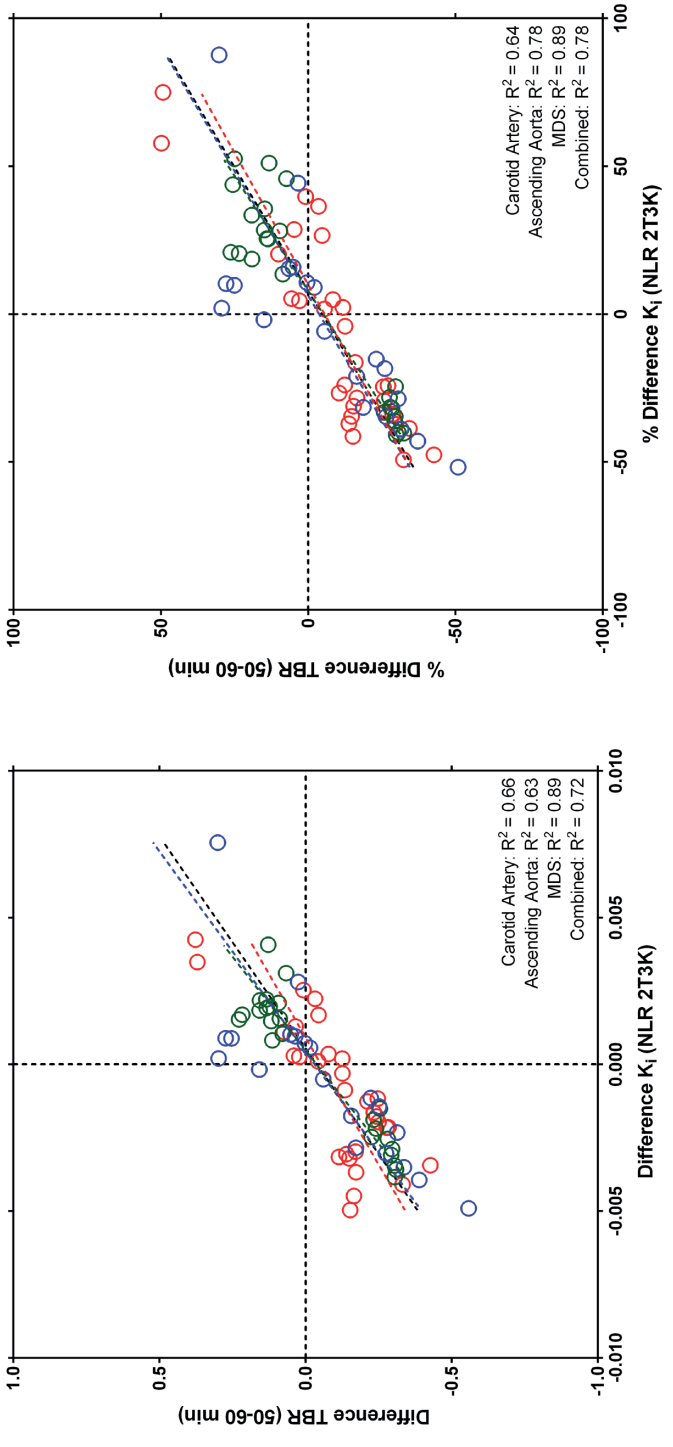

Figure 3

Scatterplots showing the correlation between absolute (Left) and relative (Right) differences in K_i (in min-1) and TBR after surgery for all regions. Carotid arteries (Blue), Ascending Aorta (Red) and Most diseased segment (MDS) (Green).

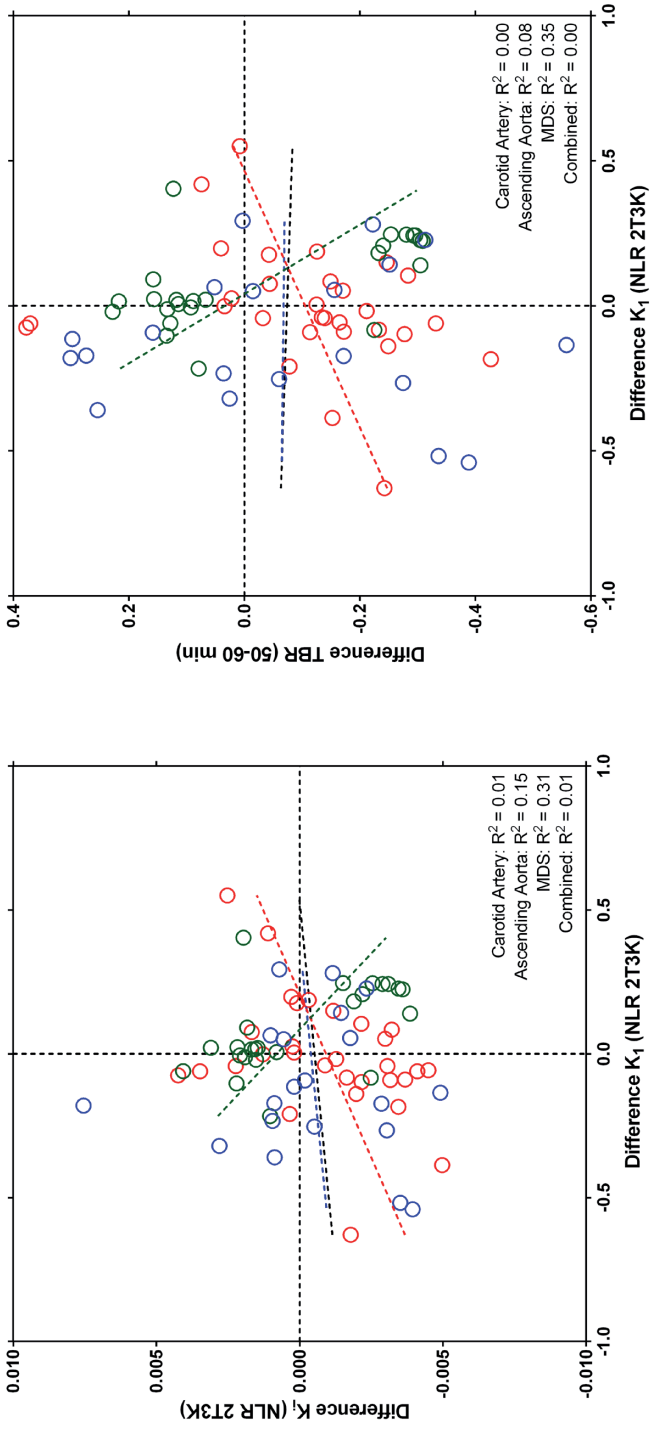

Figure 4
Scatterplots showing the correlation between change in K_1 and change in K_i (Left) and TBR (Right) for all regions. Carotid arteries (Blue), Ascending Aorta (Red) and Most diseased segment (MDS) (Green). Both K_1 and K_i are expressed in min-1.

DISCUSSION

This chapter describes the study protocol and initial results of an 18F-FDG-PET study designed to assess if major surgery can induce inflammatory activity in arterial wall, particularly in atherosclerotic lesions. Clearly, solid conclusions based on this interim-analysis (n=4 patients) cannot be drawn. Nevertheless, these preliminary results suggest that major orthopedic surgery does not evoke an increase of FDG-activity in the large vessels. In fact, the initial data point towards a decrease of inflammation in the aorta as a result of major orthopaedic surgery. If this indeed proves to be the conclusion, two explanations might be plausible:

Firstly, it is possible that plaque inflammation does not explain post-surgery cardiovascular event risk, and that the study hypothesis is therefore incorrect. Of note, lack of inflammation does not fully exclude plaque instability. An alternative explanation for post-surgery plaque instability could for example be increased shear-stress resulting from surgery or anesthesia induced hemodynamic disturbances, which may enhance plaque growth without necessarily increasing intra-plaque inflammation[17, 18]. In addition, other effects of surgery could explain post-surgical CVD risk, such as sympathetic nerve system activation[19] or activated primary and secondary hemostasis[20].

Two murine studies merit discussion. A recent study by us in ApoE -/- mice reported an increase in plaque and necrotic core area early after surgery. In parallel with the present study, less intra-plaque inflammation, as suggested by less intra-plaque macrophages, was found 15 days after major surgery[4]. To explain these results, we suggested that inflammatory cell infiltration took place before this time point and that activated macrophages in particular had already been decomposed, contributing to the necrotic core[9]. Another murine study addressed the combined effects of major blood loss and surgery, and reported increased plaque size after 72 h, along with signs of plaque vulnerability. This effect appeared to be mainly due to the excessive blood loss (20% of body weight; substantially more than in our patients[21]) rather than surgery itself. In this study, intra-plaque macrophages did not increase, further arguing that non-inflammatory conditions, such as a hyperdynamic circulation, rather than intra-plaque inflammation cause plaque vulnerability after major surgical trauma.

Secondly, it could be that increased plaque inflammation does occur after surgery, but that the 18F-FDG-PET detection technique is either not sufficiently sensitive or was inappropriately timed to capture this phenomenon. The aforementioned murine studies indeed suggest that timing is of great importance. We choose t=2 days based on the finding that risk of cardiovascular events is elevated already in the first days post-surgery, suggesting a fast inflammatory burst [1]. We cannot however exclude inflammatory cell infiltration taking place before or, more likely, after t=2 days.

A strength of the present study is the full kinetic modeling we have performed before and after surgery to correct for factors such as competitive uptake of the damaged tissue, changes in glucose metabolism, blood flow, fractional blood volume, and/or plasma clearance of 18F-FDG. Changes in all such factors can account for altered post-surgery vascular FDG-uptake. It is important for future studies to use a similar approach, or at least use appropriately calibrated TBRs, for example by using sampled venous 18F-FDG activity measurements.

To conclude, the preliminary results of this study suggest that major orthopedic surgery does not induce increased inflammation in atherosclerotic plaques of large arteries and therefore cannot help explain the high incidence of cardiovascular events following such operations. Extension of the sample size is, however, mandatory.

ACKNOWLEDGMENTS

We acknowledge the staff of the Department of Radiology and Nuclear Medicine of the VU University Medical Center, Amsterdam, The Netherlands for their help with performing the scans.

FUNDING

This study was financed by the Institute for Cardiovascular Research (ICaR-VU; Grant No.ICaR-VU-ID414-2012).

REFERENCES

1 Lalmohamed A, Vestergaard P, Klop C, Grove EL, de BA, Leufkens HG, van Staa TP and de VF. Timing of acute myocardial infarction in patients undergoing total hip or knee replacement: a nationwide cohort study. Arch Intern Med 2012;172(16):1229-1235

2 Libby P. Inflammation in atherosclerosis. Nature 2002;420(6917):868-874

3 Reid D, Toole BJ, Knox S, Talwar D, Harten J, O'Reilly DS, Blackwell S, Kinsella J, McMillan DC and Wallace AM. The relation between acute changes in the systemic inflammatory response and plasma 25-hydroxyvitamin D concentrations after elective knee arthroplasty. Am J Clin Nutr 2011;93(5):1006-1011

4 Fuijkschot WW, Morrison MC, van der Linden R, Krijnen PA, Zethof IP, Theyse LF, Kleemann R, Niessen HW and Smulders YM. Orthopedic surgery increases atherosclerotic lesions and necrotic core area in ApoE-/- mice. Atherosclerosis 2016

5 Rosenbaum D, Millon A and Fayad ZA. Molecular imaging in atherosclerosis: FDG PET. Curr Atheroscler Rep 2012;14(5):429-437

6 Tawakol A, Migrino RQ, Bashian GG, Bedri S, Vermylen D, Cury RC, Yates D, LaMuraglia GM, Furie K, Houser S, Gewirtz H, Muller JE, Brady TJ and Fischman AJ. In vivo 18F-fluorodeoxyglucose positron emission tomography imaging provides a noninvasive measure of carotid plaque inflammation in patients. J Am Coll Cardiol 2006;48(9):1818-24

7 Rudd JH, Myers KS, Bansilal S, Machac J, Pinto CA, Tong C, Rafique A, Hargeaves R, Farkouh M, Fuster V and Fayad ZA. Atherosclerosis inflammation imaging with 18F-FDG PET: carotid, iliac, and femoral uptake reproducibility, quantification methods, and recommendations. J Nucl Med 2008;49(6):871-878

8 Rominger A, Saam T, Wolpers S, Cyran CC, Schmidt M, Foerster S, Nikolaou K, Reiser MF, Bartenstein P and Hacker M. 18F-FDG PET/CT identifies patients at risk for future vascular events in an otherwise asymptomatic cohort with neoplastic disease. J Nucl Med 2009;50(10):1611-1620

9 Lee SJ, On YK, Lee EJ, Choi JY, Kim BT and Lee KH. Reversal of vascular 18F-FDG uptake with plasma high-density lipoprotein elevation by atherogenic risk reduction. J Nucl Med 2008;49(8):1277-1282

10 Yun M, Jang S, Cucchiara A, Newberg AB and Alavi A. 18F FDG uptake in the large arteries: a correlation study with the atherogenic risk factors. Semin Nucl Med 2002;32(1):70-76

11 Rudd JH, Myers KS, Bansilal S, Machac J, Rafique A, Farkouh M, Fuster V and Fayad ZA. (18)Fluorodeoxyglucose positron emission tomography imaging of atherosclerotic plaque inflammation is highly reproducible: implications for atherosclerosis therapy trials. J Am Coll Cardiol 2007;50(9):892-896

12 Mehta NN, Torigian DA, Gelfand JM, Saboury B and Alavi A. Quantification of atherosclerotic plaque activity and vascular inflammation using [18-F] fluorodeoxyglucose positron emission tomography/computed tomography (FDG-PET/CT). J Vis Exp 2012;63):e3777

13 Dunphy MP, Freiman A, Larson SM and Strauss HW. Association of vascular 18F-FDG uptake with vascular calcification. J Nucl Med 2005;46(8):1278-1284

14 Conroy RM, Pyorala K, Fitzgerald AP, Sans S, Menotti A, De BG, De BD, Ducimetiere P, Jousilahti P, Keil U, Njolstad I, Oganov RG, Thomsen T, Tunstall-Pedoe H, Tverdal A, Wedel H, Whincup P, Wilhelmsen L and Graham IM. Estimation of ten-year risk of fatal cardiovascular disease in Europe: the SCORE project. Eur Heart J 2003;24(11):987-1003

15 Boellaard R, O'Doherty MJ, Weber WA, Mottaghy FM, Lonsdale MN, Stroobants SG, Oyen WJ, Kotzerke J, Hoekstra OS, Pruim J, Marsden PK, Tatsch K, Hoekstra CJ, Visser EP, Arends B, Verzijlbergen FJ, Zijlstra JM, Comans EF, Lammertsma AA, Paans AM, Willemsen AT, Beyer T, Bockisch A, Schaefer-Prokop C, Delbeke D, Baum RP, Chiti A and Krause BJ. FDG PET and PET/CT: EANM procedure guidelines for tumour PET imaging: version 1.0. Eur J Nucl Med Mol Imaging 2010;37(1):181-200

16 Frings V, Yaqub M, Hoyng LL, Golla SS, Windhorst AD, Schuit RC, Lammertsma AA, Hoekstra OS, Smit EF and Boellaard R. Assessment of simplified methods to measure 18F-FLT uptake changes in EGFR-mutated non-small cell lung cancer patients undergoing EGFR tyrosine kinase inhibitor treatment. J Nucl Med 2014;55(9):1417-1423

17 Wang Y, Qiu J, Luo S, Xie X, Zheng Y, Zhang K, Ye Z, Liu W, Gregersen H and Wang G. High shear stress induces atherosclerotic vulnerable plaque formation through angiogenesis. Regen Biomater 2016;3(4):257-67

18 Malek AM, Alper SL and Izumo S. Hemodynamic shear stress and its role in atherosclerosis. JAMA 1999;282(21):2035-42

19 Dutta P, Courties G, Wei Y, Leuschner F, Gorbatov R, Robbins CS, Iwamoto Y, Thompson B, Carlson AL, Heidt T, Majmudar MD, Lasitschka F, Etzrodt M, Waterman P, Waring MT, Chicoine AT, van der Laan AM, Niessen HW, Piek JJ, Rubin BB, Butany J, Stone JR, Katus HA, Murphy SA, Morrow DA, Sabatine MS, Vinegoni C, Moskowitz MA, Pittet MJ, Libby P, Lin CP, Swirski FK, Weissleder R and Nahrendorf M. Myocardial infarction accelerates atherosclerosis. Nature 2012;487(7407):325-329

20 Santos-Gallego CG and Badimon JJ. The sum of two evils: pneumonia and myocardial infarction: is platelet activation the missing link? J Am Coll Cardiol 2014;64(18):1926-1928

21 Janssen H, Wagner CS, Demmer P, Callies S, Solter G, Loghmani-khouzani H, Hu N, Schuett H, Tietge UJ, Warnecke G, Larmann J and Theilmeier G. Acute perioperative-stress-induced increase of atherosclerotic plaque volume and vulnerability to rupture in apolipoprotein-E-deficient mice is amenable to statin treatment and IL-6 inhibition. Dis Model Mech 2015;8(9):1071-80

9

Inflammatory cell content of coronary thrombi is dependent on thrombus age in patients with ST-elevation myocardial infarction

Wessel W. Fuijkschot; Wouter E. Groothuizen; Yolande E.A. Appelman; Teodora Radonic; Niels van Royen; Maarten A.H. van Leeuwen; Pau A.J. Krijnen; Allard C. van der Wal; Yvo M. Smulders and Hans W.M. Niessen

J Cardiol 2017;69:394-400

ABSTRACT

Background: ST-elevation myocardial infarction (STEMI) is typically caused by an occlusive coronary thrombus. The process of intracoronary thrombus formation is poorly understood. It is known that inflammatory cells play a role in the formation and resolution of venous thrombi, however their role in coronary thrombosis is not clear. We therefore analyzed inflammatory cells in thrombi derived from patients with STEMI in relation to histologically classified thrombus age.

Methods: Thrombus aspirates of 113 patients treated with primary Percutaneous Coronary Intervention were prospectively collected and classified (fresh, lytic or organized) based on hematoxylin and eosin staining. The density of inflammatory cells neutrophils (MPO), monocytes/macrophages (CD68), lymphocytes (CD45) and the platelet area (CD31), were visualized using immunohistochemistry. Patients' history, medication and laboratory data were registered.

Results: Fresh thrombi (76.1 %) were the most abundant as compared to lytic (16.8 %) and organized (7.1 %) thrombi. Neutrophils were significantly less present in organized (169 cells/mm^2) compared to fresh (327 cells/mm^2) and lytic thrombi (311 cells/mm^2). Monocytes/macrophages were significantly more present in lytic (471 cells/mm^2) than in fresh (312 cells/mm^2) thrombi. We additionally found that thrombi from patients aged <50 years as compared to >50 years old contained significant more neutrophils and monocytes/macrophages irrespective of thrombus age. Furthermore, platelet area was smaller in patients on aspirin again irrespective of thrombus age. No gender differences were found.

Conclusions: The composition of inflammatory cells differs with thrombus age in thrombosuction material of STEMI patients that in part depends on patient age and medication.

INTRODUCTION

Acute ST-elevation myocardial infarction (STEMI) is typically caused by occlusive coronary thrombus formation superimposed on a ruptured atherosclerotic plaque[1]. Plaque disruption triggers the formation of initial platelet aggregates that expand in association with an increase in fibrin formation and subsequent trapping of erythrocytes leading to persistent coronary flow obstruction[2]. Neutrophils and monocytes are present in these thrombi at 3 hours after onset of complaints. After 6 hours T-cell and B-cell infiltration significantly increases[3-5]. Of note, inflammatory cells in thrombi were evaluated in these studies in relation to symptom to balloon time, which provides an inadequate estimate of thrombus age[6, 7]. Knowledge of the composition of inflammatory cells would be interesting since it is known that inflammatory cells play a role in the formation and resolution of venous thrombi[8, 9]. Rittersma et al. 6 described a classification method based on histological characteristics which since then is considered as the gold standard for the estimation of thrombus age of coronary thrombi. They defined thrombi as: fresh (less than one day old) when they were composed of layered patterns of fibrin and intact cells (platelets, erythrocytes and neutrophilic granulocytes); lytic (between 1 and 5 days old) when areas of colliquation necrosis and karyorrhexis of neutrophilic granulocytes were present; organized (more than 5 days old) when areas of ingrowth of smooth muscle cells, with or without depositions of young connective tissue and/or ingrowth of capillary vessels was observed. Several studies have shown that this histological appearance doesn't relate to clinical infarct duration or symptom to balloon time[6, 7, 10], indicative for a time interval of days to weeks between plaque disturbance, thrombus formation and the onset of symptoms[6]. This suggests that sudden coronary occlusion is often preceded by a variable period of plaque instability and/or thrombus formation, underlining the importance of identifying thrombus initiation and early progression before occlusion becomes clinically overt[11, 12]. In this light it is of great importance to further elucidate the timescale of thrombus formation and the factors involved.

It is known that inflammatory cells play an important role in the process of plaque instability[13], but their role in arterial thrombus formation is however less known. For this, we have studied the composition of the aspirated thrombus material in relation to their histologically defined age in a large cohort of STEMI patients undergoing primary Percutaneous Coronary Intervention (PCI) after sudden onset of symptoms. We also set out to evaluate if clinical variables like sex, age or medication influence the thrombus composition.

MATERIALS AND METHODS

Thrombus aspiration and clinical data

Patients who presented at the VU university medical center with a STEMI (defined according to the ESC guidelines for STEMI[14]) and from whom thrombus was aspirated were included in the study. All PCI's were performed according to current standard guidelines for PCI. After arrival of the ambulance or after arrival at the hospital, patients were treated with 300 mg of aspirin and 5000 IU of heparin intra venous (iv). On admission patients were directly transported to the catheterization laboratory and PCI was performed of the infarct related artery and a repeat bolus of heparin was given at the cathlab, based on the patient's body weight. After passage of the coronary artery occlusion with a guide wire, manual thrombectomy was performed with the Export AP Aspiration Catheter Medtronic, Dublin, Ireland. Typically, several suctions at the site of the occlusion were performed after smooth introduction and initial passage of catheter. Aspirated thrombus and intracoronary material were collected in the collection bottle, which was provided with a filter. Additional balloon angioplasty and stent placement were performed at the discretion of the operator, as was the additional use of glycoprotein IIb/IIIa receptor blockers. Upon thrombosuction, specimens were immediately fixed in formalin. The following baseline clinical data of the patients were collected: age, gender, cardiovascular history, medication, cardiovascular risk factors, infarct-related artery, C-reactive protein and white blood cell count in the blood. The study conforms with the principles outlined in the Declaration of Helsinki. The study protocol was approved by the medical ethical research committee at the VU university medical center.

Histology

The aspirated coronary thrombus material was embedded in paraffin after overnight fixation (4 % formalin). Tissues were deparaffinised, rehydrated and stained with a standard haematoxylin/eosin (HE)-staining. Thrombi were histopathologically classified based on the observation of two independent observers (H.W.M.N. and A.C.W), as described before[6]: fresh (less than one day old): completely composed of layered patterns of platelets, fibrin, erythrocytes and intact granulocytes; lytic (between 1 and 5 days old): areas of colliquation necrosis and karyorrhexis of granulocytes; organized (more than 5 days old): areas of ingrowth of smooth muscle cells, with or without depositions of young connective tissue and ingrowth of capillary vessels. Thrombus material with a heterogeneous composition was graded according to the age of the oldest part.

Immunohistochemistry

For immunohistochemical analysis tissues were deparaffinised, rehydrated and incubated in methanol/H2O2 (0.3%) for 30 min to block endogenous peroxidases. Antigen retrieval was performed by boiling the slides (MPO, CD68, CD31 but not for CD45) for 10 min in a citrate pH 6.0 buffer. The sections were incubated with either rabbit anti-human myeloperoxidase (1:500, A0398 Dako, Glostrup, Denmark), mouse anti-human CD68 (1:400, M0814 Dako, Glostrup, Denmark), mouse anti-human CD31 (1:40, M0823 Dako, Glostrup, Denmark) or mouse anti-human CD45 (1:50, M0701 Dako, Glostrup, Denmark) antibody for 1 hour at room temperature (RT). Next, the sections were incubated with anti-mouse/rabbit Envision (Dako, Glostrup, Denmark) for 30 min at RT. The stainings were visualized with 3,30-diaminobenzidine (0.1 mg/ml, 0.02% H2O2) for 10 minutes. The slides were subsequently counterstained with haematoxylin, dehydrated and covered. With each staining a PBS control was included. All these controls yielded negative results (not shown). All the slides were scanned with the MIRAX scan (3DHISTECH Ltd Budapest, Hungary). With the MIRAX Viewer software snapshots of all tissue were made and stored for further processing with ImageJ. Area's in thrombi (n=11; 9.7 %) that contained plaque material were left out of further analysis. The surface area of CD31-positive thrombocytes was quantitatively measured and divided by the total surface area of the scored tissue. For the slides stained with MPO, CD68 and CD45 the numbers of positive cells were scored and divided by the total surface area of the scored tissue.

Statistics

Continuous variables are expressed as mean ± standard deviation (SD) for normally distributed or median (interquartile range) for non-normally distributed ones. Differences between the groups were tested by Student t-test for normally distributed or by the Mann-Whitney U (two groups) and Kruskal-Wallis (> 2 groups) test for non-normally distributed continuous variables. The Pearson or Spearman rank correlation coefficients were calculated to test the association between two variables with a normal or non-normal distribution. $P<0.05$ was considered statistically significant. All statistical analyses were performed with SPSS software (Windows version 20, IBM corp., Armonk, NY).

RESULTS

Thrombus age and the number of inflammatory cells

Intracoronary-derived thrombus material was collected from 113 patients (see Table 1 for patient characteristics). Histological evaluation of the aspirated material in tissue sections showed that fresh thrombi (n=86; 76.1 %) were the most abundant as compared to lytic (n=19; 16.8 %) and organized (n=8; 7.1 %). Inflammatory cells and area of platelets were present (Fig. 1).

Table 1 Patient characteristics

Characteristics	
Age (years, mean ± SD)	61.1 ± 12.4
Male, n (%)	73 (82/113)
Current smoking, n (%)	38 (25/65)
Hypercholesterolemia	22 (14/65)
Hypertension, n (%)	37 (24/65)
Diabetes Mellitus, n (%)	9 (6/65)
Family history of CAD, n (%)	35 (23/65)
Chronic aspirin use, n (%)	15 (13/86)
Statin use, n (%)	13 (11/86)
Prior angina, n (%)	32 (11/34)
Prior MI, n (%)	14 (14/100)
Symptom to balloon time (hrs., median [IQR])	2.0 [2.0-3.0]
ST-resolution, n (%)	81 (56/69)
Drug eluting stent, n (%)	9 (8/85)
Stent diameter, mm mean ± SD	3.3 ± 0.4
Stent length, mm mean ± SD	23 ± 5
Infarct-related artery	
RCA, n (%)	43 (46/106)
RCx, n (%)	12 (13/106)
LAD, n (%)	44 (47/106)
Laboratory data	
Platelets 10^E9/L, median [IQR]	244 [191-289]
WBC 10^E9/L, median [IQR]	10.9 [8.4-13.3]
CRP mg/L	3.4 (2.5-6.2)
CK-MB IU/L	218 (117-328)

Variable represent mean (± SD), percentage of total patients (%), median [interquartile range]. CAD indicates coronary artery disease; MI, myocardial infarction; RCA, right coronary artery; RCx, right circumflex; LAD, left anterior descending coronary artery; CRP: C-reactive protein; CK-MB, creatine kinase MB

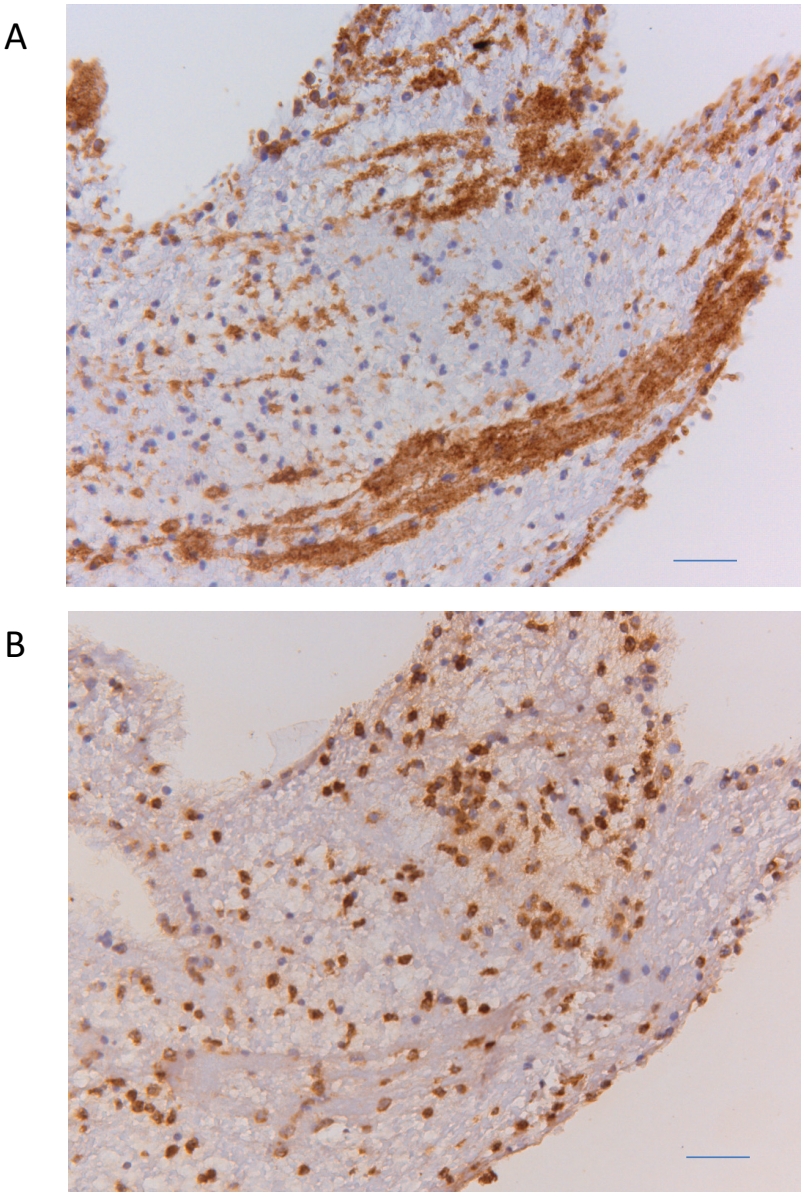

Figure 1 Example of immunohistochemical staining of aspirated coronary thrombus

A: CD31 positive area indicative for platelets. **B:** MPO positive cells indicative for neutrophilic granulocytes. Scale bar represents 100 µm.

We then evaluated the density of inflammatory cells per thrombus phase. Neutrophils were significantly less present in organized thrombi (169 [76.3-222] cells/mm^2) compared to fresh (327 [178-504] cells/mm^2) (p=0.017) and lytic thrombi (311 [191- 578] cells/mm^2) (p=0.012) (Fig. 2A). CD68 positive monocytes/macrophages, were more

present in lytic (471 [301-696] cells/mm^2) than in fresh (312 [161-466] cells/mm^2) (p=0.013) and organized (405 [249-569]) thrombi, although the difference between lytic and organized was not significant (p=0.355) (Fig. 2B). The number of lymphocytes did not differ between the three groups (fresh thrombi: 154 [72.9-284] cells/mm2, lytic thrombi; 200 [99.7-374] cells/mm^2 and organized thrombi: 120 [38.8-281] cells/mm^2). Also platelet areas were not significantly different among the 3 groups (fresh thrombi: 25.5 [15.0-39.5] %, lytic thrombi 30.5[20.0-36.0] % and organized thrombi: 37.0 [22.0-46.0] %).

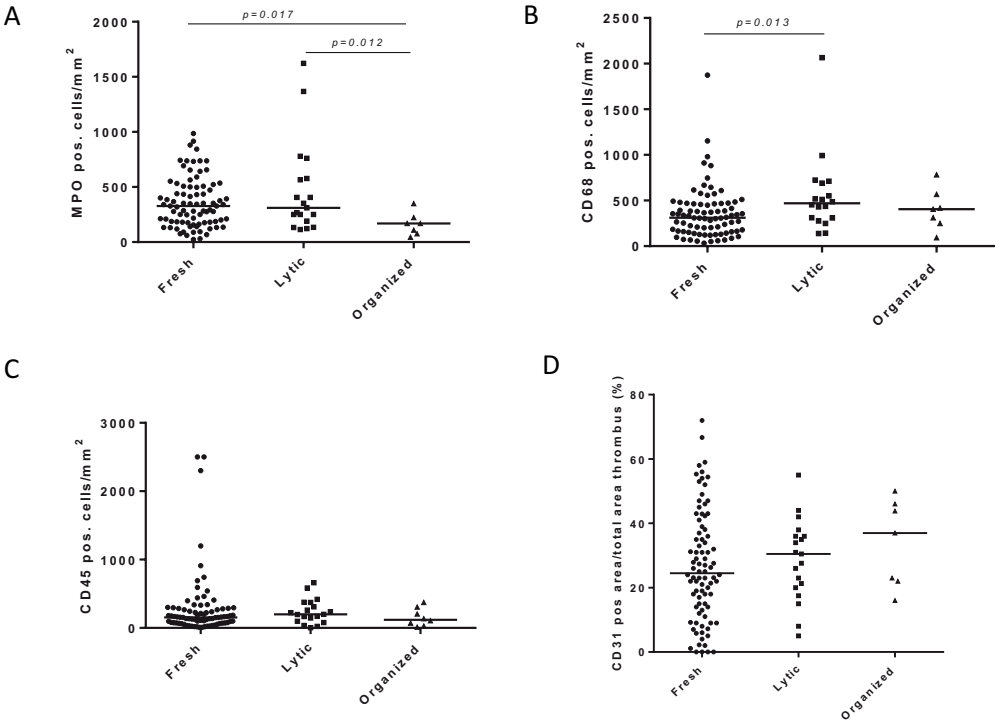

Figure 2 Amount of inflammatory cells and platelets per thrombus area at different time points.

A: MPO positive cells indicative for neutrophilic granulocytes per thrombus area. **B:** CD68 positive cells indicative for monocytes/macrophages per thrombus area. **C:** CD45 positive cells indicative for number of lymphocytes per thrombus area. **D:** CD31 positive area (indicative for thrombocytes) divided by total thrombus area in percentages. Thrombi are divided in age based on histology: fresh, lytic and organized thrombi. Bars represent median.

Next we evaluated symptom to balloon time in hours and thrombus composition. We found no significant differences between symptom to balloon time of fresh, lytic and organized thombi, respectively 2.0 [2.0-3.0], 2.8 [1.9-4.3] and 2.5 [1.6-3.8] hours (p=0.30). No correlation between symptom to balloon time and neutrophils (r=0.084; p=0.424), macrophages/monocytes (r=0.088; p=0.416) and lymphocytes (0.088; p=0.405) existed. We did found a moderate correlation between symptom to balloon time and platelet area (r=0.244; p=0.020) (Fig. 3).

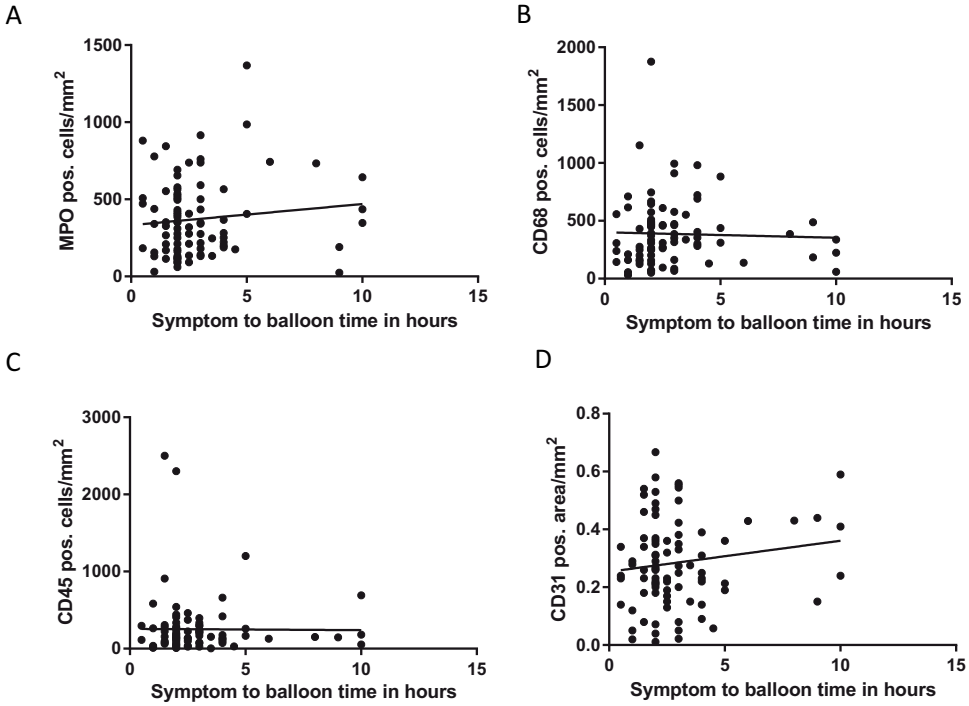

Figure 3 Relation between symptom to balloon time and thrombus composition

A: MPO positive cells indicative for neutrophilic granulocytes per thrombus area. **B:** CD68 positive cells indicative for monocytes/macrophages per thrombus area. **C:** CD45 positive cells indicative for number of lymphocytes per thrombus area. **D:** CD31 positive area (indicative for thrombocytes) divided by total thrombus area in percentages.

Clinical variables and thrombus composition

Patient age

In order to evaluate the effect of age on inflammatory cell and platelet content in thrombi, we correlated patient age with neutrophils, monocytes/macrophages, lymphocytes and platelets. Negative, but non-significant correlations were found between patients age and number of neutrophils in the thrombus (r=-0.126 p=0.190), monocytes/macrophages (r=-0.173 p=0.079), lymphocytes (r=-0.102 p=0.292) and platelet area (r=-0.109 p=0.264).

Next, we divided the population into two groups using a cut-off of 50 years. This cut-off is arbitrary, but allowed us to evaluate possible difference between patients that suffer from myocardial infarction at a relatively young age versus older patients. The percentages of fresh, lytic or organized thrombi in patients younger than 50 years (median 43; range 27-49) and in patients older than 50 years (median 63; range 50-87) did not differ and were similar to percentage for all the thrombi together. The number of neutrophils was significantly higher in thrombi of younger patients (<50 yrs) as compared to older (>50 yrs) patients (375 [277-536] vs. 267 [140-439] cells/mm2; p=0.020) (Fig. 4A). Also monocytes/macrophages were more abundant in thrombi of younger patients (<50 yrs) (413[311-543] vs. 310 [160-473 cells/mm2; p=0.006). The number of lymphocytes was not significantly different (199 [137-295] vs. 152 [71.9-285] cells/mm2; p=0.142). We also observed a significant difference between the <50 years and >50 years group for platelet count in blood (273 [252-316] vs. 235 [187-280] 109/L, p=0.012) but this was not reflected by platelet area in the thrombi (30.00[21.39-42.71] vs. 26.00 [15.00-38.05] %; p=0.264).

Gender

When comparing males (n=82; 73 %) and females (n=31; 27%) no differences in the percentages of fresh (78 % vs. 71 %), lytic (13 % vs. 26 %) or organized (9 % vs. 3 %) thrombi (p=0.212) were observed. Also the number of inflammatory cells was not different (lymphocytes 155.36 [70.37-265.26] vs. 166.67 [98.65-341.67] cells/mm^2 p=0.490, neutrophils 301.37 [163.67-462.66] vs. 282.65 [180.00-564.17 cells/mm^2 p=0.684 and monocytes/macrophages 366.96 [183.50-480.00] vs. 352.45 [174.54-611.25] cells/mm^2 p=0.456). Finally, the platelet area was neither significantly different, namely 26,35 % [11.50-42.50] vs. 27.59 % [18.00-37.00] p=0.923.

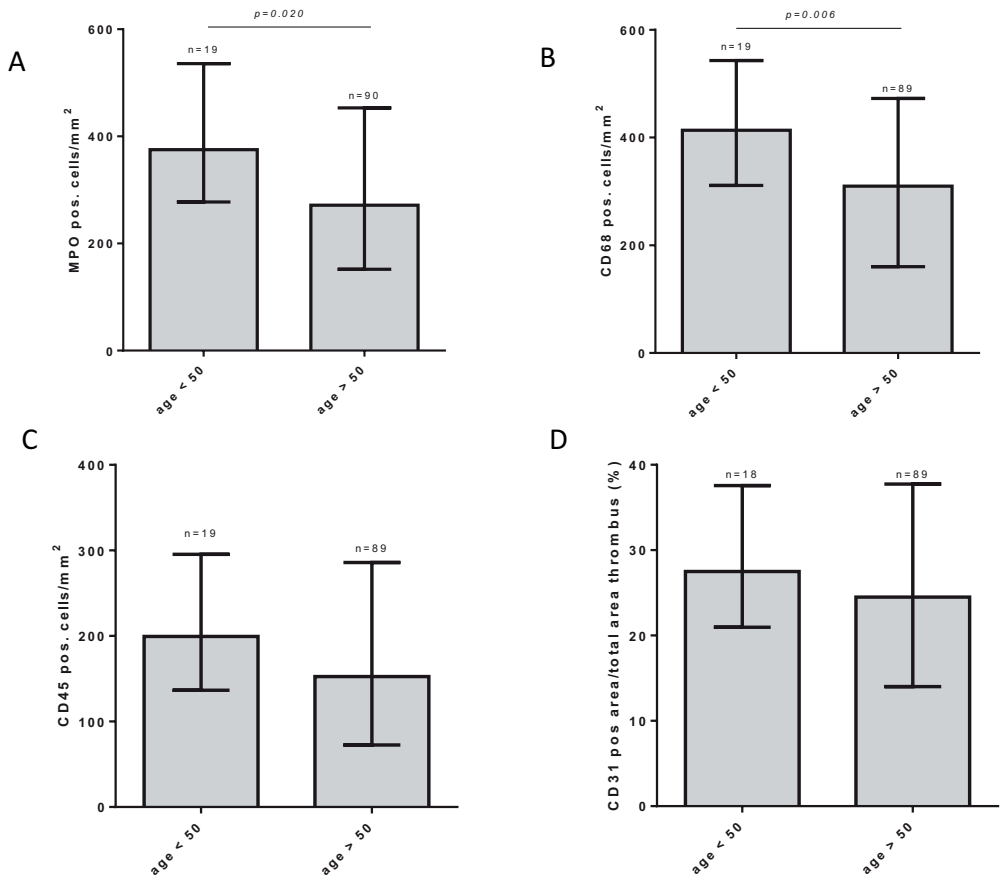

Figure 4 Relation between inflammatory cells/platelets and patients age.

Thrombus material compared between patients aged <50 years versus > 50 years for **A:** number of MPO positive cells. **B:** number of CD68 positive cells. **C:** number of CD45 positive cells. **D:** area of CD31 positivity (%).

Pre-procedural medication

We wondered whether thrombus composition in all phases of thrombi combined, would differ between chronic aspirin users (n=13) and patients without aspirin use (n=73). Platelet area was significant lower in aspirin users, namely 20.0 [7.50-31.3] vs. 27.3 [20.3-40.1] % p=0.019. No significant differences were found for lymphocytes (163 vs. 170 cells/mm2, p=0.902) monocytes/marcophages (355 vs. 345 cells/mm2, p=0.240) and neutrophils (393 [192-594] vs. 283 [159-455] cells/mm2, p=0.219) (Fig. 5). The blood platelet level did not differ significantly between chronic aspirin users and patients without a history of aspirin use (309 vs. 249 x 109/L p=0.647).

We also analyzed the effect of statin treatment that were prescribed in 11 out of 86 patients. A trend to a lower platelet area was observed in patients that used statins (18.8 [10.3-31.6] vs. 29.7 [19.8-42.5] cells/mm2, p=0.094). Statin use had no effect on neutrophil content (283 [121-564] vs. 319 [169-485] cells/mm2, p=0.555), monocytes/macrophage content, (300 [140-471] cells/mm^2 vs. 364 [228-511] cells/mm2, p=0.295) or lymphocyte content (177 [23.0-337] cells/mm^2 vs. 160 [76.3-295] cells/mm2, p=0.326).

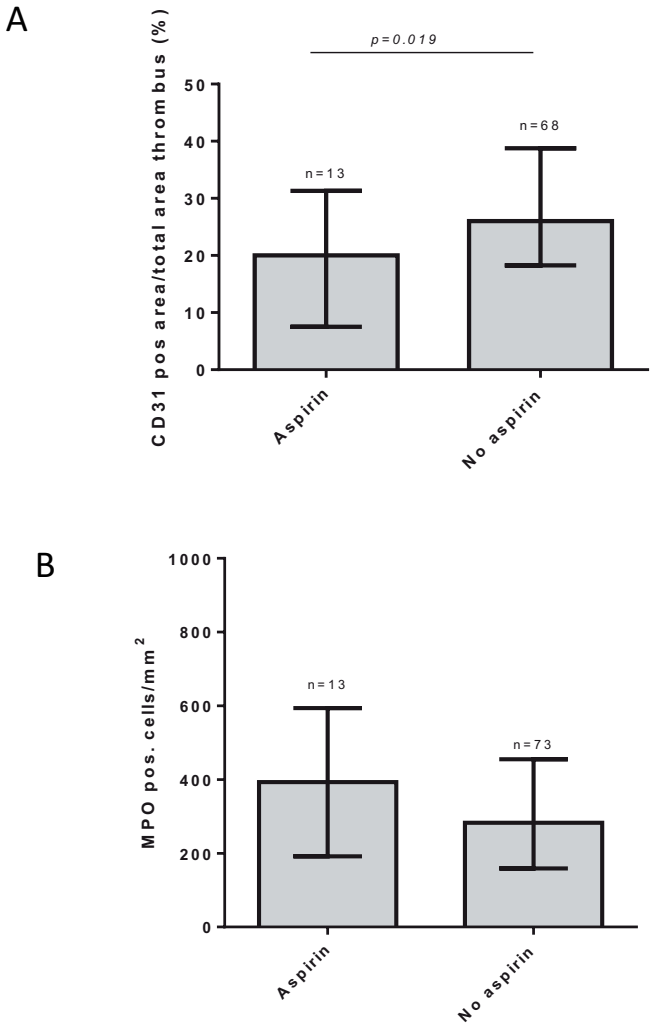

Figure 5 CD31 area and MPO positive cells in aspirin users.

A: The percentage of the CD31 positive area in aspirin users versus non-aspirin users. B: Amount of MPO positive cells/area thrombus aspirate in aspirin users versus non-aspirin users.

Coronary risk factors and serum markers

We were interested in the different coronary risk factors and their possible influence on thrombus composition. We found no significant differences in inflammatory cell/platelet content for smoking, hypertension, hypercholesterolemia, diabetes mellitus, positive family history, previous myocardial infarction or angina pectoris (data not shown). Furthermore the relationships between white blood cell count respectively C-reactive protein and the composition of inflammatory cells was evaluated (Table 2). A weak (r= 0.262; p= 0.038) positive correlation was found between white blood cell count and monocyte/macrophage content in the thrombus was found.

Table 2 Serum markers versus composition of thrombus

	MPO pos. area / mm²	CD68 pos. area / mm²	CD45 pos. area / mm²	CD31 pos. area / mm²
CRP mg/ml	r=-0.114 p=0.413	r=0.061 p=0.675	r=0.056 p=0.675	r=0.001 p=0.993
WBC 10^E9/L	r=0.055 p=0.655	r=0.262 p=0.038	r=-0.320 p=0.801	r=0.230 p=0.064

Correlations coefficients are expressed with accompanied p-values. CRP: C-reactive protein. WBC: White blood cell count. MPO positive cells indicative for neutrophilic granulocytes per thrombus area; CD68 positive cells indicative for monocytes/macrophages per thrombus area; CD45 positive cells indicative for number of lymphocytes per thrombus area; CD31 positive area (indicative for thrombocytes) divided by total thrombus area in percentages.

DISCUSSION

It is known that inflammatory cells play a role in the formation and resolution of venous thrombus. However information on inflammation in the context of coronary thrombosis is scarce. We therefore have analyzed inflammatory cells in thrombi derived from patients with STEMI in relation to histologically classified thrombus age. Thrombus aspiration after STEMI revealed thrombi at different stages of maturation (fresh 76%, lytic 17 % and organized 7 %). The number of neutrophilic granulocytes was significantly lower in organized thrombi, compared with fresh and lytic thrombi, while monocytes/macrophages were significantly higher in the lytic thrombi as compared to the fresh thrombi. Furthermore, we found that thrombi originating from younger patients (age <50) had more neutrophils and monocytes/macrophages. Also, we found no gender differences in thrombus composition. Finally, we found that chronic aspirin use alters, at least partly, thrombus composition, revealing a smaller area of platelets.

Inflammation plays an important role in the pathophysiology of AMI, namely in the initiation, progression and destabilization of atherosclerotic plaques[13], as well as in the onset of plaque rupture, resulting in thrombus formation[4, 15] and subsequent myocardial infarction[16, 17]. Since the introduction of coronary thrombus aspiration devices, thrombus

composition was studied[6, 18]. Multivariate analysis showed that high neutrophil density in aspirated thrombus was an independent predictor of impaired coronary microcirculation (myocardial blush grade ≤ 1 and ST-segment resolution < 50 %) and myocardial dysfunction (low left ventricular ejection fraction at 6 months after onset)[19]. It was furthermore suggested that systemic levels of activated neutrophilic granulocytes were positively correlated with thrombus fibrin content [4]. These studies thus indicate that inflammatory cells are not solely passively trapped in developing thrombi, but play an active role herein. It therefore is of great importance to further elucidate the timescale of infiltration of inflammatory cells in thrombi. Ramaiola et al. found that the infiltration of leukocyte subtypes changed with symptom-to-balloon time (time between onset of complaints and thrombosuction). They found in coronary thrombi aspirated 3 hours after complaints started mainly platelets and fibrinogen, while thrombi aspirated after 6 hours or more were characterized by reduced platelet content and increased T-cells and B-cells infiltration. No significant differences were found for the area of monocytes and neutrophilic granulocytes[3]. STEMI's are often preceded by a variable period of plaque instability that coincides with non-obstructive thrombi that makes classification of thrombus age based on symptom to balloon time inadequate [6, 10, 20]. This is in line with the absence of a correlation between symptom to balloon time and histological thrombus age, as we observed. This may further be established by the absence of a significant correlation between symptom to balloon time and inflammatory cell composition of the thrombus. In order to better discriminate different phases of thrombus development, we used a classification method based on histological characteristics[6, 7]. We found that lymphocytes are already present in fresh thrombi. Even more we found that neutrophils are more present in the fresh and lytic phase as compared to the organized phase, indicative that involvement of these cells is mainly contributed to the early phases of arterial thrombosis. Such a predominance of neutrophils in the earlier stages of thrombus formation (lytic more than fresh) was reported recently[21]. We found that also monocytes/macrophages were especially found in the lytic phase, likely related to their contribution in the clearance of thrombus material[22, 23].

We also looked in more detail on the role of patient age on thrombus composition, regarding the well-known age-related decline in immunologic vigor[24]. We indeed found negative but non-significant correlations between the cell types and patient age, which fits the immunosenescence hypothesis. We even more found that the number of neutrophilic granulocytes and monocytes/macrophages were significantly higher in the younger patients (<50) compared with older patients. Whether this is due to a more active immune system in younger people or f.i. due to a different etiology of infarctions still remains unclear.

It is known that mortality is higher in women with STEMI and can be explained by their unfavorable risk profile and longer symptom to balloon time[25]. We therefore also evaluated putative differences in thrombus composition in relation to gender. This we

however did not found, which is in line with an earlier report, that neither found sex differences for platelets, fibrin or erythrocytes in coronary thrombosuction material[26].

After arrival at the hospital or after arrival of the ambulance all patients were treated with 300 mg of aspirin according to standard care. Aspirin inactivates cyclooxygenase (COX) resulting in impaired synthesis of prostaglandins which are involved in both platelet aggregation and inflammation[27]. A proportion of the patients was on chronic aspirin treatment and since a substantial part of the thrombus formation takes place before the acute aspirin dose is administered, we wondered whether chronic aspirin use had effect on thrombus composition. We did find that patients with chronic aspirin treatment had a smaller platelet area in the thrombi, which is in line with the anti-platelet effect of aspirin[27]. We furthermore analyzed the effect of statin treatment, regarding its anti-inflammatory and anti-platelet effects as well[28, 29]. Although there was a general tendency of less inflammatory cells and smaller platelet area in the thrombus, no significant differences were found.

In conclusion, thrombus aspiration revealed thrombi with different amounts of inflammatory cells in relation to thrombus age that are at least to some extent influenced by patient age and aspirin use, but not by gender. These results are in line with the suggestion that inflammatory cells are not solely passively trapped in developing thrombi, but play an active role herein. Advancing knowledge of the dynamic aspects of thrombus formation and composition may contribute to tailored antithrombotic and/or anti-inflammatory treatment options in various stages of development of acute coronary syndromes.

FUNDING

This work was supported by a grant from the Institute of Cardiovascular Research of the free university (ICaR VU institute), Amsterdam, the Netherlands.

REFERENCES

1 Davies MJ, Thomas AC. Plaque fissuring--the cause of acute myocardial infarction, sudden ischaemic death, and crescendo angina. Br Heart J 1985 April;53(4):363-73

2 Yunoki K, Naruko T, Sugioka K et al. Thrombus aspiration therapy and coronary thrombus components in patients with acute ST-elevation myocardial infarction. J Atheroscler Thromb 2013;20(6):524-37

3 Ramaiola I, Padro T, Pena E et al. Changes in thrombus composition and profilin-1 release in acute myocardial infarction. Eur Heart J 2015 April 21;36(16):965-75

4 Sadowski M, Zabczyk M, Undas A. Coronary thrombus composition: links with inflammation, platelet and endothelial markers. Atherosclerosis 2014 December;237(2):555-61

5 Silvain J, Collet JP, Nagaswami C et al. Composition of coronary thrombus in acute myocardial infarction. J Am Coll Cardiol 2011 March 22;57(12):1359-67

6 Rittersma SZ, van der Wal AC, Koch KT et al. Plaque instability frequently occurs days or weeks before occlusive coronary thrombosis: a pathological thrombectomy study in primary percutaneous coronary intervention. Circulation 2005 March 8;111(9):1160-5

7 Kramer MC, van der Wal AC, Koch KT et al. Histopathological features of aspirated thrombi after primary percutaneous coronary intervention in patients with ST-elevation myocardial infarction. PLoS One 2009;4(6):e5817

8 Altmann J, Sharma S, Lang IM. Advances in our understanding of mechanisms of venous thrombus resolution. Expert Rev Hematol 2015 December 2;1-10.

9 Saha P, Smith A. Regulation of sterile inflammation in the natural resolution of venous thrombosis. Thromb Haemost 2015 November 2;114(5):875

10 Carol A, Bernet M, Curos A et al. Thrombus age, clinical presentation, and reperfusion grade in myocardial infarction. Cardiovasc Pathol 2014 January 23

11 Nishimura S, Ehara S, Hasegawa T, Matsumoto K, Yoshikawa J, Shimada K. Cholesterol crystal as a new feature of coronary vulnerable plaques: An optical coherence tomography study. J Cardiol 2016 May 4

12 Kubo T, Ino Y, Matsuo Y et al. Reduction of in-stent thrombus immediately after percutaneous coronary intervention by pretreatment with prasugrel compared with clopidogrel: An optical coherence tomography study. J Cardiol 2016 May 6

13 Libby P. Inflammation in atherosclerosis. Nature 2002 December 19;420(6917):868-74

14 Steg PG, James SK, Atar D et al. ESC Guidelines for the management of acute myocardial infarction in patients presenting with ST-segment elevation. Eur Heart J 2012 October;33(20):2569-619

15 Maier W, Altwegg LA, Corti R et al. Inflammatory markers at the site of ruptured plaque in acute myocardial infarction: locally increased interleukin-6 and serum amyloid A but decreased C-reactive protein. Circulation 2005 March 22;111(11):1355-61

16 Frangogiannis NG, Smith CW, Entman ML. The inflammatory response in myocardial infarction. Cardiovasc Res 2002 January;53(1):31-47

17 Nijmeijer R, Lagrand WK, Baidoshvili A et al. Secretory type II phospholipase A(2) binds to ischemic myocardium during myocardial infarction in humans. Cardiovasc Res 2002 January;53(1):138-46

18 Hoshiba Y, Hatakeyama K, Tanabe T, Asada Y, Goto S. Co-localization of von Willebrand factor with platelet thrombi, tissue factor and platelets with fibrin, and consistent presence of inflammatory cells in coronary thrombi obtained by an aspiration device from patients with acute myocardial infarction. J Thromb Haemost 2006 January;4(1):114-20

19 Arakawa K, Yasuda S, Hao H et al. Significant association between neutrophil aggregation in aspirated thrombus and myocardial damage in patients with ST-segment elevation acute myocardial infarction. Circ J 2009 January;73(1):139-44

20 Steiner I, Spacek J, Matejkova A, Vojacek J, Bis J, Dusek J. Histopathology of aspirated thrombi during primary percutaneous coronary intervention in patients with acute myocardial infarction. Cardiovasc Pathol 2014 September;23(5):267-71

21 Li X, de Boer OJ, Ploegmaker H et al. Granulocytes in coronary thrombus evolution after myocardial infarction - time-dependent changes in expression of matrix metalloproteinases. Cardiovasc Pathol 2015 October 17

22 Soo KS, Northeast AD, Happerfield LC, Burnand KG, Bobrow LG. Tissue plasminogen activator production by monocytes in venous thrombolysis. J Pathol 1996 February;178(2):190-4

23 Zeng S, Zhou X, Ge L et al. Monocyte subsets and monocyte-platelet aggregates in patients with unstable angina. J Thromb Thrombolysis 2014 November;38(4):439-46

24 Gruver AL, Hudson LL, Sempowski GD. Immunosenescence of ageing. J Pathol 2007 January;211(2):144-56

25 van der Meer MG, Nathoe HM, van der GY, Doevendans PA, Appelman Y. Worse outcome in women with STEMI: a systematic review of prognostic studies. Eur J Clin Invest 2015 February;45(2):226-35

26 Kovacs A, Sotonyi P, Nagy AI et al. Ultrastructure and composition of thrombi in coronary and peripheral artery disease: correlations with clinical and laboratory findings. Thromb Res 2015 April;135(4):760-6

27 Patrono C, Ciabattoni G, Patrignani P et al. Clinical pharmacology of platelet cyclooxygenase inhibition. Circulation 1985 December;72(6):1177-84

28 Jain MK, Ridker PM. Anti-inflammatory effects of statins: clinical evidence and basic mechanisms. Nat Rev Drug Discov 2005 December;4(12):977-87

29 Montecucco F, Mach F. Update on statin-mediated anti-inflammatory activities in atherosclerosis. Semin Immunopathol 2009 June;31(1):127-42

10

Inflammatory cells are not significantly increased in aspirates of coronary thrombi of STEMI patients with microvascular injury

[*] Wessel W. Fuijkschot; [*] Maarten A.H. van Leeuwen; Ivan Shelep; Raquel P. Amier; Sebastiaan Roos; Paul F. Teunissen; Stefan S. Biesbroek; Yvo M. Smulders; Allard C. van der Wal; Robin Nijveldt; Yolande E.A. Appelman; Paul A.J. Krijnen; Hans W.N. Niessen and Niels van Royen

[*] Both authors contributed equally

Submitted for publication

ABSTRACT

Background: In a proportion of patients with ST-elevation myocardial infarction (STEMI), perfusion at the microvascular level remains inadequate after successful percutaneous coronary intervention. This phenomenon of microvascular injury (MVI) is associated with worse clinical outcome. The pathogenesis is largely unknown, however inflammatory cells within the blood and coronary thrombi have been associated with the status of the microvasculature and left ventricular function after STEMI. This is the first study that evaluated a putative relationship between the composition of aspirated intracoronary thrombi and the occurrence of MVI.

Methods: Thrombus aspirates of 69 patients treated with primary percutaneous coronary intervention (p-PCI) were prospectively collected and classified (fresh or lytic) based on haematoxylin and eosin staining. Immunohistochemical stainings were performed to quantify inflammatory cells with CD68 (macrophages), CD45 (lymphocytes), MPO (neutrophilic granulocytes), CD31 (platelets) and GLUT1 (erythrocytes) within the thrombi. Cardiovascular magnetic resonance (CMR) imaging with T2-weighted and late gadolinium enhancement (LGE) imaging for IMH and MVO measurement, respectively, was performed 3-11 days after p-PCI.

Results: Patients with (n=39) and without MVI (n=30) had comparable demographics and cardiovascular risk profile. Patients with MVI had significantly higher symptom-to-balloon times (173 vs. 115 minutes; p=0.036), significantly larger enzymatic infarct size (CKMB max 324 vs. 69 µg/L; p=0.001) and significantly lower left ventricular ejection fraction (LVEF) (49 vs. 55%; p=0.003). Patients with MVI had numerically more often lytic thrombi, albeit not statistically significant ((n=18; 46% vs. n=9; 30%, p=0.17). The number of macrophages/monocytes (2.7 [1.4-5.6] vs. 1.6 [0.6-4.0]), lymphocytes (5.0 [2.5-7.7]vs. 3.5 [1.1-4.0]) and neutrophilic granulocytes (22 [11-31] vs. 13 [10-27]) was higher in patients with MVI, however this was also not statistically significant (resp. p=0.15; p=0.10; p=0.34).

Conclusions: In the present study we could not demonstrate a relationship between the composition of aspirated coronary thrombus and the occurrence of MVI.

INTRODUCTION

ST-elevation myocardial infarction (STEMI) is typically caused by occlusive coronary thrombus formation superimposed on ruptured atherosclerotic plaques[1]. Plaque disruption triggers the formation of platelet aggregates that grow in association with increased fibrin formation and subsequent trapping of erythrocytes and inflammatory cells leading to coronary flow obstruction and blood coagulation[2]. Antithrombotic drugs have reduced the incidence of STEMI in secondary prevention[3] and improved the treatment of patients[4]. However, a substantial proportion of patients with STEMI have a poor restoration of microvascular function and myocardial perfusion, despite restoration of epicardial vessel patency, a condition previously described as a 'no-reflow' phenomenon[5]. It was suggested that distal embolization of atherosclerotic plaque components and/or thrombotic material could induce mechanical obstruction of microvessels but could also cause an inflammatory response, resulting in the release of vasospastic and thrombogenic factors that further exacerbate microvascular dysfunction[6-8]. Furthermore, it was suggested that interactions between white blood cells (neutrophilic granulocytes and monocytes) and platelets likely play an important role in the pathogenesis of no-reflow following distal embolization[9]. In a pig model it was shown that blood levels of neutrophilic granulocyte-platelet aggregates and monocyte-platelet aggregates following microsphere embolization occurred prior to the onset of angiographic no-reflow[9]. In addition, it was shown in dogs that progressive leukocyte capillary plugging during myocardial ischemia prevents full restoration of capillary flow upon reperfusion[10] in a open-chest dog model, 1-5 hours after left anterior descending coronary artery occlusion and reperfusion[10].

In recent years it has become clear that angiographic no-reflow is likely to be caused by microvascular injury (MVI), and subsequent intramyocardial haemorrhage (IMH))[5, 11]. MVI has been associated with increased risk of hospital readmissions owing to cardiac failure, major adverse cardiac events, and death . Although MVI can be assessed using various imaging modalities including electrocardiography, myocardial contrast echocardiography, nuclear scintigraphy and coronary angiography, evaluation by cardiovascular magnetic resonance (CMR) is considered the gold standard [5]. CMR is the most accurate modality to assess the left ventricular ejection fraction and delineate the amount of MVI, IMH and infarct size.

Previous studies have shown that inflammation plays an important role in the occurrence of MVI. For instance, blood levels of leukocytes and CRP were positively correlated with the size of MVI[12-14]. In addition, high neutrophil density in aspirated thrombus was an independent predictor of unfavourable microvascular perfusion and left ventric-

ular ejection fraction (LVEF), as determined with angiography[15]. In the current study we studied the potential association between inflammatory cell content of coronary thrombi and the occurrence of MVI and the consequences on infarct size, as determined with CMR.

METHODS AND MATERIALS

Thrombus aspiration and baseline characteristics

Patients who presented at the VU university medical center with a STEMI (defined according to the ESC guidelines for STEMI[16]) from whom analyzable thrombus was aspirated and in which cardiovascular magnetic resonance (CMR) with late gadolinium-enhanced (LGE) imaging was performed 3-11 days after p-PCI, were selected. On admission patients were directly transported to the catheterization laboratory and PCI was performed of the infarct related artery according to current standard guidelines for PCI[17]. After passage of the coronary artery occlusion with a guide wire, manual thrombus aspiration was performed with the Export AP Aspiration Catheter Medtronic, Dublin, Ireland. Typically, several suctions at the site of the occlusion were performed after smooth introduction of the catheter. Aspirated thrombus and intracoronary material were collected in the collection bottle, which was equipped with a filter. Additional balloon angioplasty and stent placement were performed at the discretion of the operator, as was the additional use of glycoprotein IIb/IIIa receptor blockers. Upon thrombus aspiration, specimens were immediately fixated in formalin. The following baseline clinical data of the patients were collected: age, gender, cardiovascular history, medication, cardiovascular risk factors, time between start of symptoms and first balloon inflation (symptom to balloon time), C-reactive protein, CK-MB, blood leucocyte count, LDL cholesterol, creatinine and glucose. The study conforms with the principles outlined in the Declaration of Helsinki. The study protocol was approved by the human research committee at the VU University Medical Center.

Cardiovascular magnetic resonance

At day 3-11 after p-PCI, cardiovascular magnetic resonance (CMR) imaging was performed with a 1.5-Tesla clinical magnetic resonance scanner (Avanto, Siemens, Erlangen, Germany) using a phased array cardiac receiver coil. All images were ECG-gated and acquired during mild end-expiration breath-holding. Balanced steady-state free precession cine images were obtained in standard long- and short-axis orientations to examine left ventricular volumes, and ejection fraction. Typical parameters were in-plane resolution 1.6 × 2.0 mm, slice thickness/slice gap 5/5 mm, flip angle 75˚ and temporal resolution 35-40 ms. T2-weighted spin echo imaging was performed in short axis orientation covering the whole LV to visualize IMH. Typical parameters were TR = 2

× RR interval, TE 61 ms and voxel size 1.5 × 2.5 × 7 mm. Hypointense areas within the hyperintense infarcted myocardium were considered IMH. Finally, to quantify infarct size and visualize MVO, LGE images were acquired with an inversion recovery gradient echo sequence 10-15 min after 0.1 – 0.2 mmol/kg gadolinium-based contrast administration (Dotarem, Guerbet, Roissy CdG, France) in short axis orientation with whole LV coverage. Typical parameters were in-plane resolution 1.5 × 1.5 mm, slice thickness 5mm, TR = 1 × RR interval, TE 4.4 ms, flip angle 25° and TI 250-400 ms nulled to normal myocardium. Infarct size was assessed using the full-width half maximum method. MVO was defined as the areas of hypoenhancement within the hyperenhanced infarcted myocardium. All CMR analyses were performed by blinded experienced observers using a standardized protocol, using dedicated off-line software (QMassMR v7.6, Medis, Leiden, the Netherlands).

Histology

The aspirated coronary thrombus material was embedded in paraffin after overnight fixation (4 % formalin). Tissues were deparaffinised, rehydrated and stained with a standard haematoxylin/eosin (HE)-staining. Thrombi were histopathological classified based on the observation of three independent observers (H.W.M.N., A.C.W. and W.W.F.), as described before[18]: fresh (less than one day old): completely composed of layered patterns of platelets, fibrin, erythrocytes and intact neutrophilic granulocytes; lytic (between 1 and 5 days old): areas of colliquation necrosis and karyorrhexis of neutrophilic granulocytes; organized (more than 5 days old): areas of ingrowth of smooth muscle cells, with or without depositions of young connective tissue and ingrowth of capillary vessels. It is known from literature that organized thrombi are typically less common, then fresh and lytic thrombi[19]. As we in our relatively small cohort did not find sufficient organized thrombi with matching available CMR images to allow proper comparison, organized thrombi (n=4) were excluded from this study. Thrombus material with a heterogeneous composition was graded according to the age of the oldest part.

Immunohistochemistry

For immunohistochemical analysis tissues were deparaffinised, rehydrated and incubated in methanol/ H2O2 0.3%) for 30 min to block endogenous peroxidases. Antigen retrieval was performed by boiling slides (MPO, CD68, CD31 and NET) for 10 min in a citrate pH 6.0 buffer and Glut-1 in TRIS EDTA pH 9.0. No antigen retrieval was performed on CD45. Sections were incubated with either rabbit anti-human Glut-1 (1:100, Dako, Glostrup, Denmark), mouse anti-human CD68 (1:400, Dako, Glostrup, Denmark), mouse anti-human CD31 (1:40, Dako, Glostrup, Denmark), mouse anti-human CD45 (1:100, Dako, Glostrup, Denmark) or rabbit anti-human H3-histone Citrulline (1:100, Abcam, Cambridge, UK) antibody for 1 hour at room temperature (RT). Next, sections were incubated with anti-mouse/rabbit Envision (Dako, Glostrup, Den-

mark) for 30 min at RT. Staining was visualized with 3,3'-diaminobenzidine (0.1 mg/ml, 0.02% H2O2) for 10 minutes. The slides were subsequently counterstained with haematoxylin, dehydrated and covered. With each staining a PBS control was included. All these controls yielded negative results (not shown).

Immunoscoring

Immunoscoring was performed by I.S. and W.W.F. and agreement was reached between both observers. All slides were scanned with the Pannoramic Desk scan (3DHISTECH Ltd Budapest, Hungary) and were further processed with Pannoramic Viewer software. For quantitative analysis, picture of each thrombus was 5x enlarged and divided into equal sections until the whole area of the thrombus was covered. Next, snapshots were made of each section. Snapshots were further analyzed with ImageJ software. For each snapshot an area of interest (ROI) was drawn around the thrombus tissue, and atherosclerotic areas were excluded. Antibody positive surface area of the selected ROI and thrombus area were measured for each snapshot. The total antibody positive area of each thrombus was then divided by total thrombus area, which provided a percentage of stained area per thrombus.

Statistics

Continuous variables are expressed as mean ± standard deviation (SD) for normally distributed or median (interquartile range) for non-normally distributed ones. Differences between the groups were tested by Student t-test for normally distributed or by the Mann-Whitney U and test for non-normally distributed continuous variables. For the comparison between groups (MVI vs non-MVI) and the relative distribution (%) of gender, cardiovascular risk factors, procedure characteristics, CMR data and thrombus characteristics, crosstabs were used resulting in a Fisher's exact test generated p-value. All statistical analyses were performed with SPSS software (Windows version 20, IBM corp., Armonk, NY). A p-value (two sided) of less than 0.05 was considered to be significant.

RESULTS

Patient characteristics

Between Dec 2009 and Aug 2015, 2440 STEMI patients have undergone p-PCI and adjacent thrombectomy was performed in 52%, as presented in the inclusion flow chart (Fig. 1). Cardiovascular magnetic resonance (CMR) with LGE imaging was performed in 182 patients, 3-11 days after p-PCI. Our study population consisted of 69 patients (42 male; 27 female) with analysable CMR images and thrombus material. Patients with MVI (n=39) and without MVI (n=30) (Fig. 2) had comparable demographics and car-

diovascular risk factors (Table 1), except for glucose levels. In MVI patients glucose levels (8.4 mmol/L) were significant higher as compared to no MVI patients (7.2 mmol/L), although no significant differences in the number of DM patients was found.
Patients with MVI had higher symptom-to-balloon times (173 vs. 115 minutes; p=0.036), larger enzymatic infarct size (CKMB max 324 vs. 69 µg/L; p=0.001), lower left ventricular ejection fraction (49% vs. 55%; p=0.003) and more often had IMH (64% vs. 0.0 %; p<0.0001) (Table 2).

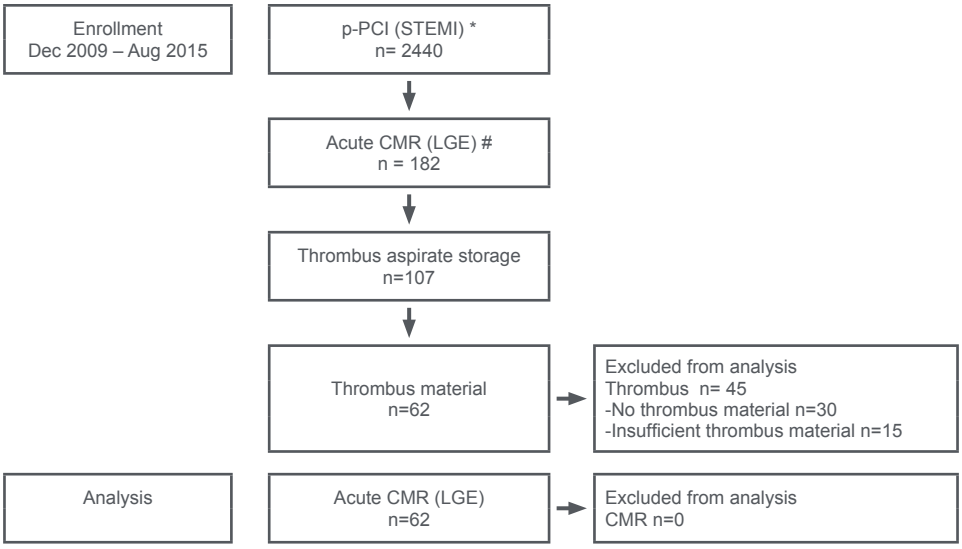

Figure 1 Enrollment flow diagram

p-PCI, primary percutaneous coronary intervention; STEMI, ST-elevation myocardial infarction; CMR, cardiovascular magnetic resonance; LGE, late gadolinium enhancement. *Thrombus aspiration n=1269 (52%); #3-11 days post PPCI

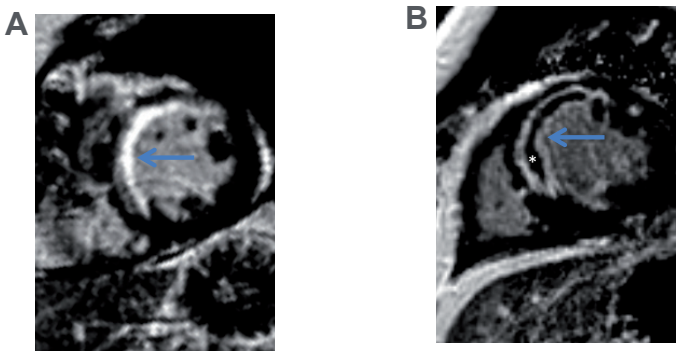

Figure 2 Example of MVI and non-MVI

Examples of short axis cardiovascular magnetic resonance (CMR) imaging with late gadolinium enhancement (LGE) showing infarcted area (anteroseptal) indicated by the arrowf. In panel A the infarcted area is hypodense, indicative of MVI. In panel B no hypodense area is present in the infarcted area, indicative of a patient without MVI.

Table 1 Baseline characteristics

	MVI (n=39)	no MVI (n=30)	p-value
Demographics			
Age (years)	57 ± 9	58 ± 10	0.59
Male, n (%)	32 (82)	20 (67)	0.14
Cardiovascular risk factors			
Current smoking, n (%)	17 (44)	12 (40)	0.77
Hypertension, n (%)	9 (23)	7 (23)	0.98
Hypercholesterolemia, n (%)	6 (15)	6 (20)	0.62
DM2, n (%)	1 (3)	0 (0)	0.38
Family history, n (%)	23 (59)	11 (37)	0.07
BMI (kg/m^2)	27 ± 3	26 ± 3	0.19
Laboratory measurements			
Creatinin µmol/L	82 (74-89)	80 (65-88)	0.47
CRP mg/L	0 (0-3)	3 (0-5)	0.30
Glucose mmol/L	8.4 (7.4-9.3)	7.2 (6.7-8.4)	0.005
Cholesterol mmol/L	5.1 (4.7-6.2)	5.4 (4.6-6.1)	0.89
LDL mmol/L	3.4 (3.0-4.3)	3.8 (3.3-4.5)	0.41
Leucocytes 10^9/L	12 (9-15)	12 (8-15)	0.99
ASAT U/L	36 (29-61)	33 (25-70)	0.47
ALAT U/L	30 (24-39)	25 (17-41)	0.17
CK U/L	480 (155-2118)	398 (171-1058)	0.57
CKMB baseline µg/L	62 (9.4-281)	44 (29-97)	0.58

Variable represent mean ± standard deviation, median (interquartile range) or number and percentage of total patients (%). DM2, type 2 diabetes; BMI, body mass index; LDL, low density lipoprotein; ASAT, L-aspartate aminotransferase; ALAT, L-alanine aminotransferase; CK, creatinine kinase; CKMB, creatinine kinase MB.

Table 2 Procedure, infarct size and LVEF

	MVI (n=39)	no MVI (n=30)	p-value
Procedure			
Multivessel disease, n (%)	16 (41)	10 (33)	0.51
LAD (IRA), n (%)	17 (44)	8 (27)	0.15
TIMI 0 pre-PCI, n (%)	35 (90)	17 (57)	0.002
Number of stents	1.2 ± 0.5	1.1 ± 0.3	0.22
Symptom-to-balloon time (minutes)	173 (104-253)	115 (75-180)	0.036
Infarct size and LVEF			
Days between presentation and CMR	5 (3-7)	5 (3-7)	0.62
MRI Infarct size (gram)	28 (19-46)	9 (13-6)	< 0.001
MRI infarct size / LV (%)	24 (65-32)	9 (3-13)	< 0.001
MRI LVEF %	49 ± 8	55 ± 9	0.003
MRI ESV ml	98 (79-132)	74 (52-86)	0.001
MRI EDV ml	189 (170-230)	166 (138-188)	0.003
IMH, n (%)	23 (64)	0	< 0.001
CKMB max µg/L	324 (155-438)	69 (43-240)	0.001

Variable represent mean ± standard deviation, median (interquartile range) or number and percentage of total patients (%). LAD, left anterior descending coronary artery; IRA, infarct-related artery; CMR, cardiovascular magnetic resonance; PCI, percutaneous coronary intervention; MRI, magnetic resonance imaging; LVEF, left ventricular ejection fraction; ESV, end systolic volume; EDS, end diastolic volume; IMH, intra-myocardial hemorrhage; CKMB, creatinine kinase MB.

Thrombus characteristics

We first evaluated the density of platelets and erythrocytes in thrombi. We found a similar percentage of platelets (37% vs. 32%; p=0.58) and erythrocytes (58% vs. 66%; p=0.47) in patients with and without with MVI.

Next we compared the relative occurrence of fresh vs. lytic thrombus in both groups (Table 3). In 18 of the 39 patients with MVI lytic thrombi were present (46%), which was higher but did not statistically differ from the 9 patients with lytic thrombi in the 30 patients without MVI (30%); p=0.17.

Table 3 Thrombus characteristics stratified by MVI

	MVI (n=39)	MVI (n=30)	p-value
General components			
Plaque components, n (%)	13 (39)	7 (32)	0.57
Platelets %	27 (27-50)	32 (10-59)	0.58
Erythrocytes %	58 (36-71)	66 (41-75)	0.47
Inflammation			
Lytic thrombys, n (%)	18 (46)	9 (30)	0.17
Monocytes / macrophages %	2.7 (1.4-5.6)	1.6 (0.6-4.0)	0.15
Lymphocytes %	5.0 (2.5-7.7)	3.5 (1.1-4.0)	0.10
Neutrophylic granulocytes %	22 (11-31)	13 (10-27)	0.34
Neutrophilic extracellular trapment %	44 (27-62)	46 (24-52)	0.70

Variable represent number and percentage of total patients (%) or median (interquartile range).

We then compared the contribution of inflammatory cells in the thrombi between patients with and without MVI. The area of inflammatory cells was enhanced in MVI vs the no MVI group, but this difference was not significant: the area of monocytes/macrophages (%) was 2.7 (1.4-5.6) in patients with MVI and 1.6 in no MVI patients (0.6-4.0); p= 0.15; the area of lymphocytes (%) was 5.0 (2.5-7.7) in patients with MVI vs. 3.5 (1.1-4.0) in patients without MVI; p=0.10; the area of neutrophilic granulocytes (%) was 22 (11-31) in patients with MVI vs. 13 (10-27) in patients without MVI; p=0.34.

Finally, the area of neutrophilic extracellular traps (NETs), a pro-thrombogenic and pro-inflammatory mediator, was evaluated[20, 21]. Also no significant difference was found: the thrombus area composed of NETs (%) was 44 (27-62) in patients with MVI vs. 46 (24-52) in patients without MVI; p=0.70.

We previously have shown that thrombus age (fresh, lytic or organized) has an effect on the composition of these inflammatory cells in the thrombus[19]. We therefore compared the area of platelets, inflammatory cells and erythrocytes in the MVI and non-MVI groups separately for fresh and lytic thrombus. Although in lytic thrombi the number of CD45 positive cells was higher in MVI vs non MVI patients (Fig. 3D), and the number of NET's in fresh thrombi was higher in MVI vs non MVI patients (Fig. 3F), these differences were not significant. In none of the other variables, significant differences were found (Fig. 3), on the contrary: the non-significant increase of monocyte/macrophages and neutrophilic granulocyte densities that was found when comparing the MVI with the non-MVI group, became less overt when thrombus age was taken into account. When we selected patients with MVI (n=39) categorizing them according to the amount of MVI (based on the median of 1.73 grams), inflammatory cell and general contents of coronary thrombus were not statistically different between patients with more pronounced MVI (≥ 1.73 grams) or less pronounced MVI (< 1.73 grams) (Table 4).

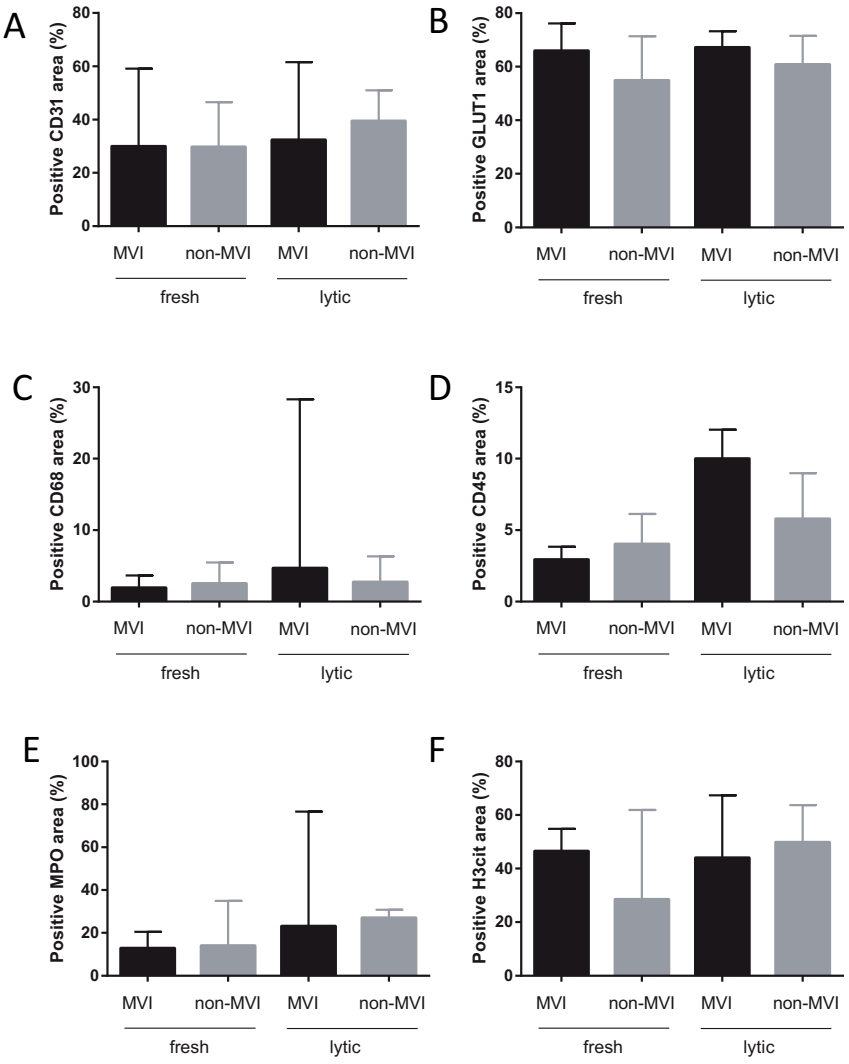

Figure 3 Thrombus composition in MVI and non-MVI patients stratified by thrombus age

Relation between platelets, erythrocytes, inflammatory cells and the occurrence of microvascular injury (MVI) subdivided by histological thrombus age (fresh or lytic). **A:** CD31 positive area (platelets); **B:** GLUT1 positive area (erythrocytes); **C:** CD68 positive area (macrophages); **D:** CD45 positive area (lymphocytes); **E:** MPO positive area (neutrophilic granulocytes); **F:** H3cit positive area (NETs). MVI fresh (n=21), MVI lytic (n=18), no MVI fresh (n=21), no MVI lytic (n=9).

Table 4 Thrombus characteristics specified for patients with more or less pronounced MVI

	Pronounced MVI (n=20)	Less pronounced MVI (n=19)	p-value
General components			
Plaque components, n (%)	14 (70)	11 (58)	0.43
Platelets %	40 (30-54)	33 (23-44)	0.16
Erythrocytes %	55 (22-70)	60 (50-76)	0.13
Inflammation			
Lytic thrombys, n (%)	11 (55)	10 (53)	0.88
Monocytes / macrophages %	2.2 (1.1-4.4)	4.1 (1.5-6.2)	0.37
Lymphocytes %	5.0 (2.4-9.0)	4.8 (3.1-6.8)	1.00
Neutrophylic granulocytes %	25 (4-31)	21 (12-36)	0.70
Neutrophilic extracellular trapment %	47 (8-64)	42 (30-61)	0.81

Variable represent number and percentage of total patients (%) or median (interquartile range).

DISCUSSION

To the best of our knowledge we were the first to evaluate whether the inflammatory cell content of coronary thrombi is related to CMR-derived MVI. Although it is suggested that inflammatory cells play a major role in thrombus formation[19, 22-24] and the occurrence of MVI, we observed no significant differences in inflammatory cell composition of obstructing coronary artery thrombi of patients with and without MVI. The current study confirms previous observations[11, 25-29] that MVI patients have a higher symptom-to-balloon time, larger enzymatic infarct size, lower left ventricular ejection fraction and a higher incidence of IMH.

This study did show a non-significant increase of inflammatory cells in thrombus in patients with MVI. However, the increased monocyte/macrophages and neutrophilic granulocyte densities, became less overt when thrombus age was taken into account. This underlines the importance of including thrombus age as a parameter in future research, in order to minimize the risk of unjustly establishing a link between thrombus inflammatory cell density and MVI. In a previous study we found that the number of neutrophilic granulocytes was significantly lower in organized thrombi, compared with fresh and lytic thrombi, while monocytes/macrophages were significantly higher in the lytic thrombi as compared to the fresh thrombi[19], indicating that inflammatory cell densities in coronary thrombi indeed depend on thrombus age.

A recent study described that neutrophil density in aspirated thrombus was an independent predictor of unfavourable myocardial outcome[15] visualized as blush grade<or=1, ST-segment resolution <50% and low left ventricular ejection fraction (LVEF) at 6 months after onset of AMI, albeit the actual occurrence of MVI was not studied

herein [15]. We however did not find increased numbers of neutrophilic granulocytes in MVI compared with non-MVI patients. In our study we used the gold standard to assess the infarcted area and LVEF, CMR, in comparison to the less favorable blush grade and segment resolution used in the referred study [15]. This could explain the discrepancy between our findings.

Several studies have evaluated the inflammatory cell content of the more distal intramyocardial vessels. In a pig model in which distal embolization was induced via microsphere embolization resulting in no-reflow, elevated blood levels of neutrophilic granulocyte-platelet aggregates and monocyte-platelet aggregates were found, suggesting that interactions between white blood cells and platelets likely play an important role in the pathogenesis of no-reflow following distal embolization[9]. Moreover, in a dog study of again the intramyocardial vessels, it was shown that progressive leukocyte capillary plugging during myocardial ischemia contributes to preventing full restoration of capillary flow upon reperfusion. This thus could point to a role of inflammatory cells in the process of thrombosis in more distal blood vessels of the heart. In humans, increased levels of white blood cells were related with increased infarct size and mortality[30]. In addition, patients with increased levels of certain inflammatory cells are also associated with the occurrence of MVO and decreased recovery of myocardial function[31]. The aforementioned studies suggest an (indirect) link between the amount of inflammatory cells in the blood (sampled distal to the coronary occlusion or systemically) and MVI, which has given rise to our hypothesis that inflammatory cell density in thrombus would be increased in patients with MVI. We could not establish such a relationship. Several studies have evaluated a possible link between systemic inflammation in the blood (defined by serum markers rather than inflammatory cell counts) and the occurrence of MVI[12-14]. Systemic activation of inflammation is increased in no-reflow/MVI, visualized via raised serum levels of C-reactive protein (CRP), hs-CRP, WBC and fibrinogen[14]. The blood levels of leukocytes and CRP were furthermore shown to positively correlate with the size of MVI[12-14]. We could however not establish a similar relationship between blood leucocyte and CRP levels and the occurrence of MVI in our study. This could be due to the fact that these studies were designed to evaluate the relationship between inflammatory markers in the blood and MVI and therefore analyzed these at multiple time points under controlled conditions. In two of these studies[12, 14], for instance, blood levels were determined serially from day 1 to day 4 after symptom onset. The third study used inflammatory markers (CRP and leukocytes) values obtained at the day of admission. Area's under the curve and peak concentrations were used for statistics. We however evaluated the levels of CRP and leukocytes retrospectively from a clinical database at non-specified time points after onset of disease. So our measurements are possibly to heterogeneous to replicate such a result.

Several limitations have to be addressed. Firstly, the number of study subjects (n=69) is relatively small. Beforehand, a proper power calculation was difficult to make, due to the exploratory character of this study. Instead, we decided to include every patient from the moment we started to collect thrombus material and performed CMR. Note that, as a result of the small sample size we have not analyzed the data for males and females separately. Secondly, we used the presence MVI (yes or no) instead of the extent of MVI, which could be used as a continuous parameter[32] and might give a more subtle reflection of MVI[33]. Lastly, it has to be noticed that the quantity of inflammatory cells in the thrombus does not represent their activation status. Therefore, we emphasize that caution is warranted when using this data to reflect on inflammatory activity.
In conclusion, in STEMI patients with MVI, inflammatory cells are not significantly increased in coronary aspirates from epicardial coronary thrombi compared with STEMI patients without MVI.

ACKNOWLEDGEMENTS

We thank the patients and their families for participating in this study. In addition, we acknowledge the staff of the Department of Cardiology and Pathology of the VU University Medical Center, Amsterdam, The Netherlands, for their help with obtaining and process thrombus material and by performing CMR.

FUNDING

This study was financed by the Institute for Cardiovascular Research (ICaR-VU; Grant No.ICaR-VU-ID414-2012).

DISCLOSURES

The authors declare that there is no conflict of interest.

REFERENCES

1 Davies MJ and Thomas AC. Plaque fissuring--the cause of acute myocardial infarction, sudden ischaemic death, and crescendo angina. Br Heart J 1985;53(4):363-373

2 Yunoki K, Naruko T, Sugioka K, Inaba M, Itoh A, Haze K, Yoshiyama M and Ueda M. Thrombus aspiration therapy and coronary thrombus components in patients with acute ST-elevation myocardial infarction. J Atheroscler Thromb 2013;20(6):524-537

3 Collaborative overview of randomised trials of antiplatelet therapy--I: Prevention of death, myocardial infarction, and stroke by prolonged antiplatelet therapy in various categories of patients. Antiplatelet Trialists' Collaboration. BMJ 1994;308(6921):81-106

4 Wallentin L, Becker RC, Budaj A, Cannon CP, Emanuelsson H, Held C, Horrow J, Husted S, James S, Katus H, Mahaffey KW, Scirica BM, Skene A, Steg PG, Storey RF, Harrington RA, Freij A and Thorsen M. Ticagrelor versus clopidogrel in patients with acute coronary syndromes. N Engl J Med 2009;361(11):1045-1057

5 Robbers LF, Eerenberg ES, Teunissen PF, Jansen MF, Hollander MR, Horrevoets AJ, Knaapen P, Nijveldt R, Heymans MW, Levi MM, van Rossum AC, Niessen HW, Marcu CB, Beek AM and van Royen N. Magnetic resonance imaging-defined areas of microvascular obstruction after acute myocardial infarction represent microvascular destruction and haemorrhage. Eur Heart J 2013;34(30):2346-53

6 Limbruno U, De Carlo M, Pistolesi S, Micheli A, Petronio AS, Camacci T, Fontanini G, Balbarini A, Mariani M and De Caterina R. Distal embolization during primary angioplasty: histopathologic features and predictability. Am Heart J 2005;150(1):102-8

7 Wu X, Mintz GS, Xu K, Lansky AJ, Witzenbichler B, Guagliumi G, Brodie B, Kellett MA, Jr., Dressler O, Parise H, Mehran R, Stone GW and Maehara A. The relationship between attenuated plaque identified by intravascular ultrasound and no-reflow after stenting in acute myocardial infarction: the HORIZONS-AMI (Harmonizing Outcomes With Revascularization and Stents in Acute Myocardial Infarction) trial. JACC Cardiovasc Interv 2011;4(5):495-502

8 Sakuma T, Leong-Poi H, Fisher NG, Goodman NC and Kaul S. Further insights into the no-reflow phenomenon after primary angioplasty in acute myocardial infarction: the role of microthromboemboli. J Am Soc Echocardiogr 2003;16(1):15-21

9 Charron T, Jaffe R, Segev A, Bang KW, Qiang B, Sparkes JD, Butany J, Dick AJ, Freedman J and Strauss BH. Effects of distal embolization on the timing of platelet and inflammatory cell activation in interventional coronary no-reflow. Thromb Res 2010;126(1):50-5

10 Engler RL, Schmid-Schonbein GW and Pavelec RS. Leukocyte capillary plugging in myocardial ischemia and reperfusion in the dog. Am J Pathol 1983;111(1):98-111

11 Betgem RP, de Waard GA, Nijveldt R, Beek AM, Escaned J and van RN. Intramyocardial haemorrhage after acute myocardial infarction. Nat Rev Cardiol 2015;12(3):156-167

12 Mayr A, Klug G, Schocke M, Trieb T, Mair J, Pedarnig K, Pachinger O, Jaschke W and Metzler B. Late microvascular obstruction after acute myocardial infarction: relation with cardiac and inflammatory markers. Int J Cardiol 2012;157(3):391-6

13 Jesel L, Morel O, Ohlmann P, Germain P, Faure A, Jahn C, Coulbois PM, Chauvin M, Bareiss P and Roul G. Role of pre-infarction angina and inflammatory status in the extent of microvascular obstruction detected by MRI in myocardial infarction patients treated by PCI. Int J Cardiol 2007;121(2):139-47

14 Reindl M, Reinstadler SJ, Feistritzer HJ, Klug G, Tiller C, Mair J, Mayr A, Jaschke W and Metzler B. Relation of inflammatory markers with myocardial and microvascular injury in patients with reperfused ST-elevation myocardial infarction. Eur Heart J Acute Cardiovasc Care 2016

15 Arakawa K, Yasuda S, Hao H, Kataoka Y, Morii I, Kasahara Y, Kawamura A, Ishibashi-Ueda H and Miyazaki S. Significant association between neutrophil aggregation in aspirated thrombus and myocardial damage in patients with ST-segment elevation acute myocardial infarction. Circ J 2009;73(1):139-144

16 Steg PG, James SK, Atar D, Badano LP, Blomstrom-Lundqvist C, Borger MA, Di MC, Dickstein K, Ducrocq G, Fernandez-Aviles F, Gershlick AH, Giannuzzi P, Halvorsen S, Huber K, Juni P, Kastrati A, Knuuti J, Lenzen MJ, Mahaffey KW, Valgimigli M, van 't HA, Widimsky P and Zahger D. ESC Guidelines for the management of acute myocardial infarction in patients presenting with ST-segment elevation. Eur Heart J 2012;33(20):2569-2619

17 Steg PG, James SK and Gersh BJ. 2012 ESC STEMI guidelines and reperfusion therapy: Evidence-based recommendations, ensuring optimal patient management. Heart 2013;99(16):1156-7

18 Rittersma SZ, van der Wal AC, Koch KT, Piek JJ, Henriques JP, Mulder KJ, Ploegmakers JP, Meesterman M and de Winter RJ. Plaque instability frequently occurs days or weeks before occlusive coronary thrombosis: a pathological thrombectomy study in primary percutaneous coronary intervention. Circulation 2005;111(9):1160-1165

19 Fuijkschot WW, Groothuizen WE, Appelman Y, Radonic T, van Royen N, van Leeuwen MA, Krijnen PA, van der Wal AC, Smulders YM and Niessen HW. Inflammatory cell content of coronary thrombi is dependent on thrombus age in patients with ST-elevation myocardial infarction. J Cardiol 2017;69(1):394-400

20 Brinkmann V, Reichard U, Goosmann C, Fauler B, Uhlemann Y, Weiss DS, Weinrauch Y and Zychlinsky A. Neutrophil extracellular traps kill bacteria. Science 2004;303(5663):1532-5

21 Fuchs TA, Brill A and Wagner DD. Neutrophil extracellular trap (NET) impact on deep vein thrombosis. Arterioscler Thromb Vasc Biol 2012;32(8):1777-1783

22 Sadowski M, Zabczyk M and Undas A. Coronary thrombus composition: links with inflammation, platelet and endothelial markers. Atherosclerosis 2014;237(2):555-561

23 Ramaiola I, Padro T, Pena E, Juan-Babot O, Cubedo J, Martin-Yuste V, Sabate M and Badimon L. Changes in thrombus composition and profilin-1 release in acute myocardial infarction. Eur Heart J 2015;36(16):965-975

24 Silvain J, Collet JP, Nagaswami C, Beygui F, Edmondson KE, Bellemain-Appaix A, Cayla G, Pena A, Brugier D, Barthelemy O, Montalescot G and Weisel JW. Composition of coronary thrombus in acute myocardial infarction. J Am Coll Cardiol 2011;57(12):1359-1367

25 Amabile N, Jacquier A, Shuhab A, Gaudart J, Bartoli JM, Paganelli F and Moulin G. Incidence, predictors, and prognostic value of intramyocardial hemorrhage lesions in ST elevation myocardial infarction. Catheter Cardiovasc Interv 2012;79(7):1101-8

26 Husser O, Monmeneu JV, Sanchis J, Nunez J, Lopez-Lereu MP, Bonanad C, Chaustre F, Gomez C, Bosch MJ, Hinarejos R, Chorro FJ, Riegger GA, Llacer A and Bodi V. Cardiovascular magnetic resonance-derived intramyocardial hemorrhage after STEMI: Influence on long-term prognosis, adverse left ventricular remodeling and relationship with microvascular obstruction. Int J Cardiol 2013;167(5):2047-54

27 Ganame J, Messalli G, Dymarkowski S, Rademakers FE, Desmet W, Van de Werf F and Bogaert J. Impact of myocardial haemorrhage on left ventricular function and remodelling in patients with reperfused acute myocardial infarction. Eur Heart J 2009;30(12):1440-9

28 Wu KC, Zerhouni EA, Judd RM, Lugo-Olivieri CH, Barouch LA, Schulman SP, Blumenthal RS and Lima JA. Prognostic significance of microvascular obstruction by magnetic resonance imaging in patients with acute myocardial infarction. Circulation 1998;97(8):765-72

29 Ito H, Tomooka T, Sakai N, Yu H, Higashino Y, Fujii K, Masuyama T, Kitabatake A and Minamino T. Lack of myocardial perfusion immediately after successful thrombolysis. A predictor of poor recovery of left ventricular function in anterior myocardial infarction. Circulation 1992;85(5):1699-705

30 Palmerini T, Brener SJ, Genereux P, Maehara A, Della Riva D, Mariani A, Witzenbichler B, Godlewski J, Parise H, Dambrink JH, Ochala A, Fahy M, Xu K, Gibson CM and Stone GW. Relation between white blood cell count and final infarct size in patients with ST-segment elevation acute myocardial infarction undergoing primary percutaneous coronary intervention (from the INFUSE AMI trial). Am J Cardiol 2013;112(12):1860-6

31 Hirsch A, Nijveldt R, van der Vleuten PA, Tijssen JG, van der Giessen WJ, Tio RA, Waltenberger J, ten Berg JM, Doevendans PA, Aengevaeren WR, Zwaginga JJ, Biemond BJ, van Rossum AC, Piek JJ and Zijlstra F. Intracoronary infusion of mononuclear cells from bone marrow or peripheral blood compared with standard therapy in patients after acute myocardial infarction treated by primary percutaneous coronary intervention: results of the randomized controlled HEBE trial. Eur Heart J 2011;32(14):1736-47

32 Timmer SAJ, Teunissen PFA, Danad I, Robbers L, Raijmakers P, Nijveldt R, van Rossum AC, Lammertsma AA, van Royen N and Knaapen P. In vivo assessment of myocardial viability after acute myocardial infarction: A head-to-head comparison of the perfusable tissue index by PET and delayed contrast-enhanced CMR. J Nucl Cardiol 2017;24(2):657-667

33 Nijveldt R, Beek AM, Hirsch A, Stoel MG, Hofman MB, Umans VA, Algra PR, Twisk JW and van Rossum AC. Functional recovery after acute myocardial infarction: comparison between angiography, electrocardiography, and cardiovascular magnetic resonance measures of microvascular injury. J Am Coll Cardiol 2008;52(3):181-9

11

Summary and general discussion

INTRODUCTION

In this thesis, we studied the interplay between inflammation and cardiovascular disease. In several mouse and human studies we not only studied the process of atherosclerosis, but also evaluated the role of inflammation in the cardiac microvasculature and atherothrombosis by using a variety of techniques, including (immuno)histochemistry, enzyme-linked immunosorbent assays, positron emission tomography, computed tomography and cardiac magnetic resonance imaging.

In Chapter 2 we described the inhibitory effect of an anti-inflammatory fish oil constituent, docosahexaenoic acid, on the accumulation of the pro-inflammatory advance glycation end product (AGE) N(ε)-(carboxymethyl)lysine (CML), in the microvasculature of the heart. In Chapters 3-8, we studied the effect of three different types of inflammatory responses, following orthopedic surgery, infection and acute myocardial infarction (AMI) on atherosclerotic plaques. In Chapter 9 and 10, we assessed the inflammatory cell composition of coronary thrombi in relation to thrombus age and the occurrence of microvascular injury.

This chapter will put the previous chapters in mutual context. To visually support these paragraphs, we have included an overview of our findings. First, the rationale for the main hypothesis will be shortly discussed, then we will summarize the main findings of the Chapters, address methodological issues and present directions for further research. We will end the general discussion with an overall conclusion.

RATIONALE

Observational studies show a peak incidence of cardiovascular events early after clinical conditions accompanied with severe systemic inflammation. For example, respiratory tract infections are associated with an approximate fivefold risk for early[1, 2] myocardial infarction [1]. Not only infections, but also major surgery is associated with a marked systemic inflammatory response[3]. As was shown in a recent nationwide cohort study indicated that the risk of myocardial infarction in patients undergoing total hip or knee replacement is increased by no less than 25-fold, again predominantly during the first days to two weeks[4]. Furthermore a landmark paper on the role of acute systemic inflammation in atherosclerosis showed increased plaque area and intra-plaque inflammation in mice briefly after acute myocardial infarction, highlighting another form of acute systemic inflammation[5]. The acuteness of the increased risk in the observational studies suggests plaque vulnerability, which is closely correlated with intra-plaque inflammation

and plaque instability[6, 7]. Indeed, in the aforementioned mouse study intra-plaque macrophage density was increased after a burst of systemic inflammation caused by AMI[5]. Furthermore, several murine studies have shown pro-atherogenic effects of serum amyloid A peptide, an important[8] marker and mediator of acute inflammation in mice[9-12], suggesting the direct effect of inflammation on the vessel wall.
We hypothesized that systemic inflammation induces vessel wall inflammation with subsequent plaque instability and addressed this hypothesis in the cardiac microvasculature and aortic roots of mice and in the atherosclerotic coronary plaques and coronary thrombi of patients using three different models for acute systemic inflammatory activation: (1) major orthopedic surgery induced tissue damage, (2) systemic infection or (3) acute myocardial infarction itself.

MAIN FINDINGS, METHODOLOGICAL CONSIDERATIONS AND DIRECTIONS FOR FURTHER RESEARCH

N(ε)-(carboxymethyl)lysine (CML) is one of the major AGEs and its formation is enhanced in the presence of inflammation[13]. CML is believed to play a role in the development and progression of atherosclerosis[13-15] and its accumulation in atherosclerotic blood vessels, increases with age. Although age-related CML accumulation was found in atherosclerotic vessels[16], it remained unknown whether age-related CML accumulation also occurs in the non-atherosclerotic microvasculature of the brain and the heart. In Chapter 2 we found age-related CML accumulation in the non-atherosclerotic microvasculature of the heart and the brain of atherosclerotic mice (Fig. 1D). Furthermore, we found that the omega-3 (n-3) long-chain polyunsaturated fatty acid, docosahexaenoic acid (DHA) polyunsaturated fatty acid DHA, the fish oil constituent known for its anti-inflammatory actions, inhibited this age-related microvascular CML accumulation in the heart only. Intra-myocardial blood vessels are more important in the induction of acute events than previously thought and potentially identify new therapeutic targets in the treatment of AMI[17]. Therefore our finding of increased CML in these vessels is of great interest. The positive effects of our study should be evaluated/validated in a large scale systematic future trial. Of note, recently published trials in patients with coronary artery disease or after AMI did not show an effect of omega-3 fatty acids on major cardiovascular endpoints (e.g. infarct induction), possibly due to state of the art concomitant drug treatment[18]. However, as suggested by the current guidelines, omega-3 fatty acids supplementation in patients with CAD or after MI and possibly in those with heart failure remains to be encouraged[18]. We add with our study a potential substrate/pathway for this encouragement.

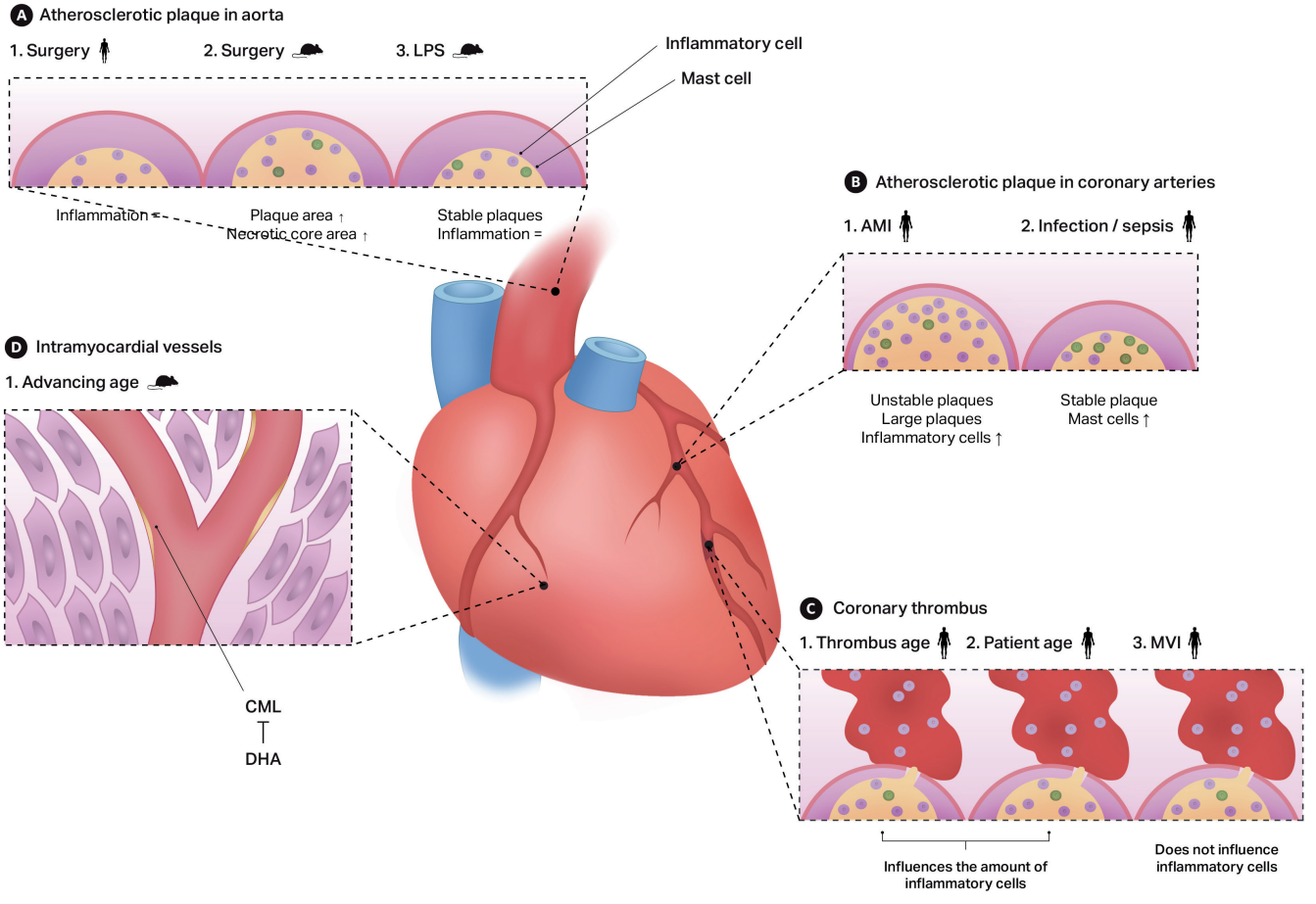

Figure 1 Intensity score of CML in 40,70 and 90 weeks old mice

Overview of the most important findings of this thesis. ND: not determined; CML: N(ε)-(carboxymethyl)lysine; DHA: docosahexaenoic acid.

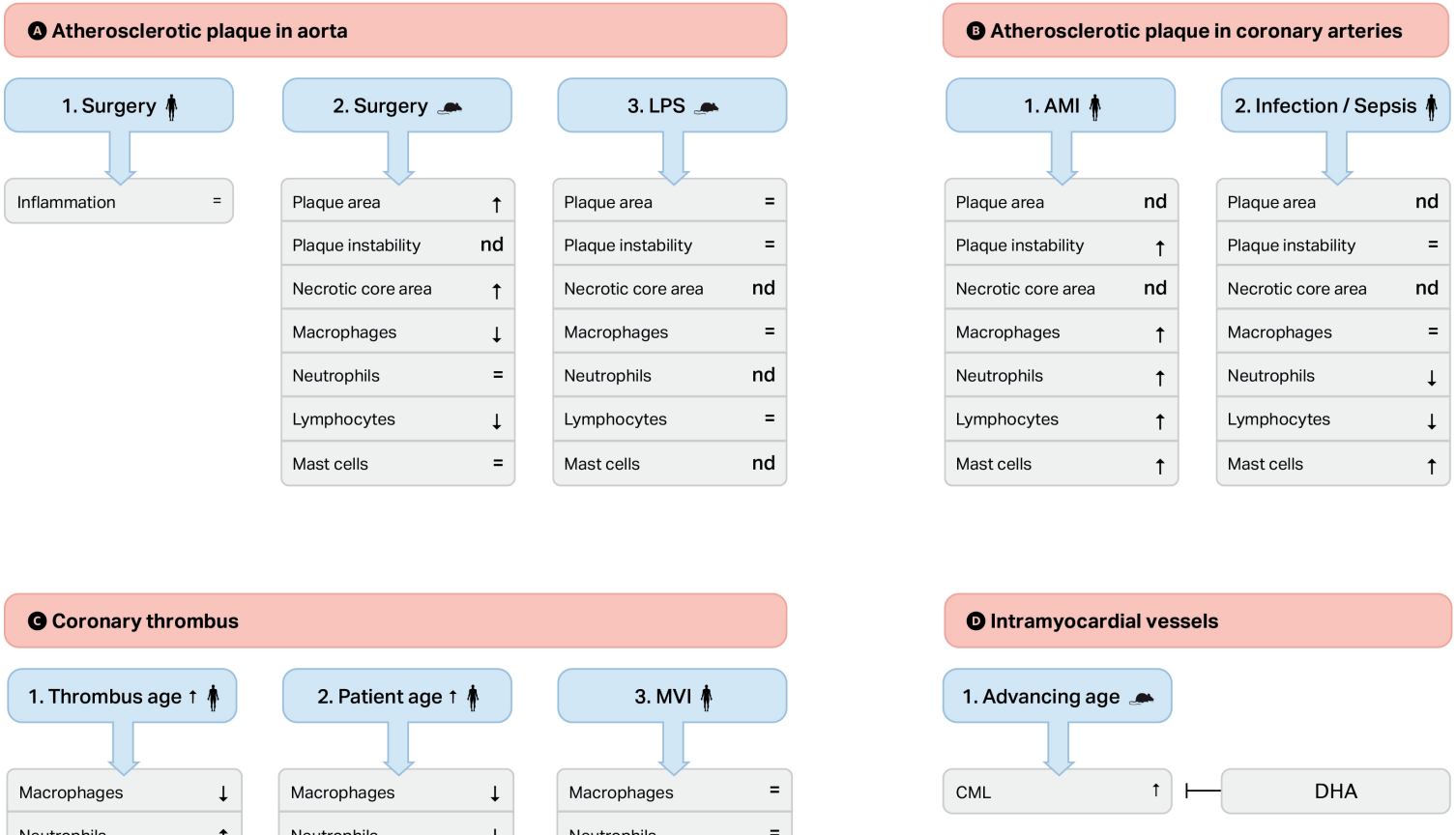
A Atherosclerotic plaque in aorta
1. Surgery
Inflammation =
2. Surgery
Plaque area ↑
Plaque instability nd
Necrotic core area ↑
Macrophages ↓
Neutrophils =
Lymphocytes ↓
Mast cells =
3. LPS
Plaque area =
Plaque instability =
Necrotic core area nd
Macrophages =
Neutrophils nd
Lymphocytes =
Mast cells nd
B Atherosclerotic plaque in coronary arteries
1. AMI
Plaque area nd
Plaque instability ↑
Necrotic core area nd
Macrophages ↑
Neutrophils ↑
Lymphocytes ↑
Mast cells ↑
2. Infection / Sepsis
Plaque area nd
Plaque instability =
Necrotic core area nd
Macrophages =
Neutrophils ↓
Lymphocytes ↓
Mast cells ↑
C Coronary thrombus
1. Thrombus age ↑
Macrophages ↓
Neutrophils ↑
Lymphocytes =
Mast cells nd
2. Patient age ↑
Macrophages ↓
Neutrophils ↓
Lymphocytes =
Mast cells nd
3. MVI
Macrophages =
Neutrophils =
Lymphocytes =
Mast cells nd
D Intramyocardial vessels
1. Advancing age
CML ↑
DHA

In Chapter 3, we studied the effect of major orthopedic surgery on atherosclerotic plaques. Major orthopedic surgery in ApoE -/- mice causes acute systemic inflammation. At 15 days post-surgery, we observed a significant increase of plaque area, mainly due to necrotic core enlargement (Fig.A1). Plaque necrosis is a characteristic hallmark of atherosclerotic lesions that causes acute atherothrombotic vascular disease[6, 19, 20]. Thus, our finding of a post-surgery increase of necrotic core area may reflect increased plaque vulnerability and could, at least in part, explain the increased incidence of cardiovascular events after major orthopedic surgery. In Chapter 4 we evaluated in a similar approach the effects of a lipopolysaccharide (LPS) evoked acute inflammatory response on atherosclerosis. LPS is part of the outer membrane of Gram-negative bacteria, and elicits strong immune responses in both animals and humans via the Toll-like Receptor 4 (TLR4), an important route in the human inflammatory response/sepsis. We chose this model over an actual infection model, such as the colon ligature and puncture model that in theory could more closely resemble the pathophysiological process of sepsis than the LPS model,[21-23] since actual infection models are very hard to reproduce and there are issues with controlling the magnitude of the septic challenge[22]. In general one could say that sepsis is one of the most difficult clinical conditions to model in animals as is also shown by the fact that several promising therapeutic agents that were effective in animal studies failed to demonstrate a similar benefit in human clinical trials[21, 22]. In order to validate our model, we measured serum amyloid A and observed indeed a marked systemic inflammatory response, similar to the orthopedic surgery model. However, in contrast to the orthopedic surgery model, we did not observe effects on plaque area, plaque severity and inflammatory cell density in the atherosclerotic lesions of the ApoE3Leiden mice at both t=3 and t=15 days after LPS injection (Fig. A2).

Although these two clinical conditions (orthopedic surgery and a LPS stimulated immune response) share the presence of an acute systemic inflammatory response, they also have many differences. Obviously the triggers of inflammation (surgery induced tissue damage vs. LPS stimulation) and therefore the profile of the inflammatory cascade differ. Furthermore, surgery, in contrast to LPS injection, was accompanied by anesthesia, pain, temporarily immobilization, and breach of the physical barrier of skin and muscle. All such factors could be responsible for the observed difference. Moreover, the difference in observed effects between the orthopedic surgery and the LPS studies, could also be explained by the different mouse models used. Although both the ApoE3*Leiden mice and the ApoE -/- mice are established models in the atherosclerotic research field, there are some differences between the two. Apolipoprotein E (ApoE) is involved in the efficient uptake of lipoprotein particles and as a result mediates the clearance of cholesterol remnants[24]. Normally, these remnant particles are rapidly removed from circulation. However, mutations in the gene encoding for ApoE (f.i. ApoE3*Leiden) or the double knock-out of the gene (ApoE -/-) cause hyperlipidemia, which can be greatly enhanced with a high-fat diet, leading to an increased susceptibility for atherosclerosis.

It is known that in the ApoE3*Leiden model plaques grow in a slower, more human-like way than the ApoE -/- model[24, 25] Furthermore ApoE is important for hepatic clearance of LPS and the complete absence of this apolipoprotein enhances the immune response to LPS[26-28]. This could have had effect on the positive outcome of the study in Chapter 3 were we used the ApoE -/- model instead of the ApoE3Leiden model.

Although our data in Chapter 3 are compatible with a causal role for surgery-induced inflammation, it would be interesting to address these findings to more in-depth studies that are designed to clarify inflammatory pathways. In addition, other, non- or indirect inflammatory effects of surgery should be further explored, such as hemodynamic disturbances[29], sympathetic nerve system activation[5] or enhanced platelet activity[30] as these are potential contributors to atherosclerotic lesion development and increased cardiovascular risk. Furthermore it would be interesting to test our findings in advanced mouse models to study actual plaque complications rather than atherosclerotic plaque development alone[31, 32].

As discussed before in Chapter 3 and 4, we used mouse models to evaluate our hypothesis. Mice models are crucial for the proof-of principle of most basic research questions and have shown to be invaluable for the progress of biomedical science. However, caution is warranted when translating these studies directly to the human situation. Hereby overcoming for example the fact that in mice, plaques seldom rupture and therefore are considered less adequate to use for the evaluation of human-like plaque complications. We therefore translated our findings from the aforementioned murine studies into clinical studies of which we report in Chapter 5, 6, 7, 8.

In Chapter 5 we studied the effect of systemic inflammation on atherosclerotic coronary plaques of post-AMI patients with or without infection at time of death. We found that AMI was accompanied by advanced inflammation of human coronary atherosclerotic plaques in patients that died 6 hrs-14 days after onset of AMI (Fig. B1). The presence of instable plaques (thin fibrous caps and/or multiple inflammatory cells reaching up to the luminal endothelial layer of the plaque) was also increased in these groups. A particularly interesting finding was that the presence of infection (e.g. sepsis, pneumonia, pancreatitis, peritonitis) at time of death enhanced the mast cell density in the intima and media of coronary arteries, but this phenomenom was not accompanied by increased plaque instability nor an increase in other cell densities (Fig. B2). It thus seems that acute systemic inflammation, both cardiac and infectious, influenced atherosclerotic lesions in a different way.

In Chapter 6 we studied the presence of mast cells (MCs) in the intima and media of unstable and stable coronary lesions at different time points after AMI. We found MCs in the intima and media of both stable and unstable atherosclerotic coronary lesions after AMI, especially increasing in the media of unstable plaques in the patients that died 5-14 days after AMI (Fig B1). These results suggest that MCs present in coronary lesions

might contribute to the onset of MI through their plaque-destabilizing or spasm-inducing properties. MI, in turn, might trigger intra-plaque infiltration of MCs, thereby inducing the transition of stable plaques into unstable plaques resulting in an increased risk of re-infarction.

Taken together, Chapters 5 and 6 thus indicate that MCs play a role in destabilizing plaques and contribute to the onset of AMI. This presumes a role for MC stabilizers, such as cromolyn, in the clinical management of patients with AMI and/or patients at risk for AMI. MC stabilizers prevent degranulation and the subsequent release of histamine, tryptase and chymase. Indeed, in several atherosclerotic murine studies inhibition of MCs reduced plaque instability[33-36], whereas activation of MCs increased plaque instability[34, 37, 38]. It has to be noticed that the conclusions of our studies are based on a tryptase staining. Tryptase is stored in the MCs' granules and is released when activated[39]. It would be interesting to include in future projects not only the MC density, but also the extent of the released MC mediators, since it is known that the mechanism by which MCs are activated affects the profile of excreted MC mediators, which in turn could influence atherogenicity[40]. For example, there is a difference in the mediators when activated by TLR4 or components of the complement system when compared to activation by IgE[34, 41, 42]. Under ischemic conditions, MCs are known to release more growth factors like VEGF instead of tryptase[40].

In Chapter 4 and 6 we evaluated plaque stability in order to identify the so called vulnerable plaques which are prone to rupture. These thin-capped, macrophage rich plaques with large necrotic cores and signs of hemorrhage have been an integral part of our understanding on the pathophysiology of the acute coronary syndromes (ACS) for decades. The vulnerable plaque is still of great value as a readout parameter for the severity of atherosclerotic disease, it is in this context however interesting to realize that plaque rupture still plays an important causal role in acute coronary syndromes, but that superficial erosion appears on the rise[43]. This is most likely explained by the changing risk profile of the studied western Caucasian population and the success of statin treatment which "stabilizes" plaques[44, 45]. This is for instance reflected by the increase of non-ST segment elevation myocardial infarction[46]. In future research it therefore would be valuable to include quantification of plaque erosion. Further it seems that the consequences of a plaque disruption depend not only on the state of the atheromatous lesion itself[47-50], indicated by the high amount of ruptured and healed plaques found in the arteries of already young patients[50], but also on the fluid phase of the blood, for example the concentrations of fibrinogen, tissue factor, endogenous inhibitors of fibrinolysis, and pro-coagulant microparticles[51, 52], which is known to be potentially altered by inflammation itself[53, 54]. Future studies must include the potential role of these factors in the development of AMI.

Next, we designed a study to replicate our finding of pro-atherogenic effects of major orthopedic surgery, in humans. In order to do so, we set out to compare large artery ^{18}FDG uptake in patients scheduled for total knee or total hip replacement. Patients underwent ^{18}F-FDG-PET/CT scanning one day prior to surgery and two to three days after surgery. [^{18}F]-2-fluoro-2-deoxy-D-glucose (FDG) imaging using positron-emission tomography (PET)/computed tomography (CT) provides a noninvasive assessment of inflammation and, as such, could be a valuable imaging biomarker in atherosclerosis. Major surgery may reduce ^{18}F-FDG uptake in atherosclerotic plaques due to competitive uptake of the surgery area and change in pharmacokinetics of ^{18}F-FDG. The aim of the study presented in Chapter 7 was to validate the use of simplified quantitative ^{18}F-FDG uptake parameters for evaluation of inflammation in atherosclerotic plaques after surgery. We found that tissue to background ratio (TBR) calibrated using venous blood samples could be used as surrogate (simplified) measures to assess changes in ^{18}F-FDG uptake in atherosclerotic plaques of patients recovering from major orthopaedic surgery. This led to further evaluation of one of our major research questions: does major orthopaedic surgery increases intra-plaque inflammation in humans? Patients are currently being enrolled for this study in the Alrijne hospital. Results are expected in 2018 and will be published separately from this thesis. The preliminary results in n=4 patients are presented in Chapter 8 and do not suggest an increase of ^{18}F-FDG uptake in the major arteries of patients recovering from major orthopaedic surgery (Fig A3).

The process of intracoronary thrombus formation and naturally occurring resolution is poorly understood. We do know that inflammatory cells play a role in the formation and resolution of venous thrombi, but their role in coronary thrombosis is less clear. In Chapter 9, we analyzed inflammatory cells in thrombi derived from patients with STEMI in relation to histologically classified thrombus age. The VU University Medical Center thrombus aspirate collection provided us the unique opportunity to study patient thrombus material. We found that fresh thrombi (76.1%) were the most abundant as compared to lytic (16.8%) and organized (7.1%) thrombi. Neutrophils were significantly less present in organized compared to fresh and lytic thrombi, respectively. Monocytes/macrophages were significantly more present in lytic than in fresh thrombi (Fig. C1). We additionally found that thrombi from patients aged <50 years as compared to >50 years old contained significantly more neutrophils and monocytes/macrophages irrespective of thrombus age (Fig. C2). Furthermore platelet area was smaller in patients on aspirin, again irrespective of thrombus age. To summarize, the composition of inflammatory cells differs with thrombus age in thrombosuction material of STEMI patients that in part depends on patient age and medication.

Angiographically successful primary percutaneous coronary intervention (p-PCI) not always restores cardiac microvascular blood flow. This phenomenon, called MicroVascular Injury (MVI), worsens prognosis and is poorly understood. We hypothesized that

inflammatory cell density of acute coronary thrombi would be increased in patients with MVI as presented in Chapter 10. In line with our expectations, we found a higher mean symptom-to-balloon time, larger enzymatic infarct size, lower left ventricular ejection fraction and a higher incidence of IMH in the MVI patients. We however could not establish a difference in thrombus content of platelets, erythrocytes, macrophages/monocytes, lymphocytes, neutrophils and neutrophil extracellular traps (NETs) between patients with MVI and patients without MVI (Fig. C3). This study thus argues against inflammatory cell alterations in the coronary thrombus as a possible influence on the occurrence of MVI.

In this Chapter, as well as in Chapters 2, 3, 4, 5, 6, 9, we used inflammatory cell densities in order to make suggestions about inflammatory status of atherosclerotic plaques and coronary thrombus. Research and diagnostics in the field of pathology has its very origin in the observation and quantification of the presence of inflammatory cells in tissues and proved to be very closely related to clinical observations. However, additional analysis of the activation status of inflammatory cells, would also be of interest when studying the pathophysiology of acute inflammation and its role in plaque destabilization and thrombus formation.

CONCLUSION

In the previous sections we gave on overview of the main findings of this thesis and what we add to the existing knowledge. We also tried to carefully address several methodological issues regarding our research. Some of these issues are not specific for our research, but are experienced by most scientists in the field of atherosclerotic research. Others give important clues for future projects, of which we make note in these sections. This thesis provides evidence for a role of systemic inflammation in the pathophysiology of acute myocardial infarction. We found, at least in part, supportive mechanistic evidence for the observational studies reporting increased incidence of cardiovascular events during or after clinical conditions that are accompanied by a systemic inflammatory response, e.g. orthopedic surgery, infection/sepsis and AMI itself.

We describe age-induced inflammatory changes in the microvasculature of the heart that can be postponed with a fish oil constituent. Furthermore, we report evidence concerning orthopedic surgery induced atherosclerotic plaque growth and increased necrotic core area, indicative of more vulnerable plaques. Next we show that mast cells (MCs) are increased in the vessel wall surrounding atherosclerotic plaques in patients that have signs of infection and that MCs are associated with more unstable plaques. Our work also shows that MCs are elevated in the vessel wall that surrounds plaques in patients that died of acute myocardial infarction. Again this was associated with a concomitant increase of unstable plaques. We hypothesize a bi-directional role of MCs as

they are not only a factor in the origin of AMI, but we believe that they are also involved in the acceleration of atherogenesis once an AMI has occurred. Besides increased coronary artery densities of MCs, we also found an increased number of macrophages, neutrophilic granulocytes and lymphocytes in atherosclerotic lesions and the surrounding vessels wall of patients that died more than 6 hours-14 days after myocardial infarction as opposed to patients that died immediately after a coronary event. This also highlights that myocardial infarction induced inflammation favors the atherosclerotic process and could explain the high amount of re-infarctions. Lastly, we found a relationship between immune cell composition of the coronary thrombus and patient characteristics and thrombus age, indicative for a role of inflammatory cells in atherothrombosis development. We did not find a clear relationship between inflammatory thrombus composition and the occurrence of the microvascular injury phenomenon. This finding argues against inflammatory cell involvement in the coronary thrombus as a possible influence on the occurrence of MVI.

Given that 17.5 million people die each year as a result of cardiovascular disease and the incidence is increased with socio-economic status, researchers should obtain a deeper insight in the pathophysiology of these diseases. Paramount in this task is increasing knowledge about triggers of acute destabilization of these mostly gradually developing conditions and subsequently the development of preventative strategies to postpone or even avoid acute myocardial infarction. This thesis provides a framework for the role of acute inflammation in causes and consequences of AMI. Based on our work we believe that one day, accumulating knowledge on the specific link between inflammation and cardiovascular events, will shift the foundation of treatment from damage control or tertiary prevention to primary prevention.

REFERENCES

1 Smeeth L, Thomas SL, Hall AJ, Hubbard R, Farrington P and Vallance P. Risk of myocardial infarction and stroke after acute infection or vaccination. N Engl J Med 2004;351(25):2611-2618

2 Meier CR, Jick SS, Derby LE, Vasilakis C and Jick H. Acute respiratory-tract infections and risk of first-time acute myocardial infarction. Lancet 1998;351(9114):1467-1471

3 Reid D, Toole BJ, Knox S, Talwar D, Harten J, O'Reilly DS, Blackwell S, Kinsella J, McMillan DC and Wallace AM. The relation between acute changes in the systemic inflammatory response and plasma 25-hydroxyvitamin D concentrations after elective knee arthroplasty. Am J Clin Nutr 2011;93(5):1006-1011

4 Lalmohamed A, Vestergaard P, Klop C, Grove EL, de BA, Leufkens HG, van Staa TP and de VF. Timing of acute myocardial infarction in patients undergoing total hip or knee replacement: a nationwide cohort study. Arch Intern Med 2012;172(16):1229-1235

5 Dutta P, Courties G, Wei Y, Leuschner F, Gorbatov R, Robbins CS, Iwamoto Y, Thompson B, Carlson AL, Heidt T, Majmudar MD, Lasitschka F, Etzrodt M, Waterman P, Waring MT, Chicoine AT, van der Laan AM, Niessen HW, Piek JJ, Rubin BB, Butany J, Stone JR, Katus HA, Murphy SA, Morrow DA, Sabatine MS, Vinegoni C, Moskowitz MA, Pittet MJ, Libby P, Lin CP, Swirski FK, Weissleder R and Nahrendorf M. Myocardial infarction accelerates atherosclerosis Nature 2012;487(7407):325-329

6 Virmani R, Burke AP, Farb A and Kolodgie FD. Pathology of the vulnerable plaque. J Am Coll Cardiol 2006;47(8 Suppl):C13-8

7 Libby P. Inflammation in atherosclerosis. Nature 2002;420(6917):868-874

8 Kleemann R, Zadelaar S and Kooistra T. Cytokines and atherosclerosis: a comprehensive review of studies in mice. Cardiovasc Res 2008;79(3):360-376

9 Thompson JC, Jayne C, Thompson J, Wilson PG, Yoder MH, Webb N and Tannock LR. A brief elevation of serum amyloid A is sufficient to increase atherosclerosis. J Lipid Res 2015;56(2):286-293

10 King VL, Thompson J and Tannock LR. Serum amyloid A in atherosclerosis. Curr Opin Lipidol 2011;22(4):302-307

11 Santos-Gallego CG, Badimon JJ and Rosenson RS. Beginning to understand high-density lipoproteins. Endocrinol Metab Clin North Am 2014;43(4):913-947

12 Tan SZ, Ooi DS, Shen HM and Heng CK. The atherogenic effects of serum amyloid A are potentially mediated via inflammation and apoptosis. J Atheroscler Thromb 2014;21(8):854-67

13 Schleicher ED, Wagner E and Nerlich AG. Increased accumulation of the glycoxidation product N(epsilon)-(carboxymethyl)lysine in human tissues in diabetes and aging. J Clin Invest 1997;99(3):457-468

14 Nerlich AG and Schleicher ED. N(epsilon)-(carboxymethyl)lysine in atherosclerotic vascular lesions as a marker for local oxidative stress. Atherosclerosis 1999;144(1):41-47

15 Wang Z, Jiang Y, Liu N, Ren L, Zhu Y, An Y and Chen D. Advanced glycation end-product Nepsilon-carboxymethyl-Lysine accelerates progression of atherosclerotic calcification in diabetes. Atherosclerosis 2012;221(2):387-396

16 Hanssen NM, Wouters K, Huijberts MS, Gijbels MJ, Sluimer JC, Scheijen JL, Heeneman S, Biessen EA, Daemen MJ, Brownlee M, de Kleijn DP, Stehouwer CD, Pasterkamp G and Schalkwijk CG. Higher levels of advanced glycation endproducts in human carotid atherosclerotic plaques are associated with a rupture-prone phenotype. Eur Heart J 2014;35(17):1137-1146

17 Baidoshvili A, Krijnen PA, Kupreishvili K, Ciurana C, Bleeker W, Nijmeijer R, Visser CA, Visser FC, Meijer CJ, Stooker W, Eijsman L, van H, V, Hack CE, Niessen HW and Schalkwijk CG. N(epsilon)-(carboxymethyl)lysine depositions in intramyocardial blood vessels in human and rat acute myocardial infarction: a predictor or reflection of infarction? Arterioscler Thromb Vasc Biol 2006;26(11):2497-2503

18 Kromhout D, Yasuda S, Geleijnse JM and Shimokawa H. Fish oil and omega-3 fatty acids in cardiovascular disease: do they really work? Eur Heart J 2012;33(4):436-443

19 Virmani R, Burke AP, Kolodgie FD and Farb A. Vulnerable plaque: the pathology of unstable coronary lesions. J Interv Cardiol 2002;15(6):439-46

20 Santos-Gallego CG, Picatoste B and Badimon JJ. Pathophysiology of acute coronary syndrome. Curr Atheroscler Rep 2014;16(4):401

21 Dyson A and Singer M. Animal models of sepsis: why does preclinical efficacy fail to translate to the clinical setting? Crit Care Med 2009;37(1 Suppl):S30-7

22 Dejager L, Pinheiro I, Dejonckheere E and Libert C. Cecal ligation and puncture: the gold standard model for polymicrobial sepsis? Trends Microbiol 2011;19(4):198-208

23 Wichterman KA, Baue AE and Chaudry IH. Sepsis and septic shock--a review of laboratory models and a proposal. J Surg Res 1980;29(2):189-201

24 Gijbels MJ, van der Cammen M, van der Laan LJ, Emeis JJ, Havekes LM, Hofker MH and Kraal G. Progression and regression of atherosclerosis in APOE3-Leiden transgenic mice: an immunohistochemical study. Atherosclerosis 1999;143(1):15-25

25 Zadelaar S, Kleemann R, Verschuren L, de Vries-Van der Weij J, van der Hoorn J, Princen HM and Kooistra T. Mouse models for atherosclerosis and pharmaceutical modifiers. Arterioscler Thromb Vasc Biol 2007;27(8):1706-21

26 Rensen PC, Oosten M, Bilt E, Eck M, Kuiper J and Berkel TJ. Human recombinant apolipoprotein E redirects lipopolysaccharide from Kupffer cells to liver parenchymal cells in rats In vivo. J Clin Invest 1997;99(10):2438-2445

27 Laskowitz DT, Lee DM, Schmechel D and Staats HF. Altered immune responses in apolipoprotein E-deficient mice. J Lipid Res 2000;41(4):613-620

28 Kattan OM, Kasravi FB, Elford EL, Schell MT and Harris HW. Apolipoprotein E-mediated immune regulation in sepsis. J Immunol 2008;181(2):1399-1408

29 Landesberg G, Beattie WS, Mosseri M, Jaffe AS and Alpert JS. Perioperative myocardial infarction. Circulation 2009;119(22):2936-44

30 Santos-Gallego CG and Badimon JJ. The sum of two evils: pneumonia and myocardial infarction: is platelet activation the missing link? J Am Coll Cardiol 2014;64(18):1926-1928

31 Chen YC, Bui AV, Diesch J, Manasseh R, Hausding C, Rivera J, Haviv I, Agrotis A, Htun NM, Jowett J, Hagemeyer CE, Hannan RD, Bobik A and Peter K. A novel mouse model of atherosclerotic plaque instability for drug testing and mechanistic/therapeutic discoveries using gene and microRNA expression profiling. Circ Res 2013;113(3):252-265

32 Van der Donckt C, Van Herck JL, Schrijvers DM, Vanhoutte G, Verhoye M, Blockx I, Van Der Linden A, Bauters D, Lijnen HR, Sluimer JC, Roth L, Van Hove CE, Fransen P, Knaapen MW, Hervent AS, De Keulenaer GW, Bult H, Martinet W, Herman AG and De Meyer GR. Elastin fragmentation in atherosclerotic mice leads to intraplaque neovascularization, plaque rupture, myocardial infarction, stroke, and sudden death. Eur Heart J 2015;36(17):1049-1058

33 Bot I, Bot M, van Heiningen SH, van Santbrink PJ, Lankhuizen IM, Hartman P, Gruener S, Hilpert H, van Berkel TJ, Fingerle J and Biessen EA. Mast cell chymase inhibition reduces atherosclerotic plaque progression and improves plaque stability in ApoE-/- mice. Cardiovasc Res 2011;89(1):244-52

34 den Dekker WK, Tempel D, Bot I, Biessen EA, Joosten LA, Netea MG, van der Meer JW, Cheng C and Duckers HJ. Mast cells induce vascular smooth muscle cell apoptosis via a toll-like receptor 4 activation pathway. Arterioscler Thromb Vasc Biol 2012;32(8):1960-9

35 Guo T, Chen WQ, Zhang C, Zhao YX and Zhang Y. Chymase activity is closely related with plaque vulnerability in a hamster model of atherosclerosis. Atherosclerosis 2009;207(1):59-67

36 Sun J, Sukhova GK, Wolters PJ, Yang M, Kitamoto S, Libby P, MacFarlane LA, Mallen-St Clair J and Shi GP. Mast cells promote atherosclerosis by releasing proinflammatory cytokines. Nat Med 2007;13(6):719-24

37 Bot I, de Jager SC, Zernecke A, Lindstedt KA, van Berkel TJ, Weber C and Biessen EA. Perivascular mast cells promote atherogenesis and induce plaque destabilization in apolipoprotein E-deficient mice. Circulation 2007;115(19):2516-25

38 Bot I, de Jager SC, Bot M, van Heiningen SH, de Groot P, Veldhuizen RW, van Berkel TJ, von der Thusen JH and Biessen EA. The neuropeptide substance P mediates adventitial mast cell activation and induces intraplaque hemorrhage in advanced atherosclerosis. Circ Res 2010;106(1):89-92

39 Shi GP, Bot I and Kovanen PT. Mast cells in human and experimental cardiometabolic diseases. Nat Rev Cardiol 2015;12(11):643-658

40 Bot I, Shi GP and Kovanen PT. Mast cells as effectors in atherosclerosis. Arterioscler Thromb Vasc Biol 2015;35(2):265-71

41 Krishnaswamy G, Ajitawi O and Chi DS. The human mast cell: an overview. Methods Mol Biol 2006;315(13-34

42 de Vries MR, Wezel A, Schepers A, van Santbrink PJ, Woodruff TM, Niessen HW, Hamming JF, Kuiper J, Bot I and Quax PH. Complement factor C5a as mast cell activator mediates vascular remodelling in vein graft disease. Cardiovasc Res 2013;97(2):311-20

43 van Lammeren GW, den Ruijter HM, Vrijenhoek JE, van der Laan SW, Velema E, de Vries JP, de Kleijn DP, Vink A, de Borst GJ, Moll FL, Bots ML and Pasterkamp G. Time-dependent changes in atherosclerotic plaque composition in patients undergoing carotid surgery. Circulation 2014;129(22):2269-76

44 Yeh RW, Sidney S, Chandra M, Sorel M, Selby JV and Go AS. Population trends in the incidence and outcomes of acute myocardial infarction. N Engl J Med 2010;362(23):2155-65

45 Underhill HR, Yuan C, Zhao XQ, Kraiss LW, Parker DL, Saam T, Chu B, Takaya N, Liu F, Polissar NL, Neradilek B, Raichlen JS, Cain VA, Waterton JC, Hamar W and Hatsukami TS. Effect of rosuvastatin therapy on carotid plaque morphology and composition in moderately hypercholesterolemic patients: a high-resolution magnetic resonance imaging trial. Am Heart J 2008;155(3):584 e1-8

46 Katz JN, Shah BR, Volz EM, Horton JR, Shaw LK, Newby LK, Granger CB, Mark DB, Califf RM and Becker RC. Evolution of the coronary care unit: clinical characteristics and temporal trends in healthcare delivery and outcomes. Crit Care Med 2010;38(2):375-81

47 van der Wal AC, Becker AE, van der Loos CM and Das PK. Site of intimal rupture or erosion of thrombosed coronary atherosclerotic plaques is characterized by an inflammatory process irrespective of the dominant plaque morphology. Circulation 1994;89(1):36-44

48 Buffon A, Biasucci LM, Liuzzo G, D'Onofrio G, Crea F and Maseri A. Widespread coronary inflammation in unstable angina. N Engl J Med 2002;347(1):5-12

49 Crea F and Liuzzo G. Pathogenesis of acute coronary syndromes. J Am Coll Cardiol 2013;61(1):1-11

50 van Dijk RA, Virmani R, von der Thusen JH, Schaapherder AF and Lindeman JH. The natural history of aortic atherosclerosis: a systematic histopathological evaluation of the peri-renal region. Atherosclerosis 2010;210(1):100-106

51 Libby P and Theroux P. Pathophysiology of coronary artery disease. Circulation 2005;111(25):3481-8

52 Libby P and Pasterkamp G. Requiem for the 'vulnerable plaque'. Eur Heart J 2015;36(43):2984-2987

53 Demetz G and Ott I. The Interface between Inflammation and Coagulation in Cardiovascular Disease. Int J Inflam 2012;2012(860301

54 Wagner DD. New links between inflammation and thrombosis. Arterioscler Thromb Vasc Biol 2005;25(7):1321-4

List of publications

LIST OF PUBLICATIONS

Abheiden CN; van Reuler AV; **Fuijkschot WW**; de Vries JI; Thijs A and de Boer MA. Aspirin adherence during high-risk pregnancies, a questionnaire study. Pregnancy hypertension 2016;6(4):350-355.

Abheiden CN; **Fuijkschot WW**; Arduc A; van Diemen JJ; Harmsze AM; de Boer MA; Thijs A and de Vries JI; Post-pregnancy aspirin resistance appears not to be related with recurrent hypertensive disorders of pregnancy. Eur J Obstet Gynecol Reprod Biol 2016;210(139-143.

* **Fuijkschot WW**; * Kramer GE; Yakub M; Krijnen PA; Niessen HW; Lammertsma AA and Smulders YM. Is large-artery ^{18}F-FDG PET/CT assessed inflammation in atherosclerotic plaques enhanced by major orthopaedic surgery? Study outline and preliminary results – in progress (* shared first authorship)

Fuijkschot WW; Woudstra L; van der Linden R; Beskers D; Zethof IPA; Krijnen IPA; Niessen HWM; Smulders YM. Systemic inflammation enhances mast cell infiltration in coronary arteries in patients who died from myocardial infarction - submitted

* **Fuijkschot WW**; * Kramer GE; Yakub M; Krijnen PA; Boellaard R; Saouti R; Niessen HW; Smulders YM and Lammertsma AA. Validation of simplified ^{18}F-FDG uptake metrics for quantitative assessment of inflammation in atherosclerotic plaques after major surgery – submitted (* shared first authorship)

* **Fuijkschot WW**; * van Leeuwen MA; Shelep I; Amier RP; Roos S; Teunissen PF; Biesbroek PS; Smulders YM; van der Wal AC; Nijveldt R; Appelman JA; Krijnen PA; Niessen HW and van Royen N. Inflammatory cells are not significantly increased in aspirates of coronary thrombi of STEMI patients with microvascular injury – submitted (* shared first authorship)

Fuijkschot WW; Zethof IP; Morrison MC; Krijnen PA; Kleemann R; Niessen HW and Smulders YM. LPS-induced systemic inflammation does not alter atherosclerotic plaque area or inflammation in ApoE3*Leiden mice in the early phase up to 15 days – accepted for publication in Schock

Fuijkschot WW; Groothuizen WE; Appelman Y; Radonic T; van Royen N; van Leeuwen MA; Krijnen PA; van der Wal AC; Smulders YM and Niessen HW. Inflammatory cell content of coronary thrombi is dependent on thrombus age in patients with ST-elevation myocardial infarction. J Cardiol 2017;69(1):394-400.

* **Fuijkschot WW**; * Kupreishvili K; Vonk AB; Smulders YM; Stooker W; Van Hinsbergh VW; Niessen HW and Krijnen PA. Mast cells are increased in the media of coronary lesions in patients with myocardial infarction and may favor atherosclerotic plaque instability. J Cardiol 2017;69(3):548-554. (* shared first authorship)

Fuijkschot WW; Morrison MC; van der Linden R; Krijnen PA; Zethof IP; Theyse LF; Kleemann R; Niessen HW and Smulders YM. Orthopedic surgery increases atherosclerotic lesions and necrotic core area in ApoE-/- mice. Atherosclerosis 2016;255(164-170.

Fuijkschot WW; de Graaff HJ; Berishvili E; Kakabadze Z; Kupreishvili K; Meinster E; Houtman M; van Broekhoven A; Schalkwijk CG; Vonk AB; Krijnen PA; Smulders YM and Niessen HW. Prevention of age-induced N(epsilon)-(carboxymethyl)lysine accumulation in the microvasculature. Eur J Clin Invest 2016;46(4):334-41.

[*] **Fuijkschot WW**; [*] van Diemen JJ; Wessels TJ; Veen G; Smulders YM and Thijs A. Evening intake of aspirin is associated with a more stable 24-h platelet inhibition compared to morning intake: a study in chronic aspirin users. Platelets 2016;27(4):351-6. ([*] shared first authorship)

van Diemen JJ; **Fuijkschot WW**; Spit K; van Reuler VA; Bonten TN; van der Bom JG; Smulders YM; Thijs A. The influence of pre-analytical time and temperature conditions on serum thromboxane B2 levels - submitted.

van Diemen JJ; Racca C; Spit K; Klaassen E; Veen G; **Fuijkschot WW**; van Reuler VA; Bonten TN; van der Bom JG; Smulders YM; Thijs A. Aspirin intake in the morning is suboptimal: a randomized cross-over study in healthy volunteers - submitted

Tonneijck L, **Fuijkschot WW**, Schouten M and Siegert CE. A 76-year-old male with a blue toe and livedo reticularis. Neth J Med 2013;71(5):257-261.

van Reuler AV; van Diemen JJ; Harmsze AM; **Fuijkschot WW** and Thijs A. Splitting aspirin tablets? Use your hands: A study on aspirin tablet splitting using four different methods – accepted for publication in Journal of Pharmacy Practice and Research

LIST OF NON-SCIENTIFIC PUBLICATIONS

Berkenbosch L; **Fuijkschot WW**; Prins G and Taks C. Een moderne arts weet wat zorg kost. Medisch Contact 2014

Buitenhuis R; **Fuijkschot WW**; Friederich H. Gamechangers in de zorg. Hype of Happening? - Published online 2017

Fuijkschot WW. Momentum voor medisch leiderschap. Onco-Hemato 2016

Fuijkschot WW; van Diemen JJ; Thijs A; Smulders YM. Crowdfunding voor medisch wetenschappelijk onderzoek. Medisch Contact 2016

Fuijkschot WW; Versteeg RI; Verweij JP; Hilders C and Levi MM. Artsen met verstand van zaken. Medisch Leiderschap, financiën en organisatie in de zorg – first print 2016

Fuijkschot WW; van Nierop KML and Saris J. Trial and (t)error: attitude leads to gratitude. Amsterdam Medical Students Journal 2015

Fuijkschot WW; de Graaf NP and Smulders YM. Titulatuur artsen vol onduidelijkheden. Medisch Contact 2015

Verhulst A; **Fuijkschot WW**. – Jonge dokter kan veel meer. Nederlands Dagblad 2016

Verhulst A; **Fuijkschot WW**. –Medische professie verdient modernisering. De Volkskrant 2016

Curriculum vitae

Wessel Willem Fuijkschot werd geboren op 20 maart 1988 op het Oversluispad in Wormerveer. Halverwege zijn jeugd verhuisde hij met zijn moeder Marlon en zijn zus Minke naar Eemnes, waar hij verder opgroeide. Hij was aldaar actief voor de Katholieke Plattelands Jongeren, waar hij door evenementen als Sterkste Man Eemnes en 24-uur barzitten leerde organiseren. Het VWO voltooide hij aan het Laar en Berg in Laren. Van 2006 tot en met 2012 studeerde hij geneeskunde aan het VUmc in Amsterdam. Gedurende zijn studietijd had hij veel plezier in het opzetten en geven van onderwijs en ontwikkelde hij een voorliefde voor de interne geneeskunde. Na stages in Peru en Zuid-Afrika raakte hij geïnspireerd door Dr. Abel Thijs en Prof. Dr. Yvo Smulders en het onderzoek dat zij deden. In 2013 startte hij zijn promotieonderzoek op de afdelingen interne geneeskunde en pathologie van het VUmc, onder leiding van Prof. Dr. Yvo Smulders, Prof. Dr. Hans Niessen en Dr. Paul Krijnen. Het resultaat van zijn werk heeft u in handen. Naast zijn gecombineerde basale en klinische onderzoek behield hij zijn voorliefde voor onderwijs en ondernemerschap. Samen met een aantal studiegenoten richtte hij de stichting Medical Business op. Deze stichting ontwikkelt onderwijs voor jonge artsen over financiën en organisatie van de zorg. Hij was verder eindredacteur van het boek: "Artsen met verstand van zaken" en schreef stukken over dit thema voor o.a. voor het Medisch Contact en de Volkskrant. Verder is hij samen met Dr. Arno Bisschop en Drs. Stefan Ottenbros oprichter van KINASE, een bedrijf dat artsen consultancy ervaring op laat doen. Op 1 juli 2017 is hij gestart als ANIOS interne geneeskunde in Alkmaar. Na het behalen van zijn doctoraat blijft Wessel actief op het grensvlak van de interne geneeskunde, onderwijs en ondernemerschap.

Wessel Willem Fuijkschot was born the 20th of March, 1988 in Wormerveer (Oversluispad), the Netherlands. During his childhood, he moved with his mother Marlon and his sister Minke to Eemnes. He was a member of a local society called "Katholieke Plattelands Jongeren", at which he developed his managerial skills during infamous events such as Strongest Man Eemnes and 24-hours bar sit-in race. He attended high school at Laar en Berg. After his graduation, he started Medical School at the VU University Medical Center in Amsterdam (2006-2012). During his studies, not only teaching and improving current education fulfilled him with great pleasure and ambition, but he also developed a strong passion for Internal Medicine. After rotations in Peru and South Africa, he was inspired by Dr. Abel Thijs, and Prof. Dr. Yvo Smulders and their research. In 2013, he started his PhD-training at the Departments of Pathology and Internal Medicine at the VU University Medical Center under advisory of Dr. Yvo Smulders, Dr. Hans Niessen and Dr. Paul Krijnen. This Thesis is the result of his work. Besides his combined basic and clinical research projects, his love for education and entrepreneurship remained, prompting him to establish the Medical Business foundation together with several fellow Medical students. This foundation develops educational programs for young medical doctors concerning the economics and organization of healthcare. His strong attachment with this area of healthcare is further underlined by the book "Artsen met verstand van zaken", for which he was editor-in-chief and his publications about this topic in e.g. Medisch Contact and Volkskrant. In addition, together with Dr. Arno Bisschop en Drs. Stefan Ottenbros, he founded KINASE, a company that allows doctors to gain experience working as a healthcare consultant. On July 1st he started as a junior doctor (not in training) at the department of Internal Medicine in Alkmaar. After finishing his PhD, he will remain active at the intersection of Internal Medicine, education and entrepreneurship.

List of co-author affiliations

LIST OF CO-AUTHOR AFFILIATIONS

Raquel P. Amier	Department of Cardiology, VU University Medical Center, Amsterdam, The Netherlands
Yolande E.A. Appelman	Department of Cardiology, VU University Medical Center, Amsterdam, The Netherlands
Ekaterina Berishvili	Department of Clinical Anatomy, Tbilisi State Medical University, Tbilisi, Georgia
Danae Beskers	Department of Pathology, VU University Medical Center, Amsterdam, the Netherlands
Stefan S. Biesbroek	Department of Cardiology, VU University Medical Center, Amsterdam, The Netherlands
Ronald Boellaard	Department of Radiology and Nuclear Medicine, VU University Medical Center, Amsterdam, The Netherlands
Amber van Broekhoven	Department of Pathology, VU University Medical Center, Amsterdam, The Netherlands
Wessel W. Fuijkschot	Department of Internal Medicine/Pathology, VU University Medical Center, Amsterdam, The Netherlands
Hjalmar J. de Graaff	Department of Cardiac Surgery, VU University Medical Center, Amsterdam, The Netherlands
Wouter E. Groothuizen	Department of ophthalmology, VU University Medical Center, Amsterdam, The Netherlands
Victor W.M. Van Hinsbergh	Department of Physiology, VUmc, Amsterdam, The Netherlands
Maaike Houtman	Department of Pathology, VU University Medical Center, Amsterdam, The Netherlands
Zurab Kakabadze	Georgian National Institute of Medical Research, Ilia State University, Tbilisi, Georgia
Robert Kleemann	Department of Metabolic Health Research, The Netherlands Organization for Applied Scientific Research (TNO), Leiden, The Netherlands
Gem M. Kramer	Department of Radiology and Nuclear Medicine, VU University Medical Center, Amsterdam, The Netherlands
Paul A.J. Krijnen	Department of Pathology, VU University Medical Center, Amsterdam, The Netherlands
Koba Kupreishvili	Department of Pathology, VU University Medical Center, Amsterdam, The Netherlands
Adriaan A. Lammertsma	Department of Radiology and Nuclear Medicine, VU University Medical Center, Amsterdam, The Netherlands
Maarten A.H. van Leeuwen	Department of Cardiology, VU University Medical Center, Amsterdam, The Netherlands

Rianne van der Linden	Department of Pathology, VU University Medical Center, Amsterdam, The Netherlands
Elisa Meinster	Department of Pathology, VU University Medical Center, Amsterdam, The Netherlands
Martine C. Morrison	Department of Metabolic Health Research, The Netherlands Organization for Applied Scientific Research (TNO), Leiden, The Netherlands
Hans W.M. Niessen	Department of Pathology/Cardiac Surgery, VU University Medical Center, Amsterdam, The Netherlands
Robin Nijveldt	Department of Cardiology, VU University Medical Center, Amsterdam, The Netherlands
Teodora Radonic	Department of Pathology, VU University Medical Center, Amsterdam, The Netherlands
Sebastiaan Roos	Department of Cardiology, VU University Medical Center, Amsterdam, The Netherlands
Niels van Royen	Department of Cardiology, VU University Medical Center, Amsterdam, The Netherlands and Department of Cardiology, Radboud University Medical Center, Nijmegen, the Netherlands
Rachid Saouti	Department of Radiology and Nuclear Medicine, VU University Medical Center, Amsterdam, The Netherlands
Casper G. Schalkwijk	Department of Internal Medicine, Maastricht University, the Netherlands
Ivan Shelep	Department of Pathology, VU University Medical Center, Amsterdam, the Netherlands
Yvo M. Smulders	Department of Internal Medicine, VU University Medical Center, Amsterdam, the Netherlands
Wim Stooker	Department of Cardiac Surgery, OLVG, Amsterdam, the Netherlands
Paul F. Teunissen	Department of Cardiology, VU University Medical Center, Amsterdam, The Netherlands
Lars F.H. Theyse	Department Clinical Sciences and Services, Royal Veterinary College London, University of London, United Kingdom
Alexander B.A. Vonk	Department of Cardiac Surgery, VU University Medical Center, Amsterdam, The Netherlands
Allard C. van der Wal	Department of Pathology, Academic Medical Center, Amsterdam, the Netherlands
Linde Woudstra	Department of Pathology, VU University Medical Center, Amsterdam, the Netherlands
Maqsood Yaqub	Department of Radiology and Nuclear Medicine, VU University Medical Center, Amsterdam, The Netherlands
Ilse P.A. Zethof	Department of Pathology, VU University Medical Center, Amsterdam, The Netherlands

Dankwoord/Acknowledgements

Van alle tradities in het wetenschappelijk onderzoek is het uitbrengen van een dankwoord misschien wel de mooiste. Het stelt de onderzoeker in staat welgemeende dank te betuigen aan de totstandkoming van zijn of haar proefschrift. Waar in het geproduceerde wetenschappelijke werk de meeste tekst opgaat aan mitsen en maren, is het dankwoord verstoken van enige kritiek. Het is een lofzang op de samenwerkingen en relaties die belangrijk waren in het proces. Het gaat over mensen. Er zit emotie in. Misschien is het daarom dat dit deel voor velen het lekkerst leest. Voor de lezer is het doorgaans belangrijk om er in genoemd te worden. Voor de schrijver om niemand te vergeten. Dat laatste is waarschijnlijk ook mij niet gelukt.

Traditiegetrouw als eerste dank voor de proefpersonen die het klinische deel mogelijk hebben gemaakt. Direct gevolgd door de donateurs, belastingbetalers en het VUmc die investeerden in dit onderzoek. Dank ook aan de leden van de leescommissie voor de aandacht die zij schonken aan mijn proefschrift.

Vervolgens, dank voor mijn promotieteam. Yvo, jouw creativiteit, schrijfvaardigheid en vasthoudendheid zijn een groot goed. Dank voor jouw vertrouwen en begeleiding van het naïeve begin tot en met het bittere eind. Hans, jouw efficiëntie is ongeëvenaard, je academisch ego opvallend in toom en de passie voor de pathologie enorm. Bedankt voor het laten afkijken van die eigenschappen. Paul, jouw ontspannen manier van werken en heldere "biologische" geest zijn van grote waarde geweest, tijdens de hele rit. Dank daarvoor.

Abel, jij zorgde voor de broodnodige spinazie. Toen ik 5 jaar geleden een wetenschappelijke stage moest kiezen, had ik de keuze tussen een uitgestippeld pad of een avontuur met een breedsprakige internist die om de andere zin zijn ongeschiktheid als onderzoeker benadrukte. O ja, hij had geen geld en dat zou er ook niet snel komen vanwege het eeuwenoude middel dat we gingen onderzoeken. Ik wist het zeker: Aspirine met Abel natuurlijk. Er is in die jaren weinig geweest waar we niet over konden discussiëren. Keer op keer bewees je jouw geschiktheid als onderzoeker, doordat je niet alleen inhoudelijk een ster bent, maar juist omdat je iets van mensen af weet en daar ook iets mee doet. Dank.

Al heel snel kwam Jeske bij het aspirineteam en wat een lol hadden we. Jij was zo mogelijk nog bijdehanter dan ik. Een uur voor de congresdeadline stuurde we ons eerste abstract langs Yvo met het verzoek het na te kijken, zodat we naar ons eerste congres in Israël konden. Als groentjes sleurden we de grijze koppen de dansvloer op en strikte jij de grote plaatjesbaas om de fout in onze poster te vinden. Later leerden we ook om op elkaar te steunen als het wat minder vlot liep. Dank voor jouw aanstekelijke optimisme, ambitie en plezier.

Het Aspirineteam is inmiddels flink uitgebreid met onderzoekers, maar vooral ook studenten die hun talent benutten. *See one, do one, teach one* geldt ook in het onderzoek. Bedankt: Karlinde, Katelijne, Cati, Vera, Estella. Jullie maken het werk leuker en beter. Datzelfde geld voor de studenten van de pathologie, zonder wie dit proefschrift er nooit was geweest. Veel dank: Rianne, Amber, Danae, Ilse, Baback, Ivan, Fabian.

Dan mijn kamergenoten. De eerste 2 jaar in kamer $0^{E}36$ op de afdeling pathologie. Ik moest aan jullie wennen en jullie zo mogelijk nog meer aan mij. We hebben veel mooie momenten gehad en ik ben jullie oneindig veel dank verschuldigd voor de steun bij het praktische werk en het uitbreiden van mijn biochemische kennis. Dank: Linde, Ibrahim, Elisa, Mark, Reindert en Ellis. De laatste 2 jaar zat ik op kamer $4^{A}45$ op de afdeling interne geneeskunde. Het aantal mensen per vierkante meter was hier zo mogelijk nog groter. Edmée, dank voor het welkom en jouw aanstekelijke non-conformisme. Nada, dank voor de tussendoorgesprekjes tijdens lange statistiekdagen. Martine, dank voor de diepgang en natuurlijk onze midpromotie-tenerific-bergtrip. Elke keer als ik moet tanken, zal ik aan je denken.

Dan kom ik gelijk aan bij mijn andere maatje van de interne. Koen, toen jij naar de VU kwam kreeg ik al een heads-up dat je lachen was en niets bleek minder waar. Rondjes lopen op een festival of in het Amsterdamse Bos tijdens de pauze. Samen kwamen we er altijd wel uit. Dank voor jouw vriendschap tijdens deze promotiejaren en wat gaaf dat ik straks naast je mag staan tijdens jouw verdediging.

Dank ook aan alle coauteurs voor de hulp bij de uitvoering van het onderzoek en het schrijven van de manuscripten. In het bijzonder wil ik noemen: Gem, aan wie ik grote dank verschuldigd ben voor de hulp bij de nucleaire studies en Martine, voor de hulp bij het muizenwerk. Heerlijk om met jullie samen op te trekken.

Vervolgens wil ik mijn beide paranimfen bedanken. Rense, we hebben samen het nodige doorleeft. Sinds de eerste dag van de middelbare school maken we elkaar aan het lachen en sta jij voor me klaar. We zijn nog steeds diezelfde plagende pubers maar dan met een serieuze baan. Jij bent altijd positief, trouw tot op het bot en ziet de dingen soms verrassend scherp. Dank dat je straks naast me staat. Rik, het is fijn om een vriend als jij te hebben. Doordat jij steeds net iets verder bent dan ik, kan ik veel van je leren. Dat begon eigenlijk al toen ik coassistent bij je was (en jij eigenlijk ook), op de kinderafdeling. Je bent altijd dichtbij, al zit je zo nu en dan in New York. Ik ben er trots op dat jullie mijn paranimfen zijn, jongens.

Dan de gym matties: Niels, Rense, Kirsty, Lennart, Rutger, Ron en ook Marjolijn. Het sporten en samen eten na een dag cellen tellen op de VU was essentieel om de vaart erin te houden. Op de Sloterkade vormde we een vrolijke, verknipte familie. Dank voor het lachen en dank voor de support. Kirsty, jij in het bijzonder bedankt voor het helpen met de lay-out van het proefschrift en de schouder om op te huilen. Niels en Marjolijn succes met jullie proefschrift, Ron met jouw bedrijf, Lennart met jouw kersverse Meesterschap en Rutger met jouw reis en straks jouw nieuwe baan. Ik kijk uit naar het feest met jullie! Iets met een band en springen.

Dank ook voor mijn vrienden uit Eemnes en Wormerveer. “Make new friends, but keep the old. One is silver, and the other gold”.

Verder dank aan de mensen waarmee ik heb samengewerkt in de stichting Medical Business. Wat een gave dingen hebben we gedaan en wat een mooie aanvulling op mijn promotietijd vormden jullie.

Dank Arno en Stefan, voor jullie geduld en ongeduld met me. Het is heerlijk om samen te werken en aan dromen te bouwen.

Dan is er een reeks mensen die niets anders gemeen hebben, dan dat ze op het juiste moment, de juiste dingen zeiden. Dank, Roland, Renate, Paul & Ellen, Marcel, Joeri, Noor, Marjolein, Casper, Carl, Sandra, Ruben, Wilma, Mike, Elselien, Jennifer, Menno & Frans voor de inspiratie en inzichten. Menno in het bijzonder bedankt voor de foto in dit proefschrift en onze bergtrips. "Het uitzicht net onder de top is ook mooi", of zoiets.

Tot slot wil ik mijn familie bedanken: Mamma, Irma, Minke, Sake, Nine en Poppy. Dank voor jullie steun, geduld en liefde bij dit soms onbegrijpelijke proces. Ik houd van jullie.

EZ, you're the best! We flamingo well together. Dank voor het samenzijn, de rust die jij brengt en het ontwerp van de figuren.